

OPG's DEEP GEOLOGIC

REPOSITORY

FOR LOW & INTERMEDIATE LEVEL WASTE

Postclosure Safety Assessment: System and Its Evolution

March 2011

Prepared by: Quintessa Ltd.

NWMO DGR-TR-2011-28

The logo for Quintessa, featuring a stylized 'Q' followed by the word 'Quintessa' in a serif font.

OPG's DEEP GEOLOGIC

REPOSITORY

FOR LOW & INTERMEDIATE LEVEL WASTE

Postclosure Safety Assessment: System and Its Evolution

March 2011

Prepared by: Quintessa Ltd.

NWMO DGR-TR-2011-28

THIS PAGE HAS BEEN LEFT BLANK INTENTIONALLY

Document History

Title:	Postclosure Safety Assessment: System and Its Evolution		
Report Number:	NWMO DGR-TR-2011-28		
Revision:	R000	Date:	March 2011
Quintessa Ltd.			
Prepared by:	R. Little, P. Humphreys, F. King, R. Metcalfe, J. Penfold, P. Suckling, G. Towler, R. Walke, J. Wilson		
Reviewed by:	M. Thorne		
Approved by:	D. Hodgkinson		
Nuclear Waste Management Organization			
Reviewed by:	H. Leung		
Accepted by:	P. Gierszewski		

THIS PAGE HAS BEEN LEFT BLANK INTENTIONALLY

EXECUTIVE SUMMARY

Ontario Power Generation (OPG) is proposing to build a Deep Geologic Repository (DGR) for Low and Intermediate Level Waste (L&ILW) near the existing Western Waste Management Facility at the Bruce nuclear site in the Municipality of Kincardine, Ontario. The Nuclear Waste Management Organization, on behalf of OPG, is preparing the Environmental Impact Statement (EIS) and Preliminary Safety Report (PSR) for the proposed repository.

The postclosure safety assessment evaluates the long-term safety of the proposed facility and provides supporting information for the EIS and PSR.

This report describes the DGR system and its evolution under a range of possible scenarios that might affect the system in the future. The DGR system comprises the waste and its packaging, the engineered repository, its geological setting, and the surface environment.

A high-level description of each of these system components is provided below.

- Waste:
- The total emplaced volume of L&ILW is about 200,000 m³, in about 50,000 containers.
 - The total amounts of organics, metals and concrete in the wastes and their packaging are approximately 22,000 tonnes, 63,000 tonnes, and 62,000 tonnes, respectively.
 - The wastes are grouped into 10 Low Level Waste and 11 Intermediate Level Waste categories, and are to be emplaced in a range of steel and concrete waste containers and overpacks.
 - The total activity at 2062, the earliest potential closure date, is about 16,000 TBq. Key radionuclides in terms of total activity include H-3, C-14, Ni-63, Nb-94 and Zr-93.
- Repository:
- The repository floor is to be about 680 m below ground surface in competent and low permeability Ordovician argillaceous limestone (the Cobourg Formation).
 - The repository will comprise two shafts, a shaft and services area, access tunnels and ventilation drifts, and 31 waste emplacement rooms in two panels.
 - The DGR will be connected to the surface via a main shaft (used for access) and a ventilation shaft.
 - The repository rooms and tunnels will not be backfilled, but after a group of emplacement rooms have been filled with waste packages, concrete closure walls will be constructed in the access tunnel and ventilation drifts to isolate this group of rooms. At closure of the DGR, the access tunnels will be sealed off from the shafts by the emplacement of a concrete monolith at the base of the shafts. The shafts will then be backfilled with a sequence of materials (bentonite/sand, asphalt, concrete and engineered fill).
 - The total amounts of concrete and metals in the repository (excluding the waste packages, and the material in the shafts other than the monoliths) will be about 170,000 and 3,500 tonnes, respectively.
- Geological Setting:
- The proposed repository location is on the eastern edge of the Michigan Basin in a large block of tectonically stable rock that has predictable geological and hydrogeological properties. There is strong evidence supporting a lack of permeable vertical discontinuities at site scale.
 - A thick sequence of sedimentary rocks overlies the gneissic granitic basement

rocks. The sequence from the ground surface down to the basement comprises approximately:

- 20 m of unconsolidated Quaternary sediments (clay, sand, silt, gravel);
 - 105 m of Devonian dolostones (dolomitic limestones);
 - 325 m of Silurian dolostones, evaporites and shales;
 - 400 m of Ordovician shales and argillaceous to shaley limestone; and
 - 15 m of Cambrian sandstone.
- The DGR is to be located within the low conductivity Ordovician and Silurian rocks (typically $<10^{-11}$ m/s) through which transport of any contaminants is expected to be diffusion dominated. Significant underpressures exist in the Ordovician rocks.
 - The low conductivity rocks are underlain by hydraulically overpressured Cambrian sandstones, and overlain by a 180 m sequence of relatively high conductivity rocks and sediments (10^{-7} to 10^{-4} m/s) through which transport of contaminants is expected to be advection dominated.
 - The porewater in the Middle and Lower Silurian, and the Ordovician sediments is highly saline brine (with total dissolved solids of 150 to 350 g/L), and reducing, with pH buffered by carbonate minerals. The porewaters in the Devonian sediments have total dissolved solids ranging from 0.1 to 2.5 g/L. They are mainly oxidizing and pH is again buffered by carbonate minerals. The porewaters in the Upper Silurian are transitional between the underlying Middle Silurian and the overlying Devonian sediments.
 - No commercially viable oil, gas, salt seams or minerals have been identified as being present.
 - The groundwater aquifer down to around a depth of 100 m is used for municipal and domestic water in the vicinity of the Bruce nuclear site. This aquifer flows into Lake Huron.

Surface Environment:

- Climate: Temperate, with annual precipitation of around 1100 mm and annual average temperature of about 8°C.
- Topography: the Bruce nuclear site is about 190 m above sea level. The area is relatively flat, with a small bluff along the eastern edge of the site.
- Surface water bodies: The dominant surface-water feature is Lake Huron with a total surface area of 60,000 km² and mean depth of 59 m. There are no major rivers in the vicinity of the Bruce nuclear site, although there are several small streams that discharge into Lake Huron.
- Soils: there is generally a shallow layer of sandy and loamy/clayey topsoil, overlying a comparatively complex sequence of surface sand and gravel from former beach deposits, in turn overlying clayey to sandy silt glacial till.
- Land uses: Bruce nuclear site land uses are currently restricted to those associated with the nuclear operations. The region around the Bruce nuclear site is mainly used for agriculture (arable and livestock), recreation and some residential development.
- Flora and fauna: The area is in the Mixedwood Plains ecozone. The site is vegetated with balsam fir, sugar maple and American beech. There is also a meadow and wetland area. There is a wide variety of wildlife in the area.

The future evolution of the DGR system, and potential exposure pathways that might occur, are addressed in part through the systematic identification and assessment of a range of “scenarios”. The purpose of these scenarios is not to predict the future; rather, it is to use field data on the past evolution of the site, and the results of models to develop a range of futures against which the performance of the repository system can be assessed.

The set of scenarios to be assessed has been identified, justified and documented in a systematic and traceable manner using a structured analysis of relevant features, events, and processes (FEPs). One scenario - the Normal Evolution Scenario – describes the expected or likely evolution of the DGR system with time. It has been identified and qualitatively described by considering those FEPs that: provide the system with its (possibly changing) boundary conditions and FEPs; and/or might cause change in the system.

Additional scenarios (Disruptive Scenarios) have also been identified and described that examine the impacts of unlikely disruptive events that would lead to possible penetration of barriers and abnormal degradation and loss of containment. These Disruptive Scenarios are unlikely or “what if” cases that test the robustness of the DGR.

The following set of scenarios is identified and described in this report.

Normal Evolution Scenario

The heat generated by radioactive decay within the repository is small – about 2 kW at the time of closure and decaying. This is low relative to the steady natural geothermal flux through the panel footprint of 10 kW. The repository will remain near its natural ambient temperature condition of around 20°C.

During the years following closure, there is corrosion of the carbon steel containers and degradation of organic materials in the wastes. The atmosphere in the repository becomes anaerobic as oxygen is consumed by corrosion. Subsequent slow anaerobic degradation of the wastes and packaging materials (i.e., containers and overpacks) in the DGR generates various decomposition products, in particular gases (predominantly CO₂ and CH₄ from the microbial decomposition of organics, and H₂ from the corrosion of metals).

The DGR’s shafts resaturate more rapidly than the DGR’s rooms and tunnels because they are: backfilled (smaller volume to be resaturated); are exposed to more permeable rock formations; tend to pull water in (bentonite); and are not a gas generation source. The low permeability of the shaft seals and the host rock, plus the gas pressure in the repository and the water consumption by corrosion reactions, all limit the resaturation of the repository. The repository might take many hundreds of thousands or even millions of years to resaturate.

Most of the waste packaging is not long-lived, and will allow water to contact the wastes as the repository resaturates (the higher activity ILW containers are more robust and are likely to take longer to degrade). All packages eventually fail. Even then, the failed packages may continue to provide some physical limitation (e.g., diffusion) or local chemistry control (e.g., alkalinity in cement containers) that inhibits the release of contaminants, especially in the case of the containers used for wastes produced from the fuel channel replacement (retubing) program.

Contaminants are released from the waste by dissolution into repository water and, especially for H-3 and C-14, the formation of radio-labelled gases. The rate of release varies with the type of wastes, with contaminants in the Zircaloy pressure tubes (containing most of the long-lived Zr-93) being released as the waste form corrodes, resulting in a slower release than for other

waste categories. Once released into the water or gas in the repository, the migration of contaminants from the repository is limited by the low-permeability shaft seals and very low permeability host rock. The excavation of the repository results in a damaged zone developing around the shaft, emplacement rooms and tunnels, with higher porosity and permeability. This is also a potential pathway for contaminant transport.

The host rock has good rock mechanical quality, and together with the emplacement room design (i.e., alignment with principal stresses, low excavation volume), results in a mechanically stable configuration. However, as the rooms and tunnels are not backfilled (the wastes occupy about 50% of the volume), it is expected that rockfall from the roofs and walls of the rooms and tunnels occurs, due to eventual degradation of engineered rock support and, in the longer term, due to seismic and/or glacial events. This process continues intermittently, over a period of a few hundred thousand years, until the collapsed rock fills the available space and is able to support the roof and prevent further failure.

The regional area around the Bruce nuclear site is tectonically stable and is characterized by low rates of seismicity. Large earthquakes are very unlikely in general, but are more likely around the time of ice-sheet retreat. The host rock is strong, and small earthquakes will have little effect. The primary effect of large earthquakes will be rockfall as noted above until the rooms and tunnels fill and stabilize. Rockfall also damages the containers.

Most radionuclides decay within the repository and the surrounding rock. However, slow migration of some dissolved or gaseous contaminants occurs into the geosphere surrounding the repository and into the repository shafts. Some contaminants may eventually discharge to the shallow groundwater system, and then to the biosphere. Potential impacts on humans are estimated based on assuming a critical group of a self-sufficient family farm located on the repository site and using groundwater from a well. These are expected to be a very small; the purpose of the postclosure safety assessment is to evaluate how small.

The surface environment will change significantly over these time frames. Initially there could be changes due to global warming, but regionally the area is expected to retain a temperate climate and ecosystem during this initial warming period.

Currently, the Earth is in a configuration where periodic ice ages occur, with nine major cycles in the past million years. Key factors contributing to these cycles – variations in solar insolation to the northern hemisphere and the arrangement of the continents – will not change appreciably over the next million years. Although global warming and a weak solar insolation variation are likely to delay the onset of the next ice-sheet advance for at least 60,000 years, it is prudent to assume that glacial cycles will resume in the long term and, therefore, to consider the potential effects on the DGR system.

As climatic conditions cool in the long term, ecosystems are expected to change from temperate to tundra. Agriculture becomes less viable. As the climate grows progressively cooler and drier, arctic conditions are established with permanent human habitation in the vicinity of the site becoming increasingly less likely (assuming present-day demographic/climatic relations), and the site is eventually covered by an advancing ice-sheet. The subsequent warming of the climate and the resulting ice-sheet retreat are followed by re-establishment of tundra and potentially temperate ecosystems and the eventual re-population of the site. Each glacial/interglacial cycle also causes biosphere change due to glacial and periglacial processes (e.g., the development of proglacial lakes, the erosion and deposition of surface deposits, the formation of soils, and the change in shoreline location).

The ice-sheet causes major changes in the shallow groundwater system, in terms of permafrost, hydraulic pressures and flow rates, and in the penetration of glacial recharge waters. Based on continental scale modelling of the last ice sheet, the repository site is expected to see shallow discontinuous permafrost. It is also likely to experience multiple cycles of glacial advance and retreat, as well as creation and loss of proglacial lakes, due to its proximity to the southern extent of the ice sheet.

However, the impacts of glacial cycles on the deep groundwater system are expected to be primarily changes in the stress and hydraulic pressure regime resulting from ice-sheet loading and unloading. This is supported by evidence from the site itself, where the deep groundwaters do not show signs of impact from past glaciations, as well as from modelling of the behaviour of the groundwater and geomechanical environment around the repository. The overall rock is expected to remain intact and solute transport remains diffusion-dominated, as in previous glacial cycles.

In the long term, the underground repository is likely to develop into an assemblage of mostly limestone rock containing magnetite, siderite and other mineral products of the wastes and their packaging, with little change in the surrounding rock beyond the vicinity of the repository. The porosity in the rock will contain a mixture of brine and methane gas.

Human Intrusion Scenario

Given the depth of the DGR, the type of human activity that might directly impact the closed repository involves a deep borehole, unintentionally drilled into the repository as part of a future geological exploration program. Such intrusion could only occur after all institutional control of the site was lost and societal memory or markers had become ineffective. Even then, the probability of occurrence is very unlikely because of the low economic resource potential of the rocks, the lack of potable groundwaters below about 100 m, the uniform geology across a large area (i.e., nothing unique about the rock at this location), and the small footprint of the DGR. Nevertheless, the possibility of such inadvertent human intrusion cannot be ruled out over the long timescales of interest to the safety assessment. If the scenario were to occur, however, the borehole could provide a direct pathway from the repository to the surface environment and the potential for direct exposure to waste inadvertently retrieved in the drill core. This scenario is referred to as the Human Intrusion Scenario.

This scenario considers the same evolution of the DGR system as for the Normal Evolution Scenario, with the only difference being that human intrusion into the repository occurs at some time after control of the site is no longer effective.

In this scenario, an exploration borehole is drilled down through the geosphere. In an exploration borehole, the investigators would most likely collect samples or conduct measurements at the repository level, which would readily identify if there were still significant residual radioactivity (e.g., gamma scanning is a standard borehole measurement). In this case, the investigators would likely initiate appropriate precautions to prevent further exposure.

Nevertheless, the Human Intrusion Scenario considers the case where the intrusion is inadvertent, the repository hazard is not recognized, the borehole and drill site are not managed and closed to current standards and material from the borehole is released around the drill site. Further, the scenario also considers the long-term consequences of the borehole being poorly sealed, resulting in the creation of a pathway for contaminants into permeable geosphere horizons above the repository. In this "what if" case, humans and non-human biota can be exposed via: direct release to the surface of pressurized gas prior to sealing of the borehole;

retrieval and examination of drill core contaminated with waste; retrieval and uncontrolled dispersal of contaminated drill core on the site; and the long-term release of contaminated water from the repository into permeable geosphere horizons via the exploration borehole, if the borehole was continued down into the pressurized Cambrian and subsequently poorly sealed. These releases could result in the exposure of the drill crew or other people at the time of intrusion, and people who might occupy the site subsequent to the intrusion event.

Severe Shaft Seal Failure Scenario

The Normal Evolution Scenario takes account of the role of engineered barriers and assumes that their performance meets design specifications; it includes an expected degree of degradation of barriers with time. The shaft seals are the most important engineered barriers, so a “what if” scenario is considered in which the shaft materials, and the shaft and repository excavation damage zones (EDZs) are assumed to have significantly degraded properties. For example, the seals may not be fabricated or installed appropriately, or the long-term performance of the seals may deteriorate due to unexpected physical, chemical and/or biological processes. The scenario is referred to as the Severe Shaft Seal Failure Scenario.

This scenario considers the same evolution of the DGR system and the same exposure pathways and group as the Normal Evolution Scenario, the difference being that there is rapid and extensive shaft seal degradation and the repository/shaft EDZs have significantly degraded properties. The scenario is a bounding, “what if” scenario that is designed to investigate the robustness of the DGR system.

Poorly Sealed Borehole Scenario

The DGR site has several deep boreholes around the repository, used for site characterization initially and for monitoring during and after operation. In all cases, the deep boreholes are licensed through the Ontario Ministry of Natural Resources and they are outside the repository footprint by at least 100 m. Furthermore, they will be appropriately sealed on cessation of site investigation/monitoring activities. However, the Poorly Sealed Borehole Scenario considers the consequences of a deep borehole not being properly sealed. It is considered as a “what if” scenario, possibly also arising due to unexpected seal degradation processes resulting in very poor seal performance.

The evolution of the system considered for the Poorly Sealed Borehole Scenario is similar to the Normal Evolution Scenario with the key difference being that a poorly sealed site investigation/monitoring borehole provides an enhanced permeability connection between the level of the repository, the overlying groundwater zones and the biosphere, thereby bypassing part of the natural geological barrier to contaminant migration from the DGR. The subsequent exposure pathways and critical group assessed are the same as those considered in the Normal Evolution Scenario.

Vertical Fault Scenario

There is strong geological, hydrogeological, and geochemical evidence that there are no vertical faults/fracture zones in the vicinity of the DGR that provide transmissive pathways from the repository horizon to higher horizons. Furthermore, the DGR site is located in a seismically stable region, and tectonic activities that can create such faults are absent for the relevant timescale.

Despite this evidence, a “what if” scenario is considered to investigate the safety implications of a hypothetical transmissive vertical fault, either undetected or representing the displacement of an existing structural discontinuity, that propagates from the Precambrian rocks into the Guelph formation in the intermediate groundwater system. The fault is in close proximity to the DGR and, consistent with regional evidence, does not extend into the shallow groundwater system. Such a fault could provide an enhanced permeability pathway that bypasses the deep groundwater system, one of the natural barriers to contaminant migration from the DGR. Groundwater flow in the Guelph is assumed to be horizontal and to discharge to the lake. Consideration is given to exposure of two critical groups: one that obtains its water and fish from the lake’s near shore; and one that farms above the repository and has the same characteristics as that considered in the Normal Evolution Scenario.

THIS PAGE HAS BEEN LEFT BLANK INTENTIONALLY

TABLE OF CONTENTS

	<u>Page</u>
EXECUTIVE SUMMARY	v
1. INTRODUCTION.....	1
1.1 PURPOSE AND SCOPE.....	2
1.2 REPORT OUTLINE.....	3
2. DGR SYSTEM DESCRIPTION	5
2.1 WASTE.....	5
2.1.1 Categories and Characteristics	5
2.1.2 Packaging	7
2.1.3 Waste Acceptance Criteria.....	7
2.1.4 Volumes	11
2.1.5 Contaminants and Other Materials	11
2.2 REPOSITORY	14
2.2.1 Layout and Construction	15
2.2.1.1 General.....	15
2.2.1.2 Shafts.....	15
2.2.1.3 Shaft and Services Area	15
2.2.1.4 Access Tunnels and Emplacement Rooms	18
2.2.2 Waste Emplacement.....	18
2.2.3 Closure.....	20
2.2.3.1 Emplacement Rooms.....	20
2.2.3.2 Access Tunnels.....	20
2.2.3.3 Shaft and Services Area	20
2.2.3.4 Shafts.....	21
2.2.3.5 Other Excavations.....	21
2.3 GEOLOGICAL SETTING	23
2.3.1 Geology.....	23

2.3.2	Stratigraphy.....	28
2.3.3	Faults and Fractures	29
2.3.4	Karst	31
2.3.5	Geological Resources	32
2.3.6	Hydrogeology.....	34
2.3.6.1	Regional.....	34
2.3.6.2	Local	34
2.3.6.3	Gas Saturation	40
2.3.6.4	Over/Underpressures.....	42
2.3.6.5	Damaged Zone	44
2.3.7	Geochemistry	44
2.3.7.1	Water Chemistry	44
2.3.7.2	Rock Chemistry.....	48
2.3.8	Seismicity	51
2.3.9	Stress Regime.....	52
2.4	SURFACE ENVIRONMENT	53
2.4.1	Atmosphere.....	56
2.4.2	Surface Water Bodies	57
2.4.3	Water Quality	62
2.4.4	Water Supply.....	63
2.4.5	Sediment.....	63
2.4.6	Surficial Geology	65
2.4.7	Land Use.....	65
2.4.8	Biota	66
2.4.8.1	Plants.....	66
2.4.8.2	Wildlife	68
2.4.8.3	Valued Ecosystem Components.....	69
3.	EXTERNAL FACTORS AFFECTING THE EXPECTED EVOLUTION OF THE DGR SYSTEM.....	70

4.	EXPECTED EVOLUTION OF THE WASTE AND REPOSITORY	81
4.1	CONTAMINANT INVENTORY	81
4.2	THERMAL EVOLUTION	82
4.3	HYDRAULIC EVOLUTION	83
4.4	MECHANICAL EVOLUTION	87
4.4.1	Emplacement Rooms and Repository Tunnels.....	87
4.4.2	Shafts.....	88
4.5	CHEMICAL AND BIOLOGICAL EVOLUTION	90
4.5.1	Corrosion of Metals	96
4.5.1.1	Corrosion of Ferrous Metals	97
4.5.1.2	Corrosion of Other Metals.....	99
4.5.1.3	Timing of Completion of Metal Corrosion Reactions.....	99
4.5.2	Degradation of Organic Materials	101
4.5.3	Degradation of Cementitious Materials	103
4.5.4	Evolution of Bentonite-Sand.....	105
4.5.5	Evolution of Asphalt	107
4.6	INTERFACES WITH THE GEOSPHERE AND BIOSPHERE SUB-SYSTEMS	108
4.7	AUDIT OF POTENTIAL INTERACTIONS	108
5.	EXPECTED EVOLUTION OF THE GEOSPHERE	110
5.1	THERMAL EVOLUTION	110
5.2	HYDRAULIC EVOLUTION	113
5.2.1	Recharge.....	113
5.2.2	Local Surface Water Bodies.....	114
5.2.3	Effects of Glaciation	114
5.3	MECHANICAL EVOLUTION	117
5.3.1	Geosphere Surrounding the Emplacement Rooms and Repository Tunnels	117
5.3.2	Geosphere Surrounding the Shafts.....	118
5.3.3	Impact of Glaciation	118

5.3.4	Impact of Earthquakes	121
5.4	CHEMICAL EVOLUTION	121
5.4.1	Impact of the Repository	121
5.4.1.1	Evolution of Gas Chemistry	121
5.4.1.2	Evolution of Mineralogy.....	122
5.4.2	Effects of Glaciation	123
5.4.2.1	Evolution of Groundwater and Porewater Chemistry.....	123
5.4.2.2	Evolution of Mineralogy.....	123
5.5	GAS MIGRATION	124
5.5.1	Evolution of Gas Pressure	124
5.5.2	Gas Transport.....	124
5.5.3	Impact of Glaciation	126
5.6	INTERFACES WITH THE WASTE/REPOSITORY AND BIOSPHERE SUB-SYSTEMS	127
6.	EXPECTED EVOLUTION OF THE BIOSPHERE.....	128
6.1	APPROACH	128
6.2	ASSESSMENT CONTEXT	130
6.3	CONSIDERATION OF BIOSPHERE CHANGE.....	130
6.3.1	Mechanisms of Change	130
6.3.1.1	Introduction	130
6.3.1.2	Global Climate Change.....	131
6.3.1.3	Human Influence on Global Climate	133
6.3.1.4	Social and Institutional Developments.....	133
6.3.2	Potential Changes to the Biosphere.....	133
6.3.2.1	Changes in Surface Features and Processes	133
6.3.2.2	Changes in Biota.....	134
6.3.2.3	Changes in Human Behaviour	135
6.3.3	Biosphere Evolution	135
6.3.4	Biosphere States.....	136

6.3.4.1	Temperate.....	137
6.3.4.2	Tundra.....	138
6.3.4.3	Glacial.....	139
6.3.4.4	Post-glacial	140
6.3.5	Sequence of Future Biosphere Change.....	141
6.4	REPRESENTATION OF BIOSPHERE SYSTEM CHANGE	143
6.5	INTERFACES WITH THE REPOSITORY AND GEOSPHERE SUB-SYSTEMS.....	143
7.	THE EXPECTED EVOLUTION OF THE DGR SYSTEM: THE NORMAL EVOLUTION SCENARIO	145
7.1	OVERALL SYSTEM EVOLUTION.....	145
7.2	WASTE AND REPOSITORY EVOLUTION.....	146
7.3	GEOSPHERE EVOLUTION	148
7.4	BIOSPHERE EVOLUTION.....	149
8.	OTHER POSSIBLE EVOLUTIONS OF THE DGR SYSTEM: DISRUPTIVE SCENARIOS	151
8.1	IDENTIFICATION OF DISRUPTIVE SCENARIOS	151
8.2	DESCRIPTION OF DISRUPTIVE SCENARIOS	173
8.2.1	Human Intrusion Scenario.....	173
8.2.2	Severe Shaft Seal Failure Scenario	174
8.2.3	Poorly Sealed Borehole Scenario	174
8.2.4	Vertical Fault Scenario	174
9.	REFERENCES.....	175
10.	ABBREVIATIONS AND ACRONYMS.....	183
APPENDIX A: MIGRATION OF GAS FROM THE DGR		
APPENDIX B: POTENTIAL GAS PRESSURES IN THE DGR		
APPENDIX C: CHEMICAL EVOLUTION OF THE DGR		
APPENDIX D: FORMATION OF METHANE AND CARBON DIOXIDE HYDRATES		
APPENDIX E: ASSESSMENT OF SHAFT SEAL DEGRADATION		

APPENDIX F: AUDIT OF COMPONENT INTERACTIONS IN THE DGR AND ITS SHAFTS

APPENDIX G: HOST ROCK DISSOLUTION BY CARBON DIOXIDE

LIST OF TABLES

	<u>Page</u>
Table 2.1: Low Level Waste Categories	6
Table 2.2: Intermediate Level Waste Categories	7
Table 2.3: Reference Containers and Overpacks	8
Table 2.4: Summary of Preliminary DGR Waste Acceptance Criteria	10
Table 2.5: Reference Forecast Waste Volumes	12
Table 2.6: Amounts of Potentially Important Radionuclides, Elements and Chemicals in Waste	13
Table 2.7: Amounts of Organics, Metals and Concrete in Wastes and their Containers and Overpacks	14
Table 2.8: Number of Emplacement Rooms Occupied by Each Waste Category in the Repository Panels	18
Table 2.9: Groundwater Flow Directions and Gradients in Deep Permeable Units	37
Table 2.10: Sampled Groundwater and Porewater Compositions	45
Table 2.11: Cobourg Model 2 Porewater Composition	47
Table 2.12: 2009 Sediment Sampling Results (µg/g) from the Hydrology and Surface Water Quality TSD	64
Table 2.13: Results of 2009 Sampling for Radionuclides in Lake Huron Sediments, Bq/kg from the Radiation and Radioactivity TSD	64
Table 3.1: External FEPs Considered	72
Table 3.2: Status of External FEPs for the Expected Evolution of the DGR System	74
Table 4.1: Summary of the Expected Evolution of Key Geochemical Parameters	93
Table 4.2: Anticipated Evolution of the Shaft Seals	109
Table 8.1: External FEPs Potentially Compromising Arguments relating to the Long-term Safety of the DGR	152
Table 8.2: Summary of Internal FEPs from the DGR FEP List	157
Table 8.3: Internal FEPs Potentially Compromising Arguments relating to the Long-term Safety of the DGR	160
Table 8.4: Potential Failure Mechanisms and Associated Scenarios	162
Table 8.5: Grouping of Alternative States for External FEPs into Additional Scenarios	165
Table 8.6: Additional Scenarios Considered in Other Safety Assessments	171

LIST OF FIGURES

	<u>Page</u>
Figure 1.1: The DGR Concept at the Bruce Nuclear Site	1
Figure 1.2: Document Structure for the Postclosure Safety Assessment	2
Figure 1.3: Approach used for the Current Postclosure Safety Assessment	4
Figure 2.1: General Layout of the Final Preliminary Design Repository	16
Figure 2.2: General Layout of the Original Preliminary Design Repository	16
Figure 2.3: Isometric View of the Final Preliminary Design Repository	17
Figure 2.4: Layout of the Shaft and Services Area for the Final Preliminary Design Repository	17
Figure 2.5: Emplacement Room Section View – P1 Profile for Bin Type Waste Packages	19
Figure 2.6: Emplacement Room Section View – P3 Profile for Resin Liner Type Waste Packages	19

Figure 2.7:	Location of Monolith in Repository Tunnels for the Final Preliminary Design	20
Figure 2.8:	Illustration showing Sequence of Shaft Sealing Materials	22
Figure 2.9:	Geologic Features of Southern Ontario	23
Figure 2.10:	Geologic Map of Southern Ontario.....	24
Figure 2.11:	Cross-section across the Michigan Basin	25
Figure 2.12:	Tectonic Boundary and Fault Contacts in Southern Ontario.....	27
Figure 2.13:	DGR Boreholes and Pre-existing US Boreholes and the Proposed DGR Layout..	28
Figure 2.14:	Geologic Stratigraphy at the DGR Site	29
Figure 2.15:	Profiles of Core Natural Fracture Frequency	31
Figure 2.16:	A) Core Photo from Shallow Devonian Lucas Formation Carbonates, Showing Karst Features and B) Remnant Paleokarst Horizon near the Top of the Bass Islands Formation.....	32
Figure 2.17:	Oil and Natural Gas Pools on Southern Ontario	33
Figure 2.18:	Reference Stratigraphic Column Showing Groundwater Zones at the Bruce Nuclear Site.....	35
Figure 2.19:	Hydraulic Conductivity Profile Based on Data from DGR Site Investigation Boreholes	36
Figure 2.20:	Groundwater Levels (mASL) and Direction of Shallow Groundwater Flow around the Bruce Nuclear Site	38
Figure 2.21:	Hypothetical Groundwater Flow Pathway in the Salina A1 Upper Carbonate (SA1UC) and Guelph Formations	39
Figure 2.22:	Major Ion Groundwater/Porewater Concentrations.....	40
Figure 2.23:	Saturation Profile in DGR Cores	41
Figure 2.24:	Groundwater Vertical Head Profiles Based on Data from the DGR-4 Site Investigation Borehole.....	42
Figure 2.25:	Groundwater Density (Salinity) Profiles Based on Data from the DGR Site Investigation Boreholes.....	43
Figure 2.26:	Profiles of Calcite and Dolomite in DGR Cores.....	48
Figure 2.27:	Profiles of Quartz and Total Sheet Silicates in DGR Cores	49
Figure 2.28:	Profiles of Illite and Chlorite Clay Mineral Content in DGR Cores	50
Figure 2.29:	Seismicity in the Bruce Region from 1985 to 2010 Overlain with Mapped Faults in Southern Ontario	51
Figure 2.30:	Location of the DGR Project and Definition of the Study Areas.....	54
Figure 2.31:	Bruce Nuclear Site and Surrounding Area	55
Figure 2.32:	Local Watersheds	58
Figure 2.33:	Stream C, Catchments and Discharge Locations	59
Figure 2.34:	Bathymetry of Lake Huron	60
Figure 2.35:	Baie du Doré Pictured from Scott Point	61
Figure 2.36:	Stream C at the Site Boundary	62
Figure 2.37:	The Railway Ditch	62
Figure 2.38:	2001 Ecological Land Classification for the Bruce Nuclear Site	67
Figure 3.1:	External, Internal and Contaminant Factors/FEPs.....	70
Figure 4.1:	Time Dependence of Radioactivity in the Waste Due to Decay.....	81
Figure 4.2:	Rockfall within and around the Emplacement Rooms after Four Glacial Cycles ...	89
Figure 4.3:	Evolution of Volumetric Strain in the Rock Adjacent to Shaft Concrete Bulkhead B1 (Lions Head Formation) Considering Time-dependent Strength Degradation, Glacial Loading and Pore Pressure.....	91
Figure 4.4:	Swelling Pressure as a Function of Clay Density and Salinity in Smectite-based Sealing Materials.....	106

Figure 5.1:	Simulated Permafrost Depth at the Bruce Nuclear Site over the Last Glacial Cycle for the Eight Cases Consistent with Historical Data	111
Figure 5.2:	Simulated Basal (Surface) Temperatures at the Bruce Nuclear Site over the Last Glacial Cycle for the Eight Cases Consistent with Historical Data	112
Figure 5.3:	Simulated Basal Meltwater Production at the Bruce Nuclear Site over the Last Glacial Cycle for the Eight Cases Consistent with Historical Data	116
Figure 5.4:	Simulated Earth Surface Elevation at the Bruce Nuclear Site over the Last Glacial Cycle for the Eight Cases Consistent with Historical Data	119
Figure 5.5:	Simulated Normal Stresses at the Bruce Nuclear Site over the Last Glacial Cycle for the Eight Cases Consistent with Historical Data	120
Figure 6.1:	Decision Tree for Use in the Identification and Justification of Biosphere Systems	129
Figure 6.2:	Simulated Proglacial Lake Depth at the Bruce Nuclear Site over the Last Glacial Cycle for the Eight Cases Consistent with Historical Data	132
Figure 6.3:	Illustration of the Temperate Biosphere State	137
Figure 6.4:	Illustration of the Tundra Biosphere State	138
Figure 6.5:	Illustration of the Glacial Biosphere State	139
Figure 6.6:	Illustration of the Post-glacial Biosphere State.....	140
Figure 6.7:	Simplified Historic Pattern of Surface Temperature at the Bruce Nuclear Site during the Last Glaciation Cycle	142
Figure 6.8:	Simplified Sequence of Past Climate States.....	143
Figure 6.9:	Assumed Sequence of Climate States and Permafrost Depth with Global Warming for the Next 120 ka	143
Figure 8.1:	Location of Disruptive Scenarios Evaluated in the Safety Assessment	172

THIS PAGE HAS BEEN LEFT BLANK INTENTIONALLY

1. INTRODUCTION

Ontario Power Generation (OPG) is proposing to build a Deep Geologic Repository (DGR) for Low and Intermediate Level Waste (L&ILW) near the existing Western Waste Management Facility (WWMF) at the Bruce nuclear site in the Municipality of Kincardine, Ontario (Figure 1.1). The Nuclear Waste Management Organization (NWMO), on behalf of OPG, is preparing the Environmental Impact Statement (EIS) and Preliminary Safety Report (PSR) for the proposed repository.

The postclosure safety assessment (SA) evaluates the long-term safety of the proposed facility and provides supporting information for the EIS (OPG 2011a) and PSR (OPG 2011b).

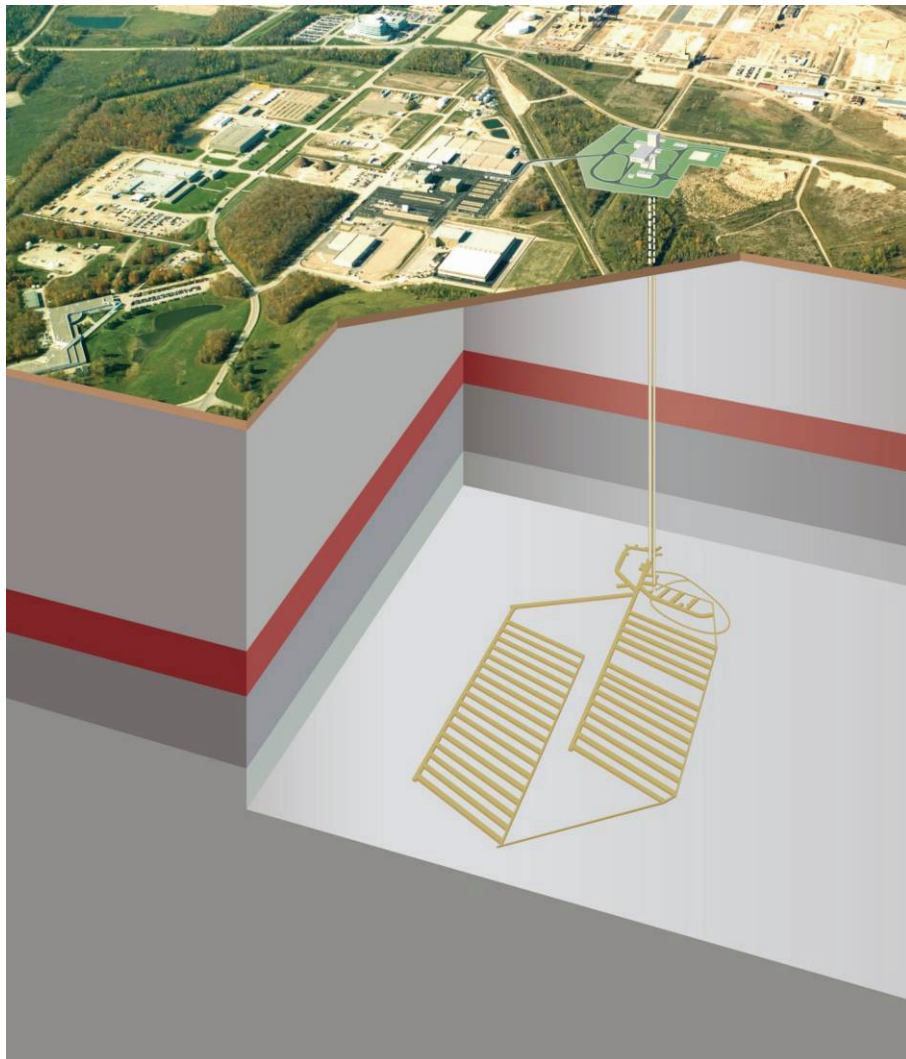


Figure 1.1: The DGR Concept at the Bruce Nuclear Site

This report (System and its Evolution) is one of a suite of documents that presents the postclosure safety assessment (Figure 1.2), which also includes the Postclosure SA main report (QUINTESSA et al. 2011a), the Normal Evolution Scenario Analysis report (QUINTESSA 2011), the Human Intrusion and Other Disruptive Scenarios Analysis report (QUINTESSA and SENES 2011), the Features, Events and Processes report (QUINTESSA et al. 2011b), the Data report (QUINTESSA and GEOFIRMA 2011), the Groundwater Modelling report (GEOFIRMA 2011), the Gas Modelling report (GEOFIRMA and QUINTESSA 2011).

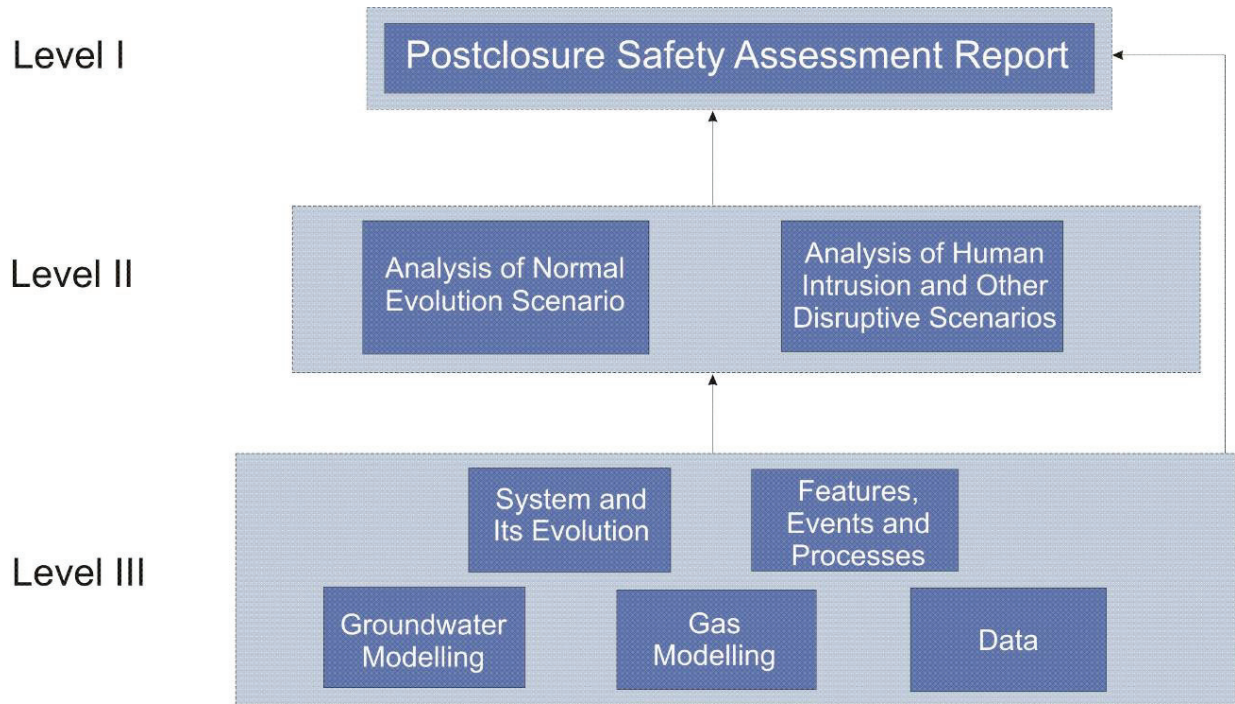


Figure 1.2: Document Structure for the Postclosure Safety Assessment

1.1 Purpose and Scope

This safety assessment has been carried out using an approach consistent with international best practice, as embodied in the draft safety standards on the safety case and safety assessment for radioactive waste disposal from the International Atomic Energy Agency (IAEA) (IAEA 2010) and the recommendations of the IAEA program for the Improvement of Safety Assessment Methodologies (ISAM) (IAEA 2004) (Figure 1.3).

The approach comprises the following basic steps.

1. The context of the assessment is defined, documenting the high-level assumptions, the constraints (reflecting the regulatory requirements), and the assessment's purpose, focus and timeframes.
2. The current information on waste, repository, geosphere and biosphere systems that is relevant to postclosure safety is reported, along with identified areas of uncertainty.

3. A range of internally consistent potential future evolutions of the disposal system (scenarios) is systematically identified.
4. Conceptual and mathematical models and data are developed for the scenarios and a range of calculation cases, which explore key areas of uncertainty, are identified and implemented in software tools.
5. Following the running of the software tools and the generation of results, the results are analyzed, interpreted and discussed to inform on the performance of the system, its overall robustness, and the nature and role of key uncertainties. Particular emphasis is given to the comparison of the results for the identified safety and performance indicators against the relevant reference levels.

The purpose of this report is to describe Steps 2 and 3 of the safety assessment approach used in the safety assessment. It, therefore, describes the DGR system (Step 2) and its evolution under a range of possible scenarios that might affect it in the future (Step 3).

A scenario is defined as “a postulated or assumed set of conditions or events. They [*scenarios*] are most commonly used in analysis or assessment to represent possible future conditions or events to be modelled, such as the possible future evolution of a repository and its surroundings” (CNSC 2006). The purpose of scenario identification and development is not to predict the future; rather, it is to use field data on the past evolution of the site, and the results of supporting modelling to develop a sufficiently comprehensive range of possible future evolutions of the DGR against which the performance of the system can then be assessed.

This report provides a primarily qualitative description of the evolution of the DGR system over timescales of up to 1,000,000 years – the timeframe over which geological events, repository evolution, and health and environmental impacts are assessed (see Section 3.8 of the Postclosure SA main report, QUINTESSA et al. 2011a). A more quantitative description of the system’s evolution is provided in the conceptual model developed in the Normal Evolution Scenario Analysis report (QUINTESSA 2011), and the Human Intrusion and Other Disruptive Scenarios Analysis report (QUINTESSA and SENES 2011). The more quantitative description in these reports is informed by the results of detailed groundwater and gas modelling presented in GEOFIRMA (2011) and GEOFIRMA and QUINTESSA (2011), respectively.

1.2 Report Outline

The key components of the DGR system are first described in Chapter 2. Based on the current understanding of the site and its processes, the key features, events and processes (FEPs) that are considered to affect the system’s evolution over the timescales of interest are then identified. External factors that are likely to impact the DGR system and its evolution are identified in Chapter 3. The impact of these external factors, together with factors internal to the disposal system, on the thermal, hydraulic, mechanical and chemical evolution of the waste and repository (Chapter 4) and the geosphere (Chapter 5) is then described. Given the significant uncertainties relating to the evolution of the biosphere, biosphere evolution is evaluated using a stylized approach¹ (Chapter 6). The resulting expected evolution of the entire system (the

¹ A stylized representation of the biosphere, and human habits and behaviour is a representation that has been simplified to reduce the natural complexity to a level consistent with the objectives of the analysis using assumptions that are intended to be plausible and internally consistent but that will tend to err on the side of conservatism.

Normal Evolution Scenario) is presented in Chapter 7, while other less likely evolutions leading to possible abnormal degradation and loss of containment (Disruptive Scenarios) are identified and described in Chapter 8.

The report has been written for a technical audience that is familiar with the scope of the DGR project; the Bruce nuclear site; and the process of assessing the long-term safety of radioactive waste disposal.

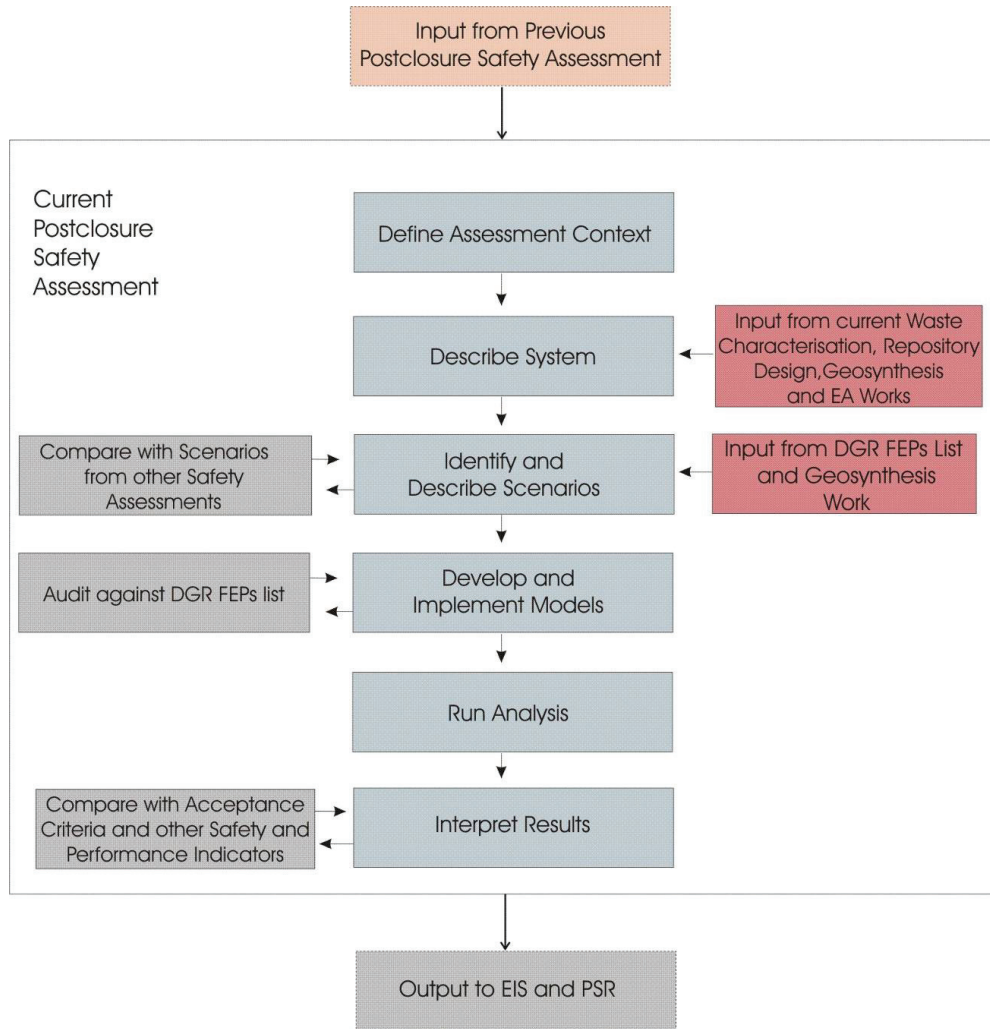


Figure 1.3: Approach used for the Current Postclosure Safety Assessment

2. DGR SYSTEM DESCRIPTION

The DGR system comprises the waste and its packaging, the engineered repository, the geological setting, and the surface environment. An overview of each of these components is presented in the following subsections which summarize the key features of the DGR system.

The primary data sources are:

- The Reference L&ILW Inventory Report (OPG 2010) for the waste and waste packaging;
- The Chapter 6 (Facility Description) of the Preliminary Safety Report (OPG 2011b) for the repository design;
- The Geosynthesis Report (NWMO 2011) and Descriptive Geosphere Site Model Report (INTERA 2011) for the geological setting (i.e., the geosphere); and
- The Technical Support Documents (TSDs) supporting the Environmental Assessment (EA) for the DGR (GOLDER 2011a to g, AMEC NSS 2011), and the EA Study Report for the WWMF (OPG 2005) for the surface environment (i.e., the biosphere).

The following sections describe the DGR system as it exists at present, or during the operational period of the DGR.

2.1 Waste

2.1.1 Categories and Characteristics

The DGR will accept operational and refurbishment wastes from OPG-owned or operated nuclear power plants. The wastes to be accepted are classified as solid low-level or intermediate-level, consistent with Canadian Standards Association (CSA) N292.3 (CSA 2008). The DGR will not accept used nuclear fuel.

Low Level Waste (LLW) typically consists of incinerator ash; compacted waste; bulk and drummed non-processible wastes; some low activity ion-exchange resins and filters from secondary side reactor process systems; system components such as heat exchangers, feeder pipes and steam generators; as well as miscellaneous low-activity items. The concentration or quantity of radionuclides in LLW is above the clearance levels established by the regulatory body (the Canadian Nuclear Safety Commission (CNSC)), and it contains primarily short-lived radionuclides (half-lives shorter than or equal to 30 years).

Intermediate Level Waste (ILW) consists of non-fuel waste containing significant quantities of long-lived radionuclides (generally with half-lives greater than 30 years). It comprises higher activity materials, such as primary side and moderator ion-exchange resins and filters; irradiated core components; and reactor fuel channel wastes (e.g., pressure tubes, calandria tubes, and end fittings) from the reactor refurbishment (retubing) program.

The L&ILW is categorized in the Reference L&ILW Inventory Report (OPG 2010) according to the characteristics of the waste. These categories and the waste characteristics are summarized in Table 2.1 and Table 2.2. Most waste categories are relatively homogeneous in their physical characteristics, especially incinerator ash, resins and sludges, and retube wastes.

Certain wastes will be conditioned at the WWMF prior to being sent to the DGR. This is current practice at the WWMF. The main waste conditioning practices undertaken by OPG at the WWMF are incineration (resulting in the generation of the bottom ash and baghouse ash) and compaction (resulting in the generation of compacted waste bales and boxes). In addition, the

steam generators from the planned refurbishment programs are assumed to be grouted and cut into smaller pieces. Some LLW has historically been conditioned by other methods, such as grouting with cement, immobilization with bitumen, and the addition of polymeric absorbers. Cementitious grout has been or will be added to some ILW to provide mechanical support for waste retrieval and handling rather than as a waste conditioning agent.

Table 2.1: Low Level Waste Categories

Waste Category	Description
Bottom ash	Heterogeneous ash and clinker from waste incineration.
Baghouse ash	Fine homogeneous ash from waste incineration.
Compacted wastes (bales)	Generally compactable solid LLW; for example compacted empty waste drums, rubber hoses, rubber area floor matting, light gauge metals, welding rods, plastic conduit, fire blankets and fire-retardant material, metal cans, insulation, ventilation filters, air hoses, metal mop buckets and presses, electric cable (<1/4" diameter), lathe turnings, metal filings, glass, plastic suits (Mark III/IV), rubbers, Vicraft hoods, rubber gloves.
Compacted wastes (boxes)	Same as compacted bales.
Non-Processible (boxes)	Solid LLW that is non-compactable or has a contact dose rate greater than 2 mSv/h; for example heavy gauge metal (e.g., beams, Ion-Exchange (IX) vessels, angle iron, plate metal), concrete and cement blocks, metal components (e.g., pipe, scaffolding pipes, metal planks, motors, flanges, valves), wire cables and slings, electric cables (>1/4" diameter), Comfo respirator filters, tools, paper, plastic, absorbent products, laboratory sealed sources, feeder pipes.
Non-Processible (drums)	Generally small, granular or solidified LLW; for example floor sweepings, cleaners and absorbents (e.g., Dust Bane, Stay Dry), metal filings, glassware, light bulbs, bitumenized low-level waste.
Non-Processible (other)	Large and irregularly shaped objects such as heat exchangers, encapsulated tile holes, shield plugs, and other miscellaneous large objects (e.g., fume hoods, glove boxes, processing equipment).
LL/ALW Resins	Spent Low-Level (LL) ion-exchange resin arising from light water auxiliary systems, and/or Active Liquid Waste (ALW) treatment systems.
ALW sludges	Sludge containing clay sorbent arising from liquid effluent treatment plant at Bruce A.
Steam generators	Redundant steam generators from refurbishment. The steam generators consist of Inconel 600 tubes, carbon steel shell and shroud, and head and tubesheet.

Table 2.2: Intermediate Level Waste Categories

Waste Category	Description
Moderator resins	Spent IX resin arising from moderator purification systems.
PHT resins	Spent IX resin arising from PHT (Primary Heat Transport) purification systems.
Misc. Resins	Spent IX resin arising from station auxiliary systems (e.g., heavy water upgraders).
CANDECON resins	Spent IX resin from chemical decontamination process for nuclear heat transport systems.
Irradiated core components	Various replaced core components, notably flux detectors and liquid zone control rods.
Filters and filter elements	Filters and filter elements from various station process systems.
IX columns	Spent IX resin mainly arising from Pickering PHT purification system, comes as package with steel container.
Retube - Pressure Tubes	Fuel channel waste from large scale retube.
Retube - End Fittings	Fuel channel waste from large scale retube.
Retube - Calandria Tubes	Fuel channel waste from large scale retube.
Retube - Calandria Tube Inserts	Fuel channel waste from large scale retube.

2.1.2 Packaging







OPG's waste packages are mostly well defined. Potential changes include the tile hole equivalent (T-H-E) Liner packaging, the amount of overpacked waste, and the possibility of pre-processing the steam generators. However, while these changes would somewhat affect the total amount of steel and concrete in the repository, the amount of radioactivity would be little changed.

The range of waste containers and overpacks that will be used by OPG for the storage and eventual disposal of L&ILW in the DGR is described in the Reference L&ILW Inventory Report (OPG 2010). It is recognized that each waste category may use several types of waste containers and overpacks, and conversely each waste container/overpack may not be exclusive to a single waste category. Furthermore, there is ongoing evolution of the packaging designs. However, for the safety assessment, the most common waste containers and overpacks for each waste category have been identified as "reference", as described in Section 3.2 of the Data Report (QUINTESSA and GEOFIRMA 2011) and summarized in Table 2.3.

2.1.3 Waste Acceptance Criteria

Preliminary waste acceptance criteria have been developed for the DGR (see Section 5.5 of the PSR, OPG 2011b) and are used to ensure that the wastes to be emplaced in the DGR are within the bounds of the safety assessment, design basis and facility licence. The criteria are summarized in Table 2.4.

Table 2.3: Reference Containers and Overpacks

Container Name, Wastes and Overpack	Picture	Container Name, Wastes and Overpack	Picture
<p>Carbon steel ash bin (AIBN)</p> <ul style="list-style-type: none"> • Bottom ash • Baghouse ash <p>Reference overpack</p> <ul style="list-style-type: none"> • LLW sheet metal overpack (BINOPK) 		<p>Mild steel bale rack (BRACK)</p> <ul style="list-style-type: none"> • Compacted waste (bales) <p>Reference overpack</p> <ul style="list-style-type: none"> • To be overpacked but details not yet specified. Assumed to be simple sheet metal cover. 	
<p>Mild steel compactor box (B25)</p> <ul style="list-style-type: none"> • Compacted waste (boxes) <p>Reference overpack</p> <ul style="list-style-type: none"> • None 		<p>Carbon steel drum bin (DBIN)</p> <ul style="list-style-type: none"> • Non-processible waste (drummed) <p>Reference overpack</p> <ul style="list-style-type: none"> • 10% overpacked in LLW sheet metal overpack (BINOPK) 	
<p>Non-pro box (NBP47)</p> <ul style="list-style-type: none"> • Non-processible waste (boxes) <p>Reference overpack</p> <ul style="list-style-type: none"> • None 		<p>Low level resin pallet tank (RTK)</p> <ul style="list-style-type: none"> • ALW resins • LLW resins <p>Reference overpack</p> <ul style="list-style-type: none"> • To be overpacked but details not yet specified. Assumed to be simple sheet metal cover. 	




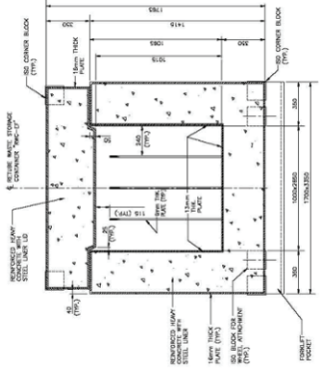

Container Name, Wastes and Overpack	Picture	Container Name, Wastes and Overpack	Picture
<p>ALW sludge box (NPBSB)</p> <ul style="list-style-type: none"> ALW sludges <p>Reference overpack</p> <ul style="list-style-type: none"> LLW sheet metal overpack (BINOPK) 		<p>Resin liner (RL)</p> <ul style="list-style-type: none"> CANDECON resins Moderator resins PHT resins Misc. resins <p>Reference shield (RLSHLD1)</p> <ul style="list-style-type: none"> Concrete cylinder each holding two resin liners 	
<p>Tile hole equivalent liner (THLIC18)*</p> <ul style="list-style-type: none"> Filters and elements Irradiated core components IX columns <p>Reference overpack*</p> <ul style="list-style-type: none"> Transported in a re-usable shield and inserted into a concrete pipe array in the emplacement room 		<p>Retube waste container (RWC-EF)</p> <ul style="list-style-type: none"> Retube wastes (end fittings) 	
<p>Retube waste container (RWC-PT)</p> <ul style="list-style-type: none"> Retube wastes (pressure tubes) Retube wastes (calandria tubes) Retube wastes (calandria tube inserts) 		<p>Notes: This table presents a simplified description of waste containers and overpacks. Pictures generally show the containers as they appear during storage at WWMF. All containers will be lidded and overpacked if necessary. Steam Generators are not shown in the table as they will not be placed in containers. * Original preliminary design. Replaced by steel and concrete ATHEL and ILW Shield containers in final preliminary design (OPG 2010).</p>	

Table 2.4: Summary of Preliminary DGR Waste Acceptance Criteria

Criteria	Summary Description
Waste characterization	- Physical, chemical, radiological characteristics of each package
Documentation	- Waste packages must be tracked in OPG's waste tracking database with waste characteristics, dose rates, description of contents, etc. - Verified load statements - Supplemental information such as radiological surveys, chemical analyses, loading checklists - Notes on package design documentation, such as drawings, technical specifications, design requirements, etc. - Transfer documents for wastes subject to additional controls
Acceptable waste package designs	- All DGR waste package designs must be approved
Condition of waste container	- No significant rusting - Sound structural integrity - No leakage - No wobbling or tilting
Mass limits	- 35 Mg, subject to maximum design limit for each waste package type
Size limits	- Must fit within internal dimensions of the DGR cage: 2.65 m wide x 5.2 m long x 14 m high
Containment	- Wastes and contamination shall be contained during handling - All containers shall have lids
Venting	- Where the potential for gas build-up exists and containers are not designed to withstand the pressure, the containers shall be vented
Identification/ labelling	- Containers bar-coded with OPG's waste tracking database tracking number on two adjacent vertical sides - Additional information including gross mass, dose rate, and significant non-radiological hazards to be marked on packaged with lettering at least 25 mm high
Stackability	- Stable, self-supporting stack of up to 6 m high - Use of standard footprints strongly encouraged
Handling	- Conventional material handling equipment such as forklifts with loads of up to 35 Mg
Fire resistance	- Non-combustible containers
Dose rate limits	- 2 mSv/h on contact with external surface of waste package or shielding - 0.1 mSv/h at 1 m from transportation package - Exceptions approved by responsible health physicist
Radionuclide composition	- Package amount must be reported for H-3, C-14, Cl-36, Co-60, Sr-90, Zr-93, Nb-94, Tc-99, I-129, Cs-135, Cs-137, U-235, U-238, Pu-239, Pu-240, Pu-241
Contamination limits	- Removable surface contamination on package exterior to be less than 4 Bq/cm ² beta-gamma and 0.4 Bq/cm ² alpha when averaged over 300 cm ²

Criteria	Summary Description
Heat load limits	<ul style="list-style-type: none"> - No restriction if less than 0.01 W/m³ of waste package external dimensions - up to 10 W/m³ by prior notification and approval for special cases
Waste form	<ul style="list-style-type: none"> - Solids only - Sludges must have slump of less than 150 mm
Residual liquids	<ul style="list-style-type: none"> - Generally must be less than 1% free liquid by volume - Bulk IX resins must be less than 5% free water by volume
Gas generation	<ul style="list-style-type: none"> - Must not generate toxic gas on exposure to water
Excluded wastes	<ul style="list-style-type: none"> - Reactive wastes, polychlorinated biphenyl (PCB) wastes, pathological wastes, ignitable wastes - Explosives, corrosives, compressed gases - Used nuclear fuel and recognizable fuel fragments - High thermal Co-60 sources
Special notice wastes	<ul style="list-style-type: none"> - Wastes containing significant levels of Occupational Health and Safety Act designated substances - Leachate toxic wastes
Chelating agents	<ul style="list-style-type: none"> - Must be less than 1% by weight of package
Petroleum oils	<ul style="list-style-type: none"> - Must be less than 1% by weight of package

2.1.4 Volumes

The volume of L&ILW to be placed in the DGR has been estimated by OPG according to several scenarios, capturing the influence on waste arisings of key decisions concerning the operating life of CANDU reactors at Bruce, Pickering and Darlington. The current reference forecast is presented in the Reference L&ILW Inventory Report (OPG 2010).

These estimated volumes are presented in Table 2.5. The raw or net volume refers to the waste material itself, whereas the emplaced volume is the volume occupied by the waste packages in the repository including an allowance for the waste containers and any overpacks.

The total volume of wastes is relatively well constrained, being based on waste volumes already stored (approximately half the total volume), plus historic experience of reactor operation combined with OPG's forecast scenario based essentially on the life of the current nuclear fleet. Therefore, the overall waste volumes are expected to be similar to this forecast. The total emplaced waste volume will be limited by the excavated volume of the repository.

2.1.5 Contaminants and Other Materials

A large number of radioactive and non-radioactive species are present in L&ILW wastes, but most of these are present in small amounts and only a subset need to be considered in safety assessment calculations. Screening calculations have been conducted that included the full set of contaminants identified in the Reference L&ILW Inventory Report (OPG 2010), and identified potentially important contaminants for consideration in the safety assessment (Appendix A of the Data report, QUINTESSA and GEOFIRMA 2011). Table 2.6 summarizes the total amounts of radionuclides, elements and chemical species in the LLW and ILW considered as contaminants in the current assessment.

Table 2.5: Reference Forecast Waste Volumes

Waste Categories	Raw (Net) Volume (m³)	Number of DGR Containers	Emplaced Volume (m³)
LLW			
Bottom ash	2,033	882	7,497
Baghouse ash	364	218	1,853
Compacted wastes (bales)	2,268	1,383	4,702
Compacted wastes (boxes)	14,110	6,135	17,177
Non-processible (boxes)	56,713	24,190	73,792
Non-processible (drums)	9,408	7,840	25,532
Non-processible (other)	3,279	164	3,279
LLW and ALW resins	3,393	2,165	6,307
ALW sludges	3,569	1,709	14,527
Steam generators	8,387	512	8,387
Sub-total LLW	103,524	45,198	163,053
ILW			
Moderator resins	1,929	430	4,779
PHT resins	1,348	301	3,340
Misc. resins	1,808	403	4,480
CANDECON resins	2,257	503	5,592
Irradiated core components	27	4,459 ⁽¹⁾ 4,453 ⁽²⁾	6,101 ⁽¹⁾ 9,453 ⁽²⁾
Filters and filter elements	1,344		
IX columns	544		
Retube Wastes (Pressure Tubes)	193	242	1,860
Retube Wastes (Calandria Tubes)	133	167	1,285
Retube Wastes (Calandria Tube Inserts)	36	45	349
Retube Wastes (End Fittings)	2,429	899	9,804
		7,449⁽¹⁾	37,590⁽¹⁾
Sub-total ILW	12,048	7,443⁽²⁾	40,942⁽²⁾
Total	115,572	52,647⁽¹⁾ 52,641⁽²⁾	200,643⁽¹⁾ 203,995⁽²⁾

Notes:

1. Based on waste packages proposed for original preliminary design (NWMO 2010a).
2. Based on waste packages proposed for final preliminary design (OPG 2010).

Table 2.6: Amounts of Potentially Important Radionuclides, Elements and Chemicals in Waste

Radio-nuclide ⁽¹⁾	Amount (Bq) at 2062			Elements/ Chemicals	Amount (kg)		
	LLW	ILW	Total		LLW	ILW	Total
H-3	8.49E+14	1.56E+14	1.00E+15	Antimony	3.23E+03	2.35E+01	3.25E+03
C-14	2.42E+12	6.07E+15	6.07E+15	Arsenic	2.83E+02	1.42E+02	4.25E+02
Cl-36	6.01E+08	1.42E+12	1.42E+12	Barium	9.42E+03	1.59E+02	9.58E+03
Ni-59	5.01E+10	3.63E+13	3.64E+13	Beryllium	1.11E+02	2.10E+01	1.32E+02
Ni-63	5.04E+12	3.95E+15	3.96E+15	Boron	1.53E+03	5.25E+03	6.78E+03
Se-79	1.54E+06	1.25E+10	1.25E+10	Bromine	1.30E+02	4.62E-01	1.30E+02
Sr-90 ⁽²⁾	8.96E+12	4.52E+13	5.42E+13	Cadmium	1.12E+04	1.96E+01	1.12E+04
Mo-93	0.00E+00	1.00E+12	1.00E+12	Chromium	7.85E+05	1.98E+05	9.84E+05
Zr-93	4.54E+06	2.13E+14	2.13E+14	Cobalt	3.42E+02	3.01E+02	6.44E+02
Nb-93m	0.00E+00	9.26E+12	9.26E+12	Copper	3.35E+06	7.01E+03	3.35E+06
Nb-94	2.46E+10	4.60E+15	4.60E+15	Gadolinium	0.00E+00	5.41E+03	5.41E+03
Tc-99	6.28E+07	6.10E+10	6.10E+10	Hafnium	0.00E+00	2.58E+02	2.58E+02
Ag-108m	3.43E+07	1.97E+13	1.97E+13	Iodine	6.60E+01	1.19E-01	6.61E+01
Sn-121m	0.00E+00	7.76E+13	7.76E+13	Lead	1.52E+06	2.85E+02	1.52E+06
I-129	1.21E+06	1.33E+08	1.34E+08	Lithium	4.47E+01	5.89E+03	5.94E+03
Cs-137 ⁽²⁾	1.32E+13	9.37E+13	1.07E+14	Manganese	8.32E+05	1.71E+04	8.49E+05
Ir-192m	0.00E+00	1.14E+10	1.14E+10	Mercury	6.83E+01	3.73E-01	6.87E+01
Pt-193	0.00E+00	1.15E+13	1.15E+13	Molybdenum	2.15E+02	9.78E+02	1.19E+03
Pb-210	3.20E+10	0.00E+00	3.20E+10	Nickel	1.63E+06	4.92E+04	1.68E+06
Ra-226	3.80E+09	0.00E+00	3.80E+09	Niobium	1.02E+02	1.10E+04	1.11E+04
U-232	2.25E+08	7.71E+06	2.33E+08	Scandium	2.29E+01	6.16E-01	2.35E+01
U-233	3.07E+08	8.88E+06	3.15E+08	Selenium	8.14E+01	5.06E+00	8.64E+01
U-234	1.34E+09	1.30E+08	1.47E+09	Silver	5.13E+00	2.13E+00	7.26E+00
U-235	2.16E+07	2.08E+06	2.36E+07	Strontium	3.24E+03	3.35E+01	3.27E+03
U-236	2.56E+08	2.38E+07	2.80E+08	Tellurium	2.03E+02	6.63E-02	2.03E+02
U-238	5.91E+09	1.60E+08	6.07E+09	Thallium	2.41E-01	3.04E-01	5.45E-01
Np-237	1.23E+08	1.07E+07	1.34E+08	Tin	1.37E+02	2.37E+03	2.51E+03
Pu-238	4.69E+11	2.77E+10 ⁽³⁾	4.96E+11 ⁽³⁾	Tungsten	1.18E+00	1.48E+02	1.49E+02
Pu-239	8.32E+11	8.51E+10	9.18E+11	Uranium	3.34E+02	2.49E+01	3.59E+02
Pu-240	1.23E+12	1.24E+11	1.35E+12	Vanadium	8.97E+01	9.56E+02	1.05E+03
Pu-241	6.75E+10 ⁽³⁾	1.76E+12	1.83E+12 ⁽³⁾	Zinc	1.47E+05	2.06E+03	1.49E+05
Pu-242	1.23E+09	1.26E+08	1.36E+09	Zirconium	7.42E+02	5.95E+05	5.96E+05
Am-241	2.16E+12	2.30E+11	2.39E+12	PAHs	3.43E+00	0.00E+00	3.43E+00
Am-242m	2.35E+09	2.39E+07	2.37E+09	Cl-Benzenes & Cl-Phenols	2.76E+00	0.00E+00	2.76E+00
Am-243	2.67E+09	4.31E+08	3.10E+09	Dioxins & Furans	9.25E-02	0.00E+00	9.25E-02
Cm-243	2.70E+09	5.30E+08	3.23E+09				
Cm-244	1.93E+11	1.25E+11	3.18E+11				
Total	8.83E+14 ⁽³⁾	1.53E+16	1.62E+16	PCBs	1.31E-01	0.00E+00	1.31E-01

Notes:

1. Radioactive progeny are not listed in the table but are included in the safety assessment calculations.
2. Sr-90 and Cs-137 activities are total including their respective progeny.
3. Values are from draft version of the Reference L&ILW Inventory Report at the time of the data freeze for the safety assessment (summer 2010). Values from final version of Reference L&ILW Inventory Report (OPG 2010) are:
Pu-238 - 3.23E+10 Bq (ILW) and 5.01E+11 Bq (total).
Pu-241 - 2.87E+12 Bq (LLW) and 4.63E+12 Bq (total).
LLW Total - 8.86E+14 Bq.

Concentrations of contaminants are subject to a degree of uncertainty, as they are based on waste-type-specific sampling and scaling factors, rather than direct measurement of each waste package. This approach is routinely used by other waste management organizations (IAEA 2009). The uncertainties associated with the inventories are described in the Reference L&ILW Inventory Report (OPG 2010). Often, the inventories have large variability between packages. However, the total repository inventory is much less uncertain, because it is summed over a large number of packages.

Table 2.7 summarizes the amount of organics, metals and concrete in the wastes and their containers and overpacks, derived from data presented in the Reference L&ILW Inventory Report (OPG 2010).

Table 2.7: Amounts of Organics, Metals and Concrete in Wastes and their Containers and Overpacks

Material		Amount (kg)			
		LLW		ILW	
		Wastes	Containers and Overpacks	Wastes	Containers and Overpacks ⁽¹⁾
Organics	Cellulose	8.2E+06	-	-	-
	Rubber and Plastics	8.2E+06	2.1E+05	-	-
	Resins	1.5E+06	-	4.2E+06	-
Metals	Carbon steel	4.1E+06	3.4E+07	9.1E+05	2.4E+06
	Stainless steel	5.3E+06	2.8E+06	2.4E+06	9.8E+06
	Zircaloy	-	-	6.0E+05	-
Concrete		1.1E+06	3.5E+06	-	5.7E+07

Note:

1. Values taken from a draft version of the Reference L&ILW Inventory Report at the time of data freeze for the safety assessment calculations (summer 2010). Values in final version of this report (OPG 2010) are 2.1E+06 kg (carbon steel), 1.0E+07 kg (stainless steel) and 6.3E+07 kg (concrete).

2.2 Repository

The final preliminary repository design is shown in Figure 2.1 and described in the Chapter 6 of the PSR (OPG 2011b). However, the postclosure safety assessment was initiated based on an original preliminary design shown in Figure 2.2 (NWMO 2010a). The change from the original to the final preliminary design was made after the present assessment was largely complete.

The design is likely to evolve further prior to the construction of the DGR, as the detailed design is prepared. Since the primary barrier is the geosphere and since long-term safety is a design requirement, it is expected that any changes would not substantively affect the postclosure safety conclusions. Key design points relevant to postclosure safety are described below. Changes from the original to final version of the preliminary design are noted where applicable.

2.2.1 Layout and Construction

2.2.1.1 General

The depth of the repository floor is around 680 m below ground surface in competent and tight limestone (the Cobourg Formation), which lies within the 400 m thick sequence of Ordovician rocks.

The repository comprises two shafts, a shaft and services area, two access tunnels, 31 waste emplacement rooms (14 rooms in the Panel 1 and 17 rooms in the Panel 2), and, in the case of final preliminary design, ventilation drifts (Figure 2.1 and Figure 2.3). The waste emplacement rooms will be oriented in the direction of major principal horizontal stress, so as to maximize stability.

2.2.1.2 Shafts

Access to the repository will be by shaft. A main shaft will be used to transfer waste packages from receipt facilities on the surface to the repository and to supply conditioned air to the repository. A ventilation shaft will be provided to allow routing of air away from underground operations. The main and ventilation shafts will have 6.5 m and 5 m finished inside diameters, respectively.

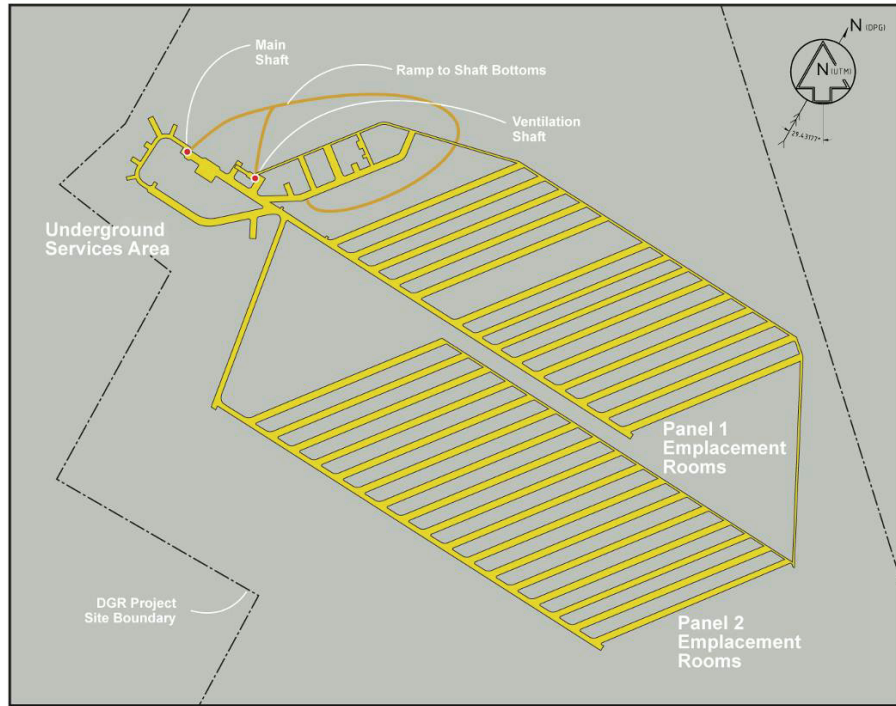
The shafts will be excavated from the ground surface down to about 720 m for the main shaft and 745 m for the ventilation shaft using controlled drill and blast techniques.

The shafts will be concrete-lined to limit potential water inflow during construction and operation. It is anticipated that there will be very little water inflow to the repository and that any inflow will be collected and pumped from the repository.

2.2.1.3 Shaft and Services Area

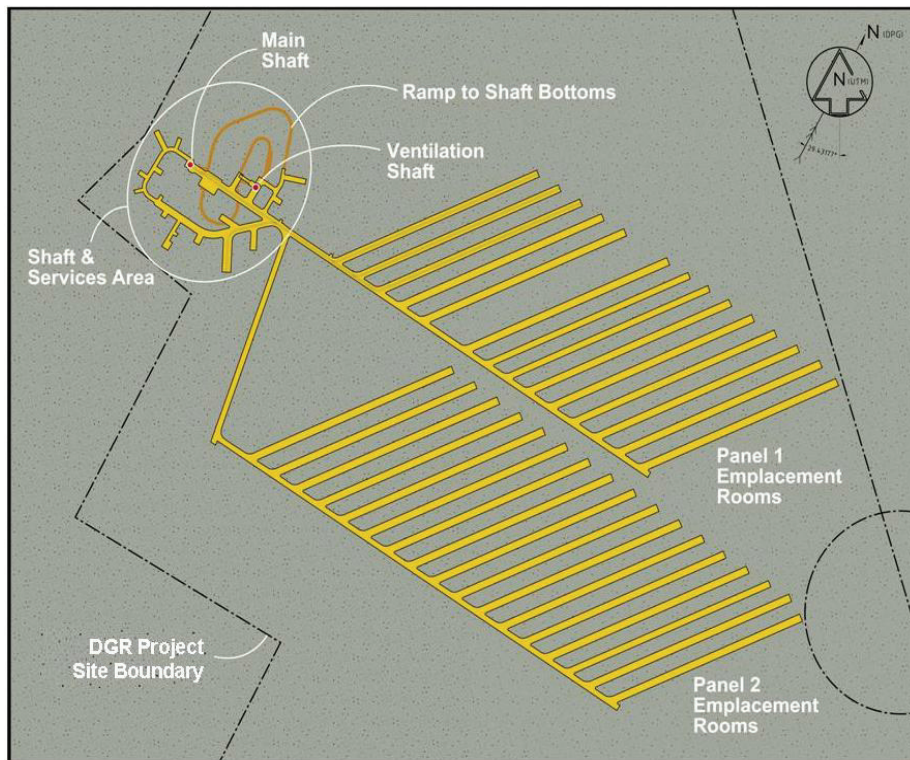
The underground layout of the repository has two vertical shafts (the main and ventilation shafts) as an islanded arrangement with a shaft and services area. A main access tunnel extends from the main shaft to the east, passing the ventilation shaft and then proceeding towards the two panels of waste emplacement room panels, as shown in Figure 2.4. Underground support facilities (offices, workshops, refuge bays, maintenance areas, etc.) will be located in the shaft and services area.

It is expected that the shaft and services area (together with the access tunnels and emplacement rooms) will be excavated using controlled drill and blast, although the use of roadheaders is being considered as an alternative. They will have concrete floors (typically 0.2 m thick), with shotcrete on the ceilings and extending down the walls, and rockbolts placed as needed in the ceiling to provide roof support.



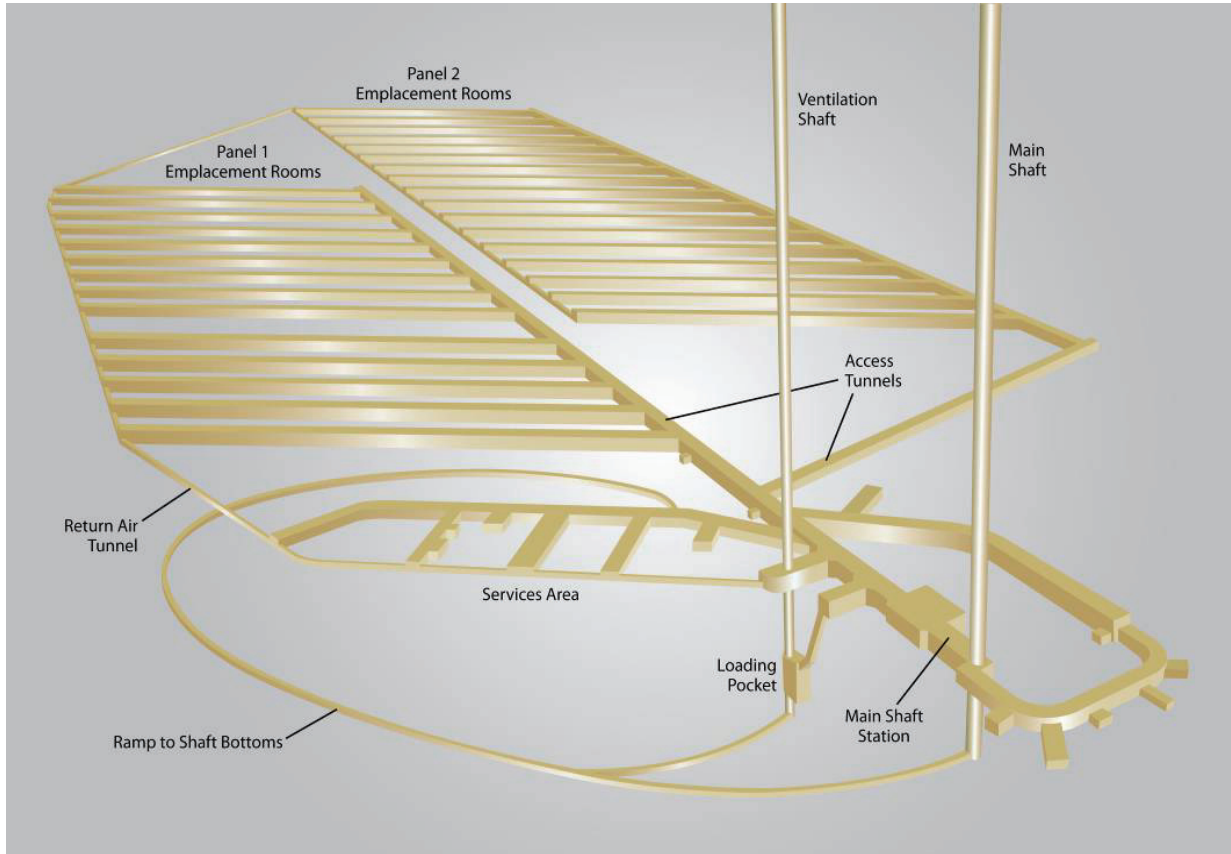
Note: Figure 6-7 in OPG (2011b).

Figure 2.1: General Layout of the Final Preliminary Design Repository



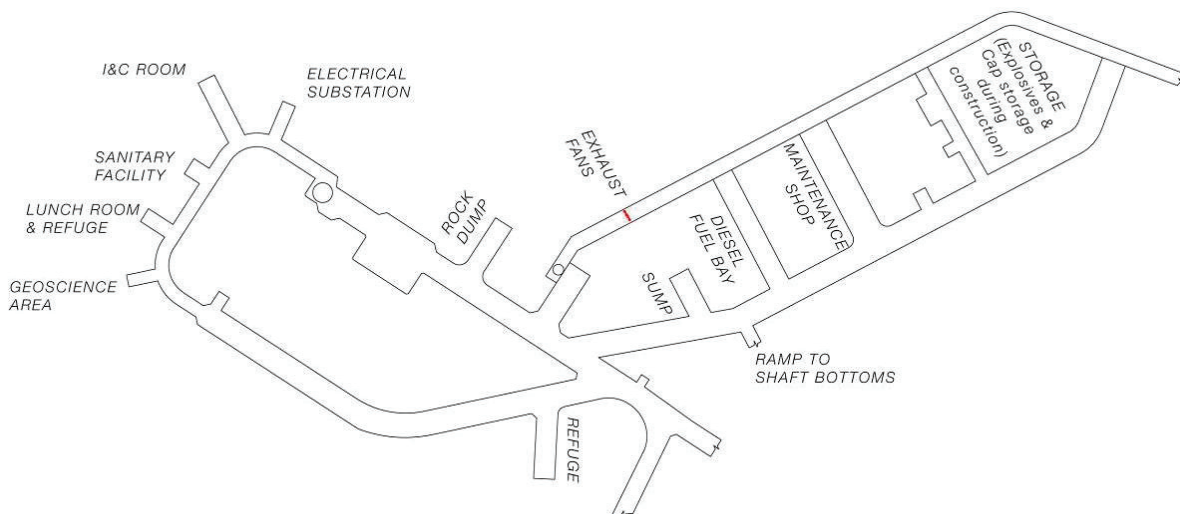
Note: Figure from NWMO (2010a).

Figure 2.2: General Layout of the Original Preliminary Design Repository



Note: Figure 6-6 in OPG (2011b).

Figure 2.3: Isometric View of the Final Preliminary Design Repository



Note: Figure 6-14 in OPG (2011b).

Figure 2.4: Layout of the Shaft and Services Area for the Final Preliminary Design Repository

2.2.1.4 Access Tunnels and Emplacement Rooms

Access to the emplacement rooms in the Panels 1 and 2 will be via tunnels with a total length of approximately 500 m and 800 m respectively. A rail line will run the along the access tunnel into the first three emplacement rooms in Panel 1. The emplacement rooms will be divided into six size profiles (P1 to P6) of varying widths (7.4 to 8.6 m) and heights (5.8 to 7.2 m), but a constant length (250 m).

All access tunnels and emplacement rooms will be ventilated, with incoming flow through the bulk volume and return air flow back to the exhaust ventilation shaft via the ventilation return drifts.

2.2.2 Waste Emplacement

Waste packages destined for Panel 2 emplacement rooms will be moved using forklift trucks. Most of the waste packages destined for Panel 1 will be similarly moved, but some will be of sufficient size and weight to require movement on self-powered rail carts. A railway line will, therefore, run from the main shaft to the access tunnel for the first three emplacement rooms in Panel 1.

Panel 2 will be filled prior to Panel 1, over the first several years of the DGR's operation, with the wastes currently in storage at the WWMF. Then the nine rooms in Panel 1 that are furthest from the shaft and services area will be filled over about 15 years. Finally, the five rooms closest to the shaft and services area will be filled. The allocation of wastes in the emplacement rooms is summarized in Table 2.8.

Table 2.8: Number of Emplacement Rooms Occupied by Each Waste Category in the Repository Panels

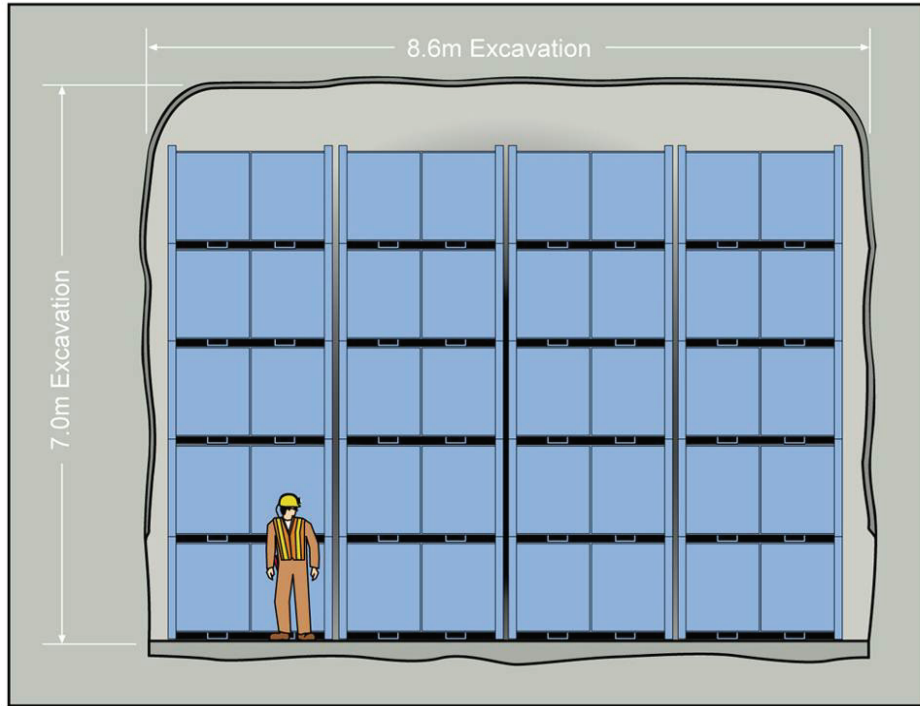
Waste Category	Panel 1		Panel 2 (Rooms 1 – 17)
	Rooms 1 – 5	Rooms 6 – 14	
LLW Non-Processible (other)	1	-	-
LLW Steam generators	-	1	1 ⁽¹⁾
All other LLW categories	1	3	13
All ILW categories	3	5	4

Note:

1. Emplaced in same room as ILW.

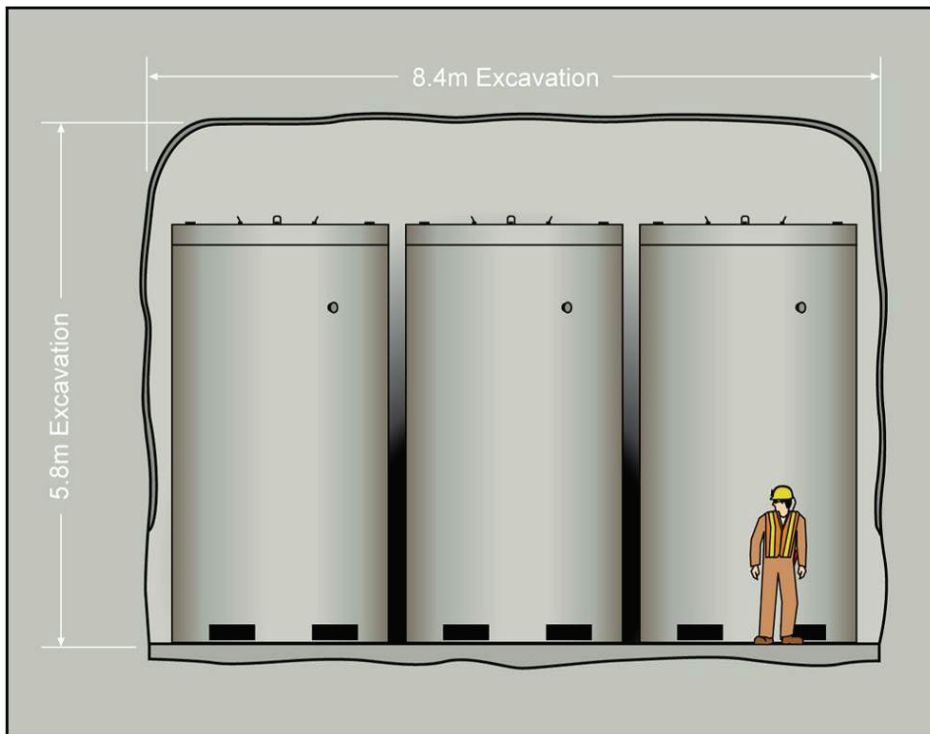
Six sizes of emplacement room with different profile types denoted as P1 – P6 are envisaged, with each type being used for the placement of particular types of waste package. These large items require in-room handling using a gantry crane, and rail lines to support it will run the whole length of the rooms concerned. Forklift trucks will be used to emplace the other types of waste package.

Potential stacking layouts for two of the emplacement room profiles are illustrated in Figure 2.5 and Figure 2.6 (Chapter 6 of OPG 2011b).



Note: Figure 6-17 in OPG (2011b).

Figure 2.5: Emplacement Room Section View – P1 Profile for Bin Type Waste Packages



Note: Figure 6-18 in OPG (2011b).

Figure 2.6: Emplacement Room Section View – P3 Profile for Resin Liner Type Waste Packages

2.2.3 Closure

2.2.3.1 Emplacement Rooms

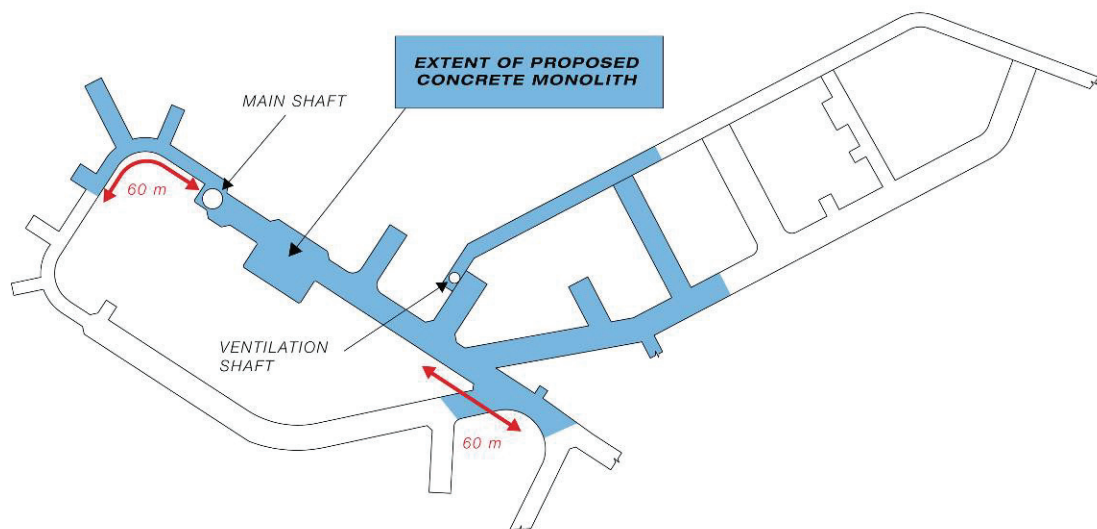
Once an emplacement room has been filled with waste, a wall may be constructed at the end of the room using reinforced concrete blocks. The wall will likely extend above the waste package height within the room, but not to the roof. The emplacement rooms will not be backfilled. For the final preliminary design, ventilation air will continue to flow through the wall opening, across the emplacement room, and out a similar opening at the back end of the room and into the ventilation drift.

2.2.3.2 Access Tunnels

The access tunnels will not be backfilled, but after a group of emplacement rooms has been filled with waste packages, concrete closure walls (around 20 m thick) will be constructed in the access tunnel and ventilation drift to isolate this group of rooms (Section 6.13 of OPG 2011b). It is expected that there may be six closure walls in place at the end of repository operations in the final preliminary design. The rail lines will remain in the tunnels.

2.2.3.3 Shaft and Services Area

Any equipment that has been used within the shaft and services area will remain in the area and all infrastructure connections (power, ventilation and water) to the panels will be disconnected. Any vehicle fuels will be removed to the surface. In addition, the steel work and shaft concrete liner removed during the closure of the ventilation shaft will be placed in the area. The concrete monoliths created at the base of each shaft (Section 2.2.3.4) will extend into the repository tunnels to form a single monolith at the repository level (Figure 2.7).



Note: Figure 13-1 in OPG (2011b).

Figure 2.7: Location of Monolith in Repository Tunnels for the Final Preliminary Design

The total amount of concrete and steel associated with the emplacement rooms (including end walls but excluding the wastes and their packaging), the access tunnels (including closure walls), and shaft and services area (including equipment, material removed from the ventilation shaft, and the monoliths in the shafts and repository) has been estimated in Chapter 4 of the Data report (QUINTESSA and GEOFIRMA 2011) to be around 140,000 tonnes of concrete and 3,300 tonnes of steel for the final preliminary design.

2.2.3.4 Shafts

Decommissioning of the shafts will consist of: the removal of shaft infrastructure; the removal of the concrete shaft liner and highly damaged zone (HDZ)² from the repository horizon up to about 180 m below ground surface (mBGS); and the installation of a shaft seal comprised of a sequence of sealing materials. The ventilation shaft will be decommissioned and its seal installed before the same operation is carried out on the main shaft.

The reference shaft seal design is illustrated in Figure 2.8, described in Section 4.3.2 of the Data report (QUINTESSA and GEOFIRMA 2011) and summarized below.

- A **concrete monolith** containing Low Heat High Performance Cement (LHHPC) will be placed at the base of each shaft to provide a stable foundation for the overlying seal materials and support to the repository openings in the vicinity of the shafts.
- **Concrete bulkheads** containing LHHPC will be placed in each shaft at specific points, to provide permeability control and structural support. One bulkhead will be located towards the top of the Silurian rock formations at the boundary between the saline lower rock formations and the upper freshwater formations. Two other bulkheads will be located around the two more permeable zones in the Silurian rock formations. Other bulkheads may be added for further structural support, or if needed to separate the bentonite/sand and asphalt seals.
- The shaft will be sealed with durable materials. A 70:30 **bentonite/sand** mix will be used for the majority of seals. An **asphalt mastic mix** will be used in one section to provide a different low-permeable material barrier that has the ability to creep and self-heal. The shaft in the upper formations will be filled with compacted **engineered fill** such as sand.
- A **concrete cap** will be constructed at the top of each shaft.

For the final preliminary design, the approximate total amount of materials used for shaft sealing has been estimated in Section 4.3.2 of the Data report (QUINTESSA and GEOFIRMA 2011) as: 56,000 tonnes of concrete for the concrete monolith; 41,000 tonnes of concrete for the concrete bulkheads; 13,000 tonnes of asphalt mastic mix; 66,000 tonnes of bentonite/sand for backfilling; and 17,000 tonnes of engineered fill for backfilling.

2.2.3.5 Other Excavations

The preliminary design for the DGR includes excavations below repository level for rock handling and ramp access to the shaft bottoms (Figure 2.3). These excavations will be backfilled with LHHPC at closure and there will be no removal of any associated HDZ or excavation damaged zone (EDZ).

² See Section 2.3.6.5 for description of the HDZ.

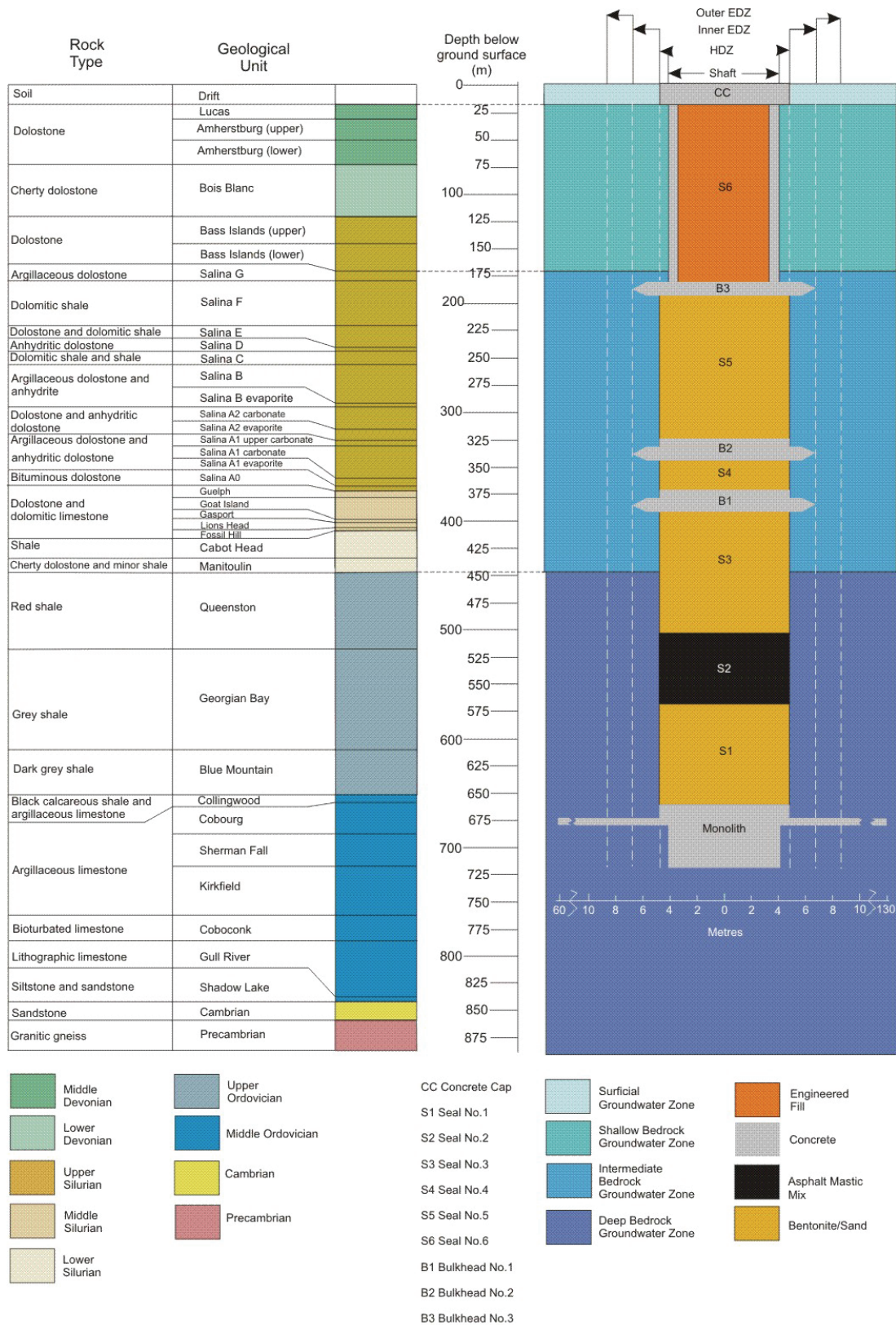


Figure 2.8: Illustration showing Sequence of Shaft Sealing Materials

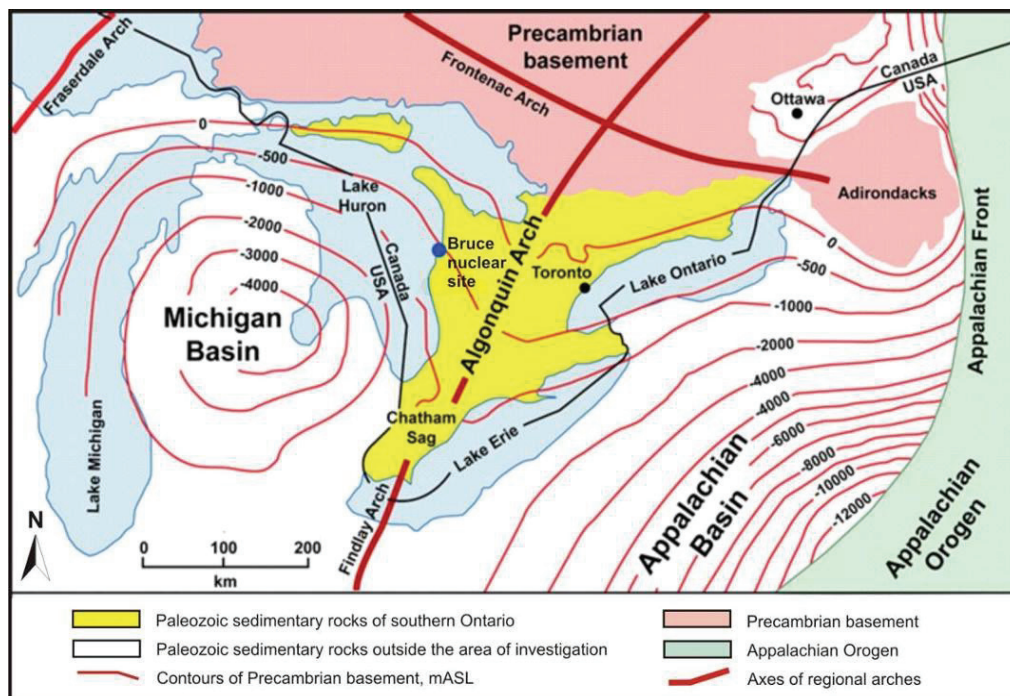
2.3 Geological Setting

The nature of the geosphere of the Bruce nuclear site and wider region is described in detail in the Geosynthesis report (NWMO 2011) and the Descriptive Geosphere Site Model (DGSM) (INTERA 2011). This section provides a summary of the geological setting to provide context for the analysis of the geosphere system evolution that underpins the safety assessment.

An overarching conclusion that can be drawn from the Geosynthesis report, and site data, is the favourable nature of the geosphere at the Bruce nuclear site for geological disposal: stable tectonic setting; laterally continuous simple predictable geology; large thickness of very low permeability rock; absence of potentially transmissive features such as faults; geochemical and hydrogeological evidence for very low rates of groundwater flow and hydraulic isolation at depth; diffusion-dominated solute transport at depth; and suitable mechanical properties for the successful development of stable excavations and sealing of access shafts.

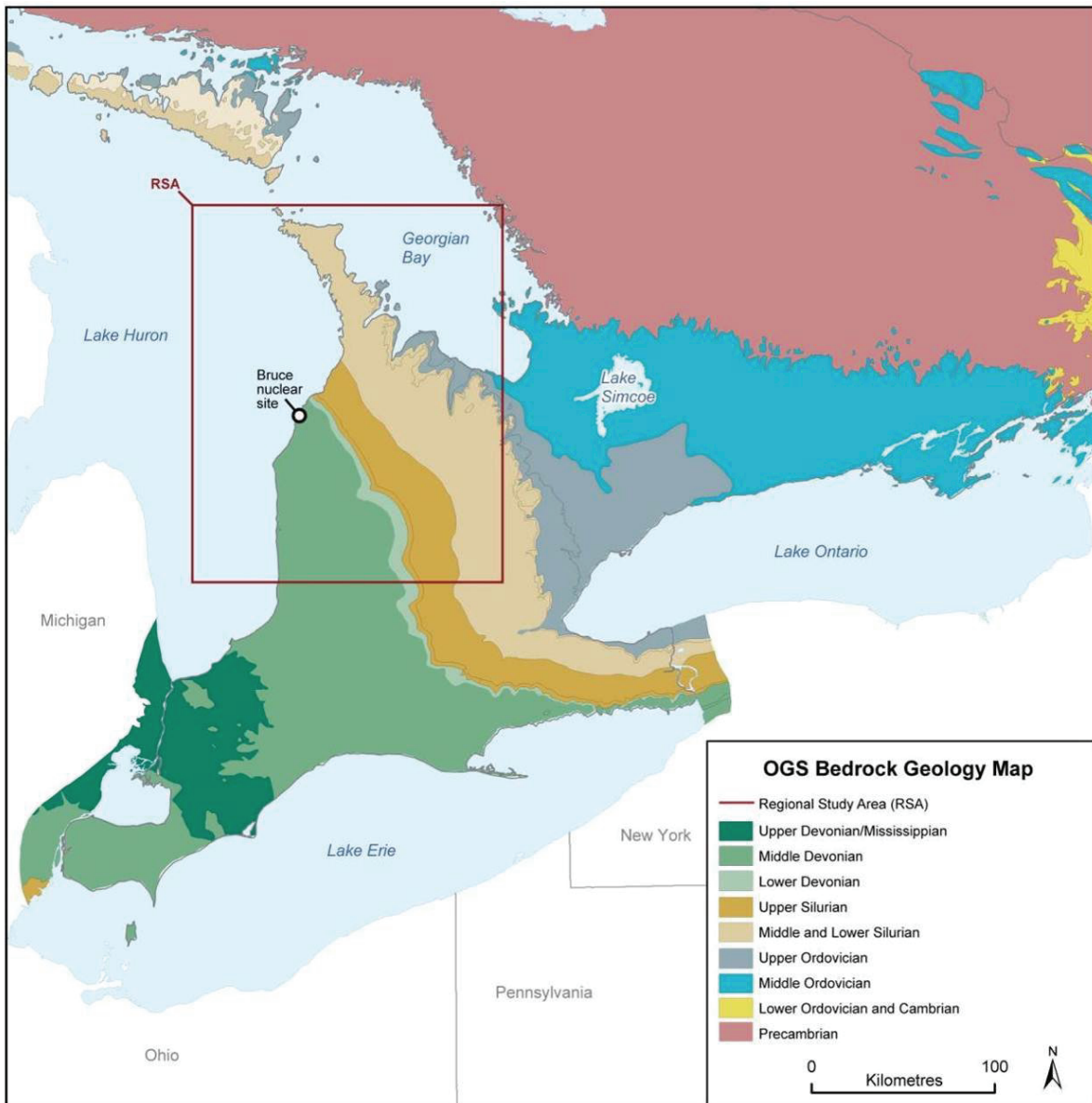
2.3.1 Geology

The proposed repository location is on the eastern edge of the Michigan Basin (Figure 2.9). The Michigan Basin is a broadly circular intracratonic basin, filled with over 4 km thickness of Paleozoic sedimentary rocks that dip gently towards the centre of the basin. The basement comprises Precambrian granitic gneiss. The Paleozoic sedimentary sequence comprises Cambrian sandstones overlain by Ordovician, Silurian and Devonian limestones, shales, dolostones and dolomitic limestones and evaporites. Figure 2.10 and Figure 2.11 show the bedrock geology for the region around the Bruce nuclear site in plan and cross-section, respectively. The cross-section also indicates the stratigraphic units encountered by the DGR-2 borehole beneath the site.



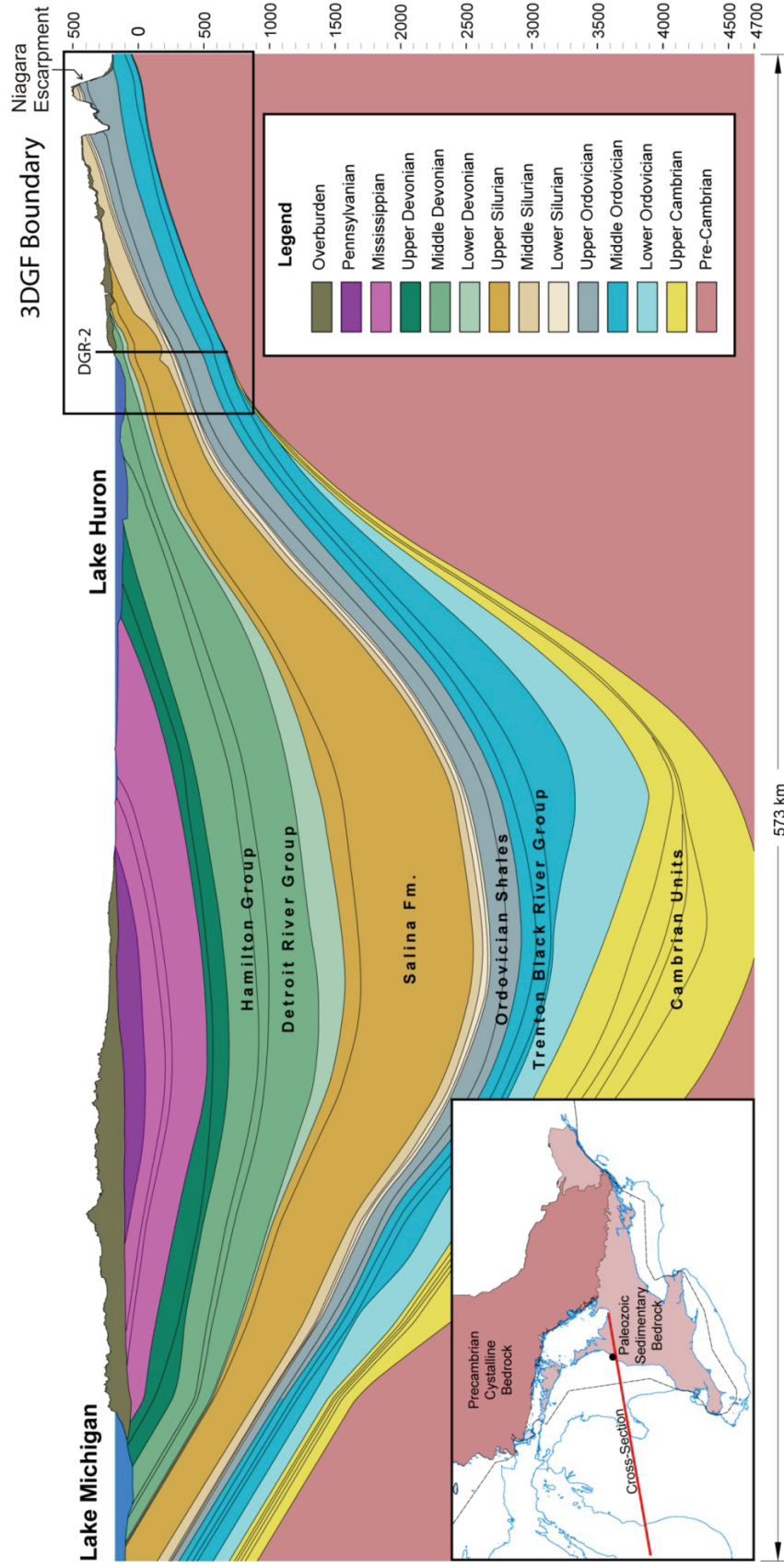
Note: Figure 2.2 in NWMO (2011).

Figure 2.9: Geologic Features of Southern Ontario



Note: Modified from Figure 2.3 in NWMO (2011). The boundary of the regional study area considered in NWMO 2011 is marked in red.

Figure 2.10: Geologic Map of Southern Ontario



Note: Figure 2.4 in NWMO (2011). Vertical axis is elevation measured in metres above sea level. Mesozoic rocks overlying the Pennsylvanian sediments are too thin and discontinuous to be shown on section. The DGR-2 borehole at the Bruce nuclear site and the boundary of the 3D Geological Framework (3DGF) model of NWMO 2011 are marked. Lower left inset indicates the line of the cross-section. Vertical exaggeration is approximately 45x.

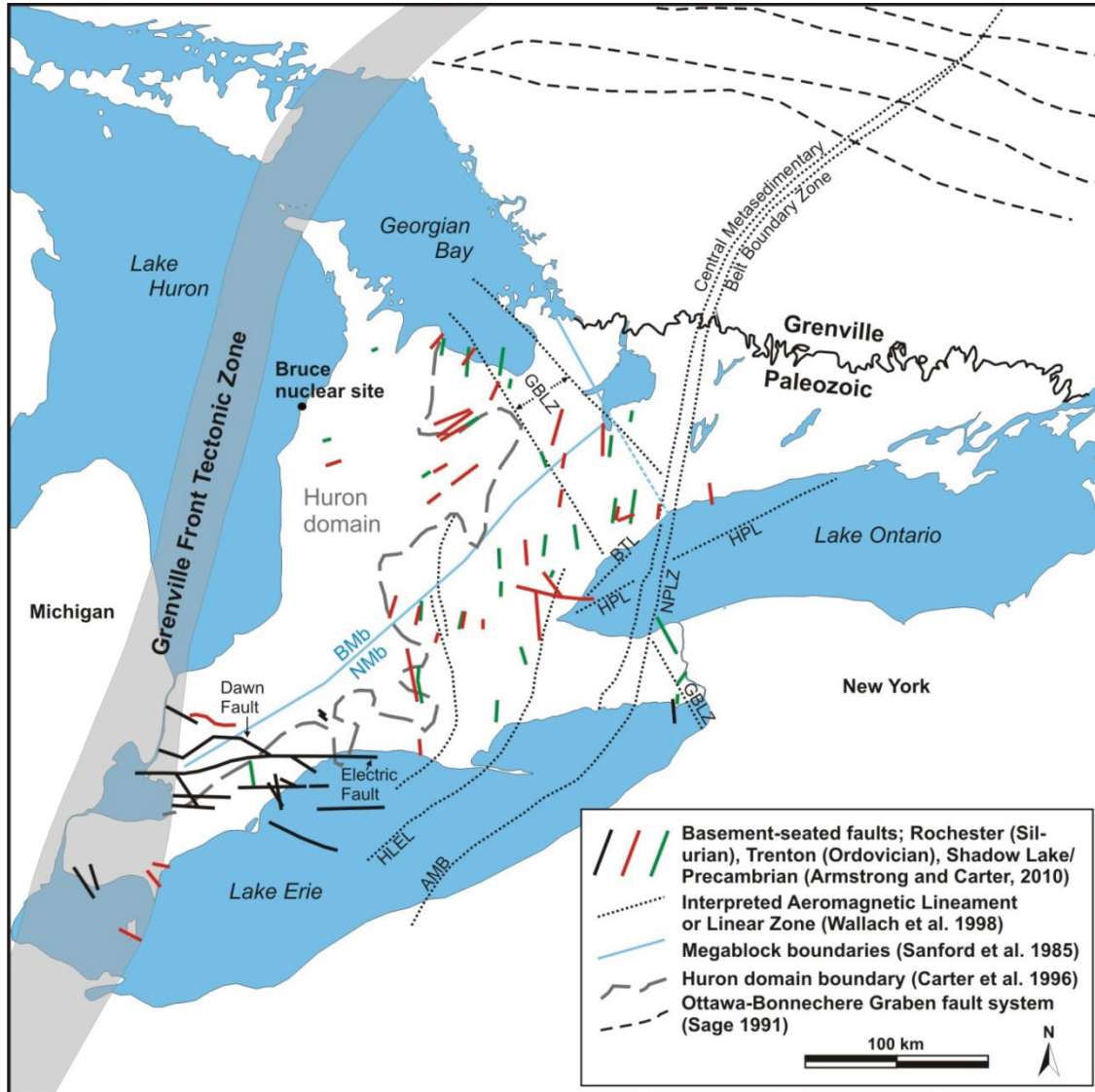
Figure 2.11: Cross-section across the Michigan Basin

NWMO (2011) collates the work of a number of authors, and summarizes the Paleozoic depositional history as follows. The Paleozoic succession was deposited northwestward of the Appalachian Orogen (Figure 2.9), a mountain chain that formed during the protracted closure of the Iapetus Ocean and assembly of the Pangaeon Supercontinent. Southwestern Ontario is underlain by two main paleo-depositional centres referred to as the Appalachian (Alleghenian) and Michigan Basins (Figure 2.9). The former is a foreland basin to the Appalachian orogen, whereas the latter is a broadly circular intracratonic basin.

These basins are separated by the northeast-trending Algonquin and Findlay arches which, along with the intervening east-southeast-trending Chatham Sag structural depression, define a regional basement high beneath southwestern Ontario. The Michigan Basin is also bounded, along its northwestern and northeastern flank respectively, by the Fraserdale and Frontenac arches. These arches acted as structural and topographic controls on depositional patterns during the Paleozoic Era, rising and falling with respect to the Michigan and Appalachian Basins in response to vertical epeirogenic (i.e., continental/sub-continental) movements, horizontal tectonic forces, and subduction at the orogenic front. The rocks forming the eastern side of the Michigan basin have been draped over the Algonquin arch. This structural control resulted in thinning, pinchouts, and erosional truncation of stratigraphic units as they approach and pass over the arch.

The Paleozoic sediments at the Bruce nuclear site unconformably overlie Precambrian basement of the Huron Domain. The Huron Domain is a subdivision within the Central Gneiss Belt of the Grenville tectonic province and is situated east of the Grenville Front Tectonic Zone. This, and other, basement features are delineated beneath the Paleozoic cover based on interpretation of aeromagnetic data, extrapolation of mapped contacts from exposed basement to the north, and by direct sampling of basement in deep boreholes where possible (Figure 2.12).

The Huron Domain basement and the overlying Paleozoic rocks are overprinted by sparse ENE to NE-trending faults of Paleozoic age reflecting the structurally simple nature of the region surrounding the Bruce nuclear site (Figure 2.12). Present and historical earthquake distribution data support the interpretation that the basement beneath the site is currently tectonically quiescent.



Note:
 AMB: Akron Magnetic Boundary; NPLZ: Niagara–Pickering Linear Zone; HLEL: Hamilton–Lake Erie Lineament; BTL: Burlington–Toronto Lineament; PL: Hamilton–Presqu’île Lineament; GBLZ: Georgian Bay Linear Zone; EF: Electric fault; DF: Dawn fault; BMb – Bruce Megablock; NMb – Niagara Megablock.
 Figure 2.5 from NWMO (2011) and references therein.

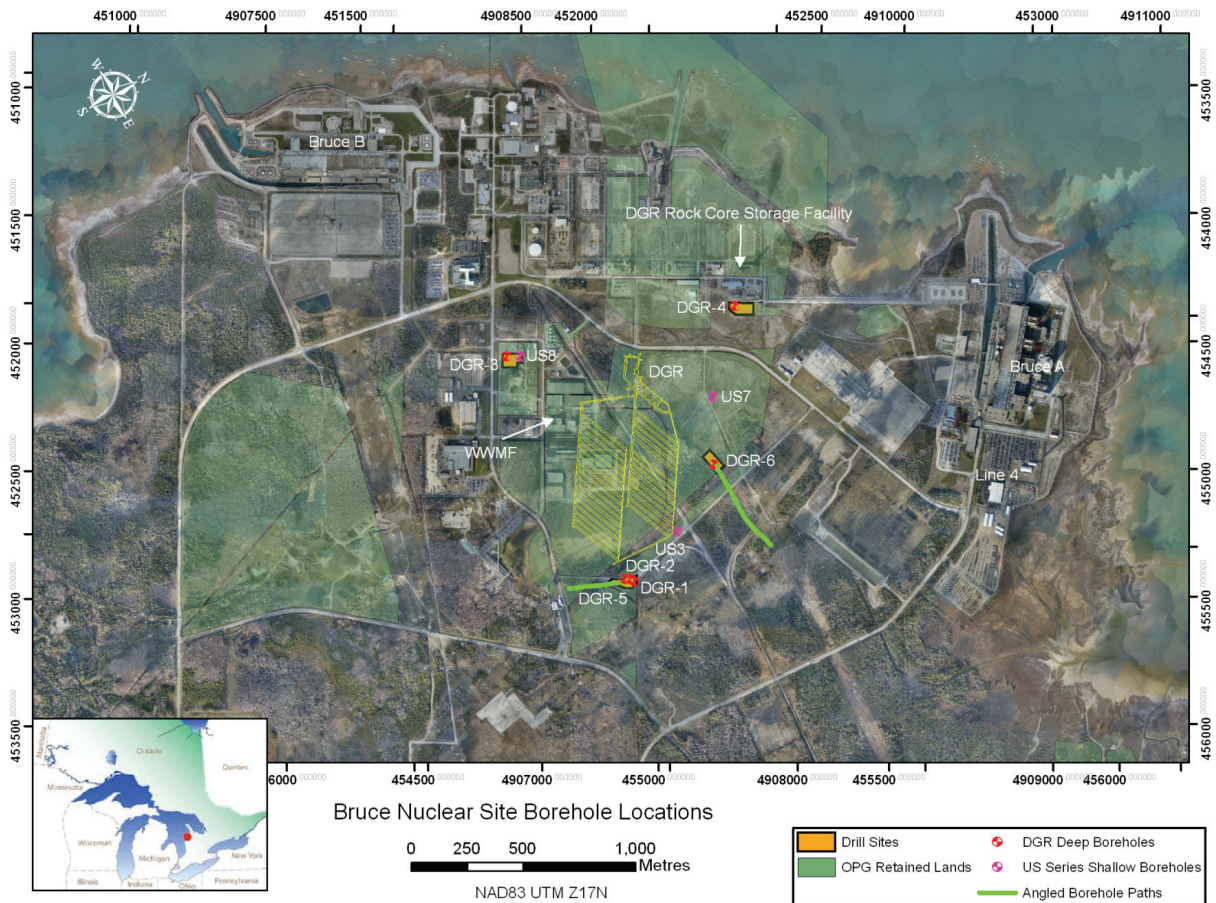
Figure 2.12: Tectonic Boundary and Fault Contacts in Southern Ontario

2.3.2 Stratigraphy

The Paleozoic bedrock sequence overlying Precambrian granitic basement has been measured to be approximately 845 m thick in the DGR site investigation boreholes (Figure 2.13). It comprises (from top to bottom) (Figure 2.14) approximately:

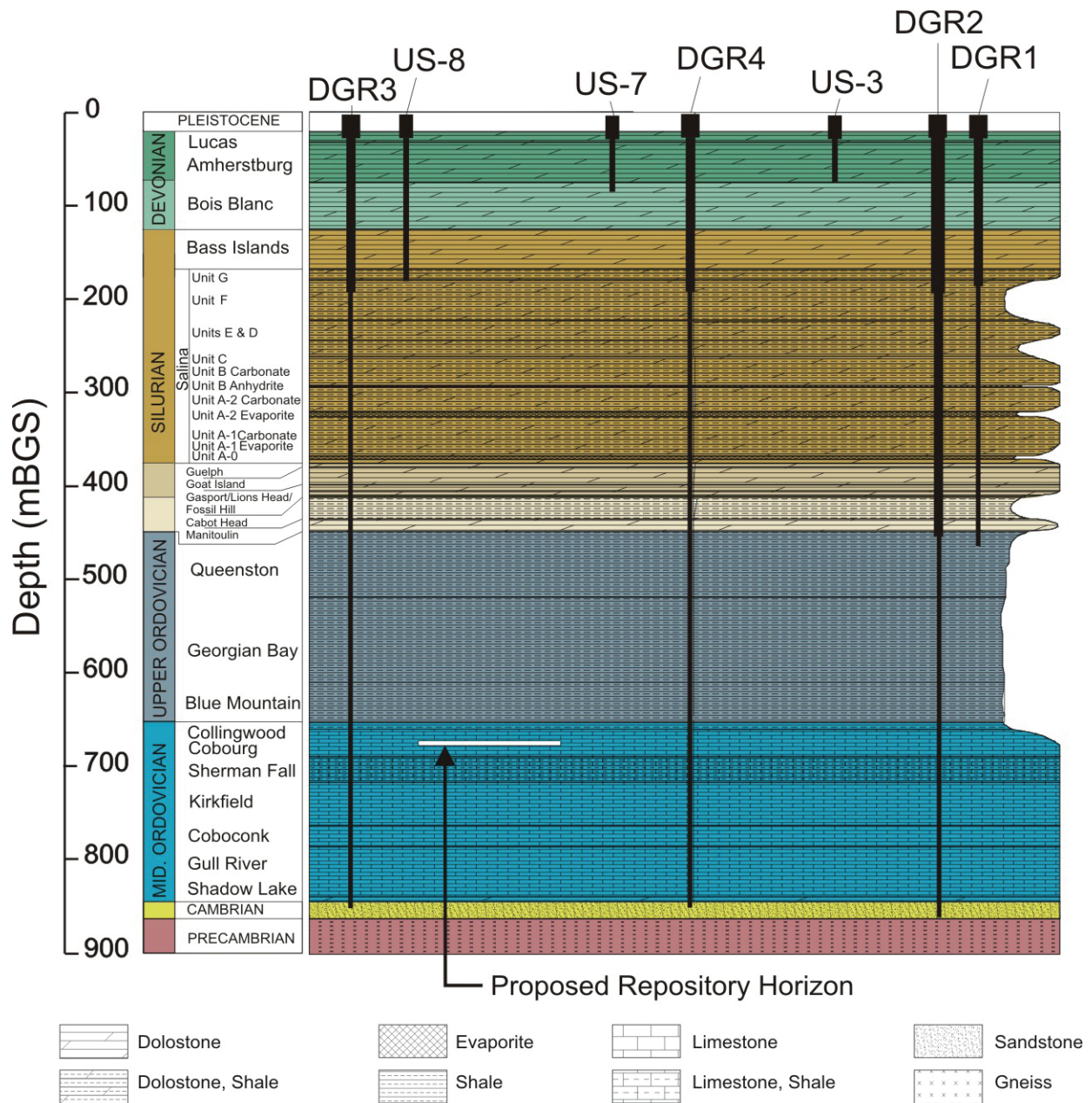
- 105 m of Devonian dolostones (dolomitic limestones);
- 325 m of Silurian dolostones and shales;
- 400 m of Ordovician shales and argillaceous to shaley limestone; and
- 15 m of Cambrian sandstone overlying Precambrian granitic gneiss.

Unconsolidated Pleistocene ('overburden') sediments overlie this bedrock sequence. The total thickness of this overburden varies from less than 1 m along the shore of Lake Huron to a maximum of about 20 m above the DGR site. The overburden typically comprises 1 to 3 m of surficial fill and sand and gravel interpreted as former beach deposits, overlying 5 to 21 m of Elma-Catfish Creek till, a clayey silt to sandy silt glacial deposit. The till is underlain by 0 to 2 m of basal gravel deposited at the weathered bedrock surface.



Note: Figure 1.2 in INTERA (2011). DGR-5 and DGR-6 are inclined boreholes.

Figure 2.13: DGR Boreholes and Pre-existing US Boreholes and the Proposed DGR Layout



Note: Figure 2.25 in NWMO (2011).

Figure 2.14: Geologic Stratigraphy at the DGR Site

2.3.3 Faults and Fractures

Figure 2.12 shows all faults known to displace the Proterozoic/Paleozoic unconformity in southern Ontario. Within southeastern Ontario, where there is an abundance of subsurface data available, these faults have been mapped with a high degree of confidence. Within the regional study area, where subsurface data are sparse, these features are inferred by subsurface

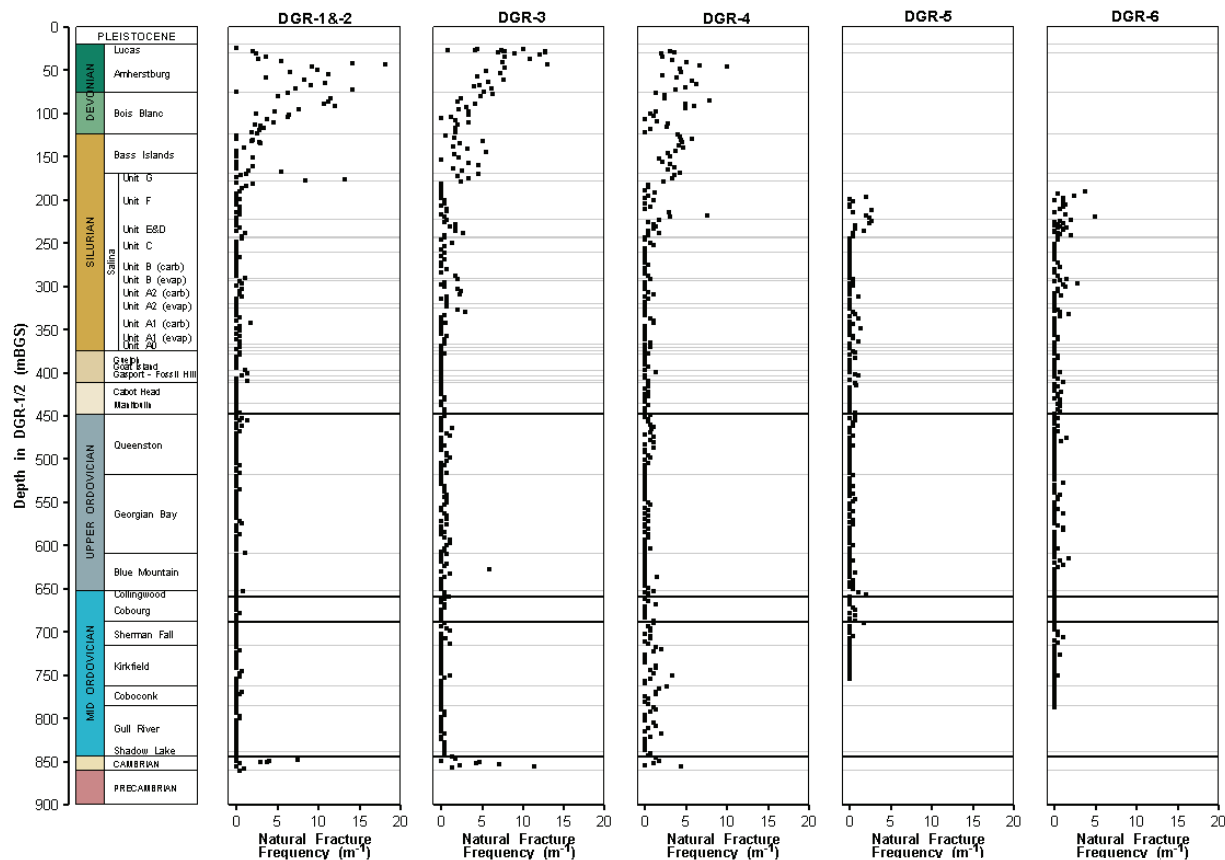
structure contouring and isopach mapping with limited well-control or through seismic interpretation. As a result, these faults are poorly constrained in terms of location and movement history and are generally mapped with a low degree of confidence. Based on the limited dataset, no mapped faults within the regional study area are interpreted to be younger than the limestones of the Ordovician Trenton Group (Cobourg, Sherman Fall and Kirkfield formations). This is consistent with the results of the site 2-D seismic survey which indicate that no faults have breached the Upper Ordovician shale. The closest interpreted fault structure is > 25 km away from the site (Sections 2.2.6.2 and 2.3.9 of NWMO 2011).

Investigations at the Bruce nuclear site have shown that the Paleozoic sediments are undeformed; dipping very gently (0.23° to 1.0°) to the southwest towards the basin depositional centre. A high degree of stratigraphic predictability and lateral facies consistency is observed between the DGR boreholes, and the DGR borehole stratigraphic data are consistent with expectations from interpolation of regional data to the site. This indicates that there is a lack of significant faulting in the vicinity of the DGR boreholes.

The 2-D seismic survey across the Bruce nuclear site identified several potential features interpreted to represent ancient and inactive basement-seated faults that extend upwards into the Upper Ordovician shales (Section 2.3.9.2 of NWMO 2011). However, the interpretation was uncertain due to data noise. Marker bed and other analyses, and two inclined DGR boreholes drilled to intersect the potential faults, have not found any evidence for the presence of faults near the DGR footprint. The most probably fault feature identified was located 1.25 km south of the DGR, and is interpreted as a Paleozoic aged fault that has been infilled. There is no evidence at the DGR for the hydrothermal dolomite-style features found in the Middle Ordovician oil and gas fields in southwestern Ontario (Section 2.2.8 of NWMO 2011).

Figure 2.15 shows the fracture frequency observed in cores from the DGR boreholes. The fracture frequency decreases with increasing depth, and is low below approximately 180 mBGS. This is to be expected because increasing overburden with increasing depth will: resist stress-relief fracturing due to the ENE orientated regional stress field; prevent fracturing due to changes in glacial loading (the percentage stress change is reduced with increasing depth); and tend to close fractures. Site data indicate that fractures are primarily shallow dipping at shallower depths, and steeper features dominate at greater depths. The majority of steeply inclined joints within the Ordovician rocks are in the shales, with a joint spacing of >1.5 m.

Hydraulic data from site investigation boreholes suggest there may be localized subhorizontal fracture zones in the Georgian Bay and Blue Mountain formations (Section 3.8 of INTERA 2011). Two-phase flow modelling (Section 5.4.9 of NWMO 2011) indicates that the data can be explained by the presence of hydraulically isolated sub-horizontal fractures that do not affect the barrier function of the geosphere. Furthermore, seismic data do not suggest that any potential fracture zones in these formations are connected by a continuous sub-horizontal feature (Section 2.3.9.2 of NWMO 2011).



Note: Figure 3.4 in INTERA (2011).

Figure 2.15: Profiles of Core Natural Fracture Frequency

2.3.4 Karst

The potential zone of karst development at the Bruce site is confined to the shallow Devonian and Upper Silurian carbonates to a depth of approximately 178 mBGS (Section 2.3.8 of NWMO 2011). Figure 2.16a shows core from the shallow Devonian carbonates. This interval is characterized by karst features such as solution-enhanced joints, stained/weathered fractures, and vuggy porosity. Groundwater in the shallow bedrock system may preferentially flow along paleokarst horizons such as those found at the top of the Bass Islands (Figure 2.16b), particularly where modern karstification has, for example, dissolved cement infilling.

Modern karst is not observed in core from the Intermediate Bedrock Groundwater Zone, nor is active karstification predicted. There is no evidence that freshwater has penetrated the Deep Bedrock Groundwater Zone during the Quaternary, and conditions for karst processes are not present.



Note: Figure 2.34 in NWMO (2011).

Figure 2.16: A) Core Photo from Shallow Devonian Lucas Formation Carbonates, Showing Karst Features and B) Remnant Paleokarst Horizon near the Top of the Bass Islands Formation

2.3.5 Geological Resources

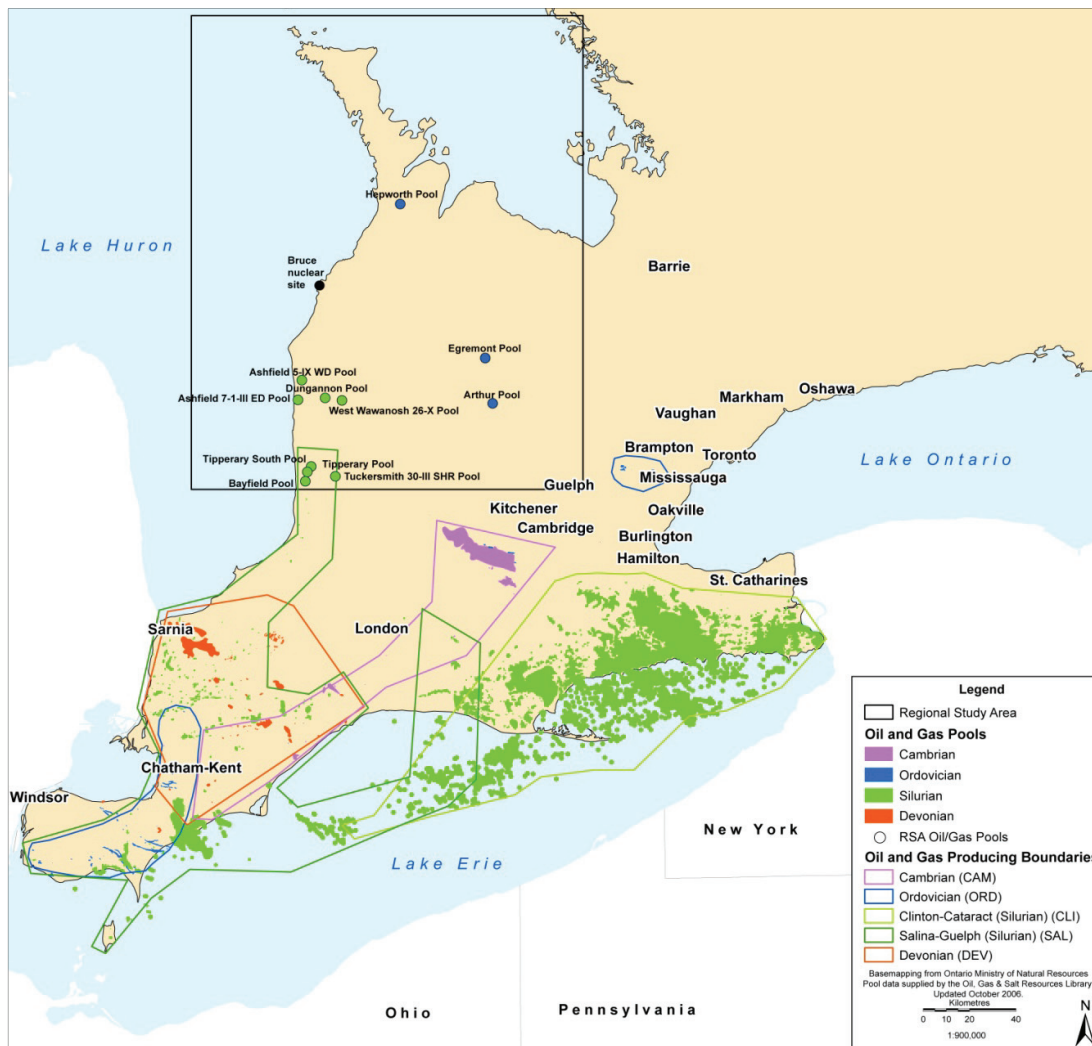
Exploration boreholes drilled throughout the regional study area have shown that there are only very localized minor oil and gas resources. The major oil and gas resources in Southern Ontario are located south of the regional study area (Figure 2.17). These findings have been confirmed by the DGR site investigation boreholes drilled at the Bruce nuclear site. These boreholes sample the Paleozoic sequence (oil and gas reserves are not found in the granitic basement), and although hydrocarbons have been detected, the quantities are small and are in discrete show zones that do not possess the permeability, source material or thermochronology to be considered commercially viable (INTERA 2011 and Section 2.2.8 of NWMO 2011).

No evidence of base minerals has been observed in the core retrieved from the DGR site investigation boreholes.

Although many of the Paleozoic rocks identified at the Bruce nuclear site are exploited elsewhere in Ontario for their aggregate potential, for landscaping rock, and for brick manufacture, generally for these industries to be economic the rock source must be close to the

surface. Most bedrock extraction operations are developed in areas where the overburden thickness is 3 m or less. Therefore, most of the rock aggregate is extracted in quarries along the Niagara Escarpment or areas of shallow overburden in Bruce County. DGR site-investigation boreholes encountered approximately 20 m of overburden at the Bruce nuclear site and so bedrock mining is not economic. Sand and gravel resources are present in the surficial deposits in the region and there is some extraction. Four disused quarries exist in the controlled development zone around the Bruce nuclear site. If shallow excavations were developed at the DGR site in the future, they would not affect the barrier performance of the geosphere.

There are only minor amounts of salt and evaporates at the Bruce nuclear site and these are not commercially viable: the formations are too thin and the salt/evaporate content is too low for brine extraction to be viable, or for the formations to be used for gas storage. Thicker and commercially viable deposits are present further to the south of the Bruce nuclear site, outside the area of interest to the postclosure safety assessment.



Note: Figure 2.20 in NWMO (2011).

Figure 2.17: Oil and Natural Gas Pools on Southern Ontario

2.3.6 Hydrogeology

2.3.6.1 Regional

A hydrogeological conceptual model has been developed for the regional study area to form the basis for regional-scale groundwater modelling centred on the Bruce nuclear site (see Chapter 5 of NWMO 2011, and references therein). Three groundwater domains are identified in this model: a shallow zone characterized by Devonian-aged formations which have a higher permeability and contain groundwaters with a relatively low Total Dissolved Solids (TDS) content; an intermediate zone which consists of Silurian formations, including low permeability shales and evaporite units in which the TDS content increases with depth; and a deep groundwater zone within the Ordovician shales and limestones, Cambrian sandstones (where present), and the Precambrian basement with a high TDS content. (Note that the Cambrian sandstones are discontinuous and pinch-out against the Precambrian basement). The surficial aquifer system represented by unconfined, semi-confined and confined aquifers present in the Quaternary glacial drift sediments is considered to be part of the shallow flow system in the regional model.

In general, modern recharge infiltrates topographic highs, such as glacial moraines and the Niagara Escarpment, and migrates through glacial drift and shallow bedrock aquifers, to ultimately discharge into topographic lows, such as streams and lakes. So the direction of groundwater flow in the shallow Devonian bedrock and glacial aquifers is gravity-driven and topographically controlled. The actual topographic variation across southern Ontario is low. Therefore, the low topographic gradients and high salinity of underlying basin formation waters prevent deep circulation of meteoric waters.

In the geological formations that form the intermediate and deep groundwater zones at the Bruce nuclear site, the only potential location for groundwater recharge or discharge is along the bands where these formations outcrop (Figure 2.10). Fresh water infiltrating into these zones is likely to have a major component of flow parallel to the formation outcrop boundaries because: i) the densities of the deeper waters in the bedrock are substantially higher than that of the infiltrating fresh water and they are, therefore, not easily displaced; ii) there is an absence of discharge areas in the basin, and therefore the hydraulic gradients are very low; and iii) the hydraulic conductivity rapidly decreases at the base of the shallow system.

2.3.6.2 Local

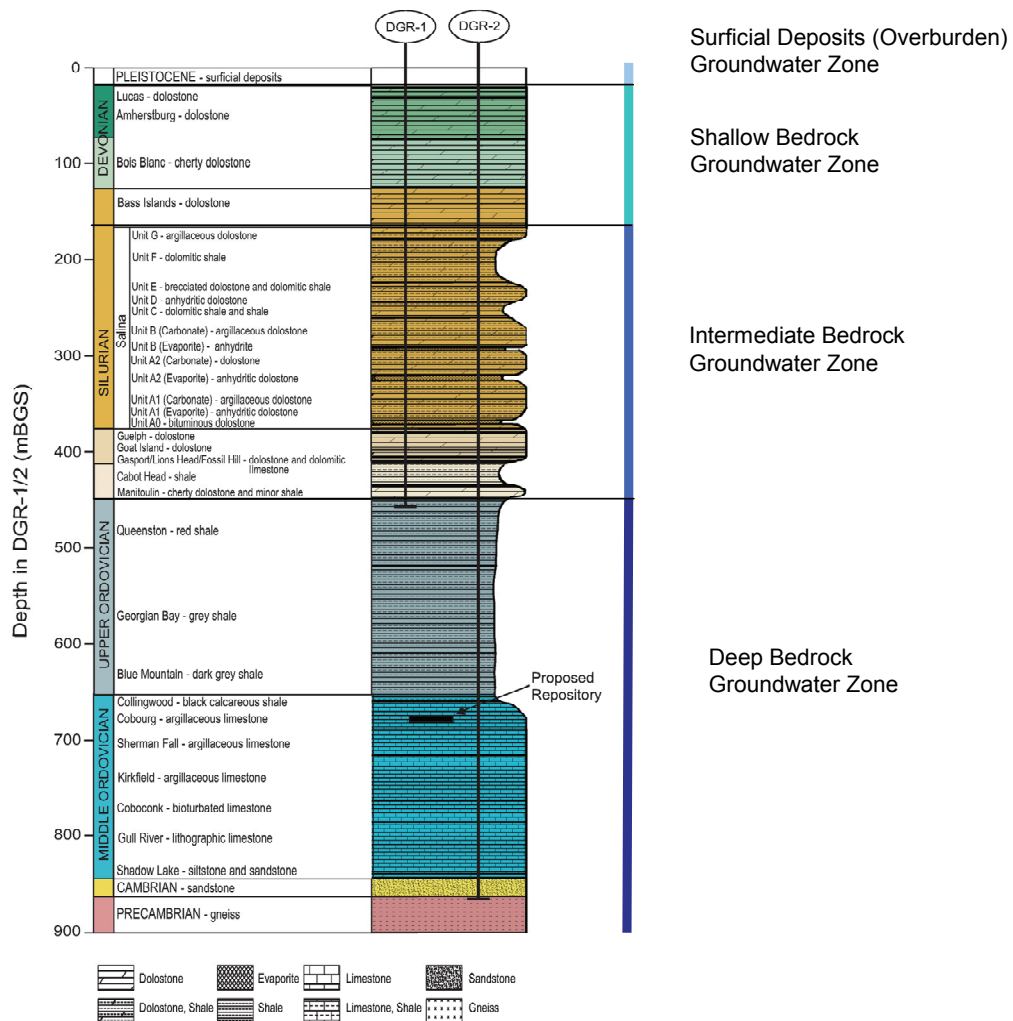
At the local or site-scale, the same groundwater zones are considered as in the regional model, except that the surficial groundwater zone is explicitly considered.

- **The Surficial Deposits (Overburden) Groundwater Zone** – the overburden sediments in which fresh water enters the groundwater system from precipitation through the recharge zone and flows vertically downwards into the underlying Shallow Bedrock Groundwater Zone. Layers of sand and gravel constitute local aquifers whereas the till layers are aquitards.
- **The Shallow Bedrock Groundwater Zone** – the Devonian and Upper Silurian dolostone sequence of the Lucas, Amherstburg, Bois Blanc and Bass Islands Formations. The direction of groundwater flow is westward to a point of near-shore discharge in Lake Huron.
- **The Intermediate Bedrock Groundwater Zone** – includes the dolostone and shale sequence of the Salina, Guelph, Goat Island, Gasport, Lions Head, Fossil Hill, Cabot Head and Manitoulin Formations. The formations are dominantly of low permeability, movement of

pore water is very slow and mass transport is considered to be diffusion dominated and due to the very low permeability. The Guelph and Salina A1 Upper carbonate are relatively more permeable, although flow is limited by the low hydraulic gradients. TDS generally increase with depth down through the zone.

- The Deep Bedrock Groundwater Zone** – is associated with the low permeability Ordovician shales and limestones and the underlying Cambrian sandstones and Precambrian granitic gneiss. Within the Ordovician sediments, movement of pore water is very slow and mass transport is considered to be diffusion dominated and due to the very low permeability. Although the Cambrian is relatively more permeable, flow is limited by the low hydraulic gradient. The proposed repository is to be located in the Deep Bedrock Groundwater Zone at a depth of around 680 m within the Cobourg Formation (argillaceous limestone).

These groundwater zones are illustrated in Figure 2.18. Figure 2.19 shows the hydraulic conductivity profile measured at the DGR site based on data from the in-situ straddle packer testing in the DGR site investigation boreholes.



Note: Adapted from Figure 3.2 in INTERA (2011).

Figure 2.18: Reference Stratigraphic Column Showing Groundwater Zones at the Bruce Nuclear Site

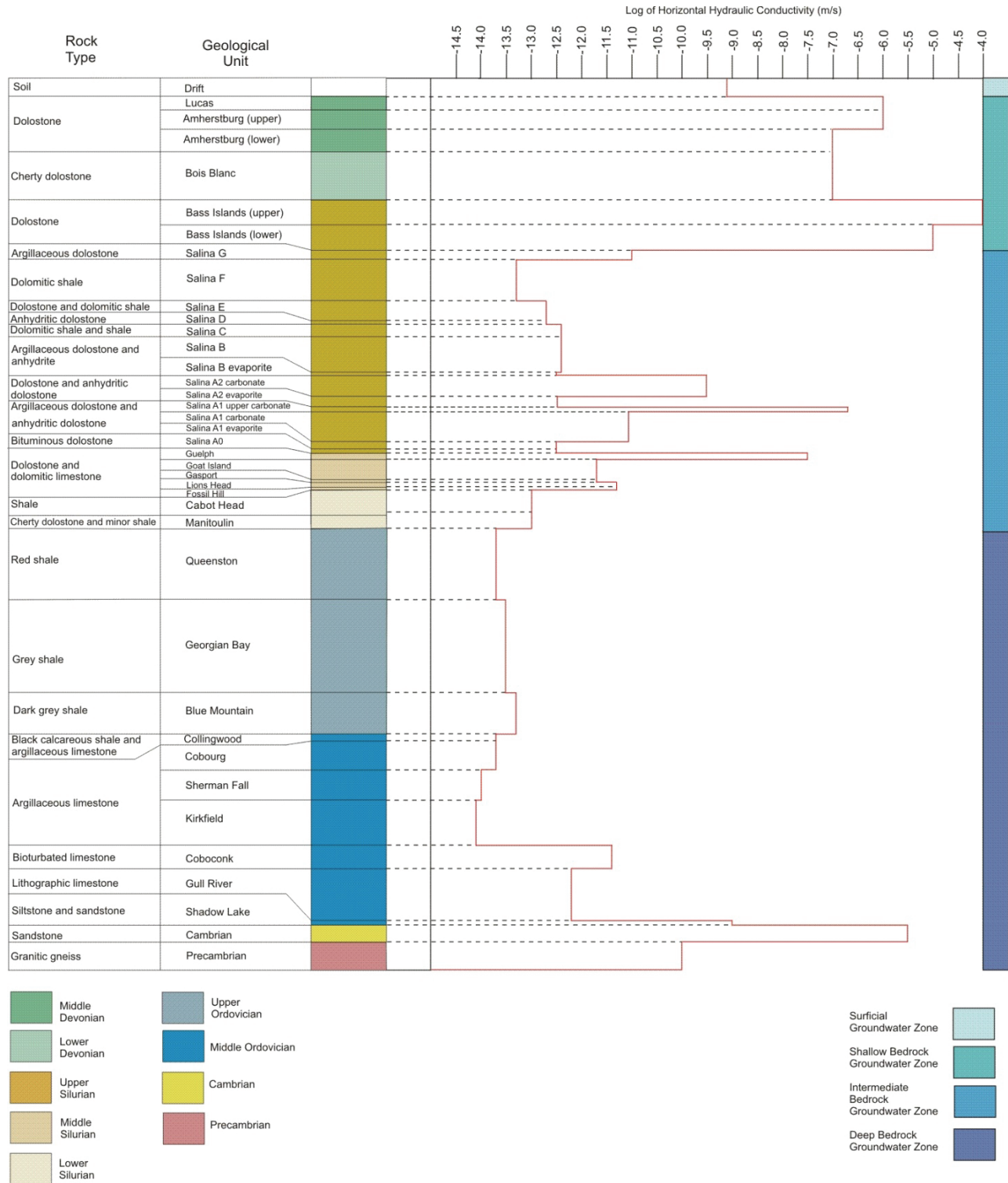


Figure 2.19: Hydraulic Conductivity Profile Based on Data from DGR Site Investigation Boreholes

The formations in the Shallow Bedrock Groundwater Zone have relatively high hydraulic conductivities compared with those in the deeper zones, resulting in topographically driven groundwater flow. Groundwater flow within the shallow zone is directed generally northwestward toward Lake Huron, generally subparallel to the well-established surface drainage pattern shown in Figure 2.20. The groundwater levels in the bedrock beneath the WWMF on the Bruce nuclear site occur between about 8 m to 10 m below ground surface. There is a slight upwards hydraulic gradient in the zone (Section 4.12.1 of INTERA 2011), and this gradient is greatest towards the base of the zone. As a result, freshwater heads towards the zone's base rise to levels above the bedrock surface, indicating artesian conditions.

The majority of the formations within the Intermediate and Deep Bedrock Groundwater Zones have very low hydraulic conductivities and, therefore, advective flows are negligible. Consequently any solute transport will be diffusion dominated. This is confirmed by water chemistry data as discussed in Section 2.3.7.

The only exceptions to this are within the Cambrian, Guelph, and Salina A1 Upper Carbonate formations.

The Cambrian formation is located below the repository and is associated with a high excess hydraulic head. The horizontal hydraulic gradient in the Cambrian is very low (Section 4.12.3 of INTERA 2011, Section 5.4.8.5 of NWMO 2011), and there is not expected to be any flow from the Cambrian to the biosphere. This is because the Cambrian formation pinches out against the Precambrian basement and is overlain by the low permeability Ordovician and younger rocks (Section 2.2.5.1 of NWMO 2011). Results from the regional groundwater flow model for the Michigan basin (Section 5.4.8 of NWMO 2011) indicate that this head is density driven. The heads are not evolving and will be stable for the timescales considered in the assessment.

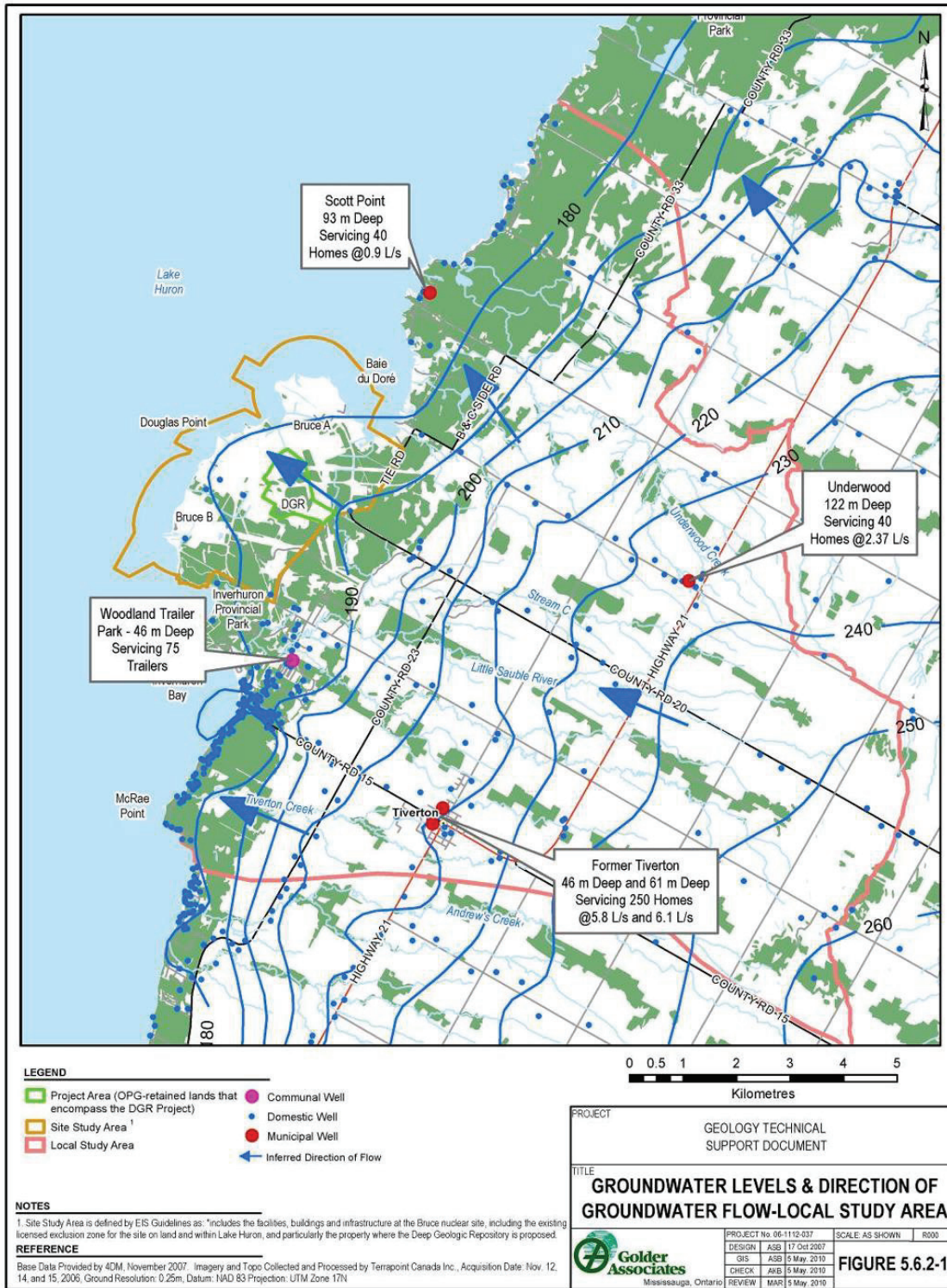
The Guelph and Salina A1 Upper Carbonate formations are located above the DGR. Even though they are of relatively high hydraulic conductivity, there is limited flow in these formations at the DGR site, because they lie between overlying and underlying, low permeability formations and the associated hydraulic gradients are low (Section 4.12.3 of INTERA 2011).

Table 2.9: Groundwater Flow Directions and Gradients in Deep Permeable Units

Parameter (Units)¹	Salina A1 Upper Carbonate	Guelph	Cambrian
Flow direction (Azimuth)	322°	78°	89°
Horizontal hydraulic gradient (-)	0.0077	0.0026	0.0031

Note: From Table 4.16 in INTERA (2011).

1. Based on freshwater heads.



Note: Figure 5.6.2-1 in GOLDER (2011d).

Figure 2.20: Groundwater Levels (mASL) and Direction of Shallow Groundwater Flow around the Bruce Nuclear Site

The hydraulic gradient in the Salina A1 Upper Carbonate formation is consistent with topographically driven strike-parallel flow, resulting in discharge to Lake Huron where the formation sub-crops to the northwest of the DGR (Figure 2.21). Due to subdued topography, the hydraulic gradient is low and the pathlength is long (tens of km) resulting in very long travel times.

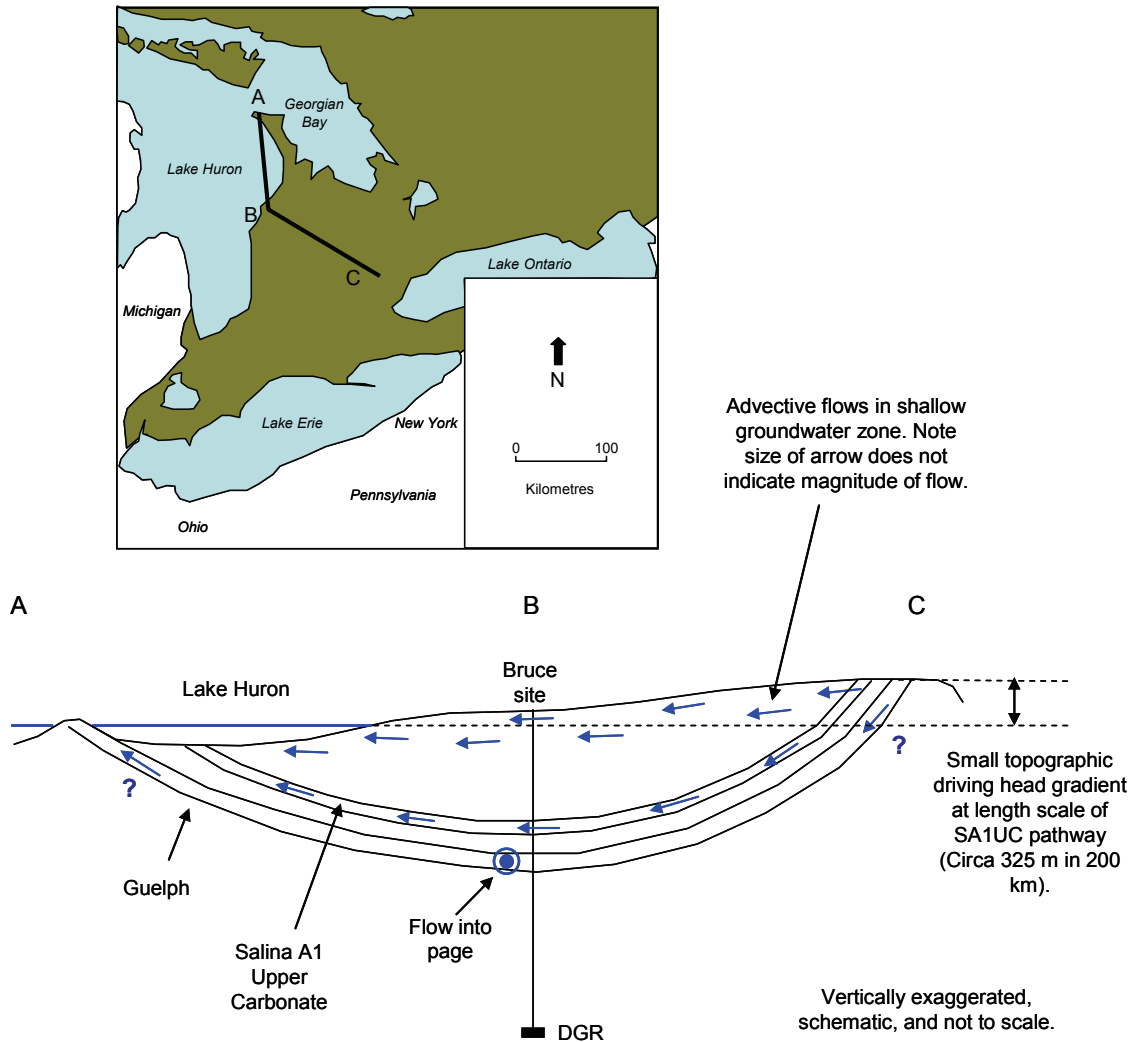
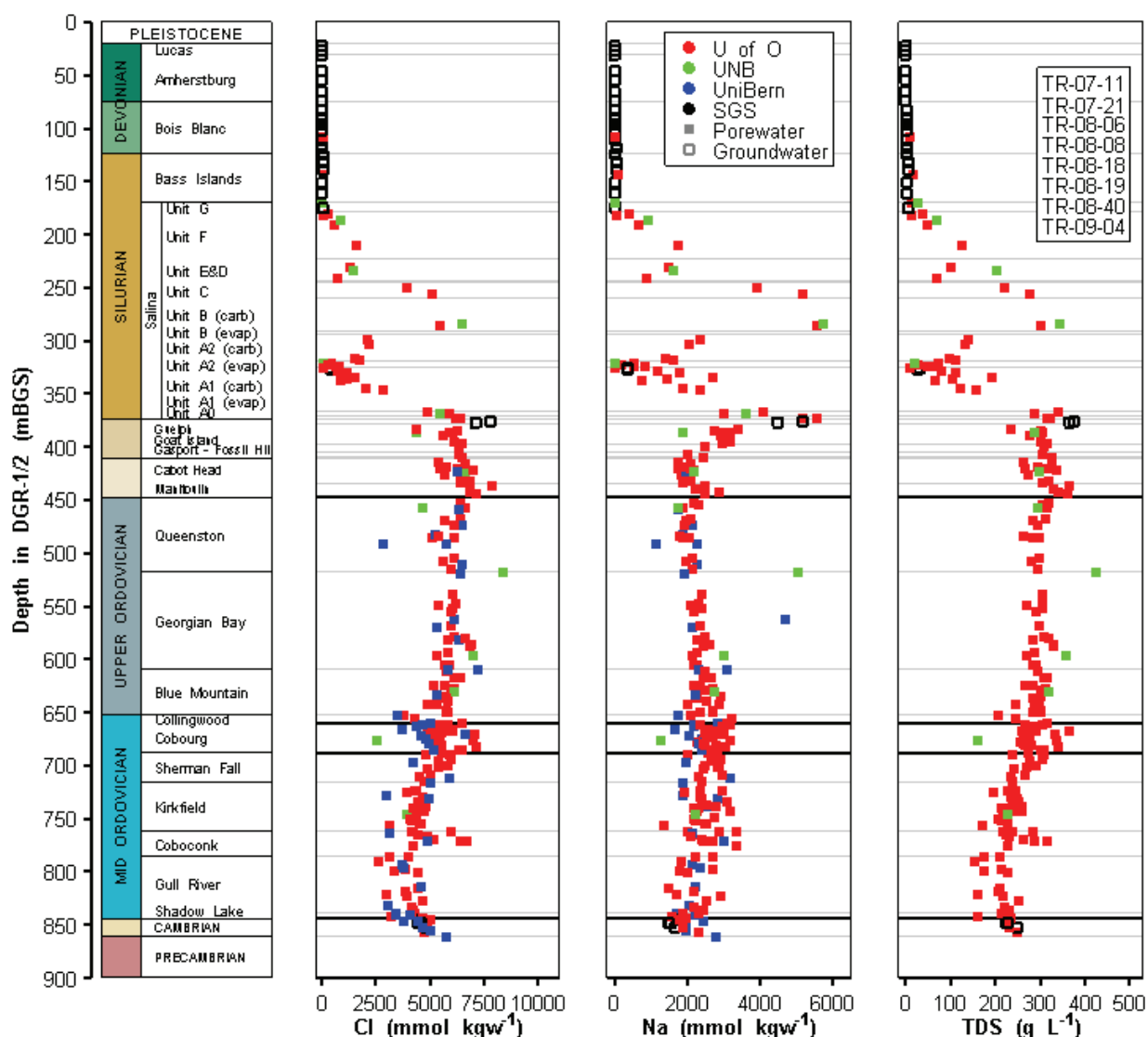


Figure 2.21: Hypothetical Groundwater Flow Pathway in the Salina A1 Upper Carbonate (SA1UC) and Guelph Formations

The hydraulic gradient in the Guelph is not strike parallel, and is orientated towards the northeast. The cause of this northeasterly gradient has not yet been established. Given that the water in the Guelph is saline (Figure 2.22), it is possible that this represents the net gradient due to topographic and density driving gradients of similar magnitude, i.e., the orientation of the hydraulic gradient in the Guelph is approximately the mean of the orientation of the gradients in the Salina A1 Upper Carbonate and the Cambrian formations.



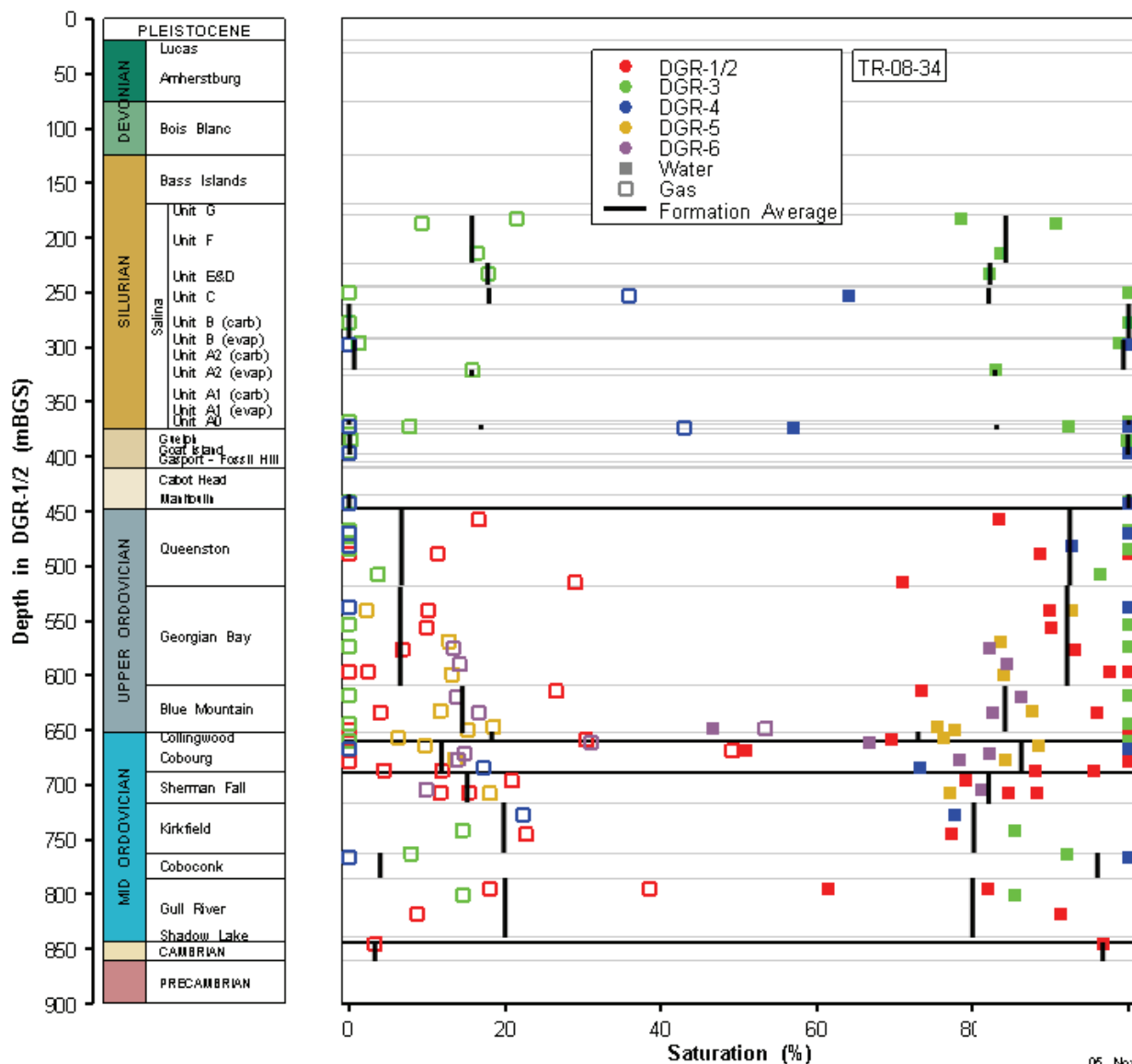
Note: Figure 4.107 in INTERA (2011).

Figure 2.22: Major Ion Groundwater/Porewater Concentrations

2.3.6.3 Gas Saturation

Free gas is present in the rock pores in the Intermediate and Deep Bedrock Groundwater Zone. Measurements (Section 4.3.3 of INTERA 2011) indicate free gas saturations of approximately 10 to 20%, and in certain cases up to 45% (Figure 2.23), although the values are uncertain due to the low rock porosity and other factors. The presence of this trapped free gas phase is a further indication of the low permeability of the zones. It is likely (for reasons noted below) that most of this gas-filled porosity is not connected due to the low porosity and narrow pore sizes, and that the included gas is not mobile.

Isotopic analysis indicates that the gas in the Middle Ordovician limestone is thermogenic in origin (i.e., formed by heating of organic matter deposited with the sediments at depth, and therefore under high pressure, within the basin). The basin subsidence history (Section 2.2.5.3 of NWMO 2011) indicates that thermogenically generated gas is likely to be ancient and most likely formed during peak burial conditions towards the end of the Paleozoic era. The low permeability of the geosphere is further confirmed by the fact that the gas of thermogenic origin in the Middle Ordovician has not mixed with gas of biogenic origin in the Upper Ordovician shale (Section 4.4.3 of NWMO 2011).



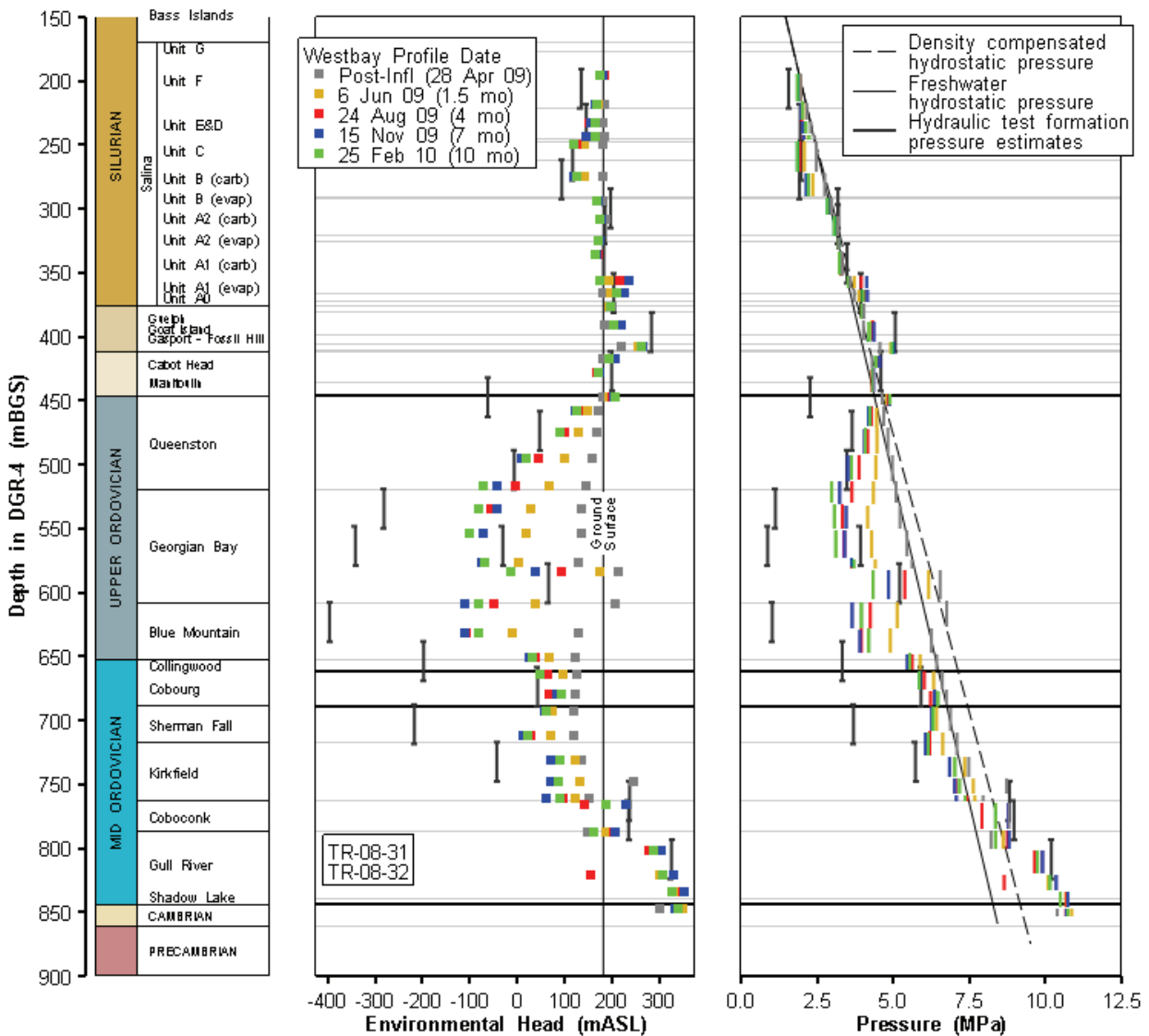
Note: Figure 4.8 in INTERA (2011).

05 Nov 2010
Pore Fl sat profile.mvw

Figure 2.23: Saturation Profile in DGR Cores

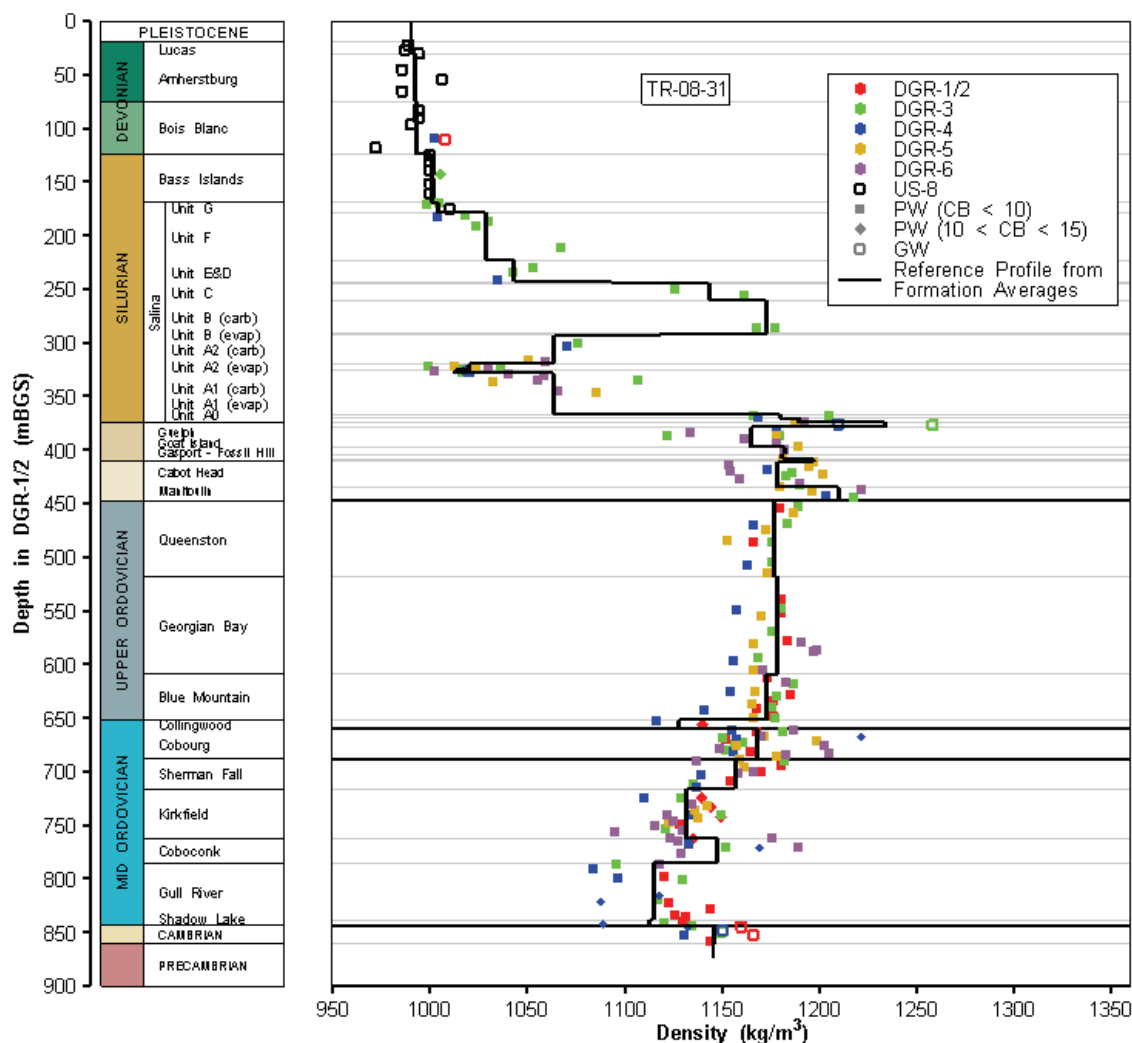
2.3.6.4 Over/Underpressures

Pressure data from the DGR boreholes indicate that the Cambrian sandstone and the Middle Silurian formations are overpressured relative to the ground surface, whereas the Ordovician limestone and shale are significantly underpressured. Given the very low hydraulic conductivities of the intermediate and deep zones, the presence of gas within these zones, the history of ice-sheet loading and unloading of the ground, and the long-term and Quaternary erosion history (NWMO 2011), this is not unexpected. Several measured head profiles for borehole DGR-4 are shown in Figure 2.24 and the associated density profile is shown in Figure 2.25.



Note: Figure 4.102 in INTERA (2011).

Figure 2.24: Groundwater Vertical Head Profiles Based on Data from the DGR-4 Site Investigation Borehole



Note: Figure 4.81 in INTERA (2011).

Figure 2.25: Groundwater Density (Salinity) Profiles Based on Data from the DGR Site Investigation Boreholes

Considerable work has been undertaken to understand the causes of these under- and over- pressures (Chapter 5 and Section 5.4.10 of NWMO 2011). The under- and over- pressures do not appear to be of ice-sheet origin since they could not be generated by paleoclimate analyses that considered various ice-sheet advance/retreat scenarios, nor can they be explained by osmotic processes. The overpressures observed in the Cambrian and Middle Silurian are consistent with the density-dependent saturated flow analyses of the Michigan Basin cross-section. The observed underpressures in the Ordovician could not be reproduced using this approach; however, they can be reproduced by assuming the presence of a non-wetting immiscible gas phase in the rock.

Regardless of their origin, the large and sustained anomalous pressure gradients indicate that the permeability is very low and that there is no transmissive vertical fracture network present within or near the DGR borehole footprint beneath the Bruce nuclear site.

2.3.6.5 Damaged Zone

The envelope of sedimentary rock surrounding underground excavations, including the shafts that will connect the DGR with the ground surface, is expected to have enhanced hydraulic conductivity as a consequence of excavation-induced damage and stress relief.

The damaged zone can be subdivided into three zones.

- HDZ where macro-scale fracturing or spalling may occur. The effective permeability of this zone is dominated by the interconnected fracture system.
- EDZ with hydromechanical and geochemical modifications inducing changes in flow and transport properties.
- Excavation disturbed Zone with possible hydromechanical and geochemical modification, but without changes in flow and transport properties.

The Geosynthesis report (Sections 6.3.1.1 of NWMO 2011) collates and analyses information from international mines and underground rock laboratories on the properties, extent and temporal evolution of the damaged zone. In high-stress environments, stress relief is the dominant control on the damaged zone, whereas in low-stress environments the excavation method is more important. The sedimentary rocks of southern Ontario have high horizontal stresses.

It is intended that the HDZ around the shafts from below about 180 mBGS will be mechanically removed as part of the backfilling and sealing process. The HDZ will be left in place around the DGR tunnels and emplacement rooms since its removal could be adversely affect worker safety.

The extent of the HDZ and EDZ are estimated from Geomechanical modelling (Section 6.4 of NWMO 2011). The properties of the HDZ and EDZ are described in Sections 5.2, 5.4.2, 5.5.2 and 5.6.2 of the Data report (QUINTESSA and GEOFIRMA 2011). Ultimately, the characteristics of the damaged zone will be verified by site-specific information as the shafts and tunnels are excavated.

2.3.7 Geochemistry

2.3.7.1 Water Chemistry

The Shallow Bedrock Groundwater Zone is permeable and groundwater samples have been taken from the US series boreholes at the Bruce nuclear site for geochemical analysis (Section 4.5.1 of INTERA 2011). Groundwater samples were also taken from permeable horizons in the Intermediate and Deep Bedrock Groundwater Zones during drilling of the DGR boreholes. These are referred to as opportunistic groundwater samples (OGWs) (Section 4.5.2 of INTERA 2011). The majority of the formations in these deeper zones have very low permeability, which made sampling difficult.

Geochemical conditions in the Intermediate and Deep Bedrock Groundwater Zones are particularly of interest because they will affect the geochemical conditions in the DGR, and contaminant transport through the geosphere barrier. Geochemical conditions of the waters in these zones are summarized in Table 2.10.

Table 2.10: Sampled Groundwater and Porewater Compositions

Sample	OGW-8	OGW-12	Salina A2	Salina A1	Georgian Bay shale	Cobourg limestone
Sample Type	Groundwater	Groundwater	Porewater	Porewater	Porewater	Porewater
Borehole	DGR-3	DGR-4	DGR-4	DGR-3	DGR-3	DGR-3
Depth (mBGS)	337.80-341.51	373.66-381.18	304.05	348.31	581.28	680.46
Formation	Salina Upper A1 Formation	Guelph	Saline A2 Unit – Carb	Salina A1 Unit - Carb	Georgian Bay	Cobourg
Source: INTERA (2011)	Table 4.7 Table 4.8, Fig. 4.53 to 4.57	Table 4.7 Table 4.8, Fig. 4.53 to 4.57	Fig. 4.53 to 4.57	Fig. 4.53 to 4.57	Fig. 4.53 to 4.57	Fig. 4.53 to 4.57
% Drill Water Contamination	3.1	0.3	N.D.	N.D.	N.D.	N.D.
pH	7.3	6.5	N.D.	N.D.	N.D.	N.D.
Eh (mV)	-13	-141.9	N.D.	N.R.D	N.R.D	N.R.D
DO (mg/L)	0.3	0.23	N.D.	N.D.	N.D.	N.D.
Fe(II) or Total Iron (mg/L)	>10	>10	N.D.	N.D.	N.D.	N.D.
Sulphide (mg/L)	5	0	N.D.	N.D.	N.D.	N.D.
Calculated TDS (mg/L)	26760	375468	131035	191664	298610	260362
Fluid Density (kg/m ³)	1019	1210	N.D.	N.D.	N.D.	N.D.
Na (mg/L)	7835	99133	47446	61626	54486	59514
Ca (mg/L)	1003	31597	2208	668	40533	9530
Mg (mg/L)	580.6	7901	2558	8738	12651	22099
K (mg/L)	125.2	3665	545	1407	16159	17303
Sr (mg/L)	17.7	589.3	252	1128	1566	1868
Fe (mg/L)	10	29.6	N.D.	N.D.	N.D.	N.D.
Mn (mg/L)	1.03	4.27	N.D.	N.D.	N.D.	N.D.
Cl (mg/L)	13615	229635	77617	54775	212431	178956
Br (mg/L)	<30	1715	167	30	2371	1824
F (mg/L)	1.9	0.3	N.D.	N.D.	N.D.	N.D.
I (mg/L)	<0.3	0.5	N.D.	N.D.	N.D.	N.D.
Si (mg/L)	2.6	987	N.D.	N.D.	N.D.	N.D.
SO ₄ (mg/L)	3568	211	8713	80999	291	1415
NO ₃ (mg/L)	<6	<5	N.D.	N.D.	N.D.	N.D.
B (mg/L)	N.D.	N.D.	75	241	182	177
Alkalinity as CaCO ₃ (mg/L)	180.6	42.5	N.D.	N.D.	N.D.	N.D.

Notes:

Porewater concentrations (apart from TDS) were reported in the original source in units of mmol/kg water. These concentrations have been converted to mg/L, based on 1 kg/L water density.

N.D. means no data.

Regional geochemical evidence (Section 4.3.2 of NWMO 2011) indicates that glacial or younger recharge has occurred in shallow environments.

Data from the DGR boreholes (Section 4.4 of NWMO 2011) are consistent with the regional data, indicating that glacial meltwater has not penetrated below the base of the Shallow Bedrock Groundwater Zone, i.e., not below 180 m except in the relatively permeable Salina A1 Upper Carbonate in the Intermediate Bedrock Groundwater Zone. The presence of waters with a glacial isotopic signature within this formation suggests injection of glacial meltwaters from outcrop/subcrop rather than via the overlying formations.

Figure 2.22 shows the major ion composition of the groundwater/porewater at the Bruce nuclear site. The Shallow Bedrock Groundwater Zone contains relatively fresh water, consistent with this being the relatively permeable, actively flowing part of the system. Major anion concentrations increase through the deeper zones; the water is dense and saline. The data indicate that porewaters in the Deep Bedrock Groundwater Zone have not mixed with, or been displaced by, surface waters, including glacial meltwaters that could have been under very high injection pressures. Coupled hydro-mechanical paleoclimatic groundwater flow models (Section 5.4.6 of NWMO 2011) support this geochemical interpretation.

Geochemical evidence presented in Chapter 4 of NWMO (2011) indicates that the brines in the Intermediate and Deep Bedrock Groundwater Zones are ancient; (more than 250 million years old). This implies that the hydraulic conductivity must be very low, which is consistent with data from the Bruce nuclear site (Figure 2.19) and is reflected in the entrapment of hydrocarbons for more than 200 million years by equivalent formations elsewhere in the Michigan Basin.

A conceptual model of the geochemical evolution of the Bruce nuclear site, and regional study area, has been developed (Section 4.5 of NWMO 2011). The model results show that the observed geochemical profiles may have evolved over a very long time period, perhaps as long as a few hundred million years.

A 'model' Cobourg porewater composition has been produced (Table 2.11) to act as the basis for the geochemical calculations presented in this report. As discussed in Appendix C of the Data report (QUINTESSA and GEOFIRMA 2011), the model composition was calculated using PHREEQC and data given in Table 2.10.

Table 2.11: Cobourg Model 2 Porewater Composition

Parameter	Composition (molality)
Ionic Strength	3.80E+00
pH	6.5
pe	-2.002
Eh	-0.12 V
Na	2.59E+00
Ca	2.38E-01
Mg	9.72E-03
K	4.43E-01
Sr	1.91E-03
Cl	3.48E+00
Br	2.28E-02
SO ₄	1.94E-02
B	1.64E-02
C	6.10E-04
Al	6.22E-11
Si	9.98E-04
% charge error	0
log pCO ₂ (g)	-2.43
log pO ₂ (g)	-65.23
Saturation Indices:	
Anhydrite	0
Calcite	0
Dolomite	0
Gypsum	0.06
Halite	-0.88
Strontianite	-0.12
Sylvite	-1.11
Celestine	0
Illite	0
SiO ₂ (am)	0

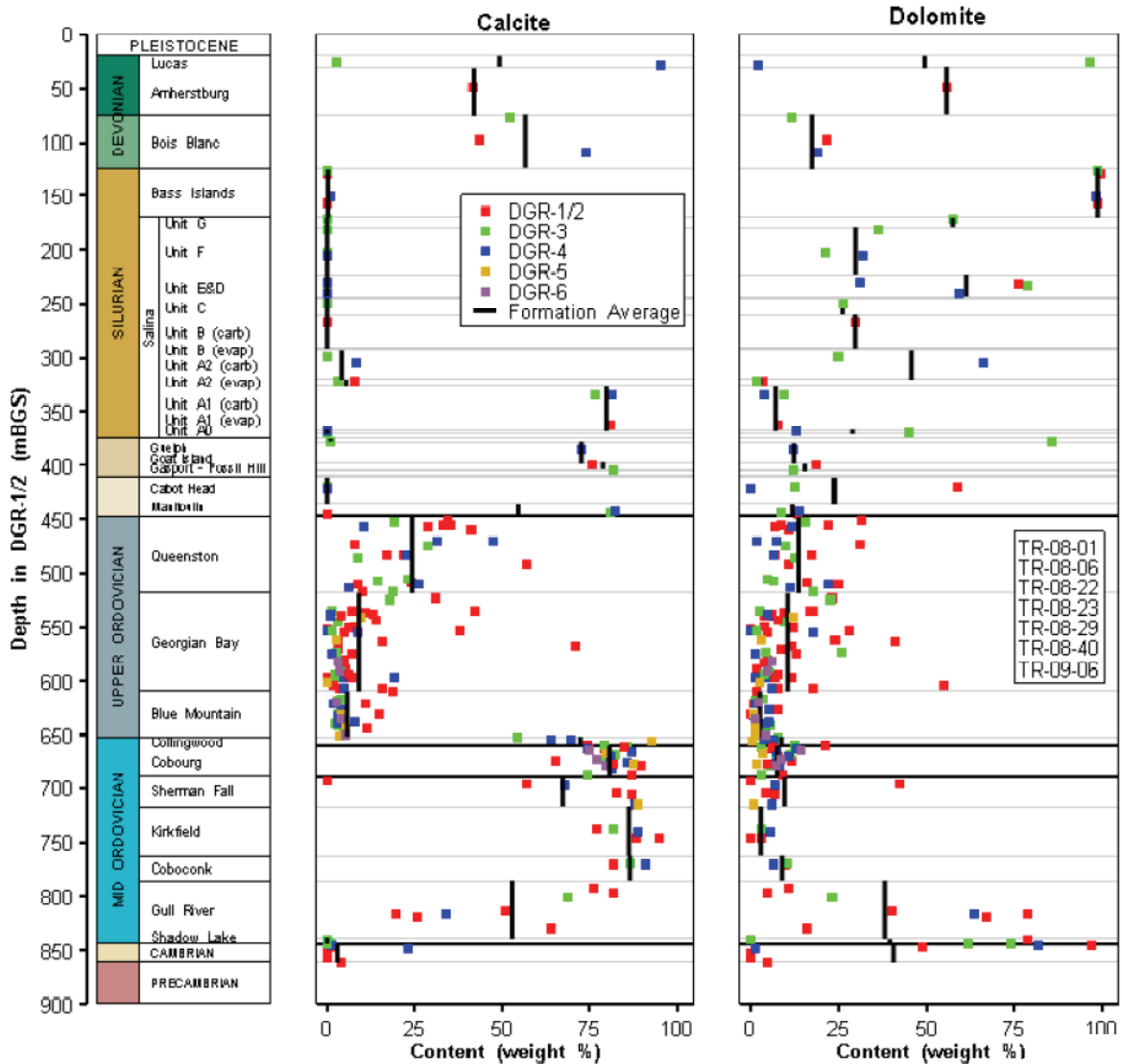
Note: Table C.3 in QUINTESSA and GEOFIRMA (2011).

2.3.7.2 Rock Chemistry

Mineralogical information is available from testing of DGR borehole core samples (Section 3.7 of INTERA 2011). The whole rock mineralogy data are shown in Figure 2.26 to Figure 2.28.

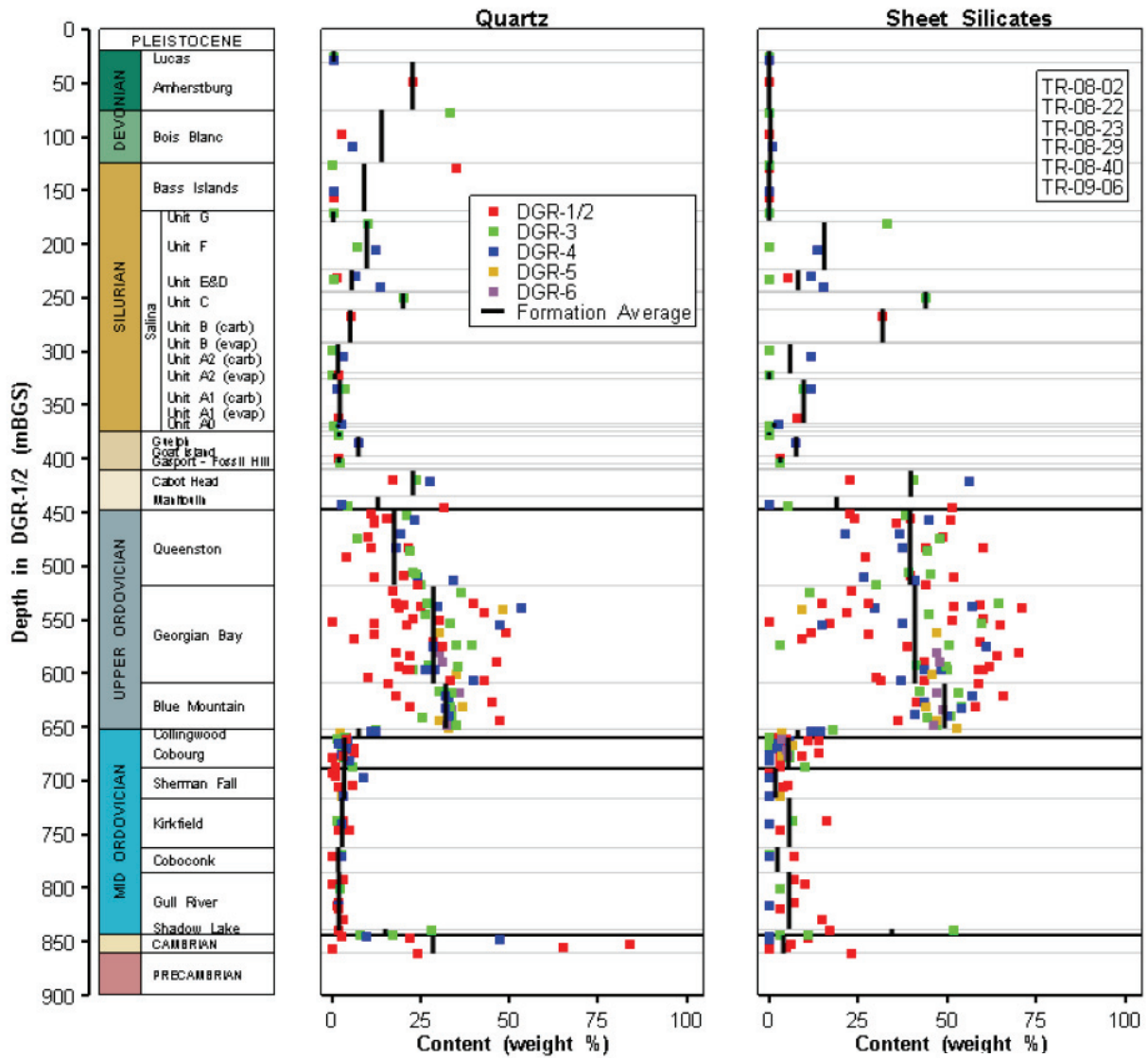
Calcite and dolomite are significant constituents of the proposed host rock (the Cobourg Formation) and surrounding lithologies. These carbonate minerals will act as an important pH buffer.

Evaporite minerals are common in minor or trace amounts (<10%). It is also noted that silicates, and most notably sheet silicates, are a minor, but not insignificant constituent of these rocks.



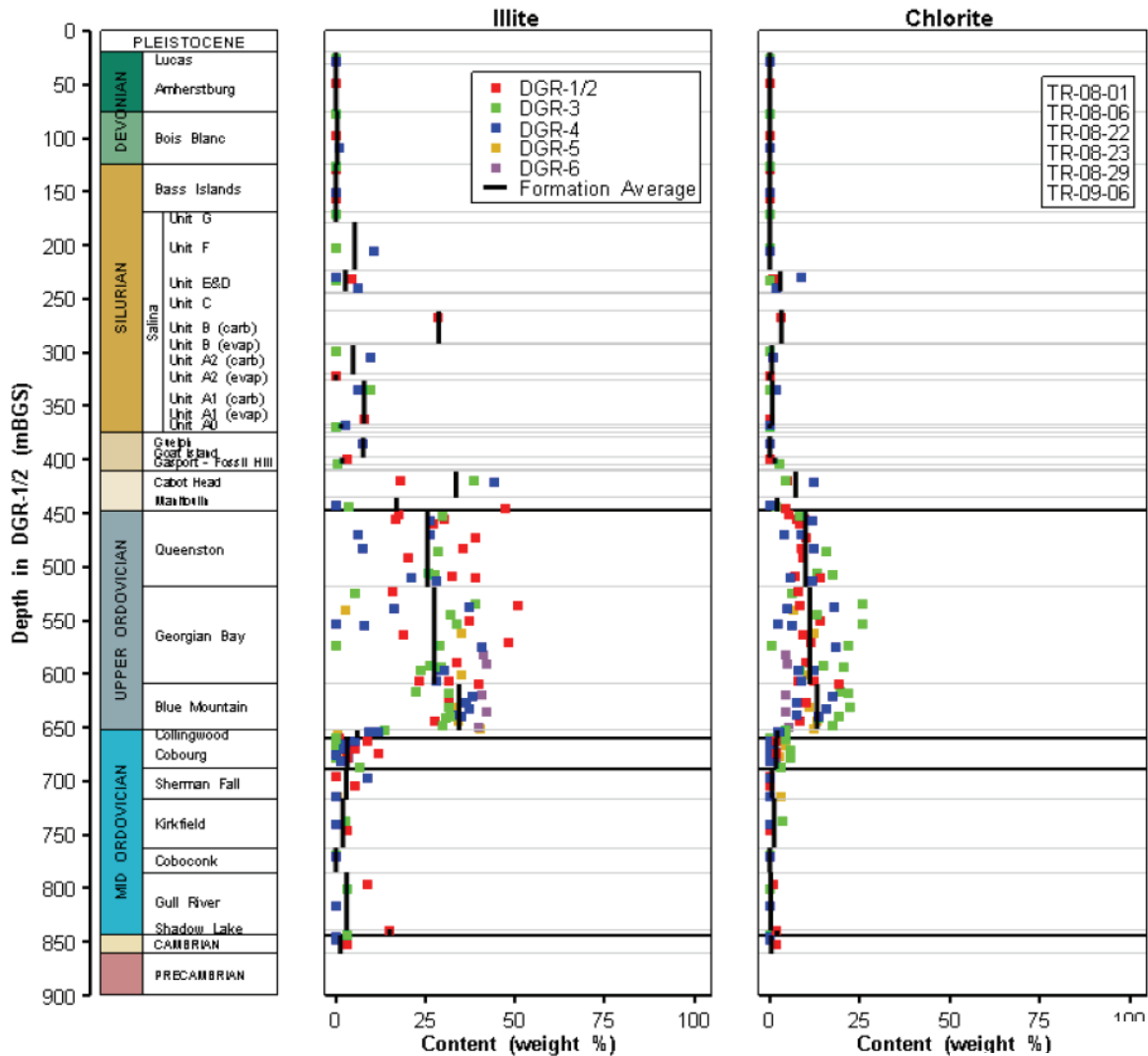
Note: Figure 3.5 in INTERA (2011).

Figure 2.26: Profiles of Calcite and Dolomite in DGR Cores



Note: Figure 3.6 in INTERA (2011).

Figure 2.27: Profiles of Quartz and Total Sheet Silicates in DGR Cores



Note: Figure 3.7 in INTERA (2011).

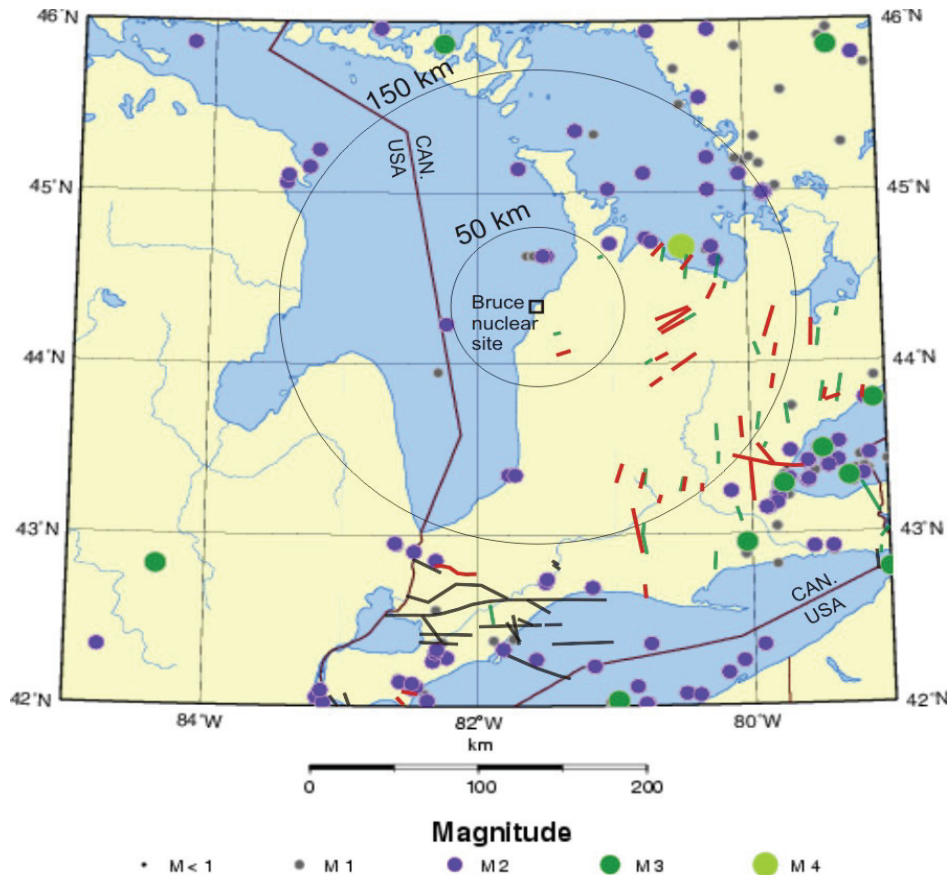
Figure 2.28: Profiles of Illite and Chlorite Clay Mineral Content in DGR Cores

Most of the formations are low in organic carbon (<0.25%). Exceptions are middle and lower parts of the Georgian Bay Formation (0.3-0.7%), the Blue Mountain Formation (0.3-1.7%), the Collingwood Member (0.75-2.5%), and the Coboconk to Shadow Lake Formations (0.3-2.0%). This organic matter is the source material for the small quantity of free gas present in the low permeability formations in the Intermediate and Deep Bedrock Groundwater Zones (Figure 2.23).

Another significant observation is that pyrite occurs in the host rocks and the surrounding rock formations. Although the abundances of this mineral are small (<<1%), the fact that it is present is good evidence that in-situ conditions are reducing.

2.3.8 Seismicity

Southwestern Ontario and the Bruce region lie within the tectonically stable interior of the North American continent, which is characterized by low rates of seismicity. There are historical records since the late 1800s. Figure 2.29 shows the monitoring results since 1985 from the seismograph stations around the Bruce nuclear site. It shows that the Bruce region experiences sparse seismic activity, with no apparent concentrations of activity that might delineate regional active faults or other seismogenic features. Most recorded events have a Nuttli magnitude³ less than **M3**, with rare occurrences of larger events up to **M4.3** within a 150 km radius from the Bruce nuclear site.



Note: Figure 2.14 in NWMO (2011).

Figure 2.29: Seismicity in the Bruce Region from 1985 to 2010 Overlain with Mapped Faults in Southern Ontario

³ Nuttli Magnitude (**M**) is the local magnitude scale used in the Bruce monitoring network. It can be related to the moment magnitude (M_m) scale by the empirical relationship $M_m = 0.98M - 0.39$ for $4 < M < 6$ (Sonley and Atkinson 2005). The moment magnitude scale was calibrated such that moment magnitude equals Richter magnitude in most cases (Hanks and Kanamori 1979), but it provides a more direct indication of earthquake fault size.

The historical seismic monitoring record is considered to be relatively complete for events of about $M > 3.5$ since the early part of the 20th century. It has become more complete at lower magnitudes over the last 10 years with the increase of station density in the region. 26 events have been detected in the Bruce region since 1952 with a maximum magnitude of $M4.3$ measured at 15 km north of Meaford near Owen Sound in 2005. Only three earthquakes had historically been detected within 50 km of the Bruce nuclear site prior to 2007. These three events occurred in Lake Huron about 20 km northwest of Southampton with magnitudes ranging from $M1.7$ to $M2.1$.

These findings provide a sense of the seismic recurrence rate of the Bruce region. With no seismic events of $M > 4.3$ recorded in the past 100+ years, the likelihood of a large event in the Bruce region is very low, exhibiting a seismicity rate comparable to that of a cratonic region. The rate could potentially be affected if there was a future episode of glaciation, as such events lead to in-situ stress changes that may temporarily increase seismicity rates (Adams 1989). However, a recently completed remote-sensing and field-based study looked at landforms within 50 km of the Bruce nuclear site and found no evidence for neotectonic activity associated with the most recent glacial cycle within the regional study area (Section 2.2.6.5 of NWMO 2011).

A Probabilistic Seismic Hazard Assessment (PSHA) has been conducted for the repository that incorporates uncertainties in the models and parameters that affect seismic hazard (Section 6.2.2.1 of NWMO 2011 and Chapter 6 of AMEC GEOMATRIX 2011). The frequency of $M6$ or greater earthquakes within 200 km of the site was estimated at 10^{-4} per year (Chapter 6 of AMEC GEOMATRIX 2011). This is approximately equivalent to an annual frequency of an $M \geq 6$ event of 10^{-6} within a 20 km radius of the site, assuming roughly uniform probability across the area.

Based on the results of the PSHA performed for the Bruce nuclear site, the estimated surface bedrock peak ground accelerations are expected to be less than 1 g for probabilities of 10^{-5} per year for the reference case and 10^{-6} per year for an extreme scenario. The 2005 National Building Code of Canada requires the peak ground acceleration associated with an event with a probability of exceedance of 1/2500 per year to be considered. For the Bruce nuclear site, the peak ground acceleration associated with such an event is very small; only 0.04 g.

The intensity of shaking due to an offsite earthquake normally decreases with depth. Therefore, for a given event, the potential for damage of the DGR and shaft seals in the Deep and Intermediate Bedrock Groundwater Zones is lower than the potential for damage to surface features. Dynamic mechanical modelling (Section 6.4 of NWMO 2011) indicates that the DGR and its shaft will not be damaged by a one in a million year event. These results are consistent with case histories that show earthquake damage to underground structures is rare, particularly below 500 m (Pratt et al. 1979; Backblom and Munier 2002).

2.3.9 Stress Regime

The compilation of regional in-situ stress data reveals a state of high compressive stress in Paleozoic bedrock formations of the Michigan Basin. At the depth of the DGR, within the Deep Bedrock Groundwater Zone, the stress ratio, σ_H/σ_v , (where σ_H is the maximum horizontal stress, and σ_v is the vertical stress) is estimated to be about 1.7 to 2.5 and the ratio σ_H/σ_h (where σ_h is the minimum horizontal stress) is approximately 1.5 to 2.1 (Section 3.3.2 of NWMO 2011). The orientation of the maximum horizontal stress, σ_H , is estimated to be in the ENE direction.

Additional site-specific data are available from the DGR boreholes. The DGSM report (Section 5.4 of INTERA 2011, Section 3.3.2 of NWMO 2011) gives the following best estimate stress values at the elevation of the DGR (~680 m bgs):

- Vertical stress (σ_v) ~18 MPa;
- Maximum horizontal stress (σ_H): $1.5 < \sigma_H/\sigma_v < 2.0$; and
- Minimum horizontal stress (σ_h): $1.0 < \sigma_h/\sigma_v < 1.2$.

Based on these stress ratios and an overburden stress of 18 MPa, the maximum and minimum horizontal stress magnitudes at the proposed repository depth would be approximately 32 MPa and 20 MPa, respectively. The horizontal stress magnitudes would be smaller in the Intermediate and Shallow Bedrock Groundwater Zones.

2.4 Surface Environment

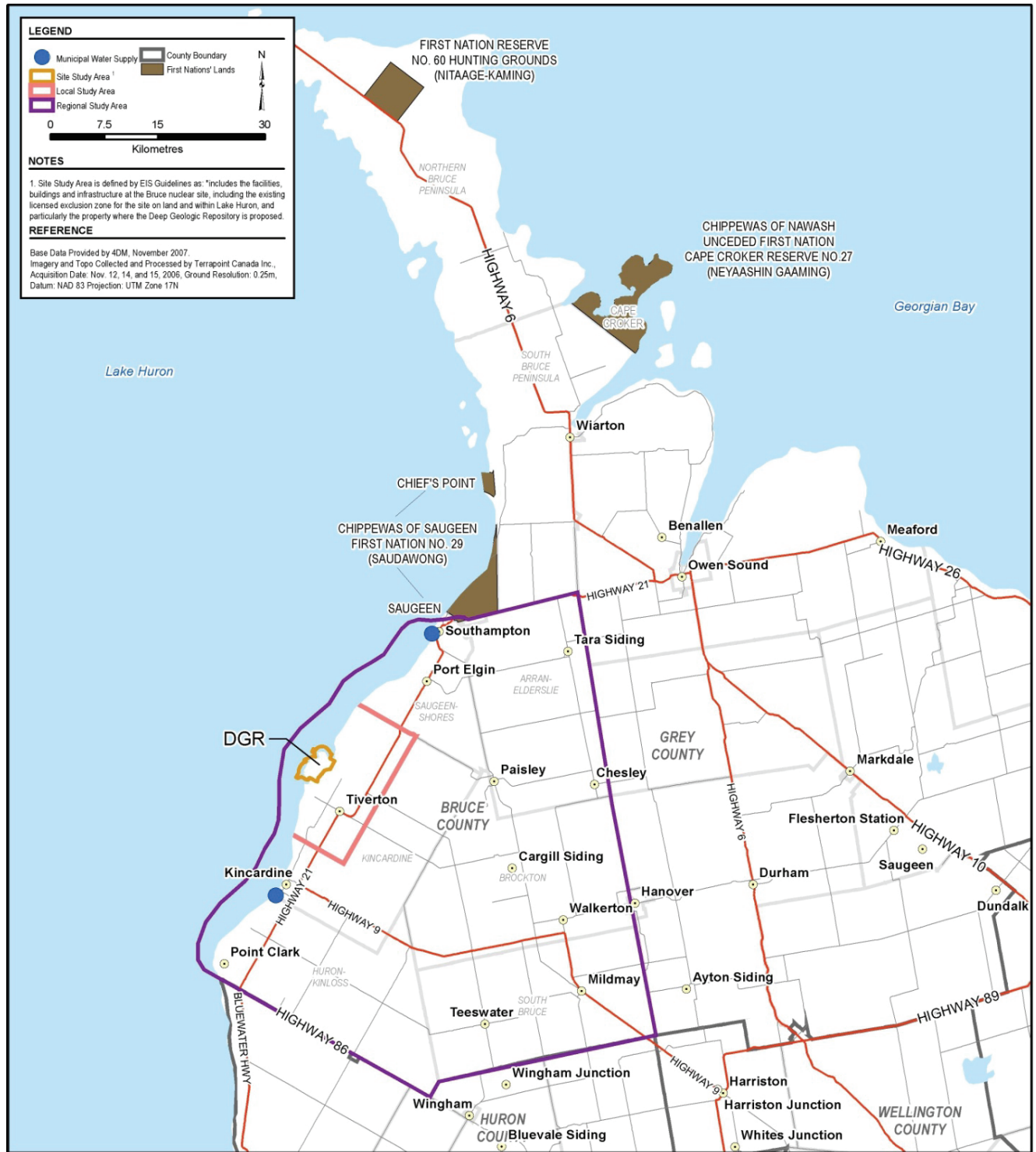
Maps showing the Bruce nuclear site are provided in Figure 2.30 at the regional and local scales and in Figure 2.31 at the site scale.

The Bruce nuclear site lies on the eastern shore of Lake Huron on the Douglas Point promontory. The topography around the Bruce nuclear site is relatively low lying, varying between 176 m above sea level (mASL) (level of Lake Huron) up to approximately 195 mASL (associated with the Nipissing Bluff). Elevations increase to approximately 230 mASL further inland to the east, associated with another bluff line, the Algonquin Bluff. Each of these bluffs represents remnants of post-glacial shorelines developed during the Holocene.

The biosphere can be defined as the surface environment, including inhabitants, in the vicinity of the proposed DGR site. Study areas adopted for the EA are convenient for describing the present-day system and are defined as follows (CEAA and CNSC 2009).

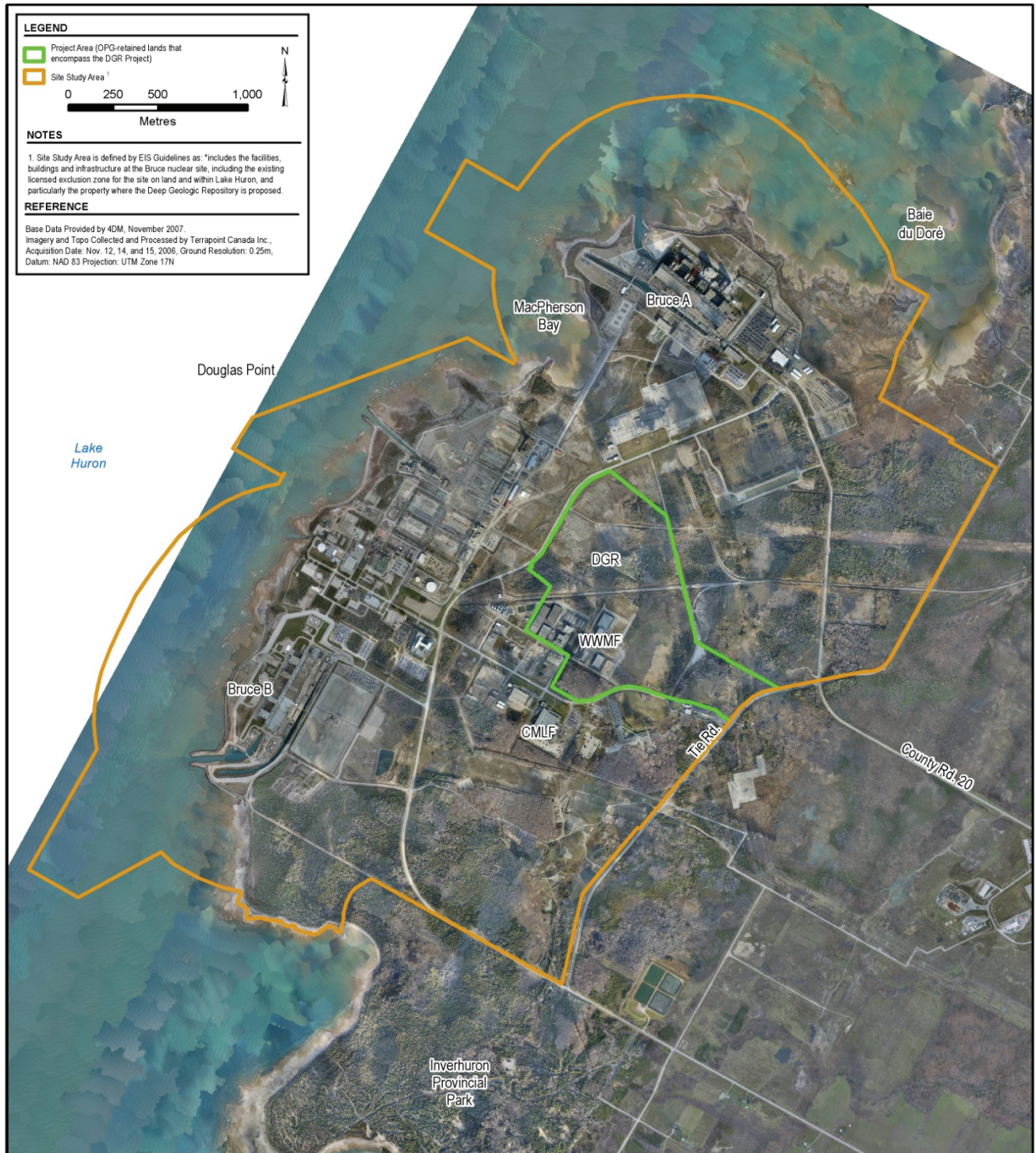
- The Project Area - the boundary of the OPG-retained lands at the centre of the Bruce nuclear site where the DGR project is being proposed.
- Site Study Area - includes the facilities, buildings and infrastructure at the Bruce nuclear site, including the existing licensed exclusion zone for the site on land and within Lake Huron, and particularly the property where the DGR is proposed.
- Local Study Area - the area existing outside the Site Study Area boundary, where there is a reasonable potential for direct effects on the environment from any phase of the project, either through normal activities, or from possible accidents or malfunctions. The Local Study Area includes all of the Bruce nuclear site and the lands within the Municipality of Kincardine closest to it, as well as the area of Lake Huron adjacent to the facility.
- Regional Study Area - the area within which there is the potential for cumulative biophysical and socio-economic effects. This area includes lands, communities and portions of Lake Huron around the Bruce nuclear site that may be relevant to the assessment of any wider-spread direct and indirect effects of the project.

The EA reports for the DGR provide descriptions of the biosphere with respect to the study areas (GOLDER 2011a to g, AMEC NSS 2011). Additional information can be found in the EA Study Report for the WWMF (OPG 2005).



Note: Figure 2.4.2-1 in AMEC NSS (2011).

Figure 2.30: Location of the DGR Project and Definition of the Study Areas



Note: Figure 2.4.2-3 in AMEC NSS (2011).

Figure 2.31: Bruce Nuclear Site and Surrounding Area

2.4.1 Atmosphere

The region has four distinct seasons with warm summers and mild winters. Because of lake effects, uncomfortably hot and humid conditions and long dry or wet spells are rare. The following description of the meteorological conditions draws on the Atmospheric Environment TSD (GOLDER 2011c), which describes conditions at the Site Study Area, and OPG (2005), which extends the description to the regional study area.

The annual mean temperature is 8.2 °C in the vicinity of the Bruce nuclear site. The mean daily temperatures fall below freezing from December through March. The coldest months are January and February, with mean daily temperature of -3.1 °C. The extreme minimum temperature recorded during the period 2005 through 2009 is -21.1 °C. During June to August, the mean daily temperature is approximately 18.8 °C. The extreme maximum temperature recorded during the period 2005 through 2009 is 31.8 °C.

There is a relatively even distribution of meteoric precipitation between winter and summer seasons (combining rainfall and snowfall), typically totalling about 1,000 mm annually. About 30% of this meteoric precipitation falls as snow.

Severe weather events in the region generally include thunderstorms and lightning, ice storms, windstorms, heavy rain or snow (winter) and fog.

The average wind speed in the Site Study Area is about 11.8 km/h (about 3.3 m/s). Winds are generally stronger in the winter season, averaging 15.3 km/h in December in comparison to 8.9 km/h in August. Annually, the prevailing winds are from the southwest. Winds at the site tend to increase towards the middle of the day, especially in the summer months when the sun is strongest and lake breezes develop.

Air quality in the regional study area is characteristic of the general air quality in Southwestern Ontario. Monitoring results for Tiverton, within the Local Study Area, show no ambient air quality criteria being exceeded for fine particulate matter (PM_{2.5}), nitrogen dioxide (NO₂) or sulphur dioxide (SO₂), whereas the ambient air quality criterion for ozone was sometimes exceeded, however this is typical of Southwestern Ontario and is contributed to by photochemical ozone from large cities in the United States (Section 4.2.1 of the Atmospheric Environment TSD, GOLDER 2011c).

Small amounts of radiological and non-radiological air pollutants are emitted to the atmosphere from operations at the Bruce nuclear site. The following summarizes the results of atmospheric monitoring conducted between 2001 and 2009 (Section 5.5 of the Radiation and Radioactivity TSD, AMEC NSS 2011).

- Annual average tritium concentrations ranged from 0.3 to 4.6 Bq/m³ in the Local Study Area and 0.1 to 0.52 Bq/m³ in the regional study area, compared with a provincial background of 0.03 to 0.2 Bq/m³.
- Average gross beta deposition rates for radioactive particulates ranged from 14 to 32 Bq/m² per month in the Local Study Area and 15 to 24 Bq/m² per month for the regional study area.

- Annual average C-14 concentrations in the local and regional study areas do not differ greatly and range from 0.04 to 0.07 Bq/m³ dry air in comparison with the provincial average of 0.04 to 0.05 Bq/m³ dry air⁴.

These values are representative of the operational Bruce nuclear site, i.e., primarily due to the operating reactors and the low-level-waste incinerator.

2.4.2 Surface Water Bodies

The following description of surface water bodies draws primarily on Chapter 5 of the Hydrology and Surface Water Quality TSD (GOLDER 2011e), but some information relating to Lake Huron is also taken from Chapter 6 of the Data report (QUINTESSA and GEOFIRMA 2011).

There are no major rivers in the regional study area, but there is an extensive network of small rivers and creeks. The largest river is the Saugeen River that enters Lake Huron at Southampton, 26 km to the northeast. There are three small east-to-west drainage courses entering the lake adjacent to the Bruce nuclear site: Underwood Creek and Stream C empty into Baie du Doré to the north; and the Little Sauble River, which forms the southern boundary of Inverhuron Provincial Park, empties into Inverhuron Bay to the south (see Figure 2.32).

The Bruce nuclear site is located adjacent to the Lake Huron shoreline, within the Stream C watershed. Stream C originates at the headwaters of the Little Sauble River and Underwood Creek and is a former tributary of the Little Sauble River that was diverted to discharge to the Baie du Doré during the initial development of the Bruce nuclear site in the 1960s (see Figure 2.33).

Lake Huron is a typical, cold and deep oligotrophic lake (i.e., a lake with low primary productivity due to low nutrient content), with a surface area of approximately 60,000 km². The bathymetry of Lake Huron is illustrated in Figure 2.34. The average depth is 59 m, whereas, in general, water depths in the near-shore zone of the lake range from 6 m to 20 m. Bedrock substrate predominates in the shallow areas of the open shorelines, grading to a mixture of pebble, cobble and boulder at the 7 and 12 m depths.

The lake contains about 3.7×10^{12} m³ of water and discharges to the St Claire River at a rate of 1.71×10^{11} m³/a (Section 6.1.2 of the Data report, QUINTESSA and GEOFIRMA 2011). Average outflows from the lake therefore represent less than 5% of the total lake volume per year, resulting in a hydraulic retention time of about 22 years. Currents in the lake are generally in the order of 2.5 cm/s, two orders of magnitude greater than the through-flow velocity, and the predominant lake-wide circulation in the main basin is cyclonic (anti-clockwise).

⁴ Converted from Bq/kg C assuming 383 ppmv CO₂, a mass of air of 1.2 kg/m³, a mean molar mass of air of 29 g/mol, and a molar mass of carbon of 12 g/mol.



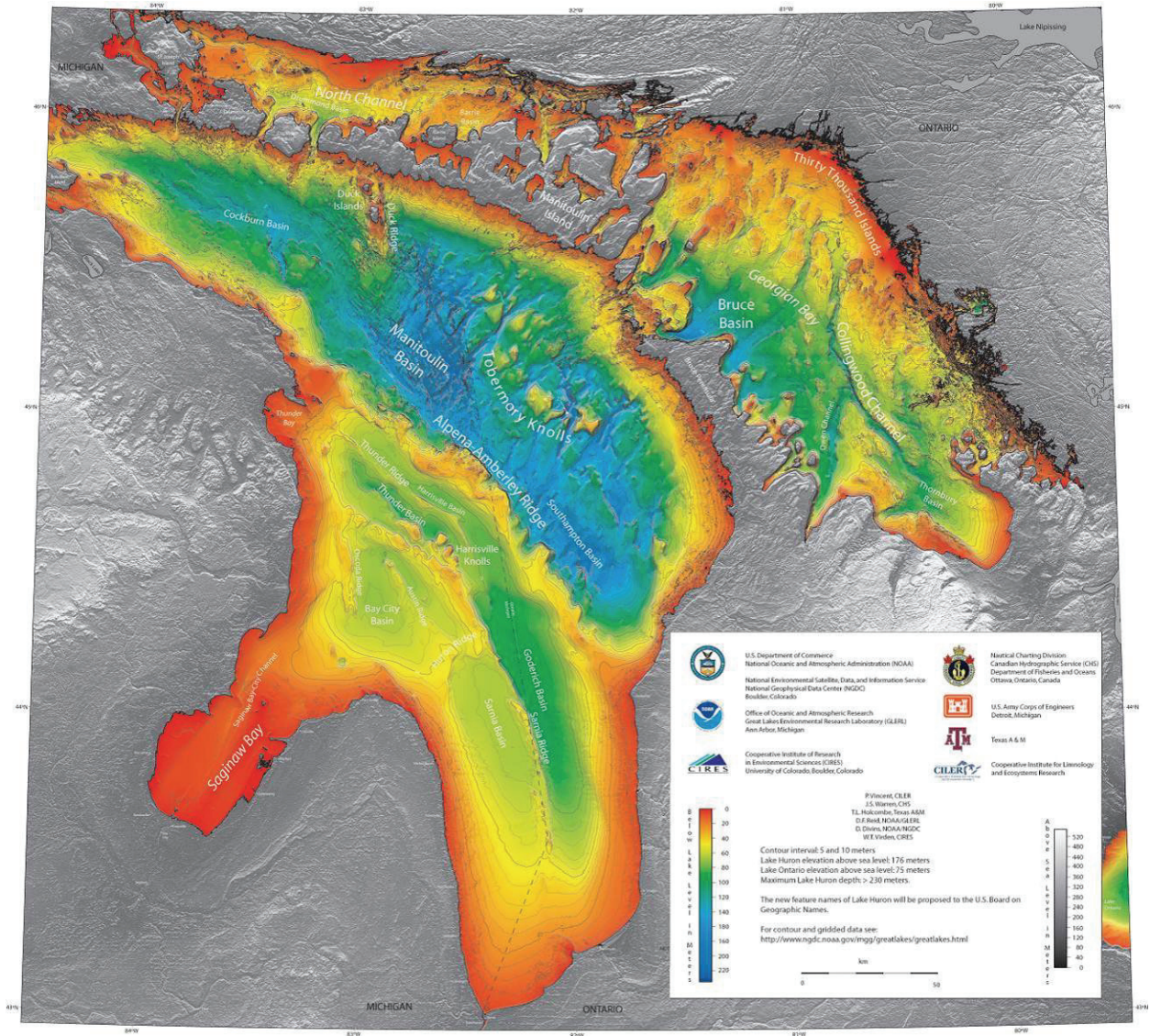
Note: Adapted from Figure 5.4.3-1 in GOLDER (2011e).

Figure 2.32: Local Watersheds



Note: Figure 5.4.2-1 in GOLDER (2011e).

Figure 2.33: Stream C, Catchments and Discharge Locations



Note: Figure from NOAA (2010).

Figure 2.34: Bathymetry of Lake Huron

The Baie du Doré, located along the northern portion of the Bruce nuclear site, is an embayment within the Local Study Area (see Figure 2.35). It is characterized by shallow depths (not exceeding 5 m) and rock outcrops. The habitat of the bay is protected from Lake Huron by two major shoals. Nevertheless, the shoreline remains subject to wave action and ice scour. Wetland areas exist at the head of the bay and are set back from the shoreline. However, they are connected to the bay through outflow channels. These wetlands provide a nursery and spawning habitat for many Great Lakes species and are very productive. Average water temperatures in Baie du Doré are generally 2°C warmer than those in the open lake, but it is often much more than 2°C warmer during the summer (Section 4.3 of OPG 2005).

Stream C is a cold water stream that is located east of the project area and flows in a northerly direction from the site to the Baie du Doré. Stream C is characterized as a slow-flowing stream with riffle and pool habitat throughout (see Figure 2.36). The stream has a mean width of 3 m with maximum depths ranging from 0.15 m to 0.8 m. Aquatic vegetation is plentiful throughout the reach consisting primarily of submergents and a small emergent component (Section 4.3 of OPG 2005).

A ditch, known as the Railway Ditch, flows to the north of the WWMF around the edge of the wetland and continues into Stream “C” beyond the wetland. The Railway Ditch is approximately 5 m wide at the top of the bank with a wetted width of 3 m and a mean water depth of 0.15 m. The side slopes of the ditch are stabilized with natural vegetation cover including grasses, trees, shrubs and cattails, as seen in Figure 2.37. The presence of cattails throughout much of the ditch provides a highly stable ditch bed and serves to reduce water velocity, thus minimizing erosion and increasing the rate of settling for sediments that may enter the ditch system (Section 4.3 of OPG 2005).



Figure 2.35: Baie du Doré Pictured from Scott Point



Figure 2.36: Stream C at the Site Boundary



Figure 2.37: The Railway Ditch

2.4.3 Water Quality

Water quality measurements show that the background lake water meets the provincial water quality objectives, Ontario drinking water objectives and Canadian environmental quality guidelines (Section 5.5.1 of the Hydrology and Surface Water Quality TSD, GOLDER 2011e).

Monitoring results over the period 2001 to 2009 for water supply plants that draw water from Lake Huron at Kincardine, Port Elgin and Southampton give tritium concentrations ranging from 3.6 to 17.4 Bq/L and gross beta concentrations ranging from 0.06 to 0.09 Bq/L (Section 5.6 of the Radiation and Radioactivity TSD, AMEC NSS 2011). Values for provincial sites over the same time period range from 1.0 to 8.0 Bq/L (tritium) and from 0.02 to 0.19 Bq/L (gross beta). Monitoring results for Stream C inside the boundary of the Bruce nuclear site give tritium

concentrations ranging from 99 to 153 Bq/L for 2001 to 2009 and total beta concentrations ranging from 0.13 to 0.20 Bq/L. Monitoring results for shallow wells in the Local Study Area in 2009 show tritium concentrations up to 95 Bq/L (Section 5.9 of the Radiation and Radioactivity TSD, AMEC NSS 2011).

Sampling of surface water in the Local Study Area has shown exceedances of provincial water quality objectives for Cu, Fe and Zn, in some samples (Section 4.2.2 of the Hydrology and Surface Water Quality TSD, GOLDER 2011e).

2.4.4 Water Supply

The towns of Port Elgin, Kincardine and Southampton, located on the shores of Lake Huron within the regional study area, have municipal water supply plants that obtain water from Lake Huron.

Most of the rural population within the regional study area obtains its water from private or communal wells, including the Village of Tiverton, the Hamlet of Underwood and some residences of Scott Point, Woodland Court Trailer Park, and Lime Kiln Cottages. Many inland cottages have water wells and septic tanks, although some lakefront properties have direct intakes from the lake. The Bruce Dale Conservation area campsites and Inverhuron Provincial Parks are supplied by wells. In the Kincardine Municipality there are approximately 1000 wells (GOLDER 2003). Water is drawn principally from the Shallow Bedrock Groundwater Zone from depths of between 30 and 100 m. Within the Local Study Area, there are four municipal wells, ranging in depth from 46 m to 122 m with licenced abstraction rates of 0.9 L/s to 6.1 L/s, and one communal well at 41 m servicing the Woodland Trailer Park (Figure 2.20).

2.4.5 Sediment

Lake Huron includes four main zones of depositional sediments underlying the deeper waters of Georgian Bay, and the southern, western and central basins (Section 6.2.2 of the Data report, QUINTESSA and GEOFIRMA 2011). The surface sediments in depositional zones are fine-grained, composed mainly of clay and silt-sized particles. Erosional zone sediments in shallower waters and inshore areas are more complex, comprising sands, lag sands and gravels. Sediments in the North Channel are likely similar to sediments in Georgian Bay.

The bed sediment in Stream C is predominantly composed of silt and sand with cobble to boulder sized material. The bank substrate comprises clay to silty sand loam (with clay). Table 2.12 provides the results of sediment sampling for non-radiological species in Stream C, the Railway Ditch and Macpherson's Bay.

Sediment samples are collected annually by Bruce Power from Lake Huron in the Regional and Local Study Areas. Sediment samples are analyzed for radionuclides including Cs-137, Co-60 and K-40 and expressed on a dry sediment basis. Results from sampling undertaken during 2008 are given in Table 2.13. The major portion of the activity in the sediments is due to the existence of K-40, a naturally occurring radionuclide.

Sediment samples were taken from the Railway Ditch during the period 2000 to 2004. Mean Cs-137 concentrations ranged from <1.1 to 25.5 Bq/kg with a maximum concentration of 27 Bq/kg (Section 5.7.1 of the Radiation and Radioactivity TSD, AMEC NSS 2011). Ground gamma surveys conducted along the shoreline focusing on the Site Study Area in 2000 and 2002 recorded maximum Cs-137 concentrations of around 50 Bq/kg (Section 5.7.2 of the Radiation and Radioactivity TSD, AMEC NSS 2011).

Table 2.12: 2009 Sediment Sampling Results ($\mu\text{g/g}$) from the Hydrology and Surface Water Quality TSD

Species	Stream C ¹	Railway Ditch ²	Macpherson's Bay
Sb	<0.2	0.9	<0.2
As	2	7	<1
Ba	28	57	4.6
Be	<0.2	0.2	<0.2
B	5	7	<5
Cd	0.1	7.5	<0.1
Cr	7	12	6
Co	2.1	8.1	1.3
Cu	9.9	110	16
Pb	4	24	1
Mn	930	1300	170
Mo	<0.5	2.8	<0.5
Ni	3.7	28	2.5
Se	0.7	2.1	<0.5
Sr	120	190	66
Tl	<0.05	0.16	<0.05
U	0.43	1.9	0.29
V	8	48	8

Notes:

From Appendix F in GOLDER (2011e). Includes species that have at least one value higher than the minimum detection limits.

1. Highest value recorded for Stream C.
2. Highest value recorded for Railway Ditch.

Table 2.13: Results of 2009 Sampling for Radionuclides in Lake Huron Sediments, Bq/kg from the Radiation and Radioactivity TSD

Radionuclide	Regional Study Area	Local Study Area
K-40	247 to 251	276 to 590
Cs-137	0.21 to 0.23	0.19 to 8.90
Co-60 ¹	Below detection limits	0.20 to 0.85

Note: From AMEC NSS (2011).

2.4.6 Surficial Geology

In the regional study area (Section 4.5.1.1 of OPG 2005), the surficial deposits below the Algonquin Bluff and underlying the Bruce nuclear site include silty to clayey till of the Elma (Catfish Creek) sequence overlying the bedrock surface. This till sequence varies in thickness by up to approximately 15 m and locally contains interbedded sequences of sand, as determined from investigations at the WWMF site.

The till below the Algonquin Bluff is locally overlain by sand and gravel beach deposits related to the former glacial Lake Algonquin and Lake Nipissing shorelines. The glacial Lake Nipissing shoreline is marked by the less prominent Nipissing Bluff situated below the Algonquin Bluff. These deposits have been locally exploited for aggregate at pit locations along the Algonquin Bluff. The shoreline areas also include deposits of till and areas of boulders, exposed by shore erosion of this till. Areas of bog and cedar swamp also occur in poorly drained areas below the Algonquin Bluff and elsewhere within other poorly drained forested areas.

Bruce Power collects soil samples and analyzes them for Cs-137, Cs-134, Co-60 and K-40 (Section 5.8.4 of the Radiation and Radioactivity TSD, AMEC NSS 2011). As found in previous years, the dominant radionuclide measured in the soil samples in 2009 was the naturally occurring K-40. K-40 concentrations in soils in the Local Study Area ranged from 295 to 626 Bq/kg (dry weight), compared with the concentrations of 446 to 500 Bq/kg observed in the provincial background locations. Cs-137 concentrations in soil samples collected in the Local Study Area were found to be in the range of 0.9 to 8.0 Bq/kg, compared with the value of 2.7 to 3.9 Bq/kg measured at provincial background locations. Co-60 and Cs-134 were negligible in all soil samples.

2.4.7 Land Use

Current land uses on the Bruce nuclear site are restricted to those associated with the nuclear operations and support activities.

The region around the Bruce nuclear site is mainly used for agriculture, recreation and some residential development. Farmland accounts for around 60% of the land use in the county, with cattle, sheep and pigs being reared and crops such as oats, canola, barley and hay being produced. Around 60% of all Bruce County farms are family owned and operated. Local people also hunt wild animals including deer and waterfowl. Farms and rural populations often obtain water from wells. The lake provides water for larger communities, and is used for recreational and commercial fishing, and boating.

There is some mineral extraction for sand and gravel in the region. Four disused quarries exist in the controlled development zone around the Bruce nuclear site.

The nearest population centre is Inverhuron (population of around 800) about 4 km to the southwest of the Bruce nuclear site. Larger towns are Port Elgin (population of over 7000) about 20 km to the northeast, and Kincardine (population of around 9300), 15 km to the southwest.

Archaeological sites exist in the vicinity showing that it was settled around 2000 years ago by the Iroquois Nation, and occupied by the Ojibway Tribe when Europeans settled in the 1800s. Two areas of archaeological interest exist on the Bruce nuclear site, neither close to the DGR site.

The traditional territory of the Ojibway in the Saugeen region covers the watersheds bounded by the Maitland River and the Nottawasaga River east of Collingwood, an area that includes the Bruce Peninsula and Grey and Bruce Counties. The Chippewas of Saugeen reserve is approximately 38 km² situated on Lake Huron, at the base of the Bruce Peninsula about 3 km northeast of Southampton. The Chippewas of Nawash reserve occupies 72 km² on the eastern shore of the Bruce Peninsula on Georgian Bay. Fishing is an important activity for the local First Nations, and the Saugeen Ojibway Nation has been responsible for managing the commercial fishery in this area (Section 4.1.1 of the Aboriginal Interests TSD, GOLDER 2011a).

2.4.8 Biota

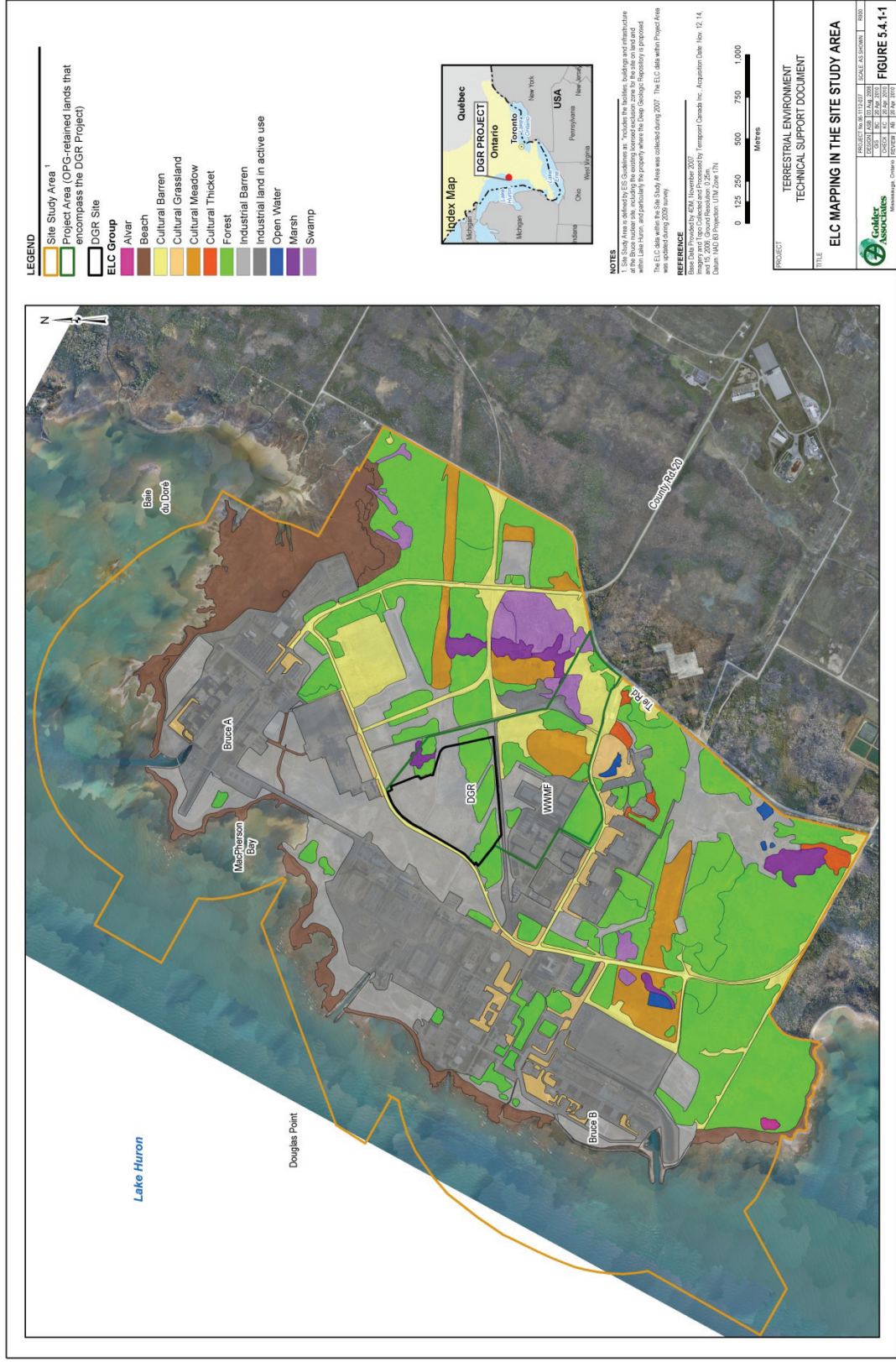
2.4.8.1 Plants

Approximately 25% of Bruce County is forested, with much of the north portion of the County, the Bruce Peninsula, under forest cover (Section 5.4.3 of the Terrestrial Environment TSD, GOLDER 2011g). The Bruce Peninsula acts as a transition zone between southern deciduous and northern boreal forests. As a result, representative species of a variety of natural areas are present in this area, often at the extreme limits of their range. These forested areas include both lowland and upland deciduous, mixed, and coniferous forests. Much of the regional study area consists of agricultural land. Consequently, few natural terrestrial features or wildlife corridors exist.

The Local Study Area is within the northern fringe of the deciduous forest zone (Section 5.4.2 of the Terrestrial Environment TSD, GOLDER 2011g). It includes the Huron Fringe woodland which contains wetland, dune and ridge areas. Vegetation in the Huron Fringe ranges from alvar, bog, swamp, fen, and marsh species to dune grasses. Much of the natural forest cover within the Local Study Area, as within the regional study area, has been historically cleared for agriculture. Remnant forested areas are primarily associated with the Lake Huron shoreline, watercourse valleys, areas with steep topography and poorly drained sites. Shallow marsh vegetation communities are present in the Baie du Doré wetland, accounting for a large area of this Provincially Significant Wetland.

An ecological land classification survey for the Bruce nuclear site was conducted in 2001, the results of which are shown in Figure 2.38 (Section 5.4.1 of the Terrestrial Environment TSD, GOLDER 2011g). The extent of anthropogenic activities is considerable and even the naturally-occurring vegetation has, in some areas, been greatly affected by past human activity. Fill has been placed in some areas and mounded up in others. Important vegetation-types found in the Site Study Area include alvar and beech.

The dominant aquatic plant along the Railway Ditch is cattail, whereas all of the species observed are common and widespread throughout southern Ontario, including muskgrass, variable leaf pondweed, sago pondweed, floating leaf pondweed and water plantain (Section 5.3.1 of the Aquatic Environment TSD, GOLDER 2011b).



Note: Figure 5.4.1-1 in GOLDER (2011g).

Figure 2.38: 2001 Ecological Land Classification for the Bruce Nuclear Site

2.4.8.2 Wildlife

The wildlife in the remnant woodland within the Site Study Area is limited by the small size of the habitats, high degree of fragmentation, and disturbed nature (Section 5.5.1 of the Terrestrial Environment TSD, GOLDER 2011g). The area is used by wildlife with larger territorial ranges (e.g., wild turkey and white-tailed deer). The Site Study and Project Areas have been extensively modified through the placement of fill, limiting the availability of topsoil. The site does not provide good habitat for burrowing species of mammals, and the stony nature of the soils limits the growth of herbaceous groundcover in some of the more open habitats.

A variety of amphibians (e.g., Green frog), reptiles (e.g., northern watersnake) and small mammals (e.g., muskrat) are recorded using the network of naturalized ditches and vernal ponds in the Project and Site Areas. Terrestrial burrowing crayfish species are found in and adjacent to the Railway Ditch and wetland areas.

Wildlife habitat in the Local Study Area is generally associated with vegetation communities such as forests, meadow and other cultural lands, wetlands and the Lake Huron shoreline (Section 5.5.2 of the Terrestrial Environment TSD, GOLDER 2011g). Coniferous and mixed forest communities in the Local Study Area, including much of the Bruce nuclear site, provide important overwintering and feeding sites for white-tailed deer. The coniferous forest habitat also supports a number of bird species, including species common to woodland edge habitats and wild turkey, which use the coniferous forests for winter cover. Mixed forests, open meadow, wetlands and cultural thickets in the Local Study Area provide habitat suitable for a variety of breeding birds, including raptors that hunt over the open field. Open-water habitat throughout the Local Study Area, particularly associated with the Lake Huron shoreline, supports waterfowl breeding. During the autumn migration period, waterfowl frequently use large water bodies as staging areas where they congregate before flying south in large flocks.

The bald eagle (designated as a species of special concern) appears to have established a winter-resident population in the Baie du Doré wetland. The golden eagle has also been observed on shoreline boulders in the Baie du Doré and is considered provincially rare.

Within the Bruce Peninsula, large stands of contiguous upland coniferous and mixed forest provide habitat for many species of wildlife (Section 5.5.3 of the Terrestrial Environment TSD, GOLDER 2011g). Mammal species commonly seen throughout the Bruce Peninsula include snowshoe hare, raccoon, eastern chipmunk, eastern grey squirrel and porcupine. This habitat is also suitable for more rarely seen species such as black bear, red fox, fisher, martin and eastern massassauga rattlesnake.

The fish community in Stream C includes brook trout, rainbow trout, brown trout, and chinook salmon. Various sucker and cyprinid species including spottail shiner are known to inhabit or have been observed in Stream C. Surveys in the pools along Stream C have also identified other species including rainbow darter, creek chub and central mudminnow.

In the open waters of Lake Huron the fish encountered are those that are well adapted to the cold water and utilize open lake or deeper coastal habitats for the majority of their life cycles or the majority of the year. Species included in this category are round whitefish, lake whitefish, lake trout and deepwater sculpin. The Baie du Doré is a calmer environment with depositional areas in the inner portion. The deposition of fine sediments allows for an increase in productivity in the Baie du Doré and a more stable/productive temperature regime for many

species. Numerous studies have noted that Baie du Doré is the most important rearing and nursery area in the Local Study Area, and is used by many fish species.

The major portion of the radioactivity found in sampling fish is C-14 and naturally occurring K-40 (Section 5.7.3 of the Radiation and Radioactivity TSD, AMEC NSS 2011). In 2009, the K-40 concentrations ranged from 125 to 146 Bq/kg, consistent with the range measured in other years. In the same year, concentrations of C-14 were found at levels above provincial background (approximately 225 to 270 Bq/kg-C) in all fish caught in the immediate vicinity of the Bruce nuclear site. In 2009, the concentration of Cs-137 in fish caught in the immediate vicinity of the site ranged from 0.18 to 0.43 Bq/kg, similar to the values found in background sampling conducted at provincial sites.

2.4.8.3 Valued Ecosystem Components

The valued ecosystem components (VECs) identified in the EA for the DGR include the following biota (GOLDER 2011a to g, AMEC NSS 2011):

- Terrestrial plants – common cattail, eastern white cedar, heal-all;
- Aquatic plants – sago pondweed, variable leaf pondweed;
- Terrestrial mammals – meadow vole, white-tail deer;
- Aquatic mammals – muskrat;
- Amphibians and reptiles – midland painted turtle, northern leopard frog, northern water snake;
- Terrestrial birds – bald eagle, great horned owl, red-eyed vireo, wild turkey, yellow warbler;
- Aquatic birds – double-crested cormorant, mallard;
- Benthic invertebrates – burrowing crayfish;
- Benthic fish – bluntnose minnow, creek chub, deepwater sculpin, lake whitefish, redbelly dace; and
- Pelagic fish – brook trout, smallmouth bass, and spottail shiner.

3. EXTERNAL FACTORS AFFECTING THE EXPECTED EVOLUTION OF THE DGR SYSTEM

The postclosure safety of the DGR is assessed through consideration of a range of potential future scenarios. In order to identify and define the scenarios of interest, the assessment considers the various external, internal and contaminant factors that could affect the DGR system and its evolution (Figure 3.1). These factors may be further categorized as FEPs. For example, an earthquake is an external event, carbon steel waste package is an internal feature, and sorption is a contaminant process.

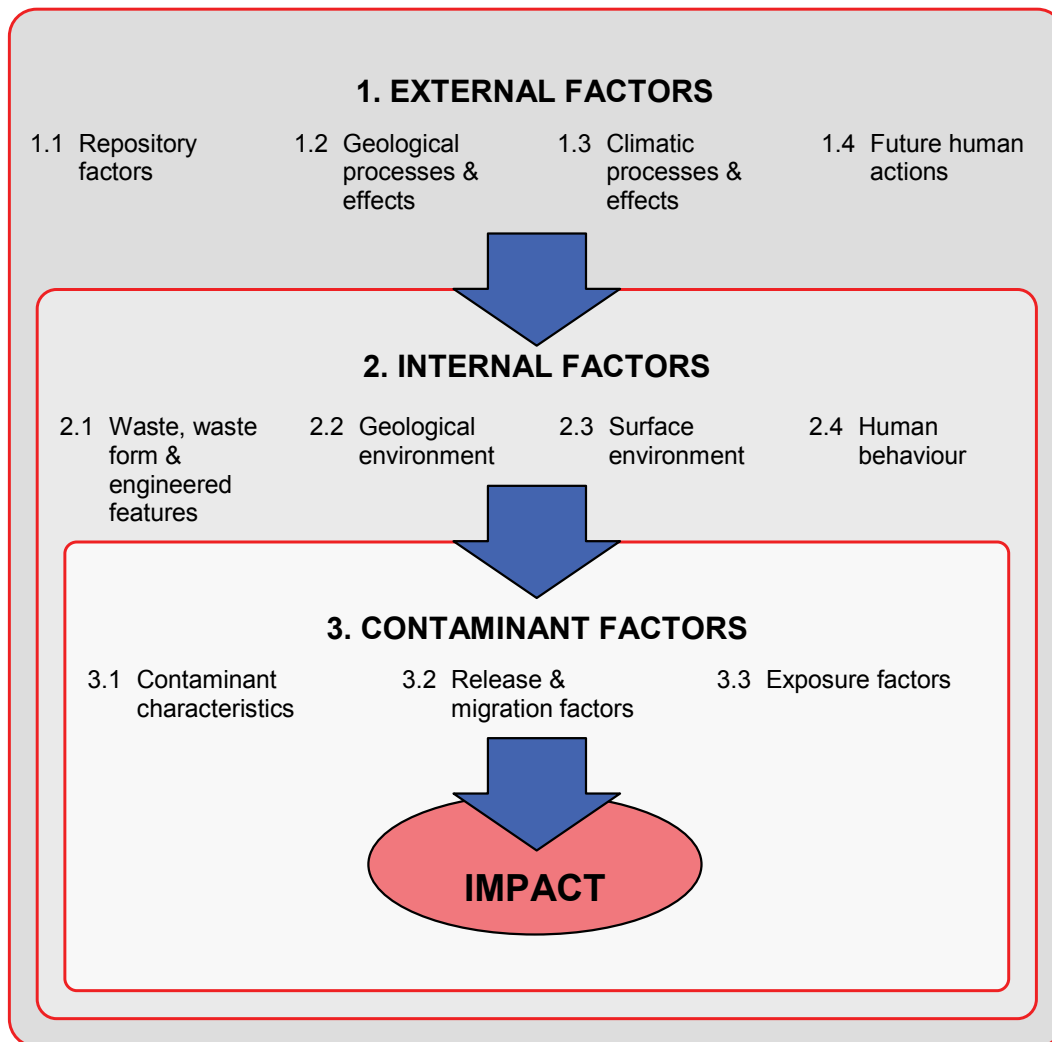


Figure 3.1: External, Internal and Contaminant Factors/FEPs

The internal and contaminant factors (Internal FEPs) occur within the spatial and temporal boundaries of the DGR system, whereas the external factors (External FEPs) originate outside these boundaries. The External FEPs provide the system with both its boundary conditions and,

in particular, include factors originating outside the DGR system that might cause change in the system. Included in this group are decisions related to repository design, operation and closure since these are outside the temporal boundary of the DGR system. If these External FEPs can significantly affect the evolution of the system and/or its safety functions (i.e., isolation and containment) within the assessment timescale (1,000,000 years), they can be considered to be scenario-generating FEPs (IAEA 2004) in the sense that whether they occur or not (or the extent to which they occur) could define a particular future scenario that should be considered within the postclosure safety assessment.

A list of potential External and Internal FEPs relevant to the DGR system has been developed (QUINTESSA et al. 2011b). This FEP list is based on lists developed in other programs, such as the international FEPs database developed by the OECD Nuclear Energy Agency (NEA 1999), the IAEA's ISAM FEP list (IAEA 2004), and the FEP list used in OPG's Third Case Study (Garisto et al. 2004). The list identifies 53 External FEPs and almost 200 Internal FEPs.

The External (scenario-generating) FEPs are listed in Table 3.1. Those that are likely to affect the DGR system and its evolution are identified and discussed in this section. The effects of less likely External FEPs and certain Internal FEPs that might lead to abnormal degradation and loss of containment (Disruptive Scenarios) are considered in Chapter 8.

The External FEPs in Table 3.1 have been reviewed, in light of information from the assessment context (documented in Chapter 3 of QUINTESSA et al. 2011a) and the system description and its supporting documents (Chapter 2 of the current report), to identify those that should be included or excluded from consideration when addressing the expected evolution of the DGR system over the timescale of interest (1,000,000 years). The resulting list of included/excluded External FEPs considered for the DGR is given in Table 3.2, together with a brief justification for their inclusion/exclusion in the assessment. Further details of the External FEPs and the justification for their inclusion/exclusion are provided in the FEPs report (QUINTESSA et al. 2011b).

From the analysis of the External FEPs presented in Table 3.2, it can be seen that the repository itself is largely unaffected by External FEPs primarily due to its depth (around 680 m below the ground surface) and the site's geological characteristics (described in Section 2.3). Although the effects of climate change resulting from continuing glacial and inter-glacial cycling are likely to cause major changes in the surface and near-surface environment, the DGR itself is intentionally isolated from the main consequences of climate change. A range of geoscientific observations can be used to provide evidence that the formations at these depths have been isolated from surface changes through the nine glacial cycles that have affected the Bruce nuclear site in the last one million years. For example, geochemical data indicate that brines in the Deep and Intermediate Bedrock Groundwater Zones are ancient (250 to 275 million years old) and that glacial meltwaters have not generally penetrated below the base of the Shallow Bedrock Groundwater Zone (Section 2.3.7). In addition, results of transient paleoclimate groundwater flow simulations undertaken for the Laurentide glacial episode (~120 ka to 10 ka BP) showed that heads in the Ordovician and Cambrian formations were little affected by Laurentide ice-sheet loading and unloading (Section 5.4.6 of the Geosynthesis report, NWMO 2011). Geomechanical modelling studies have also been undertaken to examine the impact of glacial and inter-glacial cycling on the long-term shaft integrity and emplacement room stability (Chapter 6 of NWMO 2011). While emplacement rooms would eventually collapse with repeated glacial cycles, displacements do not affect the long-term barrier integrity or permeability of the overlying Ordovician shales and the influence on EDZ evolution within the shafts is expected to be minor.

Table 3.1: External FEPs Considered

1.1	Repository Factors	
	1.1.01	Site investigations
	1.1.02	Design of repository
	1.1.03	Schedule and planning
	1.1.04	Construction
	1.1.05	Operation
	1.1.06	Waste allocation
	1.1.07	Repository closure
	1.1.08	Quality assurance
	1.1.09	Repository administrative control
	1.1.10	Accidents and unplanned events
	1.1.11	Retrieval
	1.1.12	Repository records and markers
	1.1.13	Monitoring
1.2	Geological Processes and Effects	
	1.2.01	Tectonic movement
	1.2.02	Orogeny
	1.2.03	Seismicity
	1.2.04	Volcanic and magmatic activity
	1.2.05	Metamorphism
	1.2.06	Hydrothermal activity
	1.2.07	Denudation and deposition (large-scale)
	1.2.08	Diagenesis
	1.2.09	Pedogenesis
	1.2.10	Salt diapirism and dissolution
	1.2.11	Hydrological response to geological changes
	1.2.12	Geomorphologic response to geological changes
	1.2.13	Deformation (elastic, plastic or brittle)
1.3	Climate Processes and Effects	
	1.3.01	Global climate change
	1.3.02	Regional and local climate change
	1.3.03	Sea-level change
	1.3.04	Periglacial effects
	1.3.05	Local glacial and ice-sheet effects

	1.3.06	Warm climate effects (tropical and desert)
	1.3.07	Hydrological response to climate changes
	1.3.08	Ecological response to climate changes
	1.3.09	Human behavioural response to climate changes
	1.3.10	Geomorphologic response to climate changes
1.4	Future Human Actions	
	1.4.01	Human influences on climate
	1.4.02	Social and institutional developments
	1.4.03	Knowledge and motivational issues (repository)
	1.4.04	Drilling activities
	1.4.05	Mining and other underground activities
	1.4.06	Un-intrusive site investigations
	1.4.07	Surface excavations
	1.4.08	Site development
	1.4.09	Archaeology
	1.4.10	Water management (groundwater and surface water)
	1.4.11	Explosions and crashes
	1.4.12	Pollution
	1.4.13	Remedial actions
	1.4.14	Technological developments
	1.4.15	Deliberate human intrusion
1.5	Other External Factors	
	1.5.01	Impact of meteorites and human space debris
	1.5.02	Evolution of biota

Note: From QUINTESSA et al. (2011b).

The analysis of the External FEPs shows that the DGR system might be impacted by a number of External FEPs:

- The effects of global climate change leading to glacial/interglacial cycling (FEPs 1.3.01, 1.3.02, 1.3.04, 1.3.05, 1.3.07, 1.3.08, 1.3.09, 1.3.10, 1.2.07, 1.2.09 and 1.2.13);
- The occurrence of earthquakes (FEP 1.2.03);
- Human influence on global climate (FEP 1.4.01) resulting in global warming; and
- Social and institutional developments leading to changes of land use at the Bruce nuclear site (FEP 1.4.02), and associated drilling, site development and water management (FEPs 1.4.04, 1.4.08 and 1.4.10).

Table 3.2: Status of External FEPs for the Expected Evolution of the DGR System

External FEP		Status*	Comment
1.1	Repository Factors		
	1.1.01	Included	Available data from site characterization are included (Section 2.3). All site investigation boreholes are appropriately sealed. No undetected geological features and no identified commercially viable mineral resources.
	1.1.02	Included	The DGR is built consistent with the design basis, as summarized in Section 2.2.
	1.1.03	Included	DGR is operated from 2018 to 2053 and finally closed in 2062 (Section 3.8 of the Postclosure Safety Assessment report, QUINTESSA et al. 2011a). Account is taken for decay of radioactivity prior to start of postclosure period (i.e., prior to 2062).
	1.1.04	Included	DGR is constructed as described in Section 2.2.1.
	1.1.05	Included	DGR is operated as described in Section 2.2.2.
	1.1.06	Included	LLW and ILW wastes are generally disposed in separate emplacement rooms (Table 2.8) that are laid out in the configuration describe in Section 2.2.1.4.
	1.1.07	Included	Closure of the DGR is undertaken under OPG's/NWMO's quality assurance program and is consistent with the description provided in Section 2.2.3.
	1.1.08	Included	Construction, operation, monitoring and closure of the DGR are undertaken under OPG's/NWMO's quality assurance program.
	1.1.09	Included	Controls remain effective for 300 years following DGR closure (Section 3.8 of the Postclosure Safety Assessment report, QUINTESSA et al. 2011a).
1.1.10	Excluded	Accidents and unplanned pre-closure events that could impact the long-term safety of the repository are unlikely due to the application of preventative measures. If they were to occur, then they would be mitigated before the repository was closed.	

External FEP		Status*	Comment
1.1.11	Retrieval	Excluded	The DGR design has features that improve retrievability, notably the absence of backfill in the repository rooms and tunnels, and the extended monitoring period with active ventilation of rooms before their closure. However, it is assumed that there is no retrieval of waste after repository closure.
1.1.12	Repository records and markers	Included	Any repository records are effectively maintained for 300 years following DGR closure (Section 3.8 of the Postclosure Safety Assessment report, QUINTESSA et al. 2011a).
1.1.13	Monitoring	Excluded	Monitoring during waste emplacement and after repository closure to confirm that the DGR is performing as expected is carried out in a manner to ensure that it has no consequences for the long-term safety of the DGR.
1.2 Geological Processes and Effects			
1.2.01	Tectonic movement	Excluded	Site is in a tectonically stable region away from plate margins with no tectonic activity over the timescale of interest, 1 Ma (Section 2.3.1).
1.2.02	Orogeny	Excluded	No orogenic activity over the timescale of interest (1 Ma) due to the site's location (Section 2.3.1).
1.2.03	Seismicity	Included	Earthquakes will occur over the timescale of interest (1 Ma). However, as the area is not a seismically active region, the likely magnitude, frequency and distance of earthquakes would limit their impact at the repository location (Section 2.3.8). Nevertheless, larger earthquakes could occur, in particular during retreat of ice sheets.
1.2.04	Volcanic and magmatic activity	Excluded	No volcanic or magmatic activity over the timescale of interest (1 Ma) due to the site's location (Section 2.3.1).
1.2.05	Metamorphism	Excluded	No processes occur over the timescale of interest (1 Ma) that will cause metamorphism (Section 2.3.1).
1.2.06	Hydrothermal activity	Excluded	Site is geologically stable, there are no signs of historic hydrothermal activity at the site and no drivers of hydrothermal activity are present over the timescales of interest (1 Ma) (Section 2.3.1).

External FEP		Status*	Comment
1.2.07	Denudation and deposition (large-scale)	Included	The area is topographically flat and not high above sea level so there is limited potential for large-scale denudation. However over the past 1 Ma, ice-sheet erosion and deposition has shaped the topography and could continue to do so in the future.
1.2.08	Diagenesis	Excluded	Would have negligible effect on repository safety over the timescale of interest (1 Ma).
1.2.09	Pedogenesis	Included	Glacial/ interglacial cycling will result in removal and formation of soils over the timescale of interest (1 Ma). The removal and development of soils will impact the nature of plants in the area, and therefore potentially human behaviour (e.g., feasibility of farming).
1.2.10	Salt diapirism and dissolution	Excluded	No significant salt deposits are located in the vicinity of the site (Section 2.3.2). Historically, there were salt deposits but these have already been dissolved over a long period in the distant past.
1.2.11	Hydrological response to geological changes	Included	The observed pattern of over- and underpressures in the groundwater and porewater hydraulic head data represents a state of disequilibrium due to previous geological events and related processes (Section 2.3.6.4).
1.2.12	Geomorphologic response to geological changes	Excluded	Although geomorphologic changes will occur, these will be driven by climate change (see FEP 1.3.10) rather than geological change given the site's geologically stable location and timescales of interest (Section 2.3.1).
1.2.13	Deformation (elastic, plastic or brittle)	Included	Although deformation due to tectonic movement and orogeny is unlikely over the timescale of interest (1 Ma) due to the site's tectonically stable location, deformation due to loading from ice-sheets is likely. Peltier (2011, Section 4.2.5) has estimated that the associated maximum crustal depressions might be in excess of 500 m over continental scale.

External FEP		Status*	Comment	
1.3	Climate Processes and Effects			
	1.3.01	Global climate change	Included	After an initial period of global warming, it is likely that Quaternary glacial/interglacial cycling continues since the basic solar insolation variation driving this cycling will continue (Section 6.3).
	1.3.02	Regional and local climate change	Included	Regional/local climate will respond to global climate change (Section 6.3).
	1.3.03	Sea-level change	Excluded	Changes in sea level do not affect the site due to its elevated continental location.
	1.3.04	Periglacial effects	Included	These will occur during colder climate states experienced during the glacial/interglacial cycling that is likely to occur at the site over a one million year timeframe. In particular, this would include permafrost development (Section 6.3).
	1.3.05	Local glacial and ice-sheet effects	Included	Ice-sheets are likely to cause a range of local effects. These include crustal deflection, change in rock stress (and possible earthquake initiation), changes in surface and near-surface hydrology (see FEP 1.3.07), ecosystems (see FEP 1.3.08), human behaviour (see FEP 1.3.09), and surface topography (see FEP 1.3.10).
	1.3.06	Warm climate effects (tropical and desert)	Excluded	Climate change does not result in development of tropical or hot desert conditions at the site due to its northerly latitude. There is no evidence of tropical or hot desert conditions having been present at the site during the Quaternary. An initial period of human-induced global warming will not result in extreme temperature rise resulting in tropical or desert conditions in this region.

External FEP		Status*	Comment
1.3.07	Hydrological response to climate changes	Included	Glacial/interglacial cycling impacts primarily on the hydrological conditions in the Surficial and Shallow Bedrock Groundwater Zones. Previous glaciations have had no impact on the groundwater flow in the Deep Bedrock Groundwater Zone (Section 2.3.7). Key responses are: permafrost formation; meltwater events primarily affecting the Surficial and Shallow Bedrock Groundwater Zone; and the formation of a major proglacial lake over the site during ice-sheet retreat (Section 6.3).
1.3.08	Ecological response to climate changes	Included	Flora and fauna at the site change in response to glacial/interglacial cycling (Section 6.3).
1.3.09	Human behavioural response to climate changes	Included	Human behaviour changes in response to glacial/interglacial cycling (Section 6.3).
1.3.10	Geomorphologic response to climate changes	Included	Glaciation results in significant changes to the present-day landforms found at the site (Section 6.3).
1.4 Future Human Actions			
1.4.01	Human influences on climate	Included	Human-induced global warming is likely to delay the onset of the next ice-sheet advance that affects the site (Section 6.3).
1.4.02	Social and institutional developments	Included	Controls on the development of the site are effective for 300 years following DGR closure (Section 3.8 of the Postclosure Safety Assessment report; QUINTESSA et al. 2011a). Once controls are no longer effective, land use change at the site is likely (see also FEP 1.4.08).
1.4.03	Knowledge and motivational issues (repository)	Excluded	No knowledge of the repository is assumed once controls are no longer effective. No human intrusion into the DGR due to its depth (around 680 m below ground surface - Section 2.2) and the lack of commercially viable natural resources at depth (Section 2.3.5).

External FEP		Status*	Comment
1.4.04	Drilling activities	Included	Once controls are no longer effective, the drilling of shallow water wells in the area is included since such wells currently exist in the region around the site (Section 2.4.4). However, the drilling of deep exploration boreholes at the site that penetrate to the repository is excluded from the expected evolution due to its depth (around 680 m), its relatively small panel footprint (~0.25 km ²), and the lack of commercially viable natural resources at depth in the area of the site (Section 2.3.5).
1.4.05	Mining and other underground activities	Excluded	No mining, since no commercially viable mineral resources have been identified at the site (Section 2.3.5). Other underground activities are unlikely at the site because the geology is uniform across a large area and so there is nothing unique at the site (Section 2.3). These activities would likely be preceded by exploratory drilling – see FEP 1.4.04.
1.4.06	Un-intrusive site investigation	Excluded	No direct impact on repository safety.
1.4.07	Surface excavations	Excluded	No direct impact on repository safety due to depth of repository (around 680 m).
1.4.08	Site development	Included	Site land use changes are likely once controls are no longer effective (see also FEP 1.4.02). Land uses in the previously controlled area are likely to become consistent with the land uses currently found in the area surrounding the Bruce nuclear site (i.e., predominantly agriculture and recreation – Section 2.4.7).
1.4.09	Archaeology	Excluded	No direct impact on repository safety due to depth of repository (around 680 m).
1.4.10	Water management (groundwater and surface water)	Included	The drilling of shallow water wells in the area is considered once controls are no longer effective (see FEP 1.4.04). Wells in the deeper groundwater zones are excluded since the groundwater in these zones is not potable (Section 2.3.7.1 and Table 2.10). There is present-day abstraction of groundwater in the area from the Shallow Bedrock Groundwater Zone for domestic and agricultural purposes (Sections 2.4.4 and 2.4.7). Lake Huron could also be used as a source of water.

External FEP		Status*	Comment
1.4.11	Explosions and crashes	Excluded	Surface explosions and crashes would have no direct impact on repository safety due to the depth of the repository (around 680 m). Postclosure explosions in the repository are unlikely due to absence of an ignition source and oxygen.
1.4.12	Pollution	Excluded	Impact of surface contaminants on the wastes placed in the DGR is likely to be insignificant because of the repository depth (around 680 m) and buffering capacity of the rocks above the repository (Section 2.3.2).
1.4.13	Remedial actions	Excluded	Remedial actions are unlikely following closure of repository, and if they occurred then the effects on the repository would need to be assessed at that time based on the specific remediation.
1.4.14	Technological developments	Excluded	Consistent with the recommendations of the International Commission on Radiological Protection (ICRP) (2000), Section 7.5.4 of CNSC (2006) states that human habits and characteristics should be based on current lifestyles. Therefore technological developments are not considered.
1.4.15	Deliberate human intrusion	Excluded	Excluded since it is expected that the intruders would take appropriate precaution.
1.5	Other External Factors		
1.5.01	Impact of meteorites and human space debris	Excluded	Excluded due to low probability (due to relatively small panel footprint of ~0.25 km ²) and low consequence (due to depth of repository - around 680 m).
1.5.02	Evolution of biota	Excluded	No evolution of humans assumed, consistent with ICRP's recommendation to apply the concept of (present-day) Reference Man to the disposal of long-lived solid radioactive waste (ICRP 2000). Similarly, no evolution of non-human biota assumed. General characteristics of biota are assumed to remain similar to current biota.

Notes: * Status – *Included* means that this factor is considered in the Normal Evolution Scenario. *Excluded* means that this factor is not considered in the Normal Evolution Scenario. Further discussion is provided in the FEPs report (QUINTESSA et al. 2011b).

4. EXPECTED EVOLUTION OF THE WASTE AND REPOSITORY

4.1 Contaminant Inventory

The total activity of radionuclides and the total amount of potentially important elements and or chemicals in the LLW and ILW at repository closure are presented in Section 2.1.

The inventory of contaminants in the DGR will evolve with time by decay/degradation and migration. Figure 4.1 shows the radioactivity in the repository as a function of time, considering only decay. (Contaminant migration is determined by the overall evolution of the repository.) For comparison, the figure also shows the natural radioactivity in the shale caprock above the repository as a horizontal grey band. The upper part of this band corresponds to the Bruce nuclear site area, the lower part of this band corresponds to the DGR repository footprint.

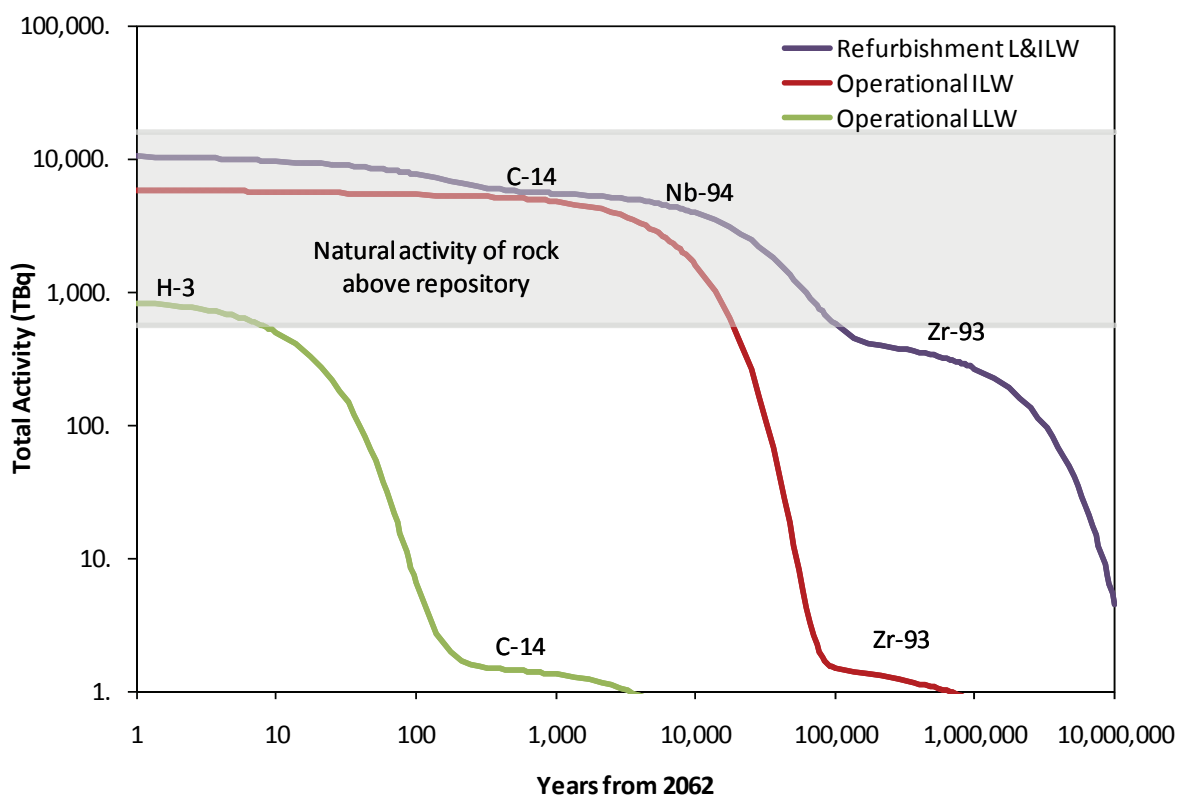


Figure 4.1: Time Dependence of Radioactivity in the Waste Due to Decay

Figure 4.1 shows that the total amount of radioactivity in the operational LLW will decay to about 1% of its 2062 value after about 100 years due to the abundance of shorter-lived radionuclides such as H-3. The total radioactivity of operational ILW and refurbishment waste will decay, though at a slower rate due to the greater amount of longer-lived radionuclides such as C-14, Nb-94 and Zr-93. Over 80% of the waste volume is LLW, and its radioactivity decays to negligible levels within a few hundred years. The long-lived radioactivity is concentrated in the 20% of ILW.

Tritium and C-14 can be present in gas or water phases, and are relatively mobile. However, while tritium is important for operational safety, its ~12 year half-life means that it decays within about a few hundred years postclosure. Nb-94 and Zr-93 are long-lived, but as they are primarily in the corrosion-resistant Zircaloy pressure tubes and as they have intrinsically low mobility in groundwater, these nuclides are very unlikely to move far from the repository. In practice, it is likely the C-14, as gas or dissolved in water, that is intrinsically of most importance to long-term safety. With its 5730 year half-life, it is potentially important for the first 60,000 years. It is worth noting that the first arrival of an ice sheet at the site, assuming that glacial cycling resumes, would occur around or after this time. That is, C-14 will have decayed by the time an ice sheet would potentially reach the site.

Figure 4.1 also shows that the residual radioactivity in the repository would have decayed towards the natural radioactivity in the rock above the repository footprint on a similar time scale of 10,000-100,000 years. After this time, the repository radioactivity remains concentrated, but from a perspective beyond the immediate DGR footprint the influence of the waste radioactivity has become small compared to the natural environmental radioactivity.

With respect to non-radioactive species in the waste, most of the wastes are common industrial type materials, and would not be considered hazardous waste. DGR waste does contain appreciable lead, present as shielding. It also contains hazardous organics (PAH, dioxins) in the incinerator ash, and asbestos waste from the stations. It does not contain PCB wastes, or hazardous liquid wastes. Some species (e.g., organic contaminants) will degrade. Even organics such as dioxins that are considered to be quite stable, are expected to degrade on assessment timescales; for example, data suggests effective half-lives of around 100 years in the subsurface environment (Adriaens et al. 1996). Other contaminants (e.g., heavy metals) will not significantly change over the entire assessment period, but can become locked into immobile mineral forms.

4.2 Thermal Evolution

The following heat-generating processes will occur in the repository:

- Radiogenic heating;
- Heat generated by corrosion of metal wastes, waste packaging and repository engineering, and microbial degradation of organic wastes;
- Heat generated by curing of the concrete monolith at the base of the shafts and shaft concrete bulkheads; and
- Heat associated with emplacement of the asphalt shaft seal.

Radiogenic heating is not significant. The only wastes that have significant heat output are the retube wastes. As this is dominated by Co-60 with a five year half-life, these packages will be stored at the surface until they have decayed enough to be emplaced without significantly affecting the rock around the emplacement rooms. At 2062, the earliest closure date for the DGR, the radiogenic heat output of the DGR will be about 2 kW (OPG 2010), less than the 10 kW geothermal flux through the ~0.25 km² panel footprint.

Heat generation from corrosion and microbial reactions will be negligible. An LLW emplacement room will contain on average about 10⁶ kg of metals and 10⁶ kg of organic wastes, and generate about 0.05 kW based on the reference corrosion rates and energy releases of 100-200 kJ/mol from each of the metals, cellulose and resins and plastic. An ILW room would have less metal and organics, and therefore even lower corrosion/degradation heat generation.

Heat generation by curing of the concrete monolith and bulkheads, and from emplacement of the asphalt seal, is of short duration and the resultant rock temperature increases are not significant. Heating can be minimized through choice of concrete and asphalt mix, and through pouring practice.

It is concluded that there will not be any significant temperature gradients in the repository postclosure, and, in the absence of glacial climate change, conditions will remain close to the ambient host rock temperature of about 22 °C. The effects of glacial cycling on repository temperature are considered in Section 5.1.

4.3 Hydraulic Evolution

Construction of the repository will draw down the porewater heads around the excavated tunnels and emplacement rooms. At the time of repository closure, the emplacement rooms will be essentially free of significant liquid water accumulations, but the atmosphere will be humid and moisture will be present in some wastes. If there is sufficient moisture in the vapour phase of the repository (i.e., for relative humidities greater than 60%), surfaces will be wetted by a thin adsorbed water layer of the order of a few nm thick. This thin water layer is sufficient to enable corrosion of metals (Appendix E of QUINTESSA and GEOFIRMA 2011).

Following closure, the repository's saturation profile will be determined by the rate of inseeping water, the rate of gas generation by degradation of organic matter and corrosion of metals (Section 4.2), and the rate at which gas migrates from the repository (Section 5.5 and Appendix A). The gas generation rate will not be constant, but will vary over time in a way that depends upon the inflow of water to support the corrosion and microbial degradation reactions. As gas is generated in the repository, the gas pressure will rise. A simple estimate of the saturation time is presented in Box 1, ignoring the effects of gas generation. The simple estimate of around 1 Ma indicates that the process will be very slow, a result that is confirmed by detailed modelling (see Figures 8.3 and 8.4 of the Gas Modelling report, GEOFIRMA and QUINTESSA 2011).

While the pressure in the repository is lower than that in the geosphere, water will seep into the repository. This will include inflow of water via the shaft. The inflow via the shaft seals and shaft EDZ will be higher than via the geosphere due to the relatively higher hydraulic conductivity of the seals and EDZ compared with the geosphere. However, the area for inflow via the shaft is small compared with the area for inflow from the geosphere. Initially the concrete and bentonite-sand shaft seals will only be partially saturated. As the shaft seals resaturate, the relative permeability for gas will decrease while that for water will increase. The shaft seals will resaturate much more rapidly than the repository due to their higher initial water saturation and the much smaller volume. A simple estimate of the resaturation time for the bentonite-sand shaft seal in the Blue Mountain formation is presented in Box 2. The resaturation time is estimated to be around 270 years. This is also consistent with detailed modelling (Figure 5.23 of GEOFIRMA AND QUINTESSA 2011), which shows that the bentonite-sand shaft seal in the Blue Mountain formation has nearly resaturated after 300 years.

If gas generation continues and the gas pressure increases above the geosphere environmental pressure, then the repository will begin to desaturate as the water is pushed back into the rock. If the gas pressure in the repository rises above the geosphere gas pressure, then gas will begin to permeate into the rock adjacent to the repository. The potential gas pressure in the DGR is explored in Box 3 and Appendix B.

BOX 1: RESATURATION TIME FOR THE DGR EMPLACEMENT ROOMS

At closure the emplacement rooms will contain air that is trapped. As water flows into the rooms the trapped air will be compressed and the pressure will increase. However, ignoring gas generation in the DGR, the pressure will not increase significantly relative to the geosphere environmental pressure until the rooms are almost fully resaturated. (The pressure increase is inversely proportional to the volume change, and the geosphere environmental pressure is approximately 60 times the initial gas pressure, i.e., atmospheric pressure). Therefore, it can be assumed that the head difference between the geosphere and the rooms is equal to the geosphere environmental pressure head throughout the resaturation period. At closure there is likely to be some desaturation of the rock around the rooms: particularly of the EDZ. It is assumed that resaturation of this desaturation fringe is instantaneous.

These simplifying assumptions mean that the inflow rate can be considered to be constant with time. The resaturation time is therefore equal to the volume to be resaturated divided by the inflow rate.

The inflow rate (Q) can be calculated using the Polubarinova-Kochina formula for inflow into a tunnel, for $R \ll D$ (Lei 1999):

$$Q = qL = \frac{2\pi K(d - \phi_0)}{\ln(2D/R)} L$$

Where,

q is the inflow rate per unit length of tunnel ($m^3/(s\ m)$),

K is the hydraulic conductivity of the rock (m/s),

d is the water depth above ground (m) (for example if the tunnel passes under a lake or river),

ϕ_0 is the hydraulic head at the tunnel perimeter (m),

D is the depth of the tunnel's centreline (m),

R is the tunnel radius (m), and

L is the tunnel length (m).

Using the following parameters, the inflow rate equals $0.011\ m^3/a$. The corresponding repository resaturation time is 1.0 Ma.

Parameter	Value	Reference
Emplacement room radius	~3.5 m	Table 4.3 of the Data report, QUINTESSA and GEOFIRMA (2011).
Emplacement room length	250 m	Table 4.3 of the Data report, QUINTESSA and GEOFIRMA (2011).
Water depth above ground	0 m	Assume water table at the ground surface.
Depth of centreline of emplacement room	678.6 mBGS	DGR operating floor is at 682.1 mBGS, Section 4.2 of QUINTESSA and GEOFIRMA (2011), plus tunnel radius of 3.5 m.
Hydraulic conductivity	2E-15 m/s	Vertical conductivity of the Cobourg in Table 5.5 of QUINTESSA and GEOFIRMA (2011) – note it assumed that the majority of flow is vertical because the repository is effectively a 2D planar feature.
Environmental pressure head	6.25 MPa	(Figure 2.24). Average density of water column = $\sim 1100\ kg/m^3$ (Figure 2.25) Pressure head at the tunnel perimeter = $6.25E6\ Pa / (1100\ kg/m^3 \times 9.81\ m/s^2) = 579\ m$.
Emplacement room void volume	$1.14E4\ m^3$	$3.53E5\ m^3$ for 31 rooms in Tables 4.5 and 4.3 of QUINTESSA and GEOFIRMA (2011).

BOX 2: RESATURATION TIME FOR THE BENTONITE-SAND SHAFT SEAL IN THE BLUE MOUNTAIN FORMATION

The resaturation time for the bentonite-sand seal in the Blue Mountain formation (i.e., near the base of the shaft) can be calculated using a similar approach to Box 1. However, the calculation is complicated bentonite-sand: when partially saturated this material exerts a strong capillary suction that will increase the hydraulic gradient. The magnitude of this suction will decrease as the bentonite-sand resaturates. The hydraulic conductivity of the bentonite-sand will also increase with resaturation.

The rate of inflow is calculated from a simple radial flow calculation (Fetter 1994):

$$Q = 2\pi r b K \left(\frac{dh}{dr} \right)$$

Where,

Q is the inflow rate through a circular section at a distance *r* from the shaft (m³/s),

(Note that *Q* is constant at any *r*, but the hydraulic gradient and area change with *r*),

r is the radial distance from the circular section to the shaft (m),

b is the aquifer thickness (m),

K is the hydraulic conductivity of the rock (m/s), and

(*dh/dr*) is the hydraulic gradient (-).

For this simple calculation any vertical flow within the shaft seals and/or EDZ is neglected. The circular section through which the inflow is calculated is taken to be in the middle of the EDZ. This is consistent with the assumption that the pressure drop from the environmental pressure head in the Blue Mountain formation to atmospheric pressure in the seal occurs across the EDZ because it is far more permeable than the undamaged rock. The relationship between saturation, capillary suction and permeability is described in Section 4.7 of the Data report (QUINTESSA and GEOFIRMA 2011).

Parameter	Value	Reference
Radius of main shaft	4.575 m	Table 4.7 of QUINTESSA and GEOFIRMA (2011).
K Blue Mountain formation	5E-14 m/s	Table 5.5 of QUINTESSA and GEOFIRMA (2011).
Thickness of Blue Mountain formation	42.7 m	Table 5.1 of QUINTESSA and GEOFIRMA (2011).
Thickness of EDZ	4.575 m	Table 5.7 of QUINTESSA and GEOFIRMA (2011).
Porosity bentonite sand	0.29	Section 4.5.4.2 of QUINTESSA and GEOFIRMA (2011).
Environmental pressure head	5 MPa	Figure 2.24. Average density of water column = ~1100 kg/m ³ (Figure 2.25)). Hydraulic head at the tunnel perimeter = 5.0E6 Pa/(1100 kg/m ³ x 9.81 m/s ²) = 463 m.
Two phase flow parameters for bentonite/sand	α = 1E-7 /Pa, m = 0.4 n = 1.8 S _{lr} = 0.01 S _{gr} = 0.01	Table 4.28 of QUINTESSA and GEOFIRMA (2011).
Initial water saturation bentonite-sand	0.8	Section 4.7.5 of QUINTESSA and GEOFIRMA (2011).

Because the capillary suction is significant, and changes with saturation, resaturation was calculated using a spreadsheet with a 1 year time step. At each time step, the hydraulic conductivity was set at the minimum of the (saturated) horizontal conductivity in the Blue Mountain formation, and the calculated unsaturated hydraulic conductivity of the bentonite sand, since the lower of the two conductivities will control the resaturation rate. The former was always lower. The resaturation time was calculated to be ~270 a.

BOX 3: POTENTIAL GAS PRESSURES

Appendix B presents simple insight calculations regarding the gas pressures that could be generated in the DGR due to corrosion of metals and microbial degradation of organics. The simple calculations assumed complete fermentation of organics to gas with no generation of biomass, and no loss of gas. The results are summarized below and show that gas pressures in the order of 10 MPa can be expected.

Case 1 considers the potential gas pressures, assuming all wastes are converted to gas and ignoring any gas-consuming reactions. Cases 2 and 3 explore the impacts of two gas-consuming reactions: CO₂ enhanced corrosion of steel forming siderite (FeCO₃) and microbial reduction of CO₂ with hydrogen forming CH₄. The summary table below shows that the latter methanogenic reaction is the most important process for reducing gas pressure.

Gas Generation	Initial Mass of Metals or Organics (kg)	Gas Pressure (MPa)		
		Case 1	Case 2	Case 3
		Anaerobic Corrosion & Degradation	Case 1 with FeCO ₃ Formation	Case 1 with Methanogenic Reaction
H ₂ from metal corrosion	6.6E+07	9.1	8.1	0.0
CO ₂ from organic degradation	2.2E+07	3.0	0.0	0.7
CH ₄ from organic degradation		4.4	4.4	6.6
N ₂ from initial air	-	0.1	0.1	0.1
Total	8.8E+07	16.6	12.6	7.4

Detailed modelling shows that gas pressures in the order of 7-9 MPa can be expected, comparable to or somewhat larger than the steady-state hydraulic pressure at repository level (7-8 MPa) and much less than the lithostatic pressure (17 MPa) (see Figures 8.1 and 8.2 of the Gas Modelling report, GEOFIRMA and QUINTESSA 2011).

Eventually gas generation will cease due to complete consumption of metals and organics. The long-term gas composition will likely be primarily methane, with some H₂ and/or CO₂ dependent in part on the extent of conversion of H₂ and CO₂ to CH₄. Once gas generation ceases, the DGR will slowly equilibrate with the surrounding host rock, due to migration of bulk gas or dissolved gas into the geosphere and shaft, or alternatively migration of formation gas from the rock into the repository space. This equilibration will be a slow process, occurring on a million year time frame (see Appendix A).

Migration of gas in the shaft is discussed in conjunction with migration of gas in the geosphere, in Section 5.5.

4.4 Mechanical Evolution

4.4.1 Emplacement Rooms and Repository Tunnels

The DGR rooms will be oriented in the direction of major principal horizontal stress, so as to maximize stability (Section 6.3 of PSR, OPG 2011b). However, the following mechanical processes are likely to occur in the repository at some point:

- Failure of waste containers due to corrosion;
- Self-compaction of the waste stacks as the wastes and containers degrade; and
- Rockfall from roofs and pillars (i.e., the rock wall between adjacent emplacement rooms) in the emplacement rooms and tunnels.

These processes will result in release of wastes from the containers, long-term compaction of the waste and reduction in the waste height.

The majority of wastes will be disposed in carbon steel containers such as drums and boxes that are not anticipated to last for more than tens to a few hundred years post-closure. As the containers corrode, they will fail and release their contents. Wastes released from the containers will fill the void spaces in the emplacement room. The corroding containers at the bottom of the waste stacks will collapse due to the weight of overlying wastes.

As the containers fail and collapse, wastes may be transferred from above the water level in the DGR to below the water level.

Failure of the rock, weakened by excavation stress relief and long-term strength degradation, and induced by ice-sheet loading/unloading, will eventually occur as the rooms will not be backfilled. Seismic events will promote the fall of already fractured and loose rock mass. The broken rock will occupy a larger volume than the in-situ rock, described as a bulking factor. For a bulking factor of 1.3 (the lower end of the range given in Whittaker and Reddish 1993), it can be shown that the 7 m high rooms would fill after about 20 m of rockfall, taking no credit for the waste packages (Box 4).

BOX 4: MAXIMUM EXTENT OF ROOF COLLAPSE

If all the collapsed material was sourced from the room/tunnel roof, then the height of the collapse zone, h_c , can be calculated using a simple volume balance:

volume prior to collapse = volume following collapse and stabilization

$$h_c v_r + h_{ro} v_{ro} = (h_c + h_{ro}) v_c$$

Where,

h_c is the height of the collapse zone (m)

v_r is the void fraction in the undamaged rock (effectively 0)

h_{ro} is the height of the room/tunnel (m)

v_{ro} is the void fraction in the room (equals 1 if the waste is ignored)

v_c is the void fraction in the collapsed rock

For a bulking factor of 1.3, i.e., the volume of the collapsed rock is 1.3 times that of undamaged rock, then v_c equals $(1.3-1)/1.3 = 0.23$.

For a 7 m high room, and ignoring the presence of the waste, the height of the collapse zone is 23 m. If the packages (minus internal volume) fill about 50% of the room volume, the collapse height is reduced to 8 m.

More detailed geomechanical modelling of the stability of the repository has been undertaken at room and panel scales, considering in situ stresses, long-term strength degradation, water/gas pressures in rock and caverns, glacial loading, and seismic loading. The modelling showed that the rooms remained largely intact at least until the first glaciation.

The seismic modelling was based on a Probabilistic Seismic Hazard Analysis that defined the likely peak ground accelerations for 10^{-5} per year and 10^{-6} per year exceedance frequencies (Section 6.2.2.1 of NWMO 2011). The analyses showed that the rooms and pillars will remain stable for seismic events of $M \leq 5$ at 15 km from the site and $M \leq 6.5$ at 50 km from the site. Seismic shaking did not cause significant additional damage or fracturing of the rock mass before first glaciation when the rock is relatively unfractured. The seismic shaking does promote unravelling of already fractured and loose rock mass (Section 6.4 of NWMO 2011).

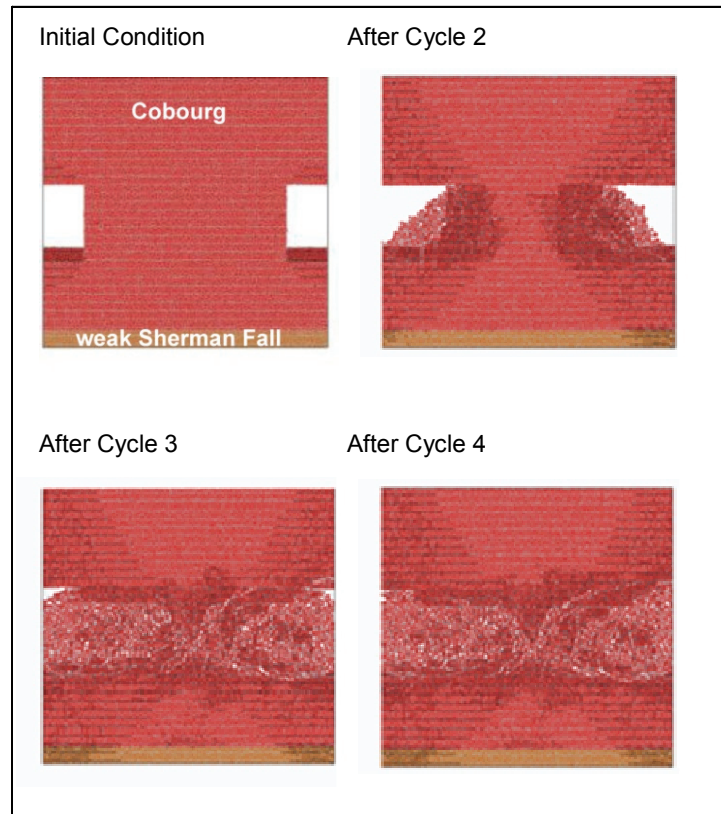
The modelling also shows that after ice-sheet loading and unloading will cause the pillars between the rooms to degrade and there will be rockfall into the rooms. After several glacial cycles, there will be no further rockfall since the fallen material has become self-supporting and the system is mechanically stable (Figure 4.2). The damage would be contained within the Cobourg formation, about 10 m into the roof (Section 6.4 of NWMO 2011) (and consistent with the simple calculation in Box 4). The models used conservative parameters, such that they will tend to overestimate the extent of damage and rate of rockfall (e.g., rock properties and no allowance for waste packages in rooms).

Under non-glacial conditions, the rockfall does not modify the total gas 'headspace' in the DGR since the total amount of void space remains constant, but is just distributed within a larger volume of rock. There are no direct consequences for the resaturation and pressure evolution of the DGR. During the first glacial cycle, panel-scale mechanical modelling (Section 6.4.5 of NWMO 2011) shows that the roof of the DGR will be compressed relative to the floor due to the transmitted mechanical load. The volume of the excavations will decrease by about 8% (the effect of a 0.45 m reduction in roof height, Figure 6.43 of NWMO 2011, on the repository void volume), and this will lead to a corresponding increase in gas pressure. The hydraulic load from the ice sheet is transmitted at a rate dependent on the overlying rock hydraulic conductivity and storativity, and generally does not fully penetrate to the repository depth (see Section 5.2.3).

4.4.2 Shafts

The chemical and biological processes that operate on the shaft materials (Section 4.5) can result in a number of physical changes which in turn will affect the mechanical evolution of the shaft and its materials. The physical changes include the following.

- Cracking due to stresses and/or phase changes in concrete. Cracking will change the hydraulic conductivity.
- Changes in concrete porosity due to leaching (especially from bulkheads that intersect the more permeable rock formations) and due to precipitation of new phases (especially at bentonite-cement interfaces). Changes in the porosity will also result in changes in the hydraulic conductivity, diffusivity and sorption.
- Changes in bentonite properties, including embrittlement and loss of swelling capacity, especially in contact with concrete. The swelling pressure against the shaft walls will affect the quality of the seal at this interface.
- Microbial degradation of asphalt possibly leading to porosity increase, embrittlement and cracking, and an increase in hydraulic conductivity.



Note: Adapted from Section 6.4 in NWMO 2011.

Figure 4.2: Rockfall within and around the Emplacement Rooms after Four Glacial Cycles

However, the rate of these chemical processes is anticipated to be very low due to the low permeability of the host rock and shaft materials which limits the rate at which the aqueous species can mix, and the low temperatures, and therefore the effects are expected to be limited to zones at interfaces (see Section 4.5). The concrete is expected to degrade the most, with the formation of cracks that result in increased hydraulic conductivity, while retaining its basic mechanical support capability through its aggregate content. As a result, in the long-term the concrete behaves more as a mechanical support than as a seal, whereas the bentonite-sand and asphalt will tend to saturate and creep/swell so as to maintain the long-term seal.

Similar to the emplacement rooms, geomechanical models have been used to understand how the rock around the shaft will evolve in response to the stress relief, ice-sheet loading and unloading, gas pressures, and seismic shaking (Section 6.4.3 of NWMO 2011). In general, the models showed that the majority of the EDZ development occurs during the initial shaft excavation phase. Once the shafts have been backfilled, they will be significantly stabilized due to the increase in confinement. The extent of the EDZ was calculated to be slightly greater than the radius of the shaft for the Cabot Head formation, which has the weakest rock, and significantly smaller for the other geological formations.

Long-term concrete bulkhead strength degradation and pore pressure evolution will both lead to active mechanical processes within the existing EDZ and some further development of the EDZ adjacent to the bulkheads and bentonite-sand backfill. Due to the vertical geometry of the shaft,

glacial loading has only a minor effect on EDZ development, because differential ground stresses in the horizontal plane are small. Consequently, the effect of EDZ increase during glaciations is minor for the shaft. Similarly, pore pressure and seismic loading will not significantly increase the predicted EDZ around the shaft (Figure 4.3).

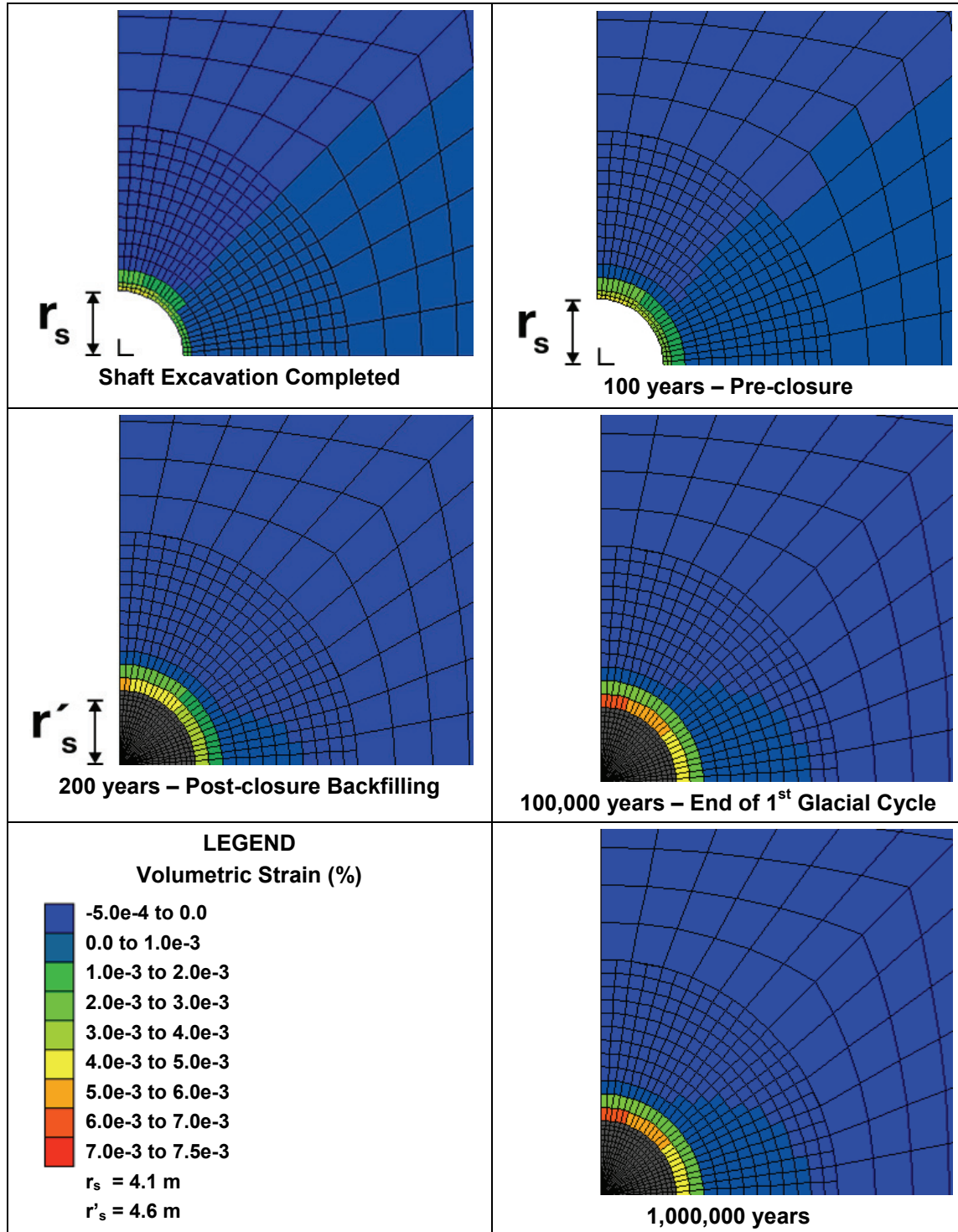
Overall, the combined effects could increase the yielding of the shaft wall, and hence the extent of the EDZ. These changes are addressed in the safety assessment through use of conservative estimates for the extent of the EDZ, e.g., using the EDZ formed in the weakest rock formations as the reference (values given in Chapter 5 of the Data report, QUINTESSA and GEOFIRMA 2011).

4.5 Chemical and Biological Evolution

Chemical and biological reactions in the waste packages and repository engineering materials will result in evolution of the repository including the shafts. The nature of the reactions will be dependent on the materials present in the waste packages and engineered structures (see Sections 2.1 and 2.2, respectively), and the hydrogeological and geochemical conditions in the DGR system (see Sections 2.3.6 and 2.3.7, respectively).

The chemical conditions in the repository and its shafts can be expressed in terms of key parameters, namely: pH, redox state, salinity, $p\text{CO}_2$, total inorganic carbon content, SO_4 concentration and quantities of any mineral precipitates (e.g., calcite in cementitious materials). These factors will influence, in particular, the characteristics of contaminant release and migration.

Key materials of interest include metals (in particular ferrous metals), organic materials, cementitious materials and engineered barrier materials (such as bentonite-sand, cement, and asphalt). Each will evolve over the period of interest as a result of the characteristic reactions discussed in this section.



Note: Figure 6.20 in NWMO (2011).

Figure 4.3: Evolution of Volumetric Strain in the Rock Adjacent to Shaft Concrete Bulkhead B1 (Lions Head Formation) Considering Time-dependent Strength Degradation, Glacial Loading and Pore Pressure

The chemical and biological evolution of the repository and its shafts will be affected by the availability of water needed for chemical and microbial reactions. The quantity of water in the repository will be a function of the porewater pressure in the rock, the gas pressure in the repository, the properties of the host rock (which is of low permeability and limited porosity, and so limits inflow) and the water inflow from the shafts. The gas pressure itself will be dependent on the rate of water inflow as well as the rock permeability, and will act to decrease the water inflow rate. The inflow of water into the shafts will be a function of the porewater pressure in the surrounding rock and the shaft seal materials, the water pressures in the shaft, and the properties of the surrounding rock and the shaft seal materials. The hydraulic evolution of the repository and shafts is discussed in Section 4.3.

The following chemical and biological processes are expected to be the most important in the repository.

- 1) Corrosion of steel, resulting in the consumption of O_2 and water, and the generation of H_2 . The process will result in the degradation of containers and rockbolts, and release of contaminants from the wastes.
- 2) The microbiological degradation of the organic wastes and the associated generation of CO_2 and CH_4 (which may be labelled with C-14). An active microbial population would also support H_2 and CO_2 reactions, including in particular methanogenic reduction of CO_2 with H_2 , forming CH_4 .
- 3) The equilibrium between CO_2 as gas, carbonate in water and carbonate rock, and possibly with cement.
- 4) The leaching and degradation of cements. Leaching of cements, and other degradation reactions such as sulphate attack and mechanical stresses, will also ultimately result in an increase in permeability of cementitious barriers.

These processes will result in the general evolution of the redox conditions from aerobic to anaerobic. The generation of gases will act to increase gas pressure and reduce pH in the repository. This reduction in pH will also result from the formation of organic acids but is expected to be offset by the leaching of concrete in the repository, generation of oxyhydroxide phases from anaerobic corrosion of steels, and buffering by the limestone (calcite) host rock. There will be an increase in salinity in the repository due to the ingress of saline porewater from the host rock and the consumption of initial water in the wastes during anaerobic corrosion of steels. The anticipated evolution of key geochemical parameters is summarized in Table 4.1.

Geochemical calculations that illustrate the potential impacts of metal corrosion and organic degradation on pH and redox conditions in the DGR are presented in Appendix C.

The processes associated with each of the key groups of materials in the emplacement rooms, repository tunnels and shafts are discussed in more detail in the following sub-sections. Although gases (principally H_2 , CO_2 and CH_4) will be generated in the DGR through metal corrosion and microbial degradation (fermentation) reactions, methane and carbon dioxide hydrates are not expected to form (see Appendix D).

Table 4.1: Summary of the Expected Evolution of Key Geochemical Parameters

Parameter	LLW Rooms	ILW Rooms	Concrete	Bentonite	Asphalt	Engineered Fill	EDZ
pH	Likely to be similar to background (~ pH 6.5) with potential increase in pH due to degradation of cement on ceilings, walls and floors and in wastes being offset by decrease caused by acidity induced by H ₂ production CO ₂ and/or organic acids from waste package degradation.	Likely to be slightly higher than LLW rooms due to increased amount of concrete associated with waste packaging. Local to cementitious waste packages higher pH conditions can be expected to develop.	In the structural concrete, there will be a rapid increase of pH > 13 in concrete pore fluids, decreasing in stages to ~12.5, pH ~10, and eventually to a pH close to that of the groundwater. In the LHHPC cement, the initial pH of pore fluids will be ~10, after which pH will decrease eventually to that of ambient groundwater in a similar fashion to structural concrete.	Front of high pH moving several cm from concrete monoliths/bulkheads. pH = 6.5-8 in rest of bentonite.	Front of high pH moving several cm into asphalt from concrete monoliths/bulkheads. No significant water in rest of asphalt.	Due to relatively high permeability of fill and surrounding geosphere, assumed to equilibrate with ambient groundwater over 100 years.	Unchanged from initial conditions (except where the EDZ is adjacent to cementitious materials in which case there may be a small (< 1 pH unit) increase).
Redox	Initially oxidizing, becoming anaerobic over 100 years Redox defined by anaerobic steel corrosion (Eh = -400 mV at pH 7). Once steel is consumed, redox conditions return to natural values	Initially oxidizing, becoming anaerobic over 100 years Redox defined by anaerobic steel corrosion (Eh = -400 mV at pH 7). Once steel is consumed, redox conditions return to natural values	Initially oxidizing, becoming anaerobic over 100 years due to equilibration with ambient groundwater.	Initially oxidizing, becoming anaerobic over 100 years due to pyrite dissolution in bentonite and equilibration with Fe ²⁺ in smectite.	Entirely anaerobic, except at interfaces during initial 100 years, owing to very little capacity to admit oxygen and consumption of any small quantity of oxygen present during small amounts of degradation.		Initially oxidizing, becoming anaerobic over 100 years initial oxygen consumption by pyrite oxidation and aerobic steel corrosion. Subsequently, redox defined

Parameter	LLW Rooms	ILW Rooms	Concrete	Bentonite	Asphalt	Engineered Fill	EDZ
	buffered by pyrite –SO ₄ (aq) and ferroan carbonate – hematite (expected to be in range -150 to 0 mV).	buffered by pyrite – SO ₄ (aq) and ferroan carbonate – hematite (expected to be in range -150 to 0 mV).					by anaerobic steel rock bolt corrosion (Eh = -400 mV at pH 7).
Salinity	Increase in salinity as high salinity porewater enters the repository and the initial water in the wastes is consumed by anaerobic corrosion of steel.	Increase in salinity as high salinity porewater enters the repository and the initial water in the wastes is consumed by anaerobic corrosion of steel.	Will become comparable with background levels with time.	Will become comparable with background levels with time.	Will become comparable with background levels with time.		No significant change with time.
pCO₂ (Defined by TIC at given temperature and pH)	Net increase initially (100 years) due to degradation of organics. Net decrease thereafter due to conversion of CO ₂ to CH ₄ .	Net decrease due to conversion of CO ₂ to CH ₄ and Ca CO ₃ .	Minor decrease due to carbonation of cement.	Minor decrease due to carbonation of bentonite/concrete interface.	Minor increase due to conservative assumption of microbial breakdown at interfaces; no change in bulk asphalt.		As per ILW or LLW according to location.
Total inorganic carbon (TIC)	Net increase initially (100 years) due to degradation of organics. Net decrease thereafter due to conversion of CO ₂ to CH ₄ .	Minor decrease due to carbonation of cement (any CO ₂ entering the ILW rooms in the gaseous phase from elsewhere in the repository would be consumed rapidly after dissolution).	Minor decrease due to carbonation of cement.	Minor decrease due to carbonation of bentonite/concrete interface.	Minor increase due to microbial breakdown at interfaces; no change in bulk asphalt.		Unchanged from initial conditions.

Parameter	LLW Rooms	ILW Rooms	Concrete	Bentonite	Asphalt	Engineered Fill	EDZ
SO₄ concentration	Small amount of SO ₄ in porewater consumed due to microbial reaction with H ₂ over 100 years.	Small amount of SO ₄ in porewater consumed due to microbial reaction with H ₂ over 100 years.	No significant change with time. Minor exchange of SO ₄ for OH ⁻ in cement.	No significant change with time. Minor exchange of SO ₄ for OH ⁻ in cement at the bentonite/concrete interface.	No significant change with time. Possible minor reduction if microbial degradation occurs at interfaces.		Repository EDZ: SO ₄ totally consumed due to microbial reaction with H ₂ over 100 a. Shaft EDZ: no significant change with time.
Porosity	No significant change with time.	No significant change with time.	Possible slow net increase due to leaching.	Porosity decrease at alteration front in bentonite due to mineral precipitation.	No significant change with time.		Possible slow decrease due to self-sealing by argillaceous components of shale or precipitation of minerals like calcite.
Main mineral precipitates	Calcite growth associated with cement carbonation. Possible ettringite/gypsum growth in cement. Iron oxyhydroxide growth on iron components during initial oxic conditions, and then minerals like magnetite and siderite ultimately under anoxic conditions.	Calcite growth associated with cement carbonation. Possible ettringite/gypsum growth in cement. Iron oxyhydroxide growth on iron components during initial oxic conditions, and then minerals like magnetite and siderite ultimately under anoxic conditions.	Calcite growth associated with cement carbonation. Possible growth of ettringite/gypsum in cement. Iron oxyhydroxide growth on iron components during initial oxic conditions, and then minerals like magnetite and siderite ultimately under anoxic conditions.	New mineral growth limited largely to interface with cement, associated with cement carbonation. Migration of C-S-H -zeolite front through bentonite.	Possible minor precipitation of sulphide minerals at interfaces if microbial degradation occurs.		Iron oxyhydroxide growth on rock bolts during initial oxic conditions, then minerals like magnetite and siderite ultimately under anoxic conditions.

4.5.1 Corrosion of Metals

There will be a number of different metallic materials present in the repository, in the form of waste container materials (typically carbon-steel, galvanized steel, or stainless steel), as structural components (such as carbon-steel rails and rock bolts), or as wastes (Zr-based retube wastes and large components such as steam generators and copper alloy heat exchangers).

For the postclosure safety assessment, these materials are classified as belonging to one of the following four corrosion categories:

1. Un-passivated carbon-steel (carbon-steel, painted carbon-steel, galvanized steel and copper alloy⁵);
2. Passivated carbon-steel (comprising carbon-steel overpacked in concrete, rebar, and rock bolts all of which are in contact with alkaline cementitious pore fluids that will result in the formation of a passive oxide film);
3. Passive alloys (all stainless steels and austenitic Ni-alloys, including alloys such as Inconel 600 used in steam generator tubes); and
4. Zirconium alloy (Zr alloy pressure tubes and calandria tubes).

These different categories represent alloy classes with a range of corrosion rates, ranging from the rapidly corroding ("active") materials, such as carbon-steel, to the more-slowly corroding passive materials, such as the steam generator Inconel and pressure tube Zircaloy alloys. As an illustration of the relative rates of corrosion, a 1 mm thick section of material would corrode under anaerobic conditions in times ranging from of the order of 500 years for the carbon steel to 100,000 years for the most-passive alloys.

In aqueous environments, corrosion is an electrochemical process involving the coupling of at least a single anodic reaction (e.g., the dissolution of carbon-steel (Fe) as ferrous ions (Fe^{2+})) and the cathodic reduction of at least one oxidant (e.g., O_2 , H_2O , or H^+). These electrochemical reactions will occur in the thin water layers formed in sufficiently humid atmospheres, with the threshold relative humidity for corrosion typically being in the range 60-70% (Leygraf and Graedel 2000, Shreir et al 1993). Therefore, corrosion of the metallic waste forms and containers will start during the operational phase, and continue with repository closure.

The mechanisms of corrosion of metallic surfaces under humid and inundated conditions are slightly different. Although many of the same reactions occur under both sets of conditions, the relative importance of different processes is affected by the difference in the rates of mass transport and differences in the chemistry of the aqueous phase. For example, the mass transport of O_2 to the corroding surface is typically higher for unsaturated surfaces exposed to humid air than for submerged surfaces, resulting in higher rates of aerobic corrosion. This effect is somewhat offset, however, by the greater propensity for the formation of (protective) corrosion product films in the thin liquid layer as super-saturation of the aqueous phase with respect to corrosion products is more readily achieved.

⁵ It is recognised that assuming the corrosion rates of copper alloys are the same as for carbon steel is a conservative assumption, both in terms of the rate of H_2 generation and the amount of gas formed. The mass of copper alloys is relatively small (Table 2.9, OPG 2010).

4.5.1.1 Corrosion of Ferrous Metals

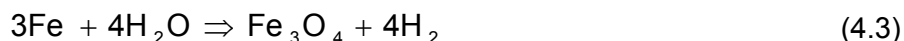
Over a relatively short period of time (less than 10 years), corrosion of the ferrous materials results in the consumption of O₂ in the closed repository and the evolution from aerobic to anaerobic conditions. The aerobic corrosion of iron-based materials can be described by the reaction:



where "FeOOH" represents a generic ferric oxyhydroxide species, which may also contain groundwater species (Cl, SO₄²⁻, CO₃²⁻) in various forms of green rust. As the environment becomes anoxic, the Fe(III) corrosion products will likely be converted to magnetite rather than Fe(OH)₂ via the Schikkor reaction:



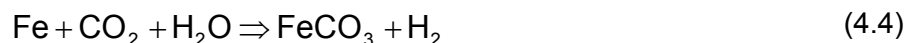
Uncorroded ferrous metals will also form magnetite through anaerobic corrosion processes such as:



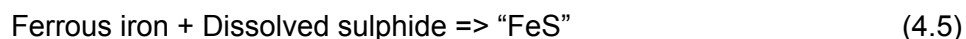
After the oxygen is consumed, the redox potential will be defined by the next most-dominant redox couple, which in turn depends on the concentrations of the redox agents and their corresponding rates of reaction. Given the large inventory of Fe-based materials in the repository, the most likely redox-controlling couple is the Fe(II)/Fe(III) couple (Box 5).

The hydrogen gas that is liberated can accumulate and contribute to the increase in gas pressure in the repository.

The degradation of organic materials, discussed in Section 4.5.2, will increase the partial pressure of CO₂ (pCO₂) initially, and may therefore stabilize siderite (FeCO₃) as the principal corrosion product:



At an early stage during the evolution of the repository environment, it is likely that sulphate will be reduced to sulphide as a result of microbial activity. Much of the sulphide formed will be precipitated as iron sulphide due to the excess Fe(II) in the system:



where "FeS" represents amorphous Fe(II) sulphide, most likely non-stoichiometric.

These reactions are expected to describe the primary corrosion behaviour of metals in the first three categories listed above, namely un-passivated carbon steel, passivated carbon steel, and the passive alloys. This is reasonable given the predominance of ferrous alloys in the repository.

BOX 5: REDOX-CONTROLLING COUPLES

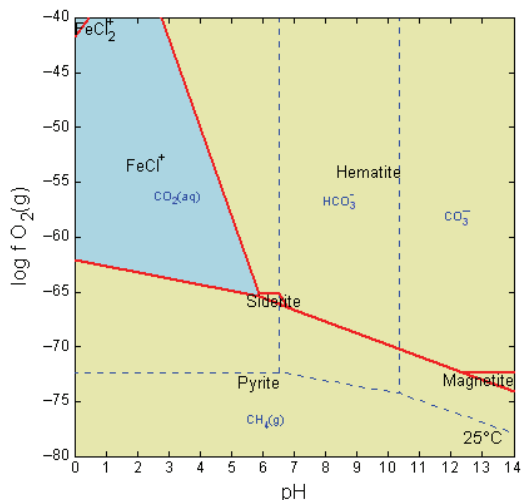
Chemical disturbances inevitably occur when sampling porewater from rock core or deep groundwater from boreholes. Therefore, it is usually impossible to determine directly from chemical analyses which oxidized and reduced aqueous species (e.g., the redox couples $\text{Fe}^{2+}/\text{Fe}^{3+}$, $\text{SO}_4/\text{H}_2\text{S}$ and $\text{CH}_3\text{CH}_2\text{OH}/\text{CH}_4$) are at chemical equilibrium and hence indicate the water's redox state. Normally it is necessary to use mineralogical information to estimate the water's redox state and then to deduce the important aqueous redox couples.

At temperatures such as those of the DGR (about 22°C), redox-sensitive minerals and dissolved redox-sensitive aqueous species are not expected to be equilibrated, unless there is microbial mediation. However, equilibrium geochemical simulations can indicate the redox conditions towards which the groundwater/rock is evolving.

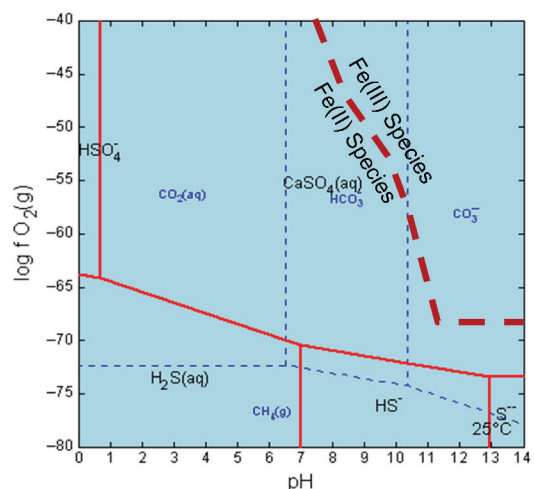
The host rock of the DGR (the Cobourg Formation) contains the following solid phases that potentially could participate in redox reactions (INTERA 2011):

- Organic matter, including bitumens;
- Sulphides (mostly pyrite, some sphalerite, marcasite and chalcopyrite);
- Sulphates (anhydrite, gypsum and some celestite);
- Ferroan carbonate minerals (Fe-bearing calcite and dolomite, and ankerite);
- Ferrous Fe-bearing silicates (principally chlorite); and
- Fe-oxides, dominantly hematite, but possibly some Fe-oxyhydroxides.

Stability of inorganic minerals and predominance fields of aqueous species are shown below, calculated with Geochemist's Workbench (Bethke 2008) using a model Cobourg Formation porewater.



Stability fields of redox-sensitive minerals (red lines) and predominance fields of aqueous carbon species (blue lines).



Predominance fields of aqueous S-species (red lines), C-species (blue lines) and Fe species (brown line) (modelled porewater pH is 6.5).

Equilibria between the porewater and pyrite/hematite, pyrite/siderite or siderite/hematite would ensure that the dominant aqueous sulphur species will be $\text{CaSO}_4(\text{aq})$. $\text{H}_2\text{S}(\text{aq})$ is expected to be negligible in this case. Only if redox is controlled by organic species, including $\text{CH}_4(\text{g})$, is it likely that $\text{H}_2\text{S}(\text{aq})$ could be the dominant S-species. However, this circumstance is inconsistent with the occurrence of anhydrite and gypsum. The dominant aqueous Fe-species is expected to be Fe(II).

4.5.1.2 Corrosion of Other Metals

Retube wastes consist mainly of various Zr alloys used as pressure and calandria tube materials. The release of activation products within the waste requires the corrosion of the Zr alloy matrix. Under aerobic conditions, the corrosion of Zr is described by:



and under anoxic conditions by:



Other metals will be present within the repository, such as aluminum, chromium and copper. However, these will not have a significant impact on either the repository environment or the release of radionuclides due to the dominance of Fe (the corrosion of which accounts for the vast majority of the H₂ generated) and Zr (the corrosion of which will result in the slow release of activation products from the Zircaloy matrix).

4.5.1.3 Timing of Completion of Metal Corrosion Reactions

An estimate of the time taken to completely corrode the inventories of the different metals in the DGR is presented in Box 6. Times range from around 4000 years for carbon steel to 36,000 years for alloys and 250,000 years for Zircaloy.

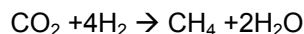
The majority of metal corrosion, and associated H₂ generation, occurs over similar timescales to cellulose degradation (Section 4.5.2). The relative rates of gas generation from organics and metals are important because CO₂ generated from microbial degradation of organics will be rapidly microbially reduced to CH₄ consuming H₂ and generating H₂O.

BOX 6: TIMING OF COMPLETION OF METAL CORROSION REACTIONS

Given the repository resaturation time estimated in Section 4.3, the saturation of the DGR is expected to be low during the period in which the majority of metal corrosion occurs, and anaerobic humid conditions are anticipated to prevail. The corrosion rates under these conditions are identical to the corrosion rates that will apply under the anaerobic saturated saline conditions once the repository has resaturated, except for un-passivated carbon steel, which will corrode twice as rapidly under saturated conditions (Table 3.20 of the Data report, QUINTESSA and GEOFIRMA 2011).

Under these anaerobic unsaturated conditions corrosion will proceed uniformly, and the time for completion of corrosion of different metals is calculated in below. This calculation assumes that conditions in the DGR are always sufficiently humid for corrosion of unsaturated wastes to proceed.

The majority of metal corrosion, and associated H₂ gas generation, will be complete after 36,000 years. The majority of metal corrosion, and associated H₂ generation, occurs over similar timescales to cellulose degradation (Section 4.5.2). The relative rates of gas generation from organics and metals are important, because CO₂ generated from microbial degradation of organics will be rapidly microbially reduced to CH₄ consuming H₂ and generating H₂O. The stoichiometry is such that one CO₂ reacts with four H₂:



This reaction, therefore, has the potential to significantly influence the pressure in the DGR and its resaturation profile, as discussed in Section 4.3.

Waste	Initial Metal Mass (kg) ¹	Density (kg/m ³) ²	Initial Metal Volume (m ³)	Surface area (m ²) ³	Thickness (m)	Corrosion Rate (m/a) ⁴	Time for uniform corrosion (a)
Unpassivated C-steel	2.9E+07	7860	3.69E+03	1.0E+06	3.69E-03	1.0E-06	3,700
Passivated C-steel	1.6E+07	7860	2.04E+03	4.3E+06	4.73E-04	1.0E-07	4,700
Passive alloys	2.0E+07	8100	2.47E+03	6.9E+05	3.58E-03	1.0E-07	36,000
Zircaloy	6.0E+05	6500	9.23E+01	3.7E+04	2.49E-03	1.0E-08	250,000

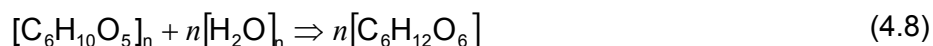
Notes:

1. Table 4.12 of QUINTESSA and GEOFIRMA (2011).
2. Section 3.4.1 of QUINTESSA and GEOFIRMA (2011).
3. Table 4.13 of QUINTESSA and GEOFIRMA (2011).
4. Table 3.20 of QUINTESSA and GEOFIRMA (2011).

4.5.2 Degradation of Organic Materials

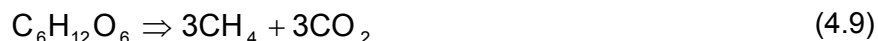
The organics present in the various DGR waste forms can be broadly classified as being cellulosic waste (generally comprising paper and other similar material) and “plastic” waste (comprising less-biodegradable organics, such as plastics and resins).

Cellulose is a polymer of glucose and can be represented by the general stoichiometry $[C_6H_{10}O_5]_n$. In the presence of microbes, cellulose is hydrolyzed to glucose ($C_6H_{12}O_6$):



with the rate of hydrolysis of cellulosic material being one to two orders of magnitude faster than that for the “plastic” wastes. Hydrolysis reactions will occur both in the unsaturated phase (in the thin liquid films adsorbed on the surface of the wastes) and in the bulk groundwater phase.

Glucose, in turn, can be microbially decomposed into CH_4 and CO_2 through several steps catalyzed by a range of microorganisms, but with an overall effective reaction according to:



This is a key process for the DGR as it results in the liberation of gas into the repository. In the safety assessment, it is assumed that this reaction essentially proceeds to completion, allowing only for some loss due to formation of microbial biomass. This maximizes the potential gas generation.

However, in the presence of H_2 generated from metal corrosion, CO_2 can be reduced to CH_4



This process is potentially important as it results in the conversion of five moles of gas to one mole, and can act to moderate the gas pressure in the repository. It also results in methane as the most common gas species in the repository at long times.

This methanogenesis reaction (Equation 4.10) is catalyzed by a commonly occurring but redox sensitive group of methanogenic bacteria. The generation of methane from cellulose and corrosion hydrogen is dependent on a range of environmental and microbiological factors such as inhibition and competition. In particular, as the DGR resaturates, the presence of sulphate in the local porewaters may result in methanogenesis being outcompeted by sulphate reduction resulting in the generation of hydrogen sulphide rather than methane. However, it is expected that there will always be niches within the repository where methane generation dominates due to sulphate being limited by the slow rate of porewater ingress, and the limitation of the latter reaction to aqueous conditions.

While biodegradation of cellulose is well established, biodegradability of resins is uncertain.

- In general, resins are resistant to both chemical and biological degradation. One group of opinions is that there would be little degradation of resins under anaerobic repository conditions. For example, Torstenfelt (1989) reviewed the stability of ion-exchange resins in a cementitious environment and noted that the resins are very stable from attack by polar, oxidizing or reducing agents.
- However, there is also evidence for the eventual degradation of resins (e.g., Bowerman et al. 1988; Bracke et al. 2004). For example, Bowerman et al. (1988) observed that the rate of

microbiological attack on resins was very low, but following irradiation (1 MGy Co-60) and/or loading with organic acid anions such as EDTA, citrate, or oxalate, their susceptibility to alteration increased.

In the present safety assessment, resin degradation is treated conservatively, assuming that all the resins do degrade and using a similar treatment to that for cellulose although with a lower reaction rate. This approach maximizes the amount of gas generated in the repository.

Similar organic degradation reactions occur in nature, and result in the conversion of cellulosic plant materials into coal, bitumen, oil or methane, depending on the conditions. Thermogenic reactions produce oil or oil/gas mixtures at lower temperatures, while higher temperatures (above 100°C) are needed to produce gas. However biogenic reactions occur at lower temperatures and generate mostly gas. At DGR temperatures, only biogenic reactions would be relevant.

Thus, the degradation of the organics (but not the corrosion of steel) requires the presence of an active anaerobic microbial community. However, the rock porewater around the repository is highly saline and not favourable for microbes – and tests of the host rock formations do not exhibit appreciable microbial activity. Although the wastes themselves will contain microbes and some water, microbial activity is expected to be inhibited as saline porewater slowly infiltrates into the DGR over long timescales (while unsaturated conditions are maintained in the DGR, it is expected that the relative humidity will be sufficiently high to allow microbial activity). Furthermore, microbial activity in certain parts of the repository could be further inhibited by relatively high concentrations of certain elements such as nickel and zinc. These factors would affect both the production of gas through Equation 4.9, as well as the reduction through Equation 4.10.

The degradation of organic waste materials will have an impact on the ambient geochemistry through the generation of a range of organic and inorganic by-products. Products are likely to include organic acids, carbon dioxide, hydrogen sulphide and ferrous iron. However, the impacts on repository pH are expected to be limited (see Appendix C.3).

The time required to completely degrade the organic materials in the wastes can be calculated. Degradation is specified in terms of decay rates (Section 3.6.6.1 of the Data report, QUINTESSA and GEOFIRMA 2011). Therefore the time for decay can be expressed in terms of the half-life:

$$T_{1/2} = \ln 2 / \lambda \quad (4.11)$$

Where,

$T_{1/2}$ is the half life (a)

λ is the decay rate (/a)

The anaerobic decay rates for cellulose and IX resins are 5×10^{-4} /a and 5×10^{-5} /a, which give half-lives of 1390 a and 13,900 a respectively (Table 3.21 of QUINTESSA and GEOFIRMA 2011).

4.5.3 Degradation of Cementitious Materials

Two main kinds of cementitious material will be used in the DGR: structural concrete; and LHHPC (Section 4.4.1 of the Data report, QUINTESSA and GEOFIRMA 2011). The structural concrete is used for all structures, other than the monoliths, bulkheads and liners, and backfilling of the rock handling and ramp excavations, which will use LHHPC. The LHHPC is sulphate resistant and has a low heat of hydration.

The structural concrete is mixed with about 15 wt% Ordinary Portland Cement (OPC), whereas the LHHPC is prepared with only around 4 wt% OPC (Section 4.4.1 of the Data report, QUINTESSA and GEOFIRMA 2011). Compared with the structural concrete, the LHHPC contains much more silica, in the form of silica fume, flour and sand. A consequence is that, whereas the cured structural concrete will initially contain free portlandite (Ca(OH)_2), the LHHPC is not expected to contain a significant amount of free portlandite (Appendix E.5.1).

Where the structural concrete is present, porewater pH will initially increase due to leaching of portlandite:



and dissolution of Calcium Silicate Hydrate (CSH) gel. Section 4.4.1 of the Data report (QUINTESSA and GEOFIRMA 2011), quoting Höglund (2001), states that there is 350 kg of cement in 1 m³ of concrete. After hydration, this amount of cement gives a paste that is able to liberate up to about 6000 moles of OH⁻ (from both portlandite and CSH gel leaching). Saturation of concrete with groundwater, therefore, leads to the development of a hyperalkaline (pH > 12.5) pore fluid.

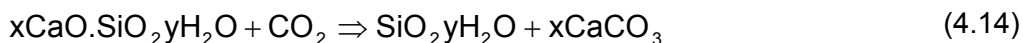
The pH decreases with time in accordance with leaching of progressively less-soluble solids. In the long-term, pH in concrete pore fluids is defined by the incongruently soluble CSH gel, with pH progressively decreasing from 12.5 to < 10.

In contrast, fresh LHHPC is expected to contain no portlandite, owing to the cement's high silica content, which reduces the Ca/Si ratio and results in CSH gel (probably with a Ca/Si ratio of ~1) being the initial pH buffer (see Appendix E.5.1). This composition has been relatively little studied and there is a lack of available information concerning the initial hydration and long-term evolution of phases present in this material. However, it is likely that the initial LHHPC porewater pH will be around 10-11, depending on the nature of the hydrated phase assemblage and pCO₂, and subsequently as it undergoes leaching and carbonation, the pH will evolve towards the "natural" pH of around 6.5 in a similar fashion to "aged" structural concrete.

Some inorganic carbon in the repository (in gaseous and aqueous phases) will be precipitated in concrete materials. In the structural concrete, CO₂ dissolved in groundwater will be involved with the carbonation of portlandite, producing calcite:

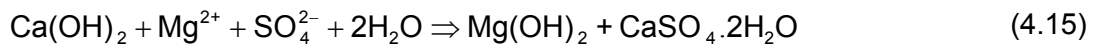


In the LHHPC, carbonation is expected to involve the reaction of CO₂ with CSH phases to eventually produce calcite and silica:



Simple scoping calculations (Appendix E.5.2) suggest that the complete carbonation of CSH present in the LHHPC may take over 1 Ma in diffusion-dominated regimes. However, it is likely that a protective layer of calcite will be formed on cement/concrete surface and in pores, thereby preventing further alteration (a process referred to as “armouring”). In addition, $p\text{CO}_2$ will decrease as a result of this reaction, and others occurring in the repository, which will decrease dissolved bicarbonate concentrations resulting in a reduction in the potential for further carbonation LHHPC. The carbonation of structural (high OPC) concrete is also likely to occur in a similar way, with surfaces being “armoured” with calcite. This leads to clogging to pores, a reduction in diffusion and concomitant decrease in reactivity of cement phases.

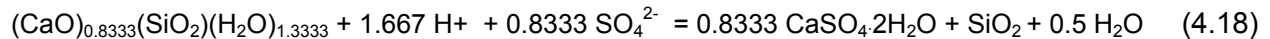
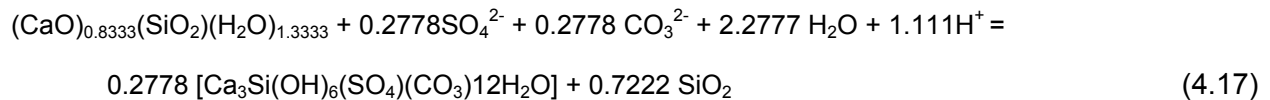
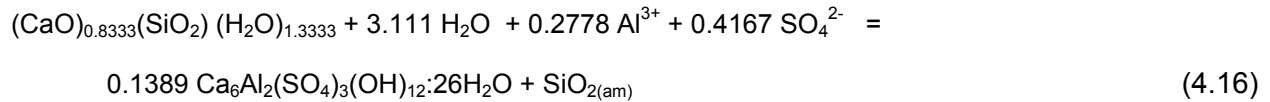
Concretes may also be subjected to sulphate attack. The presence of a MgSO_4 brine component may lead to replacement of Ca and OH^- in the cement, forming brucite ($\text{Mg}(\text{OH})_2$) and gypsum:



At high ionic strength, anhydrite (CaSO_4) may form instead of gypsum.

Glasser et al. (1999) noted that, in a mixed brine, these reactions are accelerated relative to those in either salt (NaCl , MgSO_4) separately. Sodium chloride enhances the solubility of both $\text{Mg}(\text{OH})_2$ and $\text{CaSO}_4 \cdot 2\text{H}_2\text{O}$. However, as with calcite “armouring” processes, the growth of alteration products such as gypsum or anhydrite is likely to result in the clogging of pore spaces on concrete surfaces, thereby limiting the extent of reaction.

The CSH gel component of the LHHPC could also react with sulphate to form phases such as ettringite (Equation 4-16), thaumasite (Equation 4-17) or gypsum (Equation 4-18):

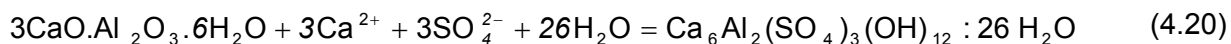


However, as shown in Appendix E, the flux of dissolved sulphate required for such reactions is such that it would take at least thousands to many tens of thousands of years for these reactions to take place to the extent that the bulkheads were completely altered, and longer when armouring of surfaces is included. In addition, the potential for significant alteration to ettringite to occur will be restricted due to the limited availability of Al and the potential for alteration to thaumasite will be limited due to the large amount of carbonate required.

Portlandite ($\text{Ca}(\text{OH})_2$) and calcium aluminate hydrate ($3\text{CaO} \cdot \text{Al}_2\text{O}_3 \cdot \text{H}_2\text{O}$, also referred to as “ C_3A ”) present in structural concrete may also react with sulphate to form ettringite ($\text{Ca}_6\text{Al}_2(\text{SO}_4)_3(\text{OH})_{12} \cdot 26\text{H}_2\text{O}$) and /or gypsum ($\text{CaSO}_4 \cdot 2\text{H}_2\text{O}$):



and



These reactions can cause the volume to increase, resulting in swelling and cracking. However, as shown for the LHHPC, these reactions are likely to be somewhat limited by Al availability. As portlandite is leached from the concrete, the pH will fall and with LHHPC, CSH gel will become the predominant solid undergoing sulphate attack.

Concrete may also undergo chloride attack, resulting in the formation of Cl-containing phases such as Friedel's salt and Kuzel's salt (Appendix E). However, these phases contain Al, the availability of which will be limited.

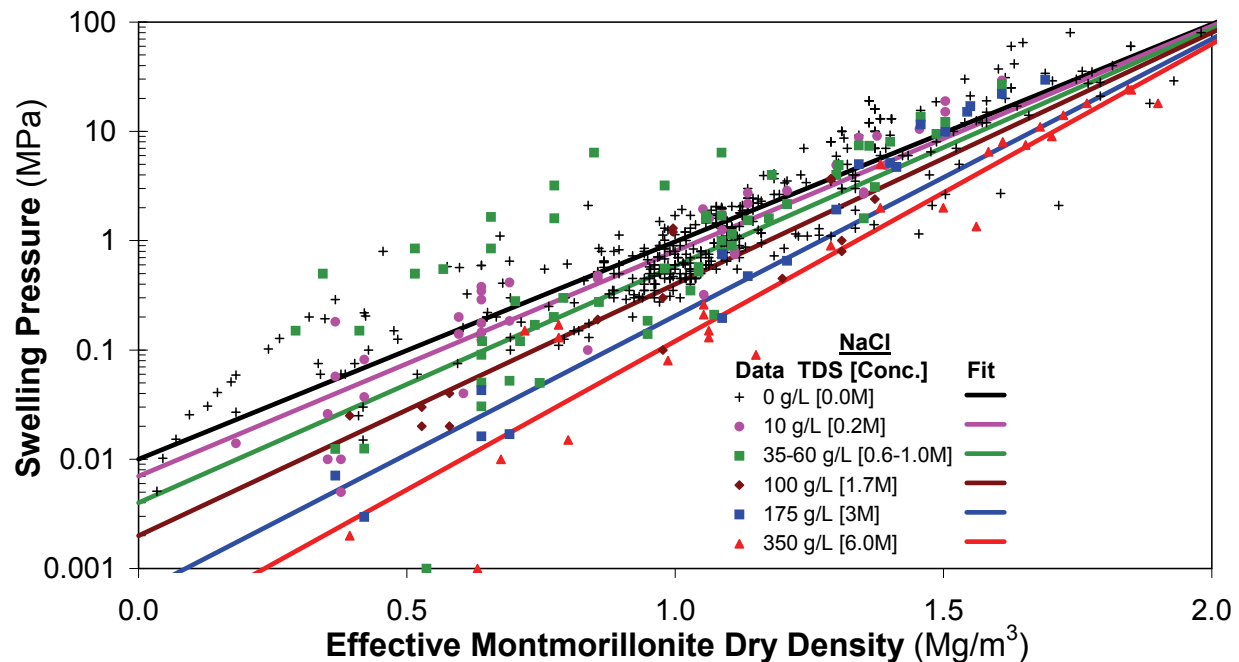
In summary, both structural cement and LHHPC may undergo carbonation and may be subject to sulphate and chloride attack. However, the availability of Al and carbonate and the possible magnitude of fluxes of dissolved components required for alteration are such that extensive depths of cement alteration is unlikely to occur over tens of thousands to hundreds of thousands (and arguably for some reactions more than a million) years. Alteration is likely to be limited to zones where concrete interfaces with the host rock/ EDZ, due to the clogging of pores by secondary solid phases and surface "armouring".

4.5.4 Evolution of Bentonite-Sand

Bentonite is known to be a durable material, with natural deposits that are many millions of years old (Laine and Karttunen 2010). Higher temperature (> 100°C) and alkaline conditions encourage mineralogical transformations, but the DGR shaft will be at low temperatures (< 25°C), with only localized alkaline conditions near the concrete monolith and bulkheads. The effects of water salinity and groundwater chemical species are more complex. There is some evidence of reduced stability under certain high salinity conditions (e.g., Herbert et al. 2004), but there is also evidence to suggest that only cation exchange is likely to occur (Kaufhold and Dohrmann 2009). Although there is no direct data on bentonite stability under the highly saline Na-Ca-Cl site groundwater conditions at the DGR site, there are some natural analogs, notably some Spanish bentonites, that have been exposed to saline Na-Cl (sea) water over millions of years, and show no significant mineral alteration (Laine and Karttunen 2010, Savage 2005).

Compacted bentonite will saturate with ambient groundwater and swell. In confined space within a shaft, the swelling will result in the creation of pressure. At an Effective Montmorillonite Dry Density of around 1.2 Mg/m³, the swelling pressure will be around 0.3-0.4 MPa, even under the highly saline groundwater conditions in the Ordovician rocks, as illustrated in Figure 4.4.

In the long term, the interaction of bentonite with saline groundwater will result in ion exchange in smectite (montmorillonite) interlayers and possible changes in physical behaviour. Ion-exchange models suggest that there will be replacement of some smectite interlayer sites with K⁺ (Appendix E.2). Although there appears to be a lack of swelling pressure data for bentonite with K-exchanged montmorillonite, it appears that it may have a lower swelling pressure than the original bentonite. Therefore, there may be some loss of swelling pressure (possibly ~ 20%) (see Appendix E.2).



Note: Figure is based after Baumgartner (2006). TDS is based on NaCl solution.

Figure 4.4: Swelling Pressure as a Function of Clay Density and Salinity in Smectite-based Sealing Materials

The process of illitization (commonly associated with burial diagenesis of sediments) involves smectite being converted to illite with a 2:1 layer charge increase as Al is substituted for Si in tetrahedral sheets, uptake of K into interlayer regions and the release of silica. The reaction is strongly dependent upon time, temperature and availability of K^+ . Significant illitization of bentonite would result in loss of swelling capacity. However, the application of the kinetic model by Huang et al. (1993) to the Bruce nuclear site indicates that illitization will be negligible (Appendix E.3) due to the prevailing chemical conditions and the low temperature.

At the interface with concrete, the clay minerals in the bentonite will be destabilized by the elevated pH of pore fluids within the concrete. Above pH 10, deprotonation of neutral aqueous silica species serves to increase silicate solubility. OH^- ions also catalyse the rate of aluminosilicate dissolution by weakening Al-O bonds, such that the rate of dissolution is typically proportional to $[OH^-]^{0.4-0.5}$.

A simple mass balance calculation based on the available moles of OH^- required from cement shows that even if all of the LHHPC present in the shaft reacted with all the bentonite, ~8% of the bentonite would be consumed (Appendix E.4). However, the mass balance is complicated by the nature of the potential secondary products of the cement-bentonite interaction. Growth of secondary minerals will contribute to consumption or generation of OH^- (Appendix E.4).

Zeolite minerals will dominate the mineral alteration products at pH < 11 (i.e., at pH conditions typical of low-pH cement), and thus tend to extend the zone of alkaline alteration. However, the availability of silica will be limited compared to higher-pH conditions because montmorillonite will not dissolve as readily and so the extent of the alteration zone will be restricted. Furthermore,

pore clogging at cement-bentonite interfaces due to mineral precipitation occurs which limits the thickness of alteration zones (e.g., Savage et al. 2002; Marty et al. 2009).

In summary, bentonite alteration is unlikely to be extensive through the shaft. As zones of alkaline alteration in published models (see Appendix E.4) have thicknesses that are confined to scales in the order of 10s of cms, the alteration zones at cement/bentonite interfaces in the DGR shaft will very likely not exceed 1 m in thickness.

4.5.5 Evolution of Asphalt

The reference asphalt mastic mix has the same composition as that proposed for use in the shaft seal for the Waste Isolation Pilot Plant (WIPP 2009). It will contain 70 wt% silica sand, 20 wt% asphalt and 10 wt% lime. The reference asphalt is AR-4000, a graded asphalt of intermediate viscosity.

Asphalt consists mainly of four components (Pettersson and Elert 2001):

- 1) Saturated hydrocarbons;
- 2) Aromatic hydrocarbons;
- 3) Resins; and
- 4) Asphaltenes.

Typically the aromatic hydrocarbons are the most abundant component, whereas the asphaltenes are the least abundant component (Pettersson and Elert 2001).

The direct evidence for long-term stability of asphalt comes from natural and anthropogenic (e.g., archaeological) analogues. For example, Miller et al. (2000) cite numerous natural asphalts that have survived for tens of thousands of years. The asphalt investigations to support WIPP's safety assessment have considered timescales of 10,000 years (WIPP 2004), whereas those at Hanford have evaluated asphalt stability over a period of 1000 years (Wing and Gee 1994; Freeman and Romine 1994). However, the timescales of these assessments were much shorter than the 1 million years relevant to the DGR.

In surface engineering applications, asphalt is principally degraded through exposure to UV light. However, this degradation mechanism is not relevant to the shaft seals. These will be emplaced underground, where there is no ultraviolet light and conditions are reducing. Under these circumstances, it is believed that asphalt would be very stable in the long-term.

Stiffening and hence increased susceptibility to cracking is a general feature of asphalt aging, but the precise degradation mechanism and its rate is highly dependent upon asphalt composition and upon the characteristics of any aggregates that are used. However, the seals in the DGR are being designed to avoid these degradation processes.

Although asphalt is a hydrophobic material, water can be transported into the asphalt matrix (Pettersson and Elert 2001). This process is usually described as diffusion of water vapour. However, unless there are impurities that are either porous themselves or that produce porosity within the asphalt, and/or that have hygroscopic properties (e.g., mineral fillers such as fly ash, hydrated limestone or stone dust), the water uptake is negligible.

Under anaerobic conditions, resins and asphaltenes are more or less unaffected by micro-organisms (Pettersson and Elert 2001) unless the surfaces of the asphalt are exposed to flowing water (Pedersen 2001). Flow is needed to provide water, to provide electron acceptors

to the site of microbial growth and to remove the waste products of microbial metabolism. Without such removal of waste products, conditions would become toxic to life and microbial activity would cease. The probable virtual absence of flow in the DGR following asphalt emplacement means that any microbial processes would be extremely slow, with the degradation products being CO₂ and CH₄ with organic acids as intermediates. The shaft designs for the WIPP in New Mexico include bitumen-bearing components that incorporate hydrated lime to inhibit microbial activity and make microbial degradation of bitumen even less likely (Hansen and Knowles 2000).

The maximum rates at which the asphalt could plausibly degrade due to microbiological activity are uncertain. Experimental rates of bitumen degradation reported by Roffey and Nordqvist (1991) and Wolf and Bachofen (1991) implies that overall degradation of the asphalt would be only about 3×10^{-7} /a (see Appendix E.6). However, even this rate is likely to be a large over-estimate since the experimental rates are probably much greater than would be achieved in the shaft, notably because:

- The bitumen degradation data are from short-term (days to months) laboratory experiments and degradation is likely to be more rapid at early times because the lighter organic components of bitumens are known to undergo microbial degradation more rapidly than the heavier components (e.g., Aitken et al. 2004; Holba et al. 2004); and
- There was effectively no nutrient limitation in the experiments, which would tend to result in very high rates of microbial activity compared with those expected for long-term in-situ degradation within a low-nutrient shaft environment in very low-permeability rocks.

For these reasons, it is not expected that chemical degradation will lead to any significant degradation of the asphalt seal's properties.

Taking into consideration the relevant thermal, hydraulic, mechanical and chemical processes described in Sections 4.2 to 4.5, the anticipated evolution of each of the major seal components is summarized in Table 4.2.

4.6 Interfaces with the Geosphere and Biosphere Sub-Systems

The processes within the waste and repository will influence the geosphere by:

- The migration of gases from the repository into the surrounding host rock;
- The migration of dissolved solutes from the repository into the host rock;
- The open repository volume that will draw in porewater during the resaturating phase;
- The gas pressure in the repository affecting surrounding rock stresses; and
- Rockfall into the repository affecting the surrounding rock integrity and stress distribution.

The waste and repository interfaces directly with the biosphere through the shafts. This is a potential path for contaminant releases in both water and gas.

4.7 Audit of Potential Interactions

Given the importance of the interactions between the various repository components (e.g., the waste packages, the engineered structures, and the engineered materials) and the interactions between these components and the surrounding geosphere in affecting the evolution of the DGR system, an audit was undertaken to ensure that key interactions had been identified. The audit confirmed that all key interactions had been identified (see Appendix F).

Table 4.2: Anticipated Evolution of the Shaft Seals

Feature	Evolution
Concrete Monolith	The monolith is located in very low permeability rock. Reaction with the host rock porewater will be limited by the rate of diffusion of reagents. It is anticipated that physio-chemical degradation of the monolith will be limited over assessment timescales. There is most likely to be some carbonation (armouring) and sulphate attack of the external surfaces exposed to CO ₂ gas and water in the DGR and the shaft EDZ. Sulphate attack and mechanical stresses may result in some cracking.
Bentonite-Sand	No significant alteration/degradation of the bentonite-sand over the assessment time scale, except where it contacts the concrete bulkheads. Here up to 1 m of chemical alteration is likely. Although this will result in a local loss of swelling pressure and cracking of the bentonite-sand, it will not significantly affect the overall performance of the seal, since the majority of the seal will be unaltered. Over assessment timescales, there will be some Ca-K exchange, which will result in a reduction in the swelling pressure. However, this is not anticipated to significantly reduce seal performance.
Asphalt Mix	No significant alteration/degradation of the asphalt mix with assessment timescale.
Concrete Bulkhead	Although the bulkheads are in contact with relatively more permeable geological formations than the monolith, the head gradient is low and groundwater flow is slow and so degradation will be limited. It is anticipated that similar to the monolith, alteration will be dominated by carbonation and sulphate attack. Sulphate attack and mechanical stresses are anticipated to result in cracking. The extent of cracking may be greater than for the monolith, which is a much larger feature.

5. EXPECTED EVOLUTION OF THE GEOSPHERE

5.1 Thermal Evolution

As noted in Section 4.2, the heat generated from the degradation of waste packages and the decay of radionuclides will have minimal impact on the temperature of the geosphere surrounding the repository.

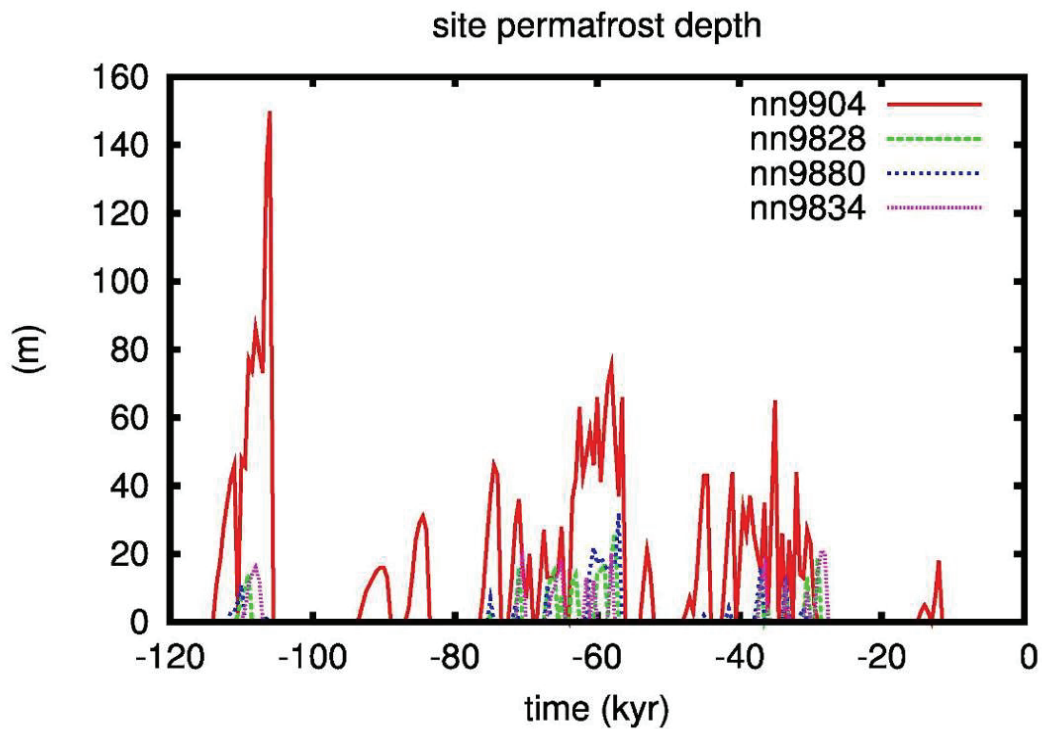
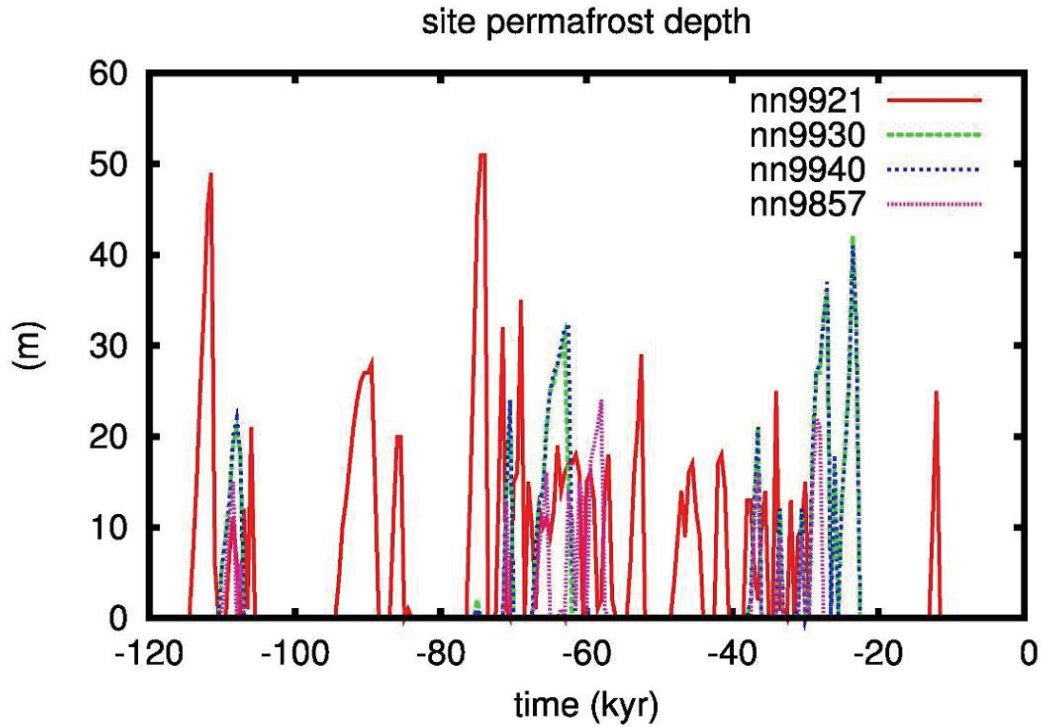
Although human-induced global warming might have some short-term impacts on temperatures in the near-surface region, it will have very little effect on the deeper geosphere which will remain with stable temperatures for tens of thousands of years.

In the longer term, thermal changes in the geosphere will be driven by the glacial and interglacial cycling discussed in Section 6. A fall in surface temperature will cause the upper part of the geosphere to cool and eventually the development of permafrost (Peltier 2004). Once an ice-sheet has covered the site, the temperature evolution beneath the ice-sheet depends upon the insulating effect of the ice and the geothermal heat flow, among other factors (Peltier 2004). The geothermal heat flow is likely to be effectively constant over the timescale of interest, but the insulating effect of the ice will depend upon the thickness of the ice-sheet. Consequently, the temperature at the interface between the earth and the ice will vary over time and permafrost may be either present or absent.

Thus, the picture that emerges is that the temperature in the geosphere will decrease as the climate cools, and long before the ice front reaches the site. After the ice front has crossed the site, the temperature may then increase once more, though conditions will remain cooler than they were prior to glaciation. Then, when the ice retreats, the temperatures will increase and eventually return to their pre-glaciation values. The temperature changes at the depth of the repository will lag behind, and be smaller than, the temperature changes at shallower depths.

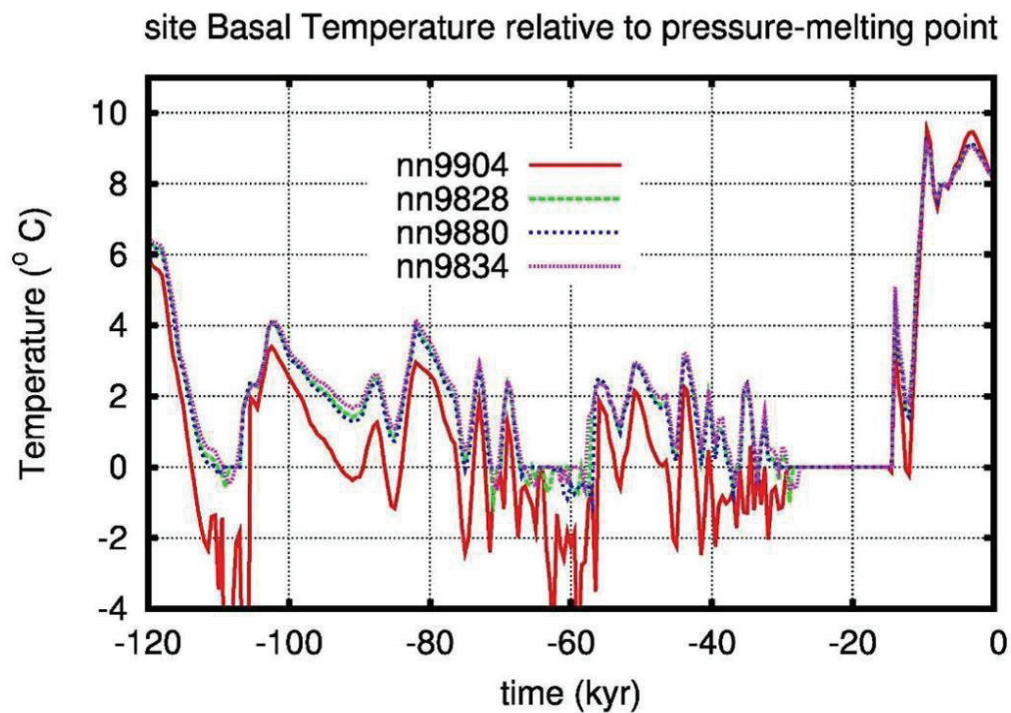
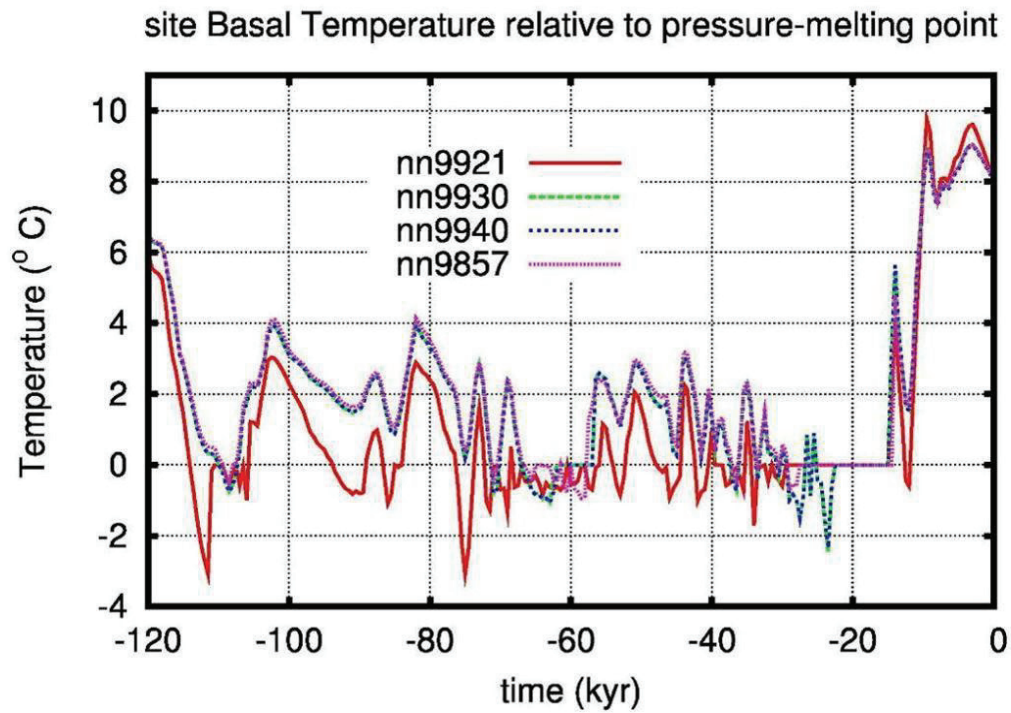
Peltier (2011) has applied the University of Toronto Glacial System Model to examine the impacts of glaciation at the DGR site over the last 120,000 years. Eight models have been developed that provide acceptable fits to the historic data. The permafrost thickness (Figure 5.1) was quite variable and rarely exceeded 60 m; an indication that this region was not covered with a continuous extensive permafrost layer.

The annual average basal (surface) temperatures at the site ranged between -4°C and $+10^{\circ}\text{C}$ (Figure 5.2). Permafrost developed when the basal (surface) temperature fell below 0°C . Using the site basal temperature time series calculated by Peltier (2011), the geosphere temperature at repository depth can be calculated. The temperature at repository depth reaches a minimum of 17°C compared with 22°C at the present day. Such a temperature change is not significant for any of the processes of interest.



Note: Figure 4.5 in Peltier (2011).

Figure 5.1: Simulated Permafrost Depth at the Bruce Nuclear Site over the Last Glacial Cycle for the Eight Cases Consistent with Historical Data



Note: Figure 4.4 in Peltier (2011).

Figure 5.2: Simulated Basal (Surface) Temperatures at the Bruce Nuclear Site over the Last Glacial Cycle for the Eight Cases Consistent with Historical Data

5.2 Hydraulic Evolution

The present-day groundwater flow regime is described in Section 2.3.6. Disequilibrium hydraulic heads have been observed in the Intermediate and Deep Bedrock Groundwater Zones at the DGR site (Section 2.3.6.4). The cause and, therefore, future evolution of these disequilibrium heads is uncertain. However, site characterization data and detailed modelling indicates that they are unlikely to be caused by glaciation, and that they likely to remain after future glacial cycles (Section 5.4.10 of NWMO 2011). Density dependent saturated flow analyses indicate that due to the properties of the host rock, it will take more than one million years for the observed underpressure in the Ordovician to equilibrate to an equilibrium pressure head profile (Section 5.4.10 of NWMO 2011).

Although human-induced global warming might have short-term impacts on the near-surface groundwater region, (e.g., elevation of the water table) it is unlikely to have an effect on the deeper geosphere due to the low permeability of the rock. In the longer term, the groundwater flow regime in the Surficial and Shallow Bedrock Groundwater Zones, plus the Salina A1 Upper Carbonate will be affected by glacial cycling through its effects on recharge, surface water bodies, and the advance and retreat of ice-sheets (Section 6.2 of NWMO 2011).

Operational dewatering of the DGR will result in localized desaturation of the host rock immediately adjacent to the excavations. Due to the very low permeability of the host rock, the extent of the desaturation fringe will be small, and the impact on geosphere porewater and gas pressures will be localized. This is supported by the results of detailed modelling presented in Section 5.1.2.1 of the Gas Modelling report (GEOFIRMA and QUINTESSA 2011).

5.2.1 Recharge

There is topographically driven sub-horizontal flow in the Surficial Groundwater Zone and in the upper part of the Shallow Bedrock Groundwater Zone, with recharge from infiltration and discharge to surface waters (local streams, wetlands, and Lake Huron). Flows in this part of the system will be sensitive to changes in climatic conditions that influence groundwater recharge, i.e., precipitation, evapotranspiration, runoff/drainage (natural and anthropogenic) and cold-climate effects such as spring snow melt. A reduction in groundwater recharge would tend to result in a lowering of the water table in the recharge areas (topographic highs) with a consequent reduction in the hydraulic gradient and hence flow rates. The decrease in hydraulic gradient due to lowering of the water table in the recharge areas will be offset to some extent by a decrease in surface water levels in the discharge areas.

Increases in recharge will have the opposite effect; however, the impacts will be self-limiting because under present-day conditions, the amount of precipitation that can infiltrate the rock is small compared with the amount occurring as runoff (Thorne and Gascoyne 1993). Relatively little increase in hydraulic gradient is possible from increased precipitation as, at some point, the water table would rise above the topographic surface.

Such changes in recharge are expected to have no significant impact on the Intermediate and Deep Bedrock Groundwater Zones due to their hydraulic isolation from the overlying zones (Section 2.3.6).

Section 10.3.2 of the Geology Technical Support Document (GOLDER 2011d) considers the impacts of climate change over the period 2011-2100 for groundwater recharge. It is concluded that the change in groundwater recharge will be within the range of annual variability. This is not

significant for geosphere flow and transport processes. Climate change beyond 2100 is discussed in Chapter 6. Global warming is not anticipated to have significant effects on groundwater flows in the geosphere, except potentially on the water table and flows in the Surficial and uppermost Shallow Bedrock Groundwater Zones.

5.2.2 Local Surface Water Bodies

Groundwater flows in the Surficial and Shallow Bedrock Groundwater Zones will also be affected by changes in the spatial location of surface water bodies and their water levels, since they are in hydraulic connection with the underlying geosphere. Surface water levels can be affected by changes in precipitation, evapotranspiration, and runoff, but also by erosion/sedimentation. The Bruce nuclear site is sufficiently elevated, and sufficiently disconnected from the sea, that surface water bodies will not be directly affected by changes in sea level.

The spatial extent and levels of surface water bodies will be affected by glaciation both in terms of the impacts of erosion and deposition on the topography, but also isostatic depression and rebound of the land surface (see Section 5.3.3). During the last glaciation cycle, large freshwater lakes existed at the ice sheet margin in the vicinity of the current site (except when covered by the ice-sheet), with Lake Huron as the present remainder. So although the location and extent of such lakes will change in the future, it is reasonable to assume that a large lake will generally be present in the vicinity of the DGR site. It is convenient to assume this lake has the same characteristics as Lake Huron so that potential impacts can be understood in terms of current conditions.

Changes in the local surface water bodies are expected to have no significant impact on the Intermediate and Deep Bedrock Groundwater Zones due to their hydraulic isolation from the overlying zones.

5.2.3 Effects of Glaciation

In the cooling stage of a glacial cycle, there could be widespread formation of permafrost and possibly reduced precipitation, which would significantly decrease recharge and alter the shallow flow system hydraulic gradients (Peltier 2002, 2004). However, by analogy with historical glacial conditions, the results of Peltier (2011) indicate that future permafrost at the DGR site would typically be only a few tens of metres thick; sufficient to reduce recharge significantly but insufficient to freeze the entire thickness of the active groundwater system. Generally, permafrost is not continuous unless the depth of permafrost exceeds 60 to 90 m (Brown and Pewe 1973).

Even under permafrost climate conditions, features such as taliks might form: these are regions of open, unfrozen ground, and typically are sustained under deeper surface water bodies. Around the Bruce nuclear site, the Lake Huron bed would likely remain unfrozen, and would continue to form a discharge location for the Shallow Bedrock Groundwater Zone.

Regions of permafrost would eventually be covered by an ice-sheet, either by the flow of an ice-sheet over the site or by the in-situ accumulation of snow. It is estimated that the maximum thickness of an ice-sheet that would cover the DGR site would be approximately 3 km (Peltier 2011).

Ice-sheet development will result in mechanical loading of the geosphere (Section 5.3.3) and isostatic depression of the ground surface, both below the ice-sheet and for tens or hundreds of

km beyond the ice-sheet margins. Although the mechanical component of the loading will be transmitted almost instantaneously through the rock, the hydraulic component will be transmitted at a rate proportional to the hydraulic diffusivity (equal to the rock hydraulic conductivity divided by its specific storage). The longer the duration of ice-sheet loading, the greater the distance the hydraulic component will propagate. For a hydraulic conductivity and specific storage representative of the Deep Bedrock Groundwater Zone (1×10^{-14} m/s and 5×10^{-6} /m, respectively), for a glacial period lasting 30,000 years, the Root Mean Squared distance the hydraulic component will propagate is 62 m. 30,000 years is slightly longer than the maximum period of Quaternary glacial loading. Therefore, the host rock porewater pressures around the DGR will be significantly isolated from the effects of glacial loading by the ~ 200 m of overlying very low permeability Ordovician rock, and the ~ 300 m of dominantly low permeability Silurian rock. This is confirmed by detailed modelling, e.g. see hydraulic head changes due to glaciation in Section 5.4.6 of NWMO (2011).

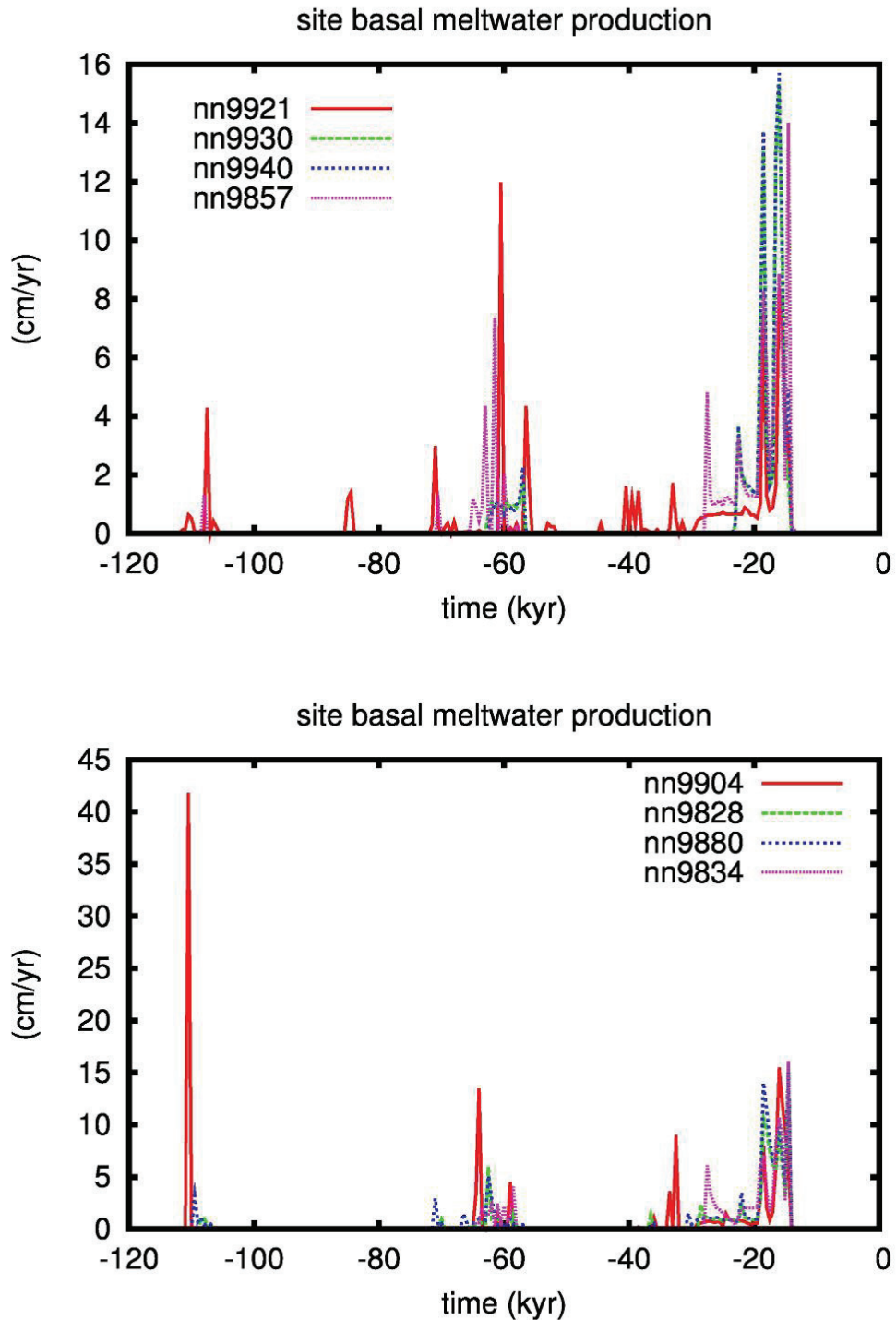
As the geosphere is compressed, the heads will increase resulting in flow (predominantly in the Shallow Bedrock Groundwater Zone) laterally to, and discharge at or beyond the ice-sheet margins. Around the DGR site, discharge would likely be to the local large lake (Lake Huron or its successor). The groundwater flow rates within the Shallow Bedrock Groundwater Zone close to the ice-sheet margins will be a function of the hydraulic conductivity and the increased head gradients in response to ice-sheet loading.

Hydrogeological conditions during glaciation also would differ depending on whether the ice-sheet is cold-based or warm-based. As long as there is no melting associated with the ice-sheet (cold-based conditions), groundwater recharge would be inhibited. A warm-based ice-sheet is one in which temperatures are above freezing at the ice-rock interface. It can occur due to several processes, including: (a) an increase in ground temperature at the ice-rock interface due to geothermal heating coupled with the insulating effect of the ice itself, (b) pressure-dependent ice melting due to the thickness of the ice-sheet, or (c) atmospheric warming (end of glacial cycle). Sub-glacial groundwater flow patterns associated with warm-based conditions are likely to involve increased volumes of water and more rapid shallow groundwater movement than under pre-glacial or cold-based conditions.

If the base of the ice-sheet was melting, liquid water would be present at the interface between the ice and the rock surface. The water would be pressurized due the hydraulic head in the ice-sheet itself, which could affect the groundwater flows and geochemistry by moving large volumes of low-salinity and possibly oxidizing meltwater through the hydraulically active part of the flow system in the rock. The maximum depth to which the fresh water penetrates the geosphere will tend to be associated with the advective path line from the point of melting furthest from the ice margin. The presence of meltwater tunnels at the base of the ice-sheet could also impact the movement of the meltwater, since such tunnels could be important routes for the release of water pressures developed at the base of the ice-sheet. A secondary control on the depth of meltwater penetration will be the density contrast with the geosphere, dependent on relative salinity.

As the ice-sheet retreats, rapid melting of the ice can be expected. Modelling by Peltier (2011) indicates that meltwater generation is confined to temporally discrete events largely constrained to a short period of time after glacial maxima (Figure 5.3). As the weight of the ice is removed, and the rock relaxes, underpressures will develop, i.e., heads below equilibrium with the current surface conditions (unless mechanical unloading associated with melting is balanced by elevated heads associated with meltwater injection). Depending on site-specific properties such

as permeability, the time required for the groundwater system to stabilize following deglaciation is likely to vary from hundreds of years to ten thousand years or longer.



Note: Figure 4.6 in Peltier (2011).

Figure 5.3: Simulated Basal Meltwater Production at the Bruce Nuclear Site over the Last Glacial Cycle for the Eight Cases Consistent with Historical Data

Coupled hydro-mechanical models developed for the Bruce nuclear site confirm the long times for the response of geosphere pressures to glacial loading and unloading (Section 5.4.6 of NWMO 2011). Groundwater flow simulations for the Laurentide glacial episode (~120 ka BP), based on the NN9930 model of Peltier (2011), show that the underpressures observed in the Ordovician shales and limestones are unlikely to be associated with the last Laurentide glacial episode. The low permeability of the majority of the geological formations, combined with the near-horizontal layering and anisotropy, all act to limit the depth to which the pressure signal can be transmitted within the duration of the glacial episode.

Glacial meltwater has been identified in the Surficial Groundwater Zone and the Shallow Bedrock Groundwater Zone (Section 2.3.7.1) confirming the above understanding. The observations are consistent with the results of the transient paleoclimate groundwater flow simulations (Section 5.4.6 and 6.2 of the Geosynthesis report, NWMO 2011).

Glacial meltwater injection into the Salina A1 Upper Carbonate formation within the Intermediate Bedrock Groundwater Zone has also been identified (Section 2.3.7.1). Glacial meltwater has mixed diffusively with porewaters in the over- and under-lying low permeability formations. The distance the diffusion front has penetrated is estimated to be 50 m from Figure 4.5 of Geosynthesis report (NWMO 2011). It is reasonable to assume that future glacial cycles would also result in meltwater injection into the Salina A1 Upper Carbonate. Meltwater could potentially also be injected into the underlying Guelph formation from outcrop, although the depth penetration associated with the Laurentide glacial maximum was insufficient to reach the Bruce nuclear site. It is very unlikely that future glacial events would be of sufficiently greater magnitude than the Laurentide glacial maximum that they would result in meltwater injection into the Deep Bedrock Groundwater Zone.

5.3 Mechanical Evolution

The host sedimentary rocks are stable and extend laterally for hundreds of kilometres. Their current stress regime reflects the lithostatic weight of the rocks in the vertical direction, and steady long-term tectonic forces in the horizontal directions. On a regional scale, these will only change after tens of thousands of years due to the added stresses from ice-sheets, particularly in the vertical direction. On the site scale, the excavation of the repository will cause redistribution of rock stresses. Seismic activity, especially after ice-sheet retreat, will also induce short-term forces on the rock.

5.3.1 Geosphere Surrounding the Emplacement Rooms and Repository Tunnels

The rock stresses in the geosphere surrounding the repository will change with repository excavation and then, as the internal pressure within the repository increases due to generation of gas and inflow of water, with repository re-pressurization. Gas pressures might reach or exceed the geosphere environmental pressure, delaying complete resaturation for hundreds of thousands of years. Ultimately the pressure in the repository and surrounding geosphere will equilibrate. Geomechanical modelling studies of the repository and surrounding geosphere have already been summarized in Section 4.4.1. The results indicate that the repository is stable, but rockfall into the unbackfilled rooms and tunnels will eventually form a stable (porous) rock-filled volume extending in the order of about 10 m above the initial ceilings of the rooms and tunnels. Geomechanical modelling of the DGR with a peak gas pressure of 7 MPa shows no fracturing, but with formation of several metres long horizontal fractures at around 15 MPa (Chapter 6.4 of the Geosynthesis report, NWMO 2011).

5.3.2 Geosphere Surrounding the Shafts

The shaft excavation activity and resulting stress redistribution can induce damage in the surrounding rock, and the formation of an HDZ (which will be removed on shaft decommissioning) and an EDZ (see Section 2.3.6.5). Geomechanical models have investigated the development of the damaged zone (Section 6.4.3 of NWMO 2011). In general, the models showed that most of the failure (and hence development of the damaged zone) will occur during the initial shaft excavation phase. Once the HDZ has been removed and the shafts have been backfilled, they will be significantly stabilized so that events such as ice-sheet loading and seismic shaking will not have significant impacts. Therefore, there is expected to be limited extension of the shaft EDZ following repository closure (see Figure 4.3).

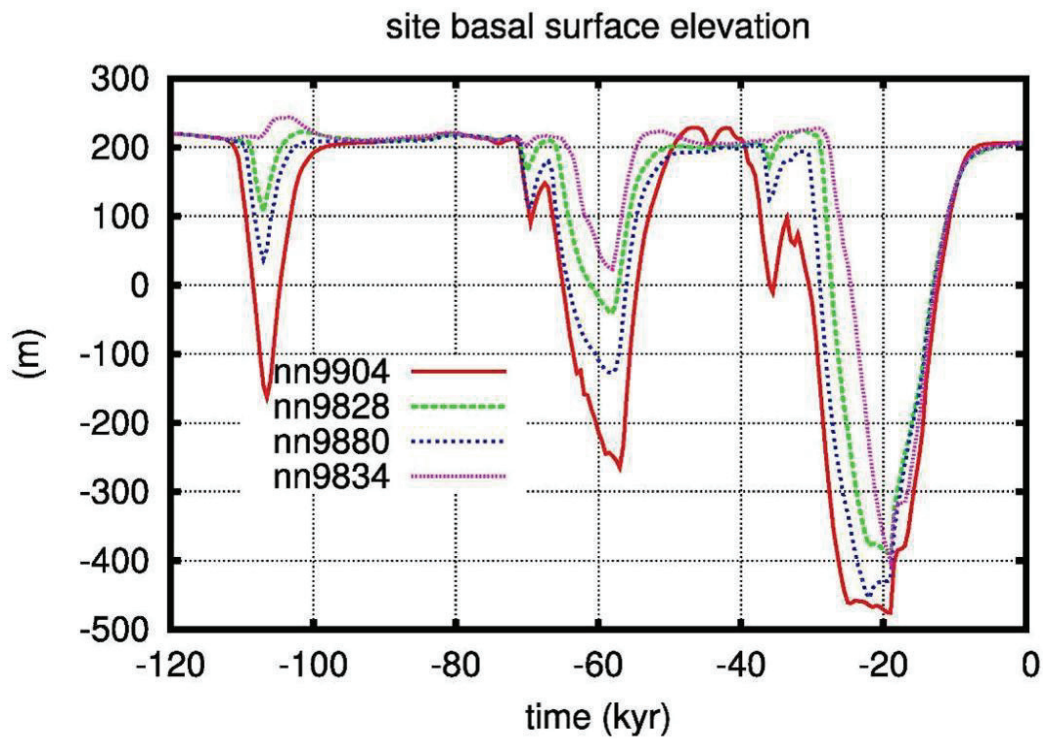
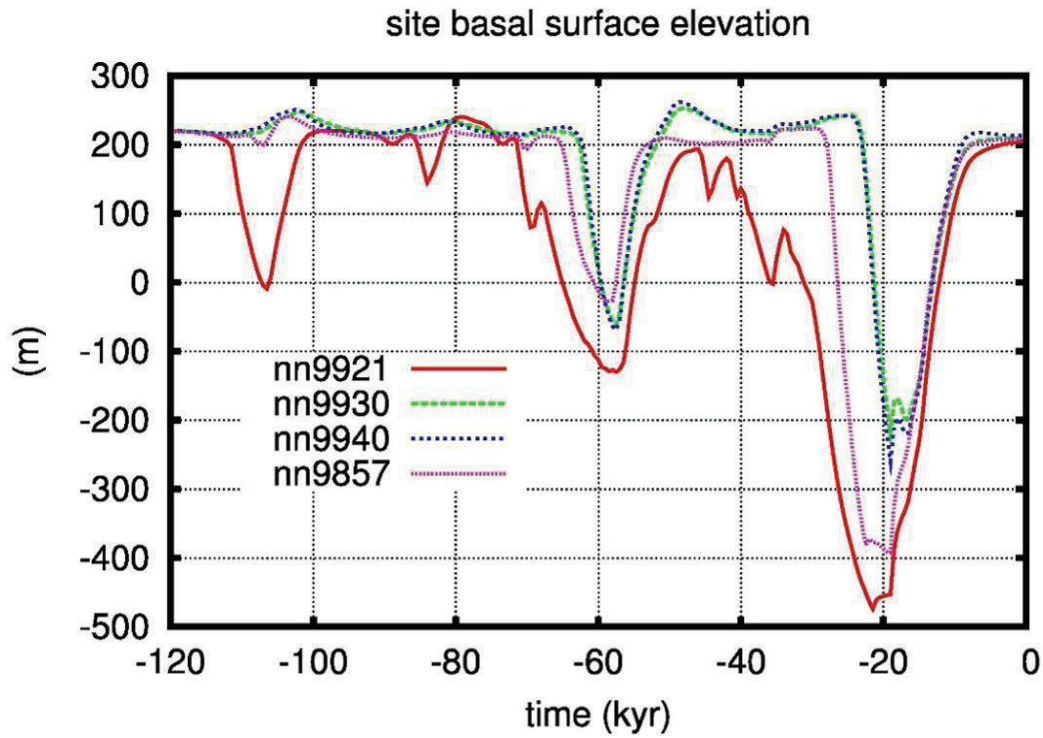
5.3.3 Impact of Glaciation

Glacial cycles will cause the rock to be depressed and rebound due to the loading and unloading caused by the advance and retreat of ice-sheets. Figure 5.4 shows the surface elevation at the site over the last 120 ka as simulated by the University of Toronto Glacial System Model and indicates a maximum depression of around 500 m at the last glacial maximum (Peltier 2011). This depression occurs over a large regional or continental scale and, due to the large scale over which it is developed, tends to be aseismic and not associated with significant displacements along fractures.

During ice-sheet advance over the site, there will be local stress changes. In advance of the ice-sheet there will be a forebulge which will change stresses at least in the top rock layer. With the ice-sheet on the site, the normal stresses will be increased due to the weight of the ice; Peltier (2011) has estimated normal stress increases of up to 30 MPa (Figure 5.5). The normal stress at repository level is about 18 MPa in the absence of an ice-sheet. It is noted that, while emplacement rooms will eventually collapse with repeated glacial cycles and be filled with rockfall, the long-term barrier integrity or permeability of the overlying Ordovician shales will not be affected (see Section 4.4.1).

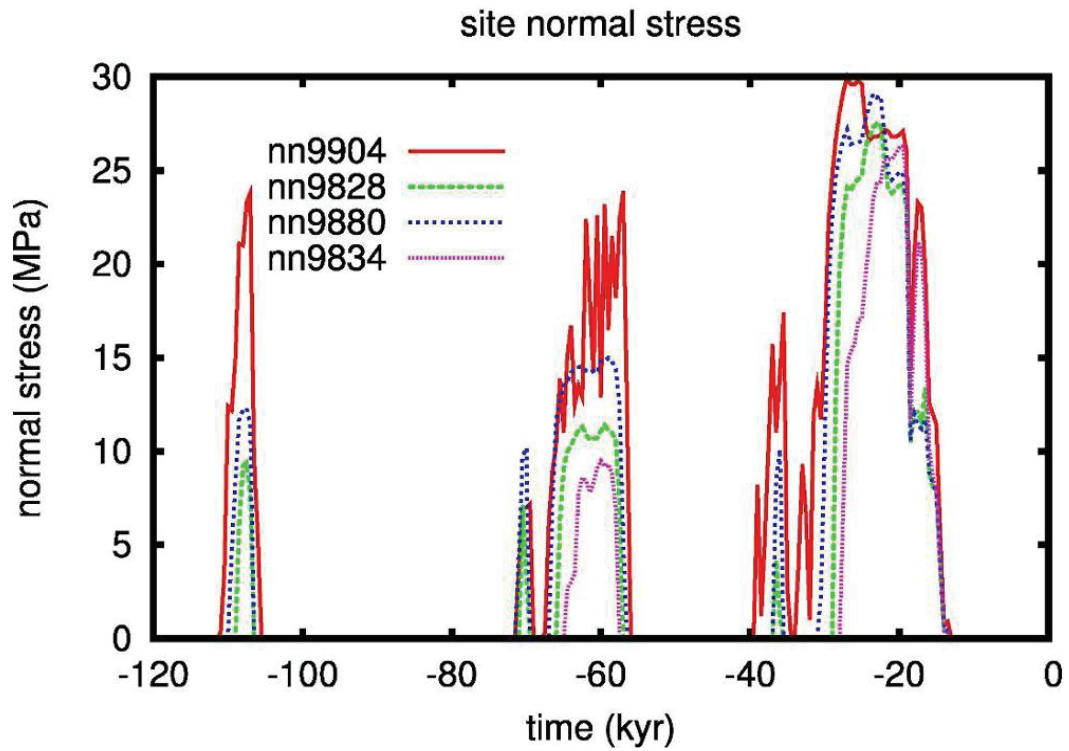
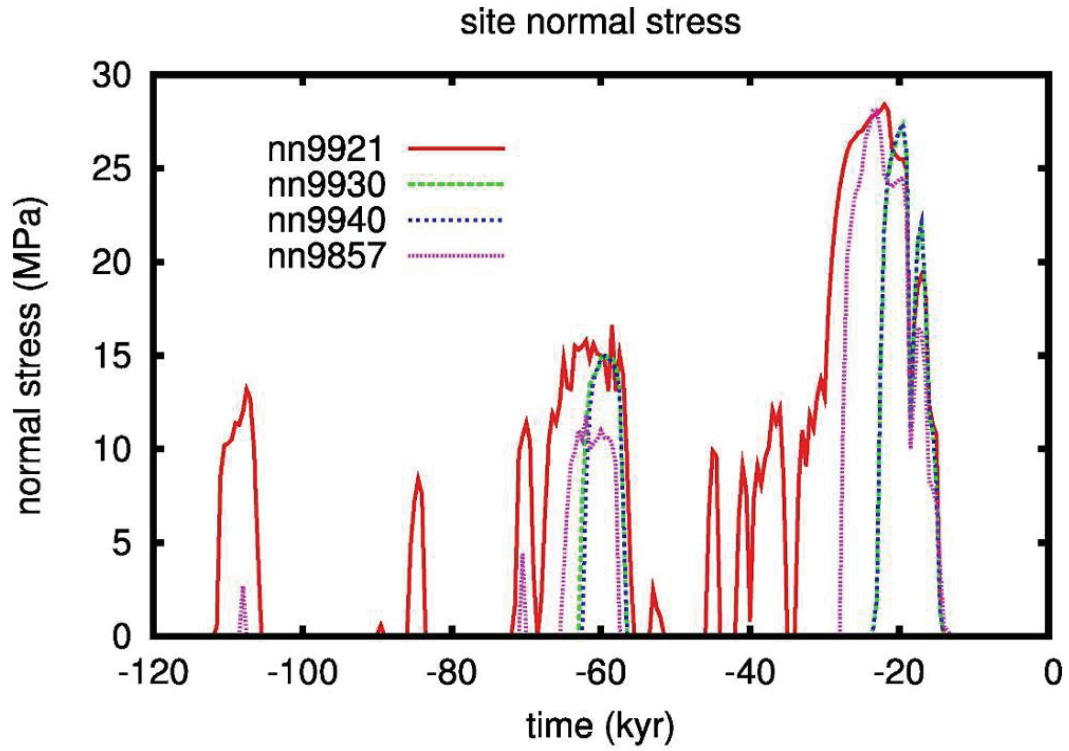
The advance and retreat of ice-sheets will also result in erosion and deposition of material. Historical cycles of glaciation have resulted in erosion at the Bruce nuclear site. Major glacial cycles are anticipated to occur with a periodicity of around 100,000 to 120,000 years. Sections 2.2.7.2 and 6.2.1.1 of NWMO (2011) and Hallet (2011) consider the amount of erosion that might be associated with each glacial cycle, considering global, regional and site-specific evidence for Quaternary ice-sheet erosion, and in particular erosion associated with the Laurentide Ice-sheet.

Although major uncertainties remain, literature data, field investigations and numerical modelling indicate that over the last 100,000 years ice-sheet erosion at the Bruce nuclear site has been of the order metres to a few tens of metres. For future erosion, a similar rate is assumed, consistent with the relatively flat local topography, due to previous glacial scouring and also considering that ice sheets can increase the local rock depth through formation of moraines or deposition of clay or sand in glacial outwash. This net erosion rate implies that, over 1 Ma, of the order of 100 m of bedrock may be eroded. This would not significantly reduce the geosphere barrier at the Bruce nuclear site given the depth of the DGR (about 680 m), although following removal of 100 m of material, some fracturing and hydraulic conductivity enhancement in the upper formations of the Intermediate Bedrock Groundwater Zone may occur due to removal of overburden, and ice-sheet loading and unloading. However, the deeper formations would remain unaffected.



Note: Figure 4.8 in Peltier (2011).

Figure 5.4: Simulated Earth Surface Elevation at the Bruce Nuclear Site over the Last Glacial Cycle for the Eight Cases Consistent with Historical Data



Note: Figure 4.3 in Peltier (2011).

Figure 5.5: Simulated Normal Stresses at the Bruce Nuclear Site over the Last Glacial Cycle for the Eight Cases Consistent with Historical Data

5.3.4 Impact of Earthquakes

Southwestern Ontario and the Bruce region lie within the tectonically stable interior of the North American continent; a region characterized by low rates of seismicity. The Bruce nuclear site is in one of the more stable parts of the interior. This has been confirmed by analysis of over 100 years of earthquake and seismic records for the regional and wider area. Seismic activity may also be triggered by crustal uplift and the release of stresses after the retreat of an ice-sheet (Wu 1998). However, there is no evidence for any ongoing neotectonic activity as a result of ongoing stress relief from the last glaciation (Section 2.2.6.5 of NWMO 2011).

Based on existing site and regional information, the likelihood of fault rupture is extremely low, as it would require a very large event to occur right at the repository site. Furthermore, since the repository is sited in an area where no faults have been observed, it would require fracturing of previously unfaulted rock. The tectonic setting is incompatible with the generation of sufficient forces, even considering the stress relief associated with glacial melting.

Most of the seismic activity that does occur is deep (≥ 5 km), and occurs on pre-existing basement faults that are very rare in the site area. Sections 6.2.2.2 and 6.4.4 of NWMO (2011) indicate that reactivation of any as yet undetected fault or creation of a new fault through the bedrock is unlikely.

Also, repository-scale modelling of the effect of earthquakes has not indicated any tendency for formation of fractures extending from the repository itself.

5.4 Chemical Evolution

At the repository horizon, the present-day chemical conditions in the geosphere are isolated and buffered by several hundred metres of low permeability rock. Geochemical studies reported in Chapter 4 of the Geosynthesis report (NWMO 2011) indicate that the deep geosphere has not been significantly affected by the passage of previous glaciations, and it is not expected to be affected by future ones.

On a site scale, the repository and the waste packages will present a change in the chemical conditions. The rock and repository chemistry will tend to evolve towards a (meta) stable equilibrium state on long time scales.

5.4.1 Impact of the Repository

5.4.1.1 Evolution of Gas Chemistry

Gas generation, primarily CH_4 , CO_2 and H_2 , will occur within the repository due to microbially mediated degradation (producing CO_2 and CH_4) and anaerobic corrosion (producing H_2) of the wastes and packaging. Over time some of these gases will migrate into the surrounding host rock. There are also some natural gas and trace liquid hydrocarbons present in the Silurian and Ordovician formations at the Bruce nuclear site (Section 2.3.6.3).

The quantity of CO_2 in the repository is expected to generally be low due to microbially mediated reduction with H_2 to form CH_4 . There could be minor reactions between the small quantity of CO_2 in the repository and with cement or host rock minerals; particularly carbonates within the limestones and dolomites. Scoping calculations presented in Appendix G and more detailed calculations presented in ARC (2010) indicate that the CO_2 will have limited impact on these carbonate rocks.

The primary gas species in the long term will be CH₄, which is generally unreactive with the host sedimentary rocks, as demonstrated through existence of natural gas fields in similar rocks elsewhere in Southern Ontario. If CO₂ reduction does not occur in the DGR, much of the CO₂ will be consumed through reaction with the limestone host rock until carbonate equilibrium conditions are reached. The long-term gas composition would then comprise a mix of CH₄, H₂ and some CO₂.

5.4.1.2 Evolution of Mineralogy

Large-scale mineralogical changes resulting from geosphere interactions with the repository materials and wastes are very unlikely. The natural deep porewaters are reducing, of very high total dissolved solids, and buffered by the rock minerals. Reaction with repository materials is not likely to alter the major chemistry to such an extent that repository fluids will drive large-scale mineralogical changes.

It is expected that any mineralogical changes that do occur are likely to involve localized mineral precipitation/dissolution in the immediate vicinity of the repository. The precise chemical evolution of the geosphere adjacent to the repository is uncertain owing to the heterogeneity of the wastes and packages. However, the impacts associated with these interactions are expected to be small.

During excavation and the operational phase, dewatering of the repository and thus drying of the EDZ may result in the precipitation of salts such as halite and gypsum in fractures or joints or open porosity associated with the EDZ. These precipitation reactions could seal such features and reduce permeability.

Equally, dissolution of minerals could result in an increase of rock permeability. The alteration would most probably involve the following kinds of reactions:

- Dissolution of carbonate minerals;
- Oxidation of pyrite;
- Alteration of feldspar; and
- Cation exchange involving expandable clay minerals.

Small amounts of sulphide minerals (pyrite and sphalerite) occur within the Cobourg Formation at the Bruce nuclear site. There is a possibility that due to ingress of oxygen during excavation and operation of the DGR, localized oxidation will cause the generation of some acidity. This acidity will be neutralized by reaction with the calcareous host rock. This reaction will tend to increase porosity and permeability in the nearby rock. However the effect will be small since the amount of sulphide minerals is small.

Following closure, CO₂ generated by the microbially mediated degradation of the wastes will dissolve in the repository waters and porewaters, leading to some dissolution of the calcareous host rock, which will act to buffer the pH. Therefore, there is not expected to be a significant change in the pH of the repository waters and porewaters. Dissolution of carbonate minerals will tend to increase porosity and permeability in the near-field rock; but little dissolution is expected (see Appendix G).

Reaction of CO₂ with concrete in the wastes and repository engineering, CO₂ enhanced corrosion of steel and microbial reduction of CO₂ with H₂ forming CH₄ will act as competing sinks for CO₂. Therefore, reaction between CO₂ and the host rock may be limited. Reduction in the CO₂ partial pressure due to reaction with concrete and microbial reduction, combined with

the generation of aqueous iron (II) through corrosion reactions, may result in precipitation of minerals such as siderite (iron (II) carbonate) in both the repository waters and rock porewaters.

Alteration of feldspars by CO₂ could be more extensive, but these reactions are much slower than carbonate dissolution reactions, and feldspars only constitute a minor component of the Ordovician rocks. Cation exchange reactions coupled to the pH evolution of the groundwater in the repository would be minor, since expandable clay minerals are present only in relatively minor quantities.

Characteristic products of any near-field oxidation of iron sulphides would be Fe-oxyhydroxide minerals. Also, the carbonate minerals present in the rock may contain Fe(II) and Mn(II). Any dissolution of these minerals while oxygen is still present in the repository may also be accompanied by oxidation of Fe- and Mn- to produce Fe- and Mn-oxyhydroxides. The mineral products of such oxidation reactions would have high specific surface areas. Potentially any radionuclides that might migrate into this EDZ could sorb on these minerals.

5.4.2 Effects of Glaciation

5.4.2.1 Evolution of Groundwater and Porewater Chemistry

An extended period of global warming with elevated levels of CO₂ might affect the chemical properties of the uppermost near-surface waters, with increased dissolution and total dissolved solids, but the influence would not penetrate deeply due to the buffering capacity of the rock.

The extent and magnitude of geochemical changes during any glacial cycle will depend on the site-specific conditions of the geosphere and of the particular glacial episode. Changes will be most evident in the shallow, hydraulically active portion of the flow system, where oxygenated, low-salinity meltwaters will have the potential to react with redox-sensitive elements or to cause dissolution or precipitation of minerals in fractures (Guimerá et al. 1999).

The historical impact of ice-sheets on groundwater and porewater chemistry is discussed in Section 2.3.7.1. Fresh glacial meltwater was injected into the permeable formations that make up the Shallow Bedrock Groundwater Zone, and the permeable Salina A1 Upper Carbonate formation within the Intermediate Bedrock Groundwater Zone. Freshwater was not able to displace the dense saline porewaters in the low permeability formations within the Intermediate and Deep Bedrock Groundwater Zone, or within the Cambrian formation and basement rocks, which are hydraulically isolated by the overlying low permeability formations. Future glacial cycles are anticipated to be of similar duration and magnitude to the historic Quaternary glacial cycles. The impacts on groundwater and porewater chemistry are, therefore, anticipated to be similar to those associated with the historic Quaternary glacial cycles.

5.4.2.2 Evolution of Mineralogy

Enhanced recharge of fresh oxidizing waters under glacial conditions, particularly during ice-sheet retreat, would affect the geochemistry of the Surficial Deposits Groundwater Zone and Shallow Bedrock Groundwater Zone. The existence of pyrite is further evidence that the deep system has not experienced change due to recent glacial cycles, and is, therefore, likely to remain unchanged over the course of future glacial cycles. Dolomite and calcite form up to 90% of some rocks in the Shallow Bedrock Groundwater Zone (Section 3.7.1.1 of INTERA 2011, Figure 2.26) and dissolution of these phases would likely have the most significant effect on rock porosity. Anhydrite and gypsum also occur in small quantities and would also tend to

dissolve. These processes would probably increase the porosity and permeability of the rock. However, dissolution would not occur uniformly and would be focussed along pre-existing groundwater flow pathways, such as fractures. Additionally, the secondary oxide and oxyhydroxide phases would tend to have higher specific surface areas and sorption capacities than the original oxidized minerals, thereby increasing the ability of the rock to retard radionuclide migration.

In contrast to the rocks of Shallow Bedrock Groundwater Zone, the Intermediate and Deep Bedrock Groundwater Zones are typically much less permeable (Figure 2.19) and contain dense brines. Furthermore, there is no evidence that there have been mineralogical changes caused by past glaciations. For these reasons, surficial environmental changes are not expected to influence significantly the evolution of mineralogy in these zones. Instead, the only mineralogical changes that occur will be caused by the DGR itself; these are described in Section 5.4.1.2.

5.5 Gas Migration

Microbial degradation of organic wastes and corrosion of metallic wastes will cause gas generation within the repository (Section 4.5). Gas can migrate from the repository and through the geosphere by a number of processes:

1. Diffusion of dissolved gas molecules in water;
2. Advection of water containing dissolved gas;
3. Movement of gas as a discrete phase within the original pore space of the material;
4. Movement of gas as a discrete phase within stress- or pressure-induced porosity in the rock matrix (pathway dilation); and
5. Migration of gas as a discrete phase in fractures (i.e., in the EDZ).

5.5.1 Evolution of Gas Pressure

Gas generation rates under the anaerobic, saline, low-water conditions expected in the repository are expected to be low. Nonetheless, over long time scales it is expected that the steel containers and the wastes will degrade, producing gases. The slow gas generation rate is expected to be higher than the rate at which dissolved gas can diffuse away (process 1), due to the low permeability of the host rock and the shaft seals. Analyses indicate that the gas pressures will rise over thousands of years to values comparable to or somewhat above the steady-state hydraulic pressure in the host rock. See, for example, the simple calculations presented in Box 3 (Section 4.3).

If the pressure in the DGR rises above the natural host rock hydraulic pressure, gas and water are pushed out of the repository into the rock and shaft (processes 2, 3 and 5), so that the system returns to a long-term equilibrium with the host rock. As a result, the gas pressures never approach lithostatic pressures and so there is no fracturing or dilation, and processes (4) and (5) can be excluded for the geosphere.

5.5.2 Gas Transport

The potential rates of migration of gas in the free gas phase and dissolved in water are explored in Appendix A.

Movement of bulk gas will occur at a faster rate within the shafts and EDZ compared with the geosphere, due to their relatively higher hydraulic conductivity. The shaft seal-rock interfacemay

also be a preferential gas pathway, although smaller in area, due to a potentially lower effective gas entry pressure. Dissolution of gas into water, and potentially also exsolution of gas from water, will occur along geosphere and shaft/shaft EDZ pathways.

Gas cannot enter the shaft seals until the gas pressure exceeds the water pressure plus the capillary pressure in the shaft seal (i.e. bentonite-sand). The capillary pressure of the shaft seals and EDZ are a function of the degree of saturation. The shafts are expected to saturate relatively quickly compared with the DGR emplacement rooms (within several hundred years, see Section 4.3, Box 2), due to their smaller free volume and connection to water-bearing formations in the Intermediate Bedrock Groundwater Zone. Therefore, bulk gas within the repository will be contained by the saturated shaft seals.

Dilation of the bentonite-sand shaft seals due to the gas pressure is a potentially relevant process. Dilation is most likely to occur at the interface between the shaft seal and shaft wall. For this to occur, the gas pressure would have to overcome the forces acting to seal the interface, which include:

- Compressive force from the rock;
- Cohesion forces between the bentonite-sand and the rock;
- The horizontal component of the lithostatic loading by overlying shaft seal materials; and
- Seal swelling.

In the DGR, the compressive force from the rock is not expected to be significant since the shaft wall rock is expected to be in a stable equilibrium, in which the horizontal stresses in the rock are largely self-supported (not including any potential long-term creep, which is possible in the shales).

The clays will have an internal tensile strength due to their internal cohesive forces. It is assumed that there is little cohesive force with the rock at the interface, although chemical interactions over time could form a bond with the host rock.

The weight and consolidation forces from the placement of the shaft seals will create a horizontal force at the interface. A simple estimate of this force can be obtained as in Box 7. The effective stress is about 2.6 MPa. Including the swelling pressure of the bentonite-sand, the effective stress is about 3 MPa.

Therefore for gas to enter this interface, the gas pressure will have to be greater than the hydrostatic pressure by this amount (if less than hydrostatic, it would not exist as a bulk gas phase). For a hydrostatic pressure of 7 MPa, the gas pressure would need to be at least 10 MPa.

BOX 7: EFFECTIVE STRESS AT SHAFT SEAL - SHAFT WALL INTERFACE

Assuming that the shaft is a column of bentonite-sand, then the total vertical stress at the bottom of the shaft is:

$$\sigma_v = \rho_{sat}gh$$

Where

ρ_{sat} is the saturated density of bentonite-sand,

g is acceleration due to gravity: 9.81 m/s²,

h is the height of the column from surface to top of monolith: 660 m (Table 4.14, QUINTESSA and GEOFIRMA 2011).

The 70:30 bentonite-sand mixture is compacted in-situ to a 1600 kg/m³ dry density (Section 4.5.2.2 of QUINTESSA and GEOFIRMA 2011). Based on 29% porosity, and assuming that it saturates with saline water with an average density of 1100 kg/m³, then the saturated bentonite-sand density is $\rho_{sat}=1900$ kg/m³.

The total vertical stress is then $\sigma_v = 12.3$ MPa.

The effective vertical stress is $\sigma'_v = \sigma_v - u$, where u is the porewater pressure; $u = \rho_wgh = 7.1$ MPa.

The effective lateral stress is given by $\sigma'_h = K_o \sigma'_v$, where K_o is the lateral earth pressure coefficient (Section 7.6 of Holtz and Kovacs 1981).

For clays, typical values for K_o range from 0.4 to 0.8, with higher values corresponding to preloaded deposits (Section 11.11, Holtz and Kovacs 1981). Assuming a value of 0.5, then the effective horizontal stress due to the shaft seals is $\sigma'_h = 2.6$ MPa.

The bentonite-sand has an effective montmorillonite dry density of 1215 kg/m³ (Section 4.5.2.2 of QUINTESSA and GEOFIRMA 2011). The swelling pressure is estimated to be 0.4 MPa (Section 4.5.4).

Therefore, the effective lateral stress of the shaft seal on the shaft wall near the bottom of the shaft is 2.6 MPa + 0.4 MPa = 3 MPa.

The gas will not be able to cause dilation at the interface between the concrete monolith or bulkheads and rock, due to the concrete's resistance to compression, creep and shear. The asphalt will behave similarly to the bentonite-sand, except that its resistance to dilation, shear and creep will be different to the bentonite-sand. In summary, the use of multiple layers of shaft seal materials, with some keying of bulkheads into the host rock, will tend to inhibit formation of simple gas pathways, including a continuous pathway at the shaft seal-rock interface.

If gas migrates sufficiently far up the shafts that it reaches the permeable Guelph or Salina A1 upper carbonate formations, it will tend to then move laterally into these formations due to their relatively high permeability and low gas entry pressure.

5.5.3 Impact of Glaciation

Under future glacial conditions, the presence of permafrost or coverage by a cold-base ice-sheet would restrict the release of gas from the geosphere into the biosphere. Gas would be driven to migrate laterally within the Shallow Bedrock Groundwater Zone. This would increase the dispersion of any gas release to surface, and the dissolution of gas within the groundwater.

5.6 Interfaces with the Waste/Repository and Biosphere Sub-Systems

The most important effects of the geosphere on the repository (including wastes) occur as a result of resaturation. Water from the geosphere will infiltrate into the repository and promote:

- Degradation of the waste packages;
- Generation of gases from degradation of waste packages; and
- Release of contaminants from the waste.

The geosphere will influence the biosphere. In the absence of continuous permafrost, these influences are likely to occur as a result of:

- Groundwater discharge to the surface at natural discharge locations (e.g., into lake sediment) or through wells; and
- Gas discharge to the surface.

6. EXPECTED EVOLUTION OF THE BIOSPHERE

6.1 Approach

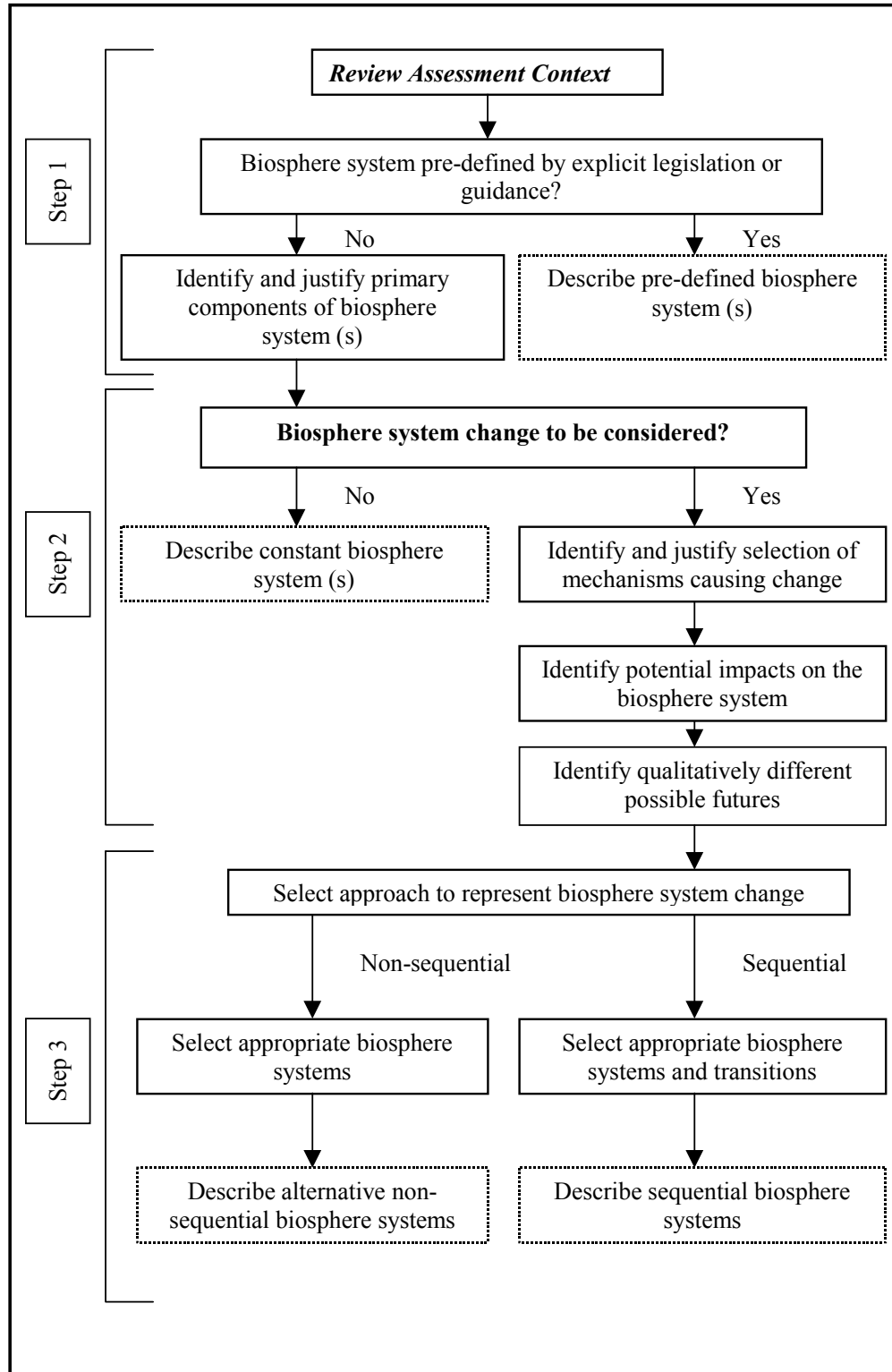
Over the timescale over which the DGR system evolution is to be considered, it is unrealistic to predict human habits and behaviour. Further, major changes to the surface and near-surface environment are also likely to occur over such timescales, either as a result of natural changes such as ice-sheet advance/retreat or as a result of future human actions.

Thus, in order to estimate the potential impacts in the future, a series of assumptions relating to the biosphere and its evolution must be made. Some of these assumptions will necessarily be arbitrary to some extent. However, such assumptions should be consistent with providing a reasonable level of assurance regarding the potential impact of the DGR on humans and the environment.

In particular, any description of the biosphere that is adopted for impact assessment should be considered a 'reference' or 'assessment' biosphere that acts as a 'measuring instrument' for evaluating representative indicators of the potential long-term impact of the repository.

A systematic process (the 'Reference Biosphere Methodology') for establishing a logical audit trail to justify the scope, constituents and definition of such biospheres was developed in Phase II of the Biosphere Model Validation Study (BIOMOVS II 1996) for use in the assessment of deep geologic repositories. It has been subsequently tested and enhanced under the International Atomic Energy Agency's International Programme on Biosphere Modelling and Assessment Methods (BIOMASS) (IAEA 2003) and the BIOCLIM project of the European Commission (BIOCLIM 2004). It is helpful to take the methodology into account when considering the representation and documentation of biosphere evolution. In particular, the practical, three-step approach used for the identification of future biosphere systems (Figure 6.1) is applied in Sections 6.2, 6.3 and 6.4 below.

A consequence of the application of the BIOMASS approach is that this chapter of the report has a somewhat different structure from the repository and geosphere evolution chapters (Chapters 4 and 5), with their focus on the thermal, hydraulic, mechanical and chemical evolution of the repository and geosphere.



Note: Figure is from IAEA (2003).

Figure 6.1: Decision Tree for Use in the Identification and Justification of Biosphere Systems

6.2 Assessment Context

The assessment context, as documented in Chapter 3 of the Postclosure Safety Assessment report (QUINTESSA et al. 2011a), does not define the biosphere system(s) to be considered. However, the context does constrain the definition of the assessment biosphere by the following.

- The primary postclosure safety and performance indicators are: radiological impact on humans as represented by the annual individual effective dose to an average adult member of a hypothetical potential exposure group expected to receive the highest annual dose (i.e., the critical group) from each scenario that is assessed; radiological impact on non-human biota identified through the evaluation of site-specific VECs; and environmental concentrations of hazardous substances.
- A range of representative exposure groups needs to be considered in order to allow confirmation of the identification of the critical group and to illustrate the range of doses that might be received by different exposure groups. Their habits and characteristics should be based on reasonably conservative and plausible assumptions that consider current lifestyles.
- The assessment is to be carried out to a point in time that allows a clear demonstration that the peak calculated impacts have been reached (CNSC 2006).

Consistent with this context, we consider a present-day biosphere since that supports consideration of current lifestyles and site-specific VECs. The primary components of the present-day biosphere system are described in Section 2.4. (i.e., proceeding down the left-hand side of Step 1 shown in Figure 6.1).

Given the long timescales to be considered, it is necessary to give consideration to biosphere system change (i.e., proceed down the right-hand side of Step 2 shown in Figure 6.1) and to identify mechanisms of change and the possible future biosphere systems.

6.3 Consideration of Biosphere Change

6.3.1 Mechanisms of Change

6.3.1.1 Introduction

The BIOMASS program identified seven External FEPs that can act as mechanisms of global change in the biosphere, which can then propagate change down to the regional and local scales (IAEA 2003). These are listed below together with their reference number in the FEP list given in Table 3.1 and whether they are included or excluded from consideration in the DGR Normal Evolution Scenario as a consequence of the External FEPs identification process documented in QUINTESSA et al. (2011b) and summarized in Section 3 and Table 3.2.

- Orogeny (FEP 1.2.02) – excluded.
- Seismicity (FEP 1.2.03) – included.
- Volcanic and magmatic activity (FEP 1.2.04) – excluded.
- Global climate change (FEP 1.3.01) – included.
- Human influence on global climate (FEP 1.4.01) – included.
- Social and institutional developments (FEP 1.4.02) – included.
- Impact of meteorites (FEP 1.5.01) – excluded.

Global climate change is the principal External FEP causing long-term environmental change in the biosphere. Human influence on global climate, and social and institutional developments, will also have important impacts on the biosphere. These External FEPs are discussed further below.

Seismicity is not expected to cause long-term environmental change in the biosphere. As noted in Section 2.3.8, with no seismic events of $M > 4.3$ recorded in the past 100+ years, the likelihood of a large event in the Bruce region is very low - an event of $M \geq 6$ somewhere within a 20 km radius of the Bruce nuclear site has an annual frequency of approximately 10^{-6} . Although such an event might cause some disruption in the biosphere (for example the collapse of buildings), its effects are expected to be limited in magnitude and temporal extent.

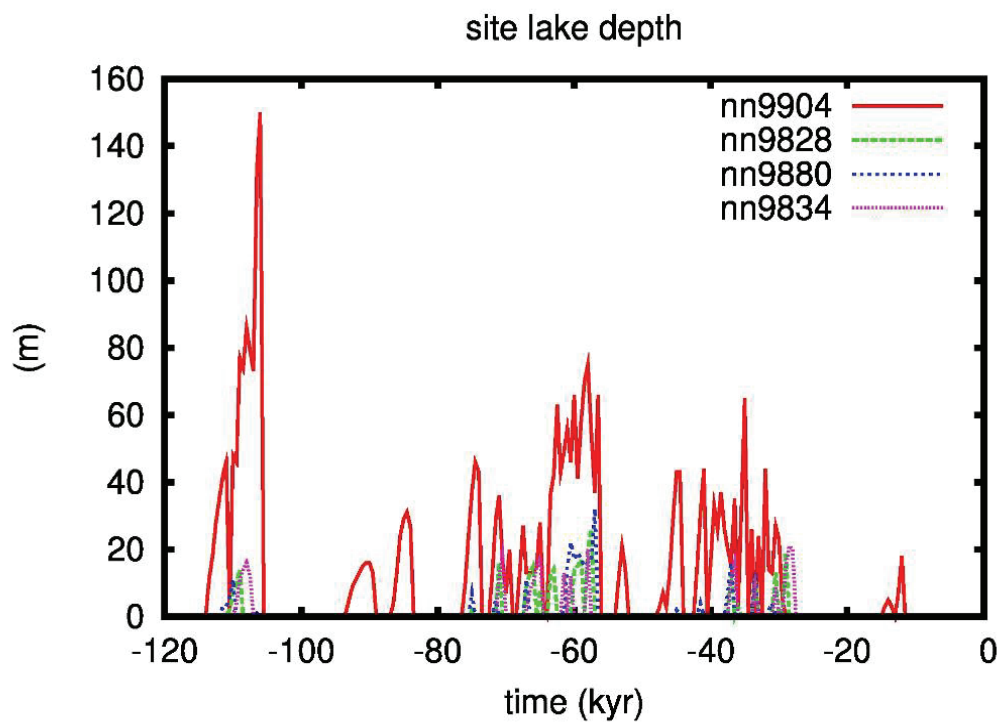
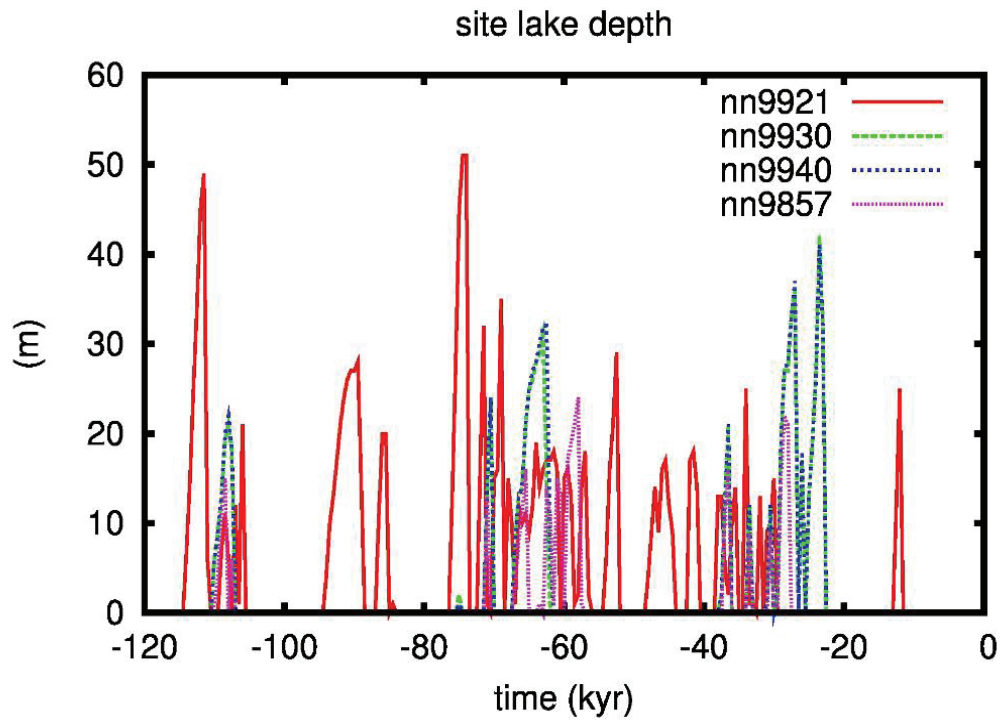
6.3.1.2 Global Climate Change

In the past million years, Canada has experienced approximately nine cycles of glaciation, with relatively short interglacials between them (Peltier 2011). The last glaciation began at about 120,000 years before the present. At its maximum, more than 97 percent of Canada was covered by ice, primarily the Laurentide ice-sheet. The final retreat of the ice-sheet occurred between approximately 9,000 and 6,500 years ago.

Understanding gained from evidence of past ice-sheets can be used to provide information on the likely effects of future ice-sheets on the Bruce nuclear site. To this end, work using the University of Toronto Glacial Systems Model (UoT GSM) has been undertaken to describe the evolution of the Canadian land mass in response to glacial events over the last 120,000 years (Peltier 2011). The work indicates that the site will be affected substantially by the development, presence, and retreat of an ice-sheet.

A range of conclusions are identified by Peltier (2011) that are important in framing the response of the DGR system to climate change for the purposes of safety assessment modelling. Principally, these are:

- Calculated permafrost depth at the site has not been substantial historically, typically being tens of metres in depth (Figure 5.1);
- Meltwater generation is confined to temporally discrete events as the ice sheet is retreating (Figure 5.3);
- The site is likely to be covered with a proglacial lake, as the lake boundary expands and contracts following the advance and retreat of the ice-sheet even though the latter is not actually covering the site (Figure 6.2);
- Crustal deflection of up to 500 m at the last glacial maximum (Figure 5.4); and
- Three distinct periods of ice sheet coverage over the last 120,000 years (Figure 5.4 and Figure 5.3).



Note: Figure 4.7 in Peltier (2011).

Figure 6.2: Simulated Proglacial Lake Depth at the Bruce Nuclear Site over the Last Glacial Cycle for the Eight Cases Consistent with Historical Data

6.3.1.3 Human Influence on Global Climate

There is a evidence that man-made emissions of gases such as carbon dioxide and methane are contributing to global warming (IPCC 2007).

In the near term (i.e., on the scale of centuries or perhaps a thousand years), global warming is likely to cause average annual global surface temperatures to increase by several degrees Celsius, with the increase being rather greater at high northern latitudes. The resulting changes in meteoric precipitation and evapotranspiration could affect the surface and near-surface environments and could change patterns of human activity. Such global warming will also result in a global sea-level rise of several metres. Although the sea-level rise is unlikely to impact the DGR site (due to its elevated inland location), the impacts of temperature and precipitation changes on the surface and near-surface systems might be locally important. For example, there could be changes in Lake Huron water levels and, therefore, changes in the current shoreline, streams and wetlands.

In the longer term, the effects are more uncertain. However, Peltier (2011) notes that the initiation of a glacial episode in the next 60,000 years could be inhibited. Long-term climate modelling in the BIOCLIM project (BIOCLIM 2004) also indicated that no significant glaciations would occur for considerably longer than 60,000 years (and potentially well in excess of 100,000 years). Ultimately, however, it is expected that atmospheric carbon dioxide concentrations will return to historic levels and glacial cycling, on a timescale of around 100,000 years, will be re-established (BIOCLIM 2004).

6.3.1.4 Social and Institutional Developments

Potentially significant social and institutional developments include:

- Changes in planning controls and environmental legislation;
- Demographic change and urban development;
- Changes in land use; and
- Loss of records or societal memory of the DGR location and hazards.

Societal knowledge of the DGR is likely to provide control for at least 300 years from the closure of the DGR (see Section 3.8 of the Postclosure Safety Assessment report, QUINTESSA et al. 2011a). Thereafter, it is assumed for the assessment that the land uses in the previously controlled area are likely to become consistent with those in the wider region around the Bruce nuclear site (i.e., predominantly agriculture and recreation – Section 2.4.7).

6.3.2 Potential Changes to the Biosphere

6.3.2.1 Changes in Surface Features and Processes

Topography

The current-day topography around the Bruce nuclear site and the larger region is relatively flat. It is expected that a relatively low-lying topography with bluffs (representing former lake shorelines), or hills due to glacial moraines, will be maintained during subsequent ice-sheet advances and retreats.

Lake

Lake Huron is a dominant feature in the present-day biosphere at Bruce. Modelling results (Peltier 2011) and field observations indicate that there has been a large lake in this area for a considerable period, although the size, lake levels, and possibly flow outlet have varied. Although the details of the shoreline and extent of Lake Huron will change in the future, it is expected that a large lake will generally be in the vicinity of the DGR site, except during periods of glacial maxima when the area will be overridden by an ice-sheet.

Changes in the size of the lake will have consequences for surface and groundwater conditions, and will also change the areas of land that can be utilized by humans.

Streams and Wetlands

There are currently streams and wetlands present in the vicinity of the site (Section 2.4.2). Future climate change will affect surface water systems and their associated sediments. Changes in precipitation, evapotranspiration and the lake margin location, associated with general climate evolution (including global warming), will be reflected in an evolving pattern of surface drainage with the associated erosion and deposition of sediment. The presence of an ice-sheet will change the nature of “surface” flows. Ice-margin effects will also be significant, especially during retreat when there are likely to be large volumes of meltwater produced and a proglacial lake is likely to be present over the site. Sediment can also be eroded and deposited during the advance/retreat of an ice-sheet. Consequently, the presence and character of surface water courses and their associated sediments will be dynamic, especially in the periods before and after ice-sheet cover occurs.

Soil

The migration of streams and changes in the location of lake margins will result in the exposure/submersion of sediment/soil. In addition to the effects of changes in location of surface water courses, soils and lake sediments will be affected by the advance and retreat of an ice-sheet through erosive and depositional processes and subsequent pedogenesis. The soils currently found at the Bruce nuclear site have developed from former lake bed sediments exposed by the recession of the Lake Huron shoreline following the retreat of the last ice-sheet to affect the site. The flow of water through the soils will be affected by: the climate, through its effects on precipitation and evapotranspiration rates; and the hydraulic characteristics of the soil, which in turn can be affected by the climate, e.g., through the formation of permafrost (Figure 5.1).

6.3.2.2 Changes in Biota

The current distribution of biota in the vicinity of the Bruce nuclear site is described in Section 2.4.8. This distribution can be expected to evolve as a result of natural and human-induced climate change. The climate is currently in a warm phase of the glacial cycle and is expected to warm further in the next millenium, due to human-induced global warming, resulting in some changes to the nature and distribution of biota in the vicinity of the Bruce nuclear site. Thereafter, during glacial cycling, the climate is likely to oscillate between cool and warm periods as it has for the past 1,000,000 years. During the cool periods, the ecosystem is expected to evolve to approximately resemble that currently present at inland tundra locations at higher latitudes in central Canada.

6.3.2.3 Changes in Human Behaviour

It is assumed that eventually land use at the site (currently industrial), will be consistent with that in the surrounding area (i.e., predominantly agriculture and recreation). Wells could be drilled into the Shallow Bedrock Groundwater Zone on the site since the water in the upper parts of this zone is potable and such wells currently exist in the region around the site (Section 2.4.7). Wells in the deeper groundwater zones are not credible since the groundwater in these zones is not potable (Section 2.3.7.1 and Table 2.10).

Natural and human-induced climate change will also impact human behaviour. It is likely that, for some periods of the glacial cycle, conditions will be sufficiently inhospitable that permanent human habitation is very unlikely. However, for the remaining periods, when permanent habitation is feasible, human habits can be expected to remain broadly the same as found today; the main differences being the parameter values that describe the human habits (e.g., the ingestion rates of different foodstuffs and the occupancy rates in different parts of the biosphere system). Present-day practice at farms and individual households in the area is to obtain water from wells rather than the lake or other surface water sources (Section 2.4.4). The wells are typically between 30 and 100 m deep. During climate conditions in which there is some formation of permafrost, it may be necessary to obtain water from other sources such as the lake, because the available water supply may be constrained by the permafrost, and the deeper waters below the permafrost are likely to be saline.

6.3.3 Biosphere Evolution

From consideration of the above mechanisms of change and the associated potential changes, the following illustrative description of the evolution of the biosphere system through a series of stylized biosphere states has been developed for consideration in the current safety assessment.

Although the DGR system will be affected by global warming in the short term (i.e., on the scale of centuries or perhaps a thousand years), the associated changes will not be significant from the perspective of the postclosure safety assessment, since they will not modify the fundamental nature of the biosphere system and its processes. However, global warming will mean that the onset of the next glacial cycle is likely to be delayed, and the next ice sheet coverage of the site would not occur for at least 60,000 years.

Following the onset of climatic cooling, the climate will become drier and the present-day temperate ecosystem will gradually evolve into a tundra ecosystem characterized by sparse vegetation such as lichens, grasses, sedges and arctic-adapted low-lying plants, and dwarf shrubs and discontinuous permafrost. The timescale over which this evolution will occur is uncertain, but previous work for a slightly more northerly latitude has suggested that it could be up to a few thousands of years (McMurry et al. 2003). This tundra period is likely to be the predominant biosphere state during a glacial cycle.

With further cooling, the land surface temperature will fluctuate around the freezing point and the amount of snow accumulation will become greater than the amount melted. An ice-sheet will eventually advance over the site, developing to a maximum thickness of 3 km, resulting in the removal of unconsolidated sediments and some scouring of the underlying bedrock. As the ice provides insulation against heat loss from the earth's interior, the interface between the ice and the underlying solid earth will reach temperatures that are around freezing.

Towards the end of the glacial cycle, the ice-sheet will start to retreat relatively rapidly by melting, resulting in voluminous discharges of meltwater. Regionally, this will be likely to lead to the formation of large proglacial lakes, the further erosion of poorly resistant rocks and sediments in some locations, and deposition of thick layers of glacially derived sediments elsewhere.

Subsequently, further warming will result initially in the re-establishment of tundra conditions, and the eventual warming to present-day temperatures will result in the re-establishment of a temperate ecosystem. Based on historical records, the warm conditions will persist for about 20,000 years until another cooling period initiates the next cycle of glaciation.

This new cycle of glaciation will have a different behaviour in detail, due in part to the different solar insolation variations in the future. However it is sufficient to model it based on the previous historic cycle modelled by Peltier (2011) including its three glacial maxima, as this cycle includes the key aspects of a glacial cycle. This results in the following sequence of biosphere states:

temperate => tundra => glacial => post-glacial => tundra => glacial => post-glacial =>
tundra => glacial => post-glacial => tundra => temperate

This sequence of glacial cycling can be considered to be repeated for the remainder of the assessment timeframe with a periodicity of around 100,000 to 120,000 years, consistent with historic records over the Late Quaternary (Peltier 2011).

6.3.4 Biosphere States

From the above description of the evolution of the biosphere, four biosphere states can be identified:

- Temperate;
- Tundra;
- Glacial; and
- Post-glacial.

Each state has been defined to represent a configuration of the system that is reasonably likely to occur during the evolution of the biosphere at the DGR site, and is of interest in relation to assessing the safety of the DGR system.

6.3.4.1 Temperate

The temperate biosphere state is illustrated in Figure 6.3.

The characteristics of the soils, surface waters and biota are similar to the present day. Human habits are the same as at the present day, with the land being used for agricultural and recreational purposes. Groundwater discharges to the lake and is assumed to be pumped from a well in the Shallow Bedrock Groundwater Zone. Well-water is used for agricultural and domestic purposes. Wetlands and other natural environments are sources of wild food.

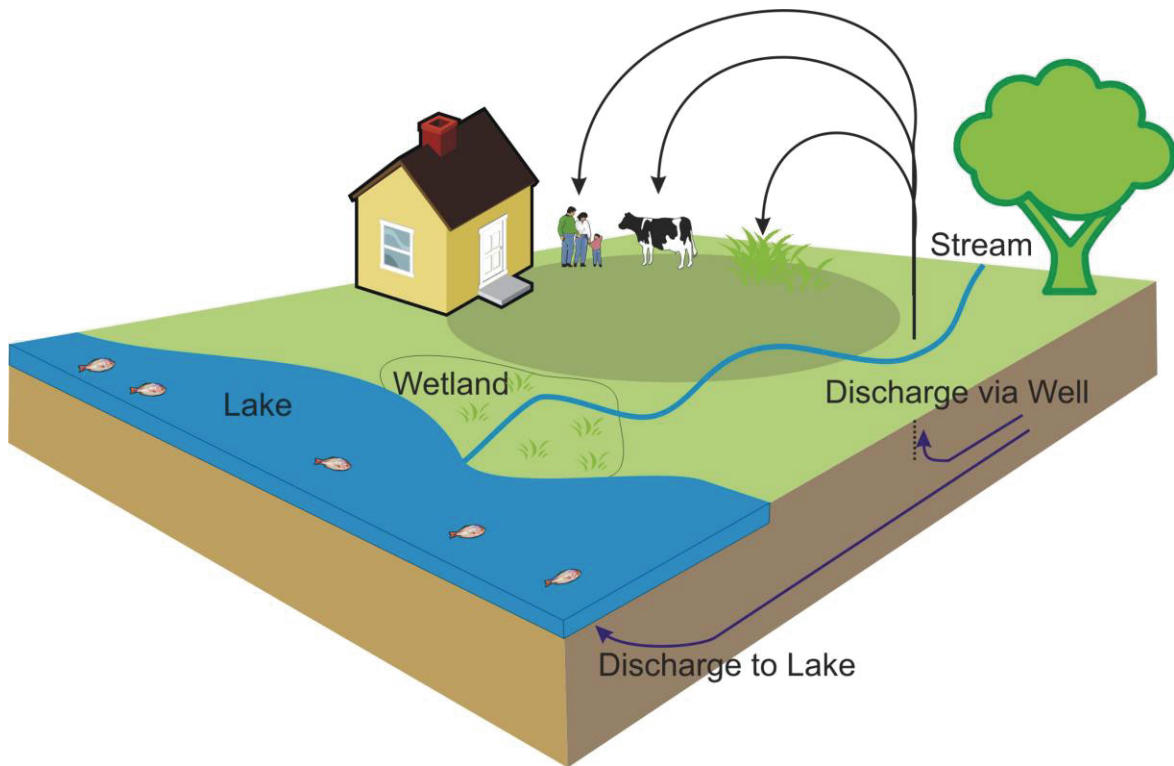


Figure 6.3: Illustration of the Temperate Biosphere State

6.3.4.2 Tundra

The tundra biosphere state is illustrated in Figure 6.4.

The lake may retreat as a result of reduced precipitation, exposing former lake sediments. Other soils may become peaty in nature due to the slow decomposition of newly deposited organic matter in the cold climate. Any permafrost that might be present would be discontinuous and limited to less than a few tens of metres. The biota that are present are comparable with the biota found in present-day tundra environments.

Human habitation is expected to continue to be feasible, but reduced temperatures and precipitation means that agriculture is limited to growing of crops under cover and there is greater reliance on subsistence hunting, fishing, and trapping.

Groundwater continues to discharge to the lake and the retreat of the lake may lead to some limited discharge of water from the Shallow Bedrock Groundwater Zone to a stream. Although there is likely to be reduced demand for water (due to reduced agricultural activity), it is likely that water will continue to be pumped from a well in the Shallow Bedrock Groundwater Zone.

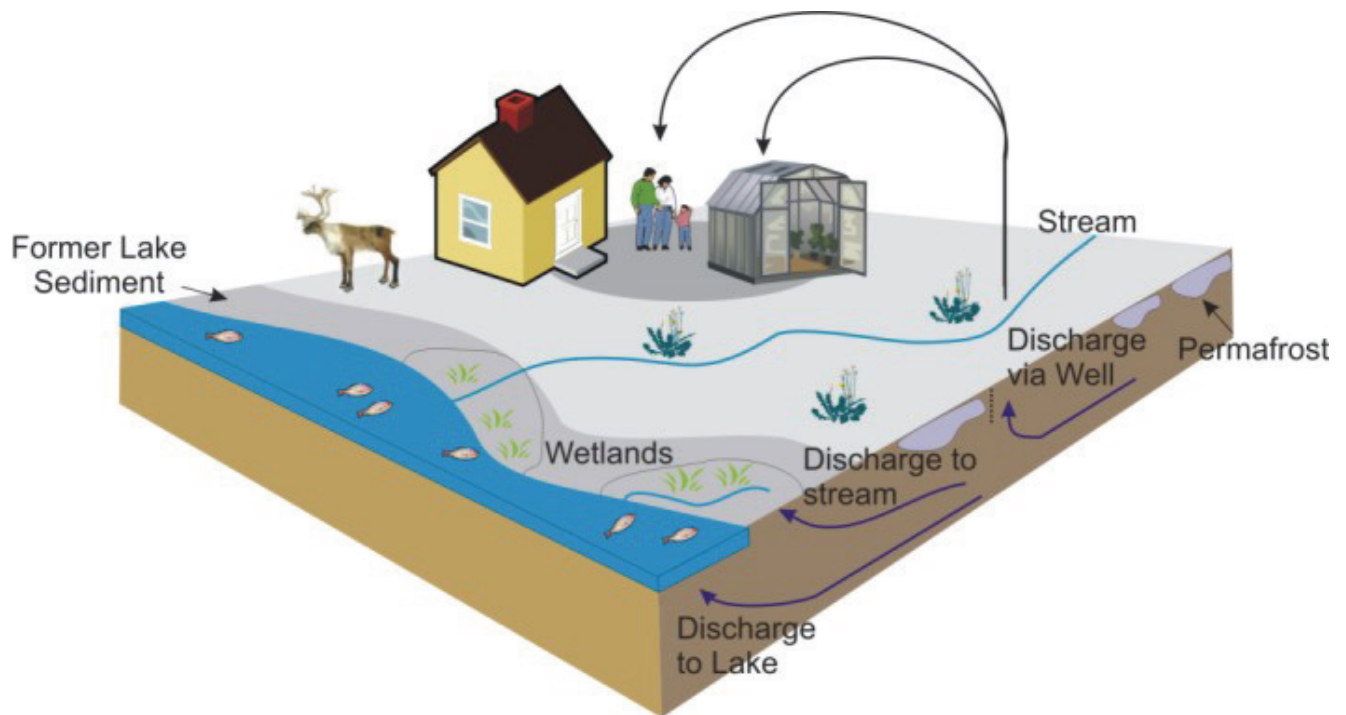


Figure 6.4: Illustration of the Tundra Biosphere State

6.3.4.3 Glacial

The glacial biosphere state is illustrated in Figure 6.5.

The ice-sheet will approach and the biota more limited. The lake may also continue to retreat due to reduced precipitation, exposing sediments. However, this retreat could be mitigated by meltwater coming from a warm-based ice-sheet, especially if other lobes of the ice-sheet cut off the water outlet. As the ice-sheet advances sediments and bedrock will be eroded due to the action of the ice and meltwater, and moraines (accumulations of unconsolidated soil and rock) will develop at the front of the ice-sheet. Groundwater releases are expected to continue to the lake basin and also potentially to other surface waters that may form in advance of the ice-sheet (if warm-based). Permafrost might continue to develop but it is likely to remain discontinuous and is unlikely to extend to a depth in excess of 60 m. If the ice-sheet is warm-based, the permafrost is likely to disappear as the ice-sheet advances over the site. Recharge to the shallow groundwater will decrease if the ice-sheet is cold-based, and increase if it is warm-based.

Self-sufficient permanent human habitation in the region is very unlikely as the environment will be harsh and inhospitable, especially once the site has been overrun by the ice-sheet. Prior to the site being overrun by the ice-sheet, there might be some limited use of resources in the region (e.g., the lake) by temporary visitors (e.g., fishers, nomadic people).

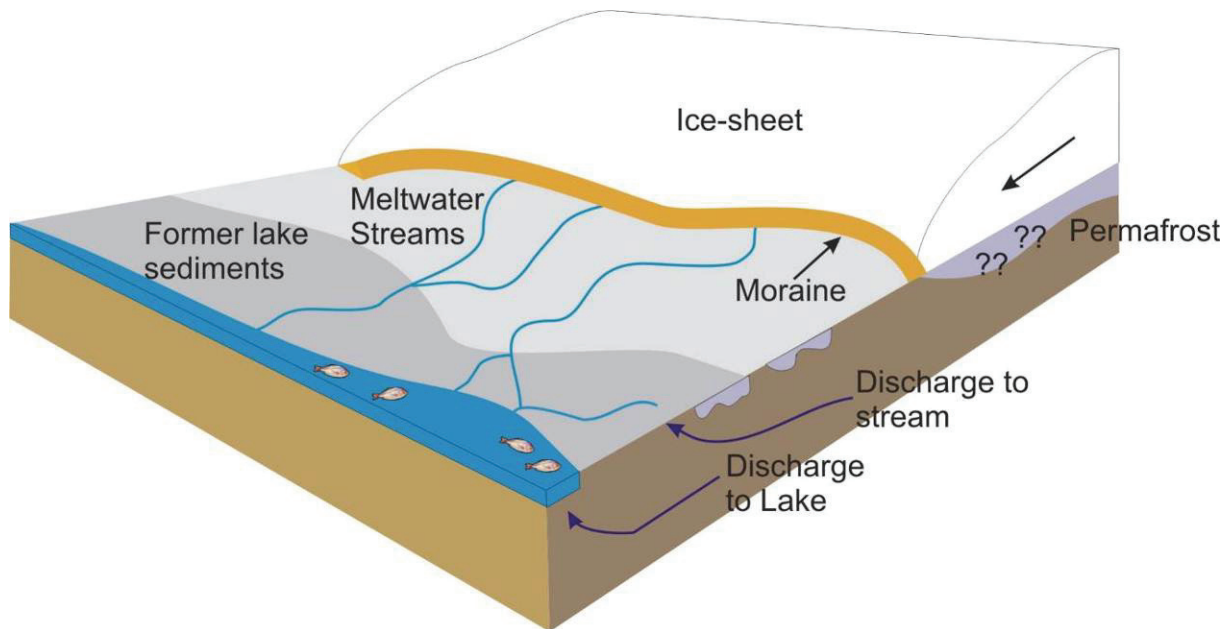


Figure 6.5: Illustration of the Glacial Biosphere State

6.3.4.4 Post-glacial

The post-glacial biosphere state is illustrated in Figure 6.6.

Figure 6.2 indicates that the DGR site is likely frequently covered by a proglacial lake. This would follow the retreat of the ice-sheet from the site, but also more generally reflects the expanding lake size as it collects meltwater from a more distant retreating ice-sheet. Eventually, for a period, the proglacial lake is expected to overlie the site completely, before gradually receding as a result of ameliorating climatic conditions, drainage and isostatic rebound.

The vicinity of a retreating ice-sheet will consist primary of sands, clays and gravels, and exposed bedrock; there will be little soil development. Some nomadic animals (e.g., caribou herds, migratory birds) will be present and vegetation will be limited to a few hardy species. There could be a transient presence of people who make use of the local resources, especially fish.

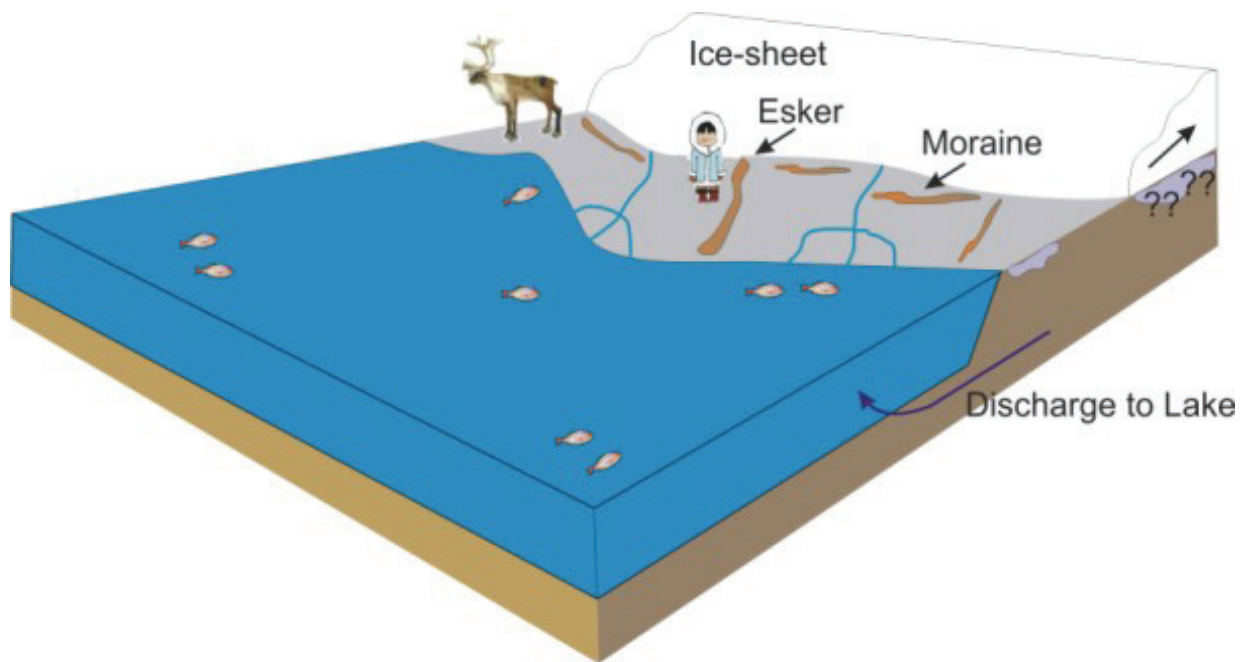


Figure 6.6: Illustration of the Post-glacial Biosphere State

6.3.5 Sequence of Future Biosphere Change

The analysis of the last glaciation cycle by Peltier (2011) has been reviewed and simplified in order to determine basic trends that can be used in a safety assessment representation of the sequence of future climate change at the Bruce nuclear site. Projecting past patterns of climate change forward in time is valid because the key initiators of glacial cycles, variations in the Earth's orbit, have a characteristic timescale. This is known as the Milankovitch effect. A key period of 41 ka is associated with the temporal variability in orbital obliquity (the precession of the spin axis with respect to the plane of the ecliptic). A dominantly 100 ka periodic variation of orbital eccentricity modulates the amplitude of the precessional effect. This means that, while characteristic timescales can be identified, the magnitude of glaciations varies. However, the Milankovitch theory does not fully explain the dominant 100 ka periodicity of observed glacial cycles in the Quaternary.

Figure 6.7 presents a simplified pattern of change for site basal temperature derived for the last full glacial cycle, based on data given in Peltier (2011). This figure has been developed by judgement from the reported results of Peltier's ensemble of model runs, seeking to identify the key trends, and representative measures of temperature corresponding to the Bruce nuclear site.

It is clear that three glaciation maxima occurred, peaking at approximately 110ka, 60ka and 20 ka BP, with varying magnitude (the 20 ka BP event being by some margin the most severe).

Throughout most of the last glacial cycle, site basal temperatures were below 4 °C, with only the last 10 ka showing temperatures that would comfortably correspond to a temperate climate. Over the rest of this cycle (i.e., unaffected by global warming effects) the climate is tundra or glacial in nature at the Bruce nuclear site.

A simplified sequence of climate states can be assigned using the biosphere states identified in Section 6.3.4 and is shown in Figure 6.8. This corresponds to typical climatic variations, with no influence of increased greenhouse gas concentrations due to human activity. There is some uncertainty as to whether the 41 ka or 100 ka periodicity will dominate in the future (the former dominated during most of the last few million years, but the latter has been most prevalent during the last 800 ka). Results in Peltier (2011) are presented on a 120 ka timescale and therefore, for consistency with these, this timescale is adopted as being representative, although it is noted that variations will occur.

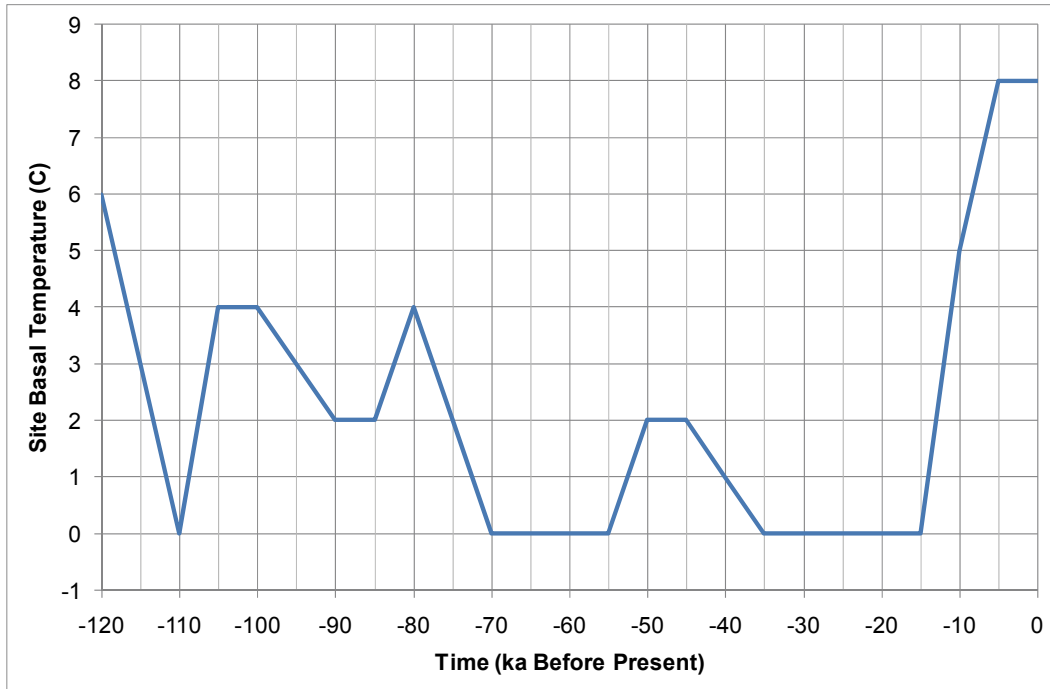


Figure 6.7: Simplified Historic Pattern of Surface Temperature at the Bruce Nuclear Site during the Last Glaciation Cycle

The UoT GSM does not take account of the influence of human-induced global warming as a result of the increased concentrations of atmospheric greenhouse gases. No detailed information on the impact of global warming at the Bruce nuclear site is, therefore, available. However, Peltier (2011) notes that a glacial cycle in the next 60 ka could be inhibited. Furthermore, work on long-term climate modelling using Earth Models of Intermediate Complexity in the BIOCLIM project (BIOCLIM 2004) indicate that no significant glaciations would occur for considerably longer than 60 ka (potentially well in excess of 100 ka).

It is, therefore, reasonable to assume that temperate conditions persist at the Bruce nuclear site for 60 to 70 ka before there is a possibility for the historical pattern of glaciations to recommence, as illustrated in Figure 6.9. The rest of the sequence is based on the pattern shown in Figure 6.8, but projected forward in time with the first 70 ka of the cycle assumed to be temperate.

Subsequent cycles are then assumed to follow a pattern similar to that experienced in the last 120 ka (shown in Figure 6.8).

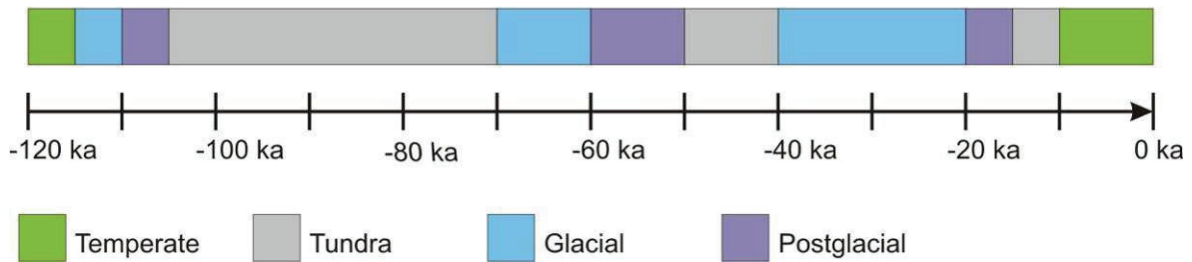


Figure 6.8: Simplified Sequence of Past Climate States

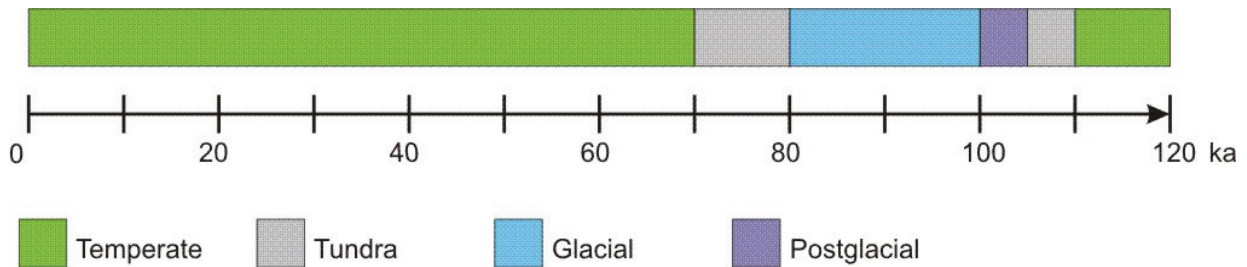


Figure 6.9: Assumed Sequence of Climate States and Permafrost Depth with Global Warming for the Next 120 ka

6.4 Representation of Biosphere System Change

The final step in the identification and justification of the biosphere system (per Figure 6.1) is the selection of an approach to represent biosphere system change in the development of assessment biospheres. This is a modelling decision that is discussed in the Normal Evolution Scenario Analysis report (QUINTESSA 2011) rather than this system description and evolution report.

6.5 Interfaces with the Repository and Geosphere Sub-Systems

It is expected that there will be no direct impact of the biosphere on the repository for the Normal Evolution Scenario due to the isolation of the repository from the biosphere and its processes provided by the depth of the repository. Nevertheless, there could be a limited number of indirect impacts such as the increased loading and associated stresses at depth resulting from an ice-sheet, causing rockfall in the repository rooms and tunnels. Furthermore, since the Main and Ventilation shafts are part of the repository system and they extend up from below the level of the emplacement rooms through the geosphere to the surface environment, the repository system can direct interface with the biosphere.

The interface between the geosphere and biosphere is important to consider in any safety assessment since its nature can have a significant impact on the release of contaminants from the geosphere into the biosphere.

Contaminant releases into a biosphere consistent with that currently found at the site can occur via the following pathways:

- Groundwater discharge via the Shallow Bedrock Groundwater Zone into a lake;
- Groundwater wells near the repository in the Shallow Bedrock Groundwater Zone; and
- Gaseous releases into the soil and atmosphere above the repository, primarily focussed around the main and ventilation shafts.

However, with evolution of the biosphere described above, the nature of the interface can be expected to change. With the onset of cooler conditions, the location of contaminant discharge is expected to be redirected, for example to former lake bed sediments exposed due to a fall in lake level (see Section 6.3.2.1). The advance and subsequent retreat of ice-sheets over the site is likely to cause significant changes in the configuration of the biosphere and the nature of the Shallow Bedrock Groundwater Zone, due to the effects of erosion and deposition caused by the ice-sheet and its associated meltwaters. The response of surface-water and groundwater systems may also be complex (see discussion in Section 5.2). Therefore, a number of interfaces could be envisaged for the post-glacial biosphere state in addition to the lake and well identified for the present-day biosphere state:

- Groundwater discharge via the Shallow Bedrock Groundwater Zone into a stream/river;
- Groundwater discharge via the Shallow Bedrock Groundwater Zone into a marsh; and
- Groundwater discharge via the Shallow Bedrock Groundwater Zone to a lake shore.

7. THE EXPECTED EVOLUTION OF THE DGR SYSTEM: THE NORMAL EVOLUTION SCENARIO

The guidelines for the preparation of the PSR and EIS for the DGR (CEAA and CNSC 2009) and the guidance on assessing the long-term safety of radioactive waste management (CNSC 2006) both identify the need for the postclosure safety assessment to include a scenario of the normal (or expected) evolution of the site and facility that is based on reasonable extrapolations of present-day site features and receptor lifestyles. This scenario should include the expected evolution of the DGR system and its degradation (loss of barrier function) with time.

The expected evolution of the DGR system has been described in Chapters 3 to 6 in terms of:

- The External FEPs affecting the expected evolution of the entire system (Chapter 3);
- The FEPs affecting the expected evolution of the waste and repository (Chapter 4);
- The FEPs affecting the expected evolution of the geosphere (Chapter 5); and
- The FEPs affecting the expected evolution of the biosphere (Chapter 6).

The role of this section is to synthesize the information provided in Chapters 3 to 6 in order to provide a high-level narrative of the expected evolution of the DGR system that can be used to inform the subsequent development of conceptual models.

Chapter 3 identifies the following External (scenario-generating) FEPs as needing to be considered in the Normal Evolution Scenario:

- Climate change with initial global warming, and subsequent reversion to the glacial/interglacial cycling experienced over the last million years;
- Large-scale denudation and deposition due to ice-sheet advance and retreat;
- Seismic events;
- The development of soils from unconsolidated parent material (particularly after the retreat of ice-sheets);
- The deformation of rocks (including the EDZ) and shaft materials due to loading from ice-sheets; and
- Land-use change once controls are no longer effective.

Taking these External FEPs into account, together with the Internal FEPs discussed in Chapters 4 to 6 and the FEPs report (QUINTESSA et al. 2011b), the following description of the Normal Evolution Scenario has been developed.

7.1 Overall System Evolution

The construction, operation, monitoring and closure of the DGR are undertaken under OPG's quality assurance program and are consistent with the description provided in Section 2.2. Following closure of the repository, some combination of active and passive controls (e.g., monitoring, planning controls, markers, and societal memory) remains effective for a reference period of 300 years (Section 3.8 of the Postclosure Safety Assessment report, QUINTESSA et al. 2011a). Once these controls are relaxed or become ineffective, it is assumed that land uses in the previously controlled area become consistent with the wider region, i.e., predominantly agriculture and recreation (Section 2.4.7).

Although global warming is likely in the near term (i.e., over the next thousand years), it is expected that its impact will not be significant from the perspective of the postclosure safety assessment because:

- The inland location of the Bruce nuclear site means that sea-level rise does not impact the site;
- The hydraulic isolation of the repository and the deep geosphere from the surface and near-surface systems prevent the effects of any temperature and precipitation changes significantly impacting the repository and the deep geosphere; and
- Releases of contaminants are very unlikely to occur from the repository over such a timescale due to the isolation provided by the geosphere and shaft seals.

However, global warming does delay the onset of the next glacial episode, which does not occur for 60,000 years (Peltier 2011). After around 60,000 years, a cooling in surface temperature occurs resulting in the transition from present-day temperate conditions through tundra to glacial conditions. A warming in surface temperature then occurs resulting in the retreat of the ice-sheet from the site, the development of a proglacial lake and the subsequent re-establishment of tundra conditions. Further warming results in the eventual re-establishment of temperate conditions. These warm conditions persist until another cooling period initiates the next cycle of glaciation around 100,000 to 120,000 years from present. This new cycle of glaciation is not affected to the same extent by global warming and so has characteristics similar to the historic cycle modelled by Peltier (2011) including its three glacial maxima. This sequence of glacial/interglacial cycling is repeated for the remainder of the assessment timeframe with a periodicity of around 100,000 to 120,000 years, consistent with historic records over the Late Quaternary (Peltier 2011).

7.2 Waste and Repository Evolution

The evolution of the waste and repository can be divided into three phases:

- 1) An aerobic humid period immediately following closure of the repository during which the levels of oxygen in the repository decrease due to degradation of the waste packages;
- 2) An anaerobic humid period during which degradation of waste packages continues, and repository is unsaturated or partly saturated; and
- 3) An anaerobic inundated period following the eventual resaturation of the entire repository.

The aerobic humid phase is expected to be relatively short, with the main consequence being the removal of oxygen and establishment of anaerobic conditions in the repository.

During the anaerobic phases, the waste packages (i.e., wastes, containers and any overpacks) in the repository degrade at differing rates due to corrosion and microbial degradation. If sufficient moisture is present, the carbon steel containers degrade significantly on timescales of decades, whereas other packages (e.g., those with stainless steel containers) might take centuries. Following the degradation of the packages, the waste and the contaminants can be contacted by water that has entered the repository. The extent of contact depends on the resaturation level in the DGR.

The shafts resaturate more rapidly than the rooms/tunnels because they are backfilled, and therefore the volume to be resaturated is smaller. Capillary suction in the shaft seal materials also increases the rate of water inflow, and hence resaturation, compared with the repository where there is no backfill and hence no capillary suction. Also, unlike the DGR, there is no gas

generation in the shaft (the presence of gas acts to increase the pressure and reduce the hydraulic gradient driving resaturation). Water is also able to move vertically within the shaft and the associated EDZ because the seals and EDZ are relatively more permeable than the Deep and Intermediate Bedrock Groundwater Zones. This allows water from the Shallow Bedrock Groundwater Zone and the more permeable formations in the Intermediate Bedrock Groundwater Zone (i.e., the Guelph and Salina A1 Upper Carbonate) to flow into the shafts. Once the shafts have resaturated, the potential for the migration of bulk gas through them is significantly reduced due to the reduction in the relative permeability for gas.

The repository gradually resaturates with water from the surrounding geosphere and the shafts. Resaturation is limited by the repository gas pressure, the low permeability of the shaft seals and the very low permeability of the host rock. The repository might take many hundreds of thousands or even millions of years to resaturate.

The host rock has good rock-mechanical quality, and the emplacement room design (i.e., alignment with principal stresses, low excavation volume) results in a mechanically stable configuration. However, as the rooms and tunnels are not backfilled (the wastes occupy about 50% of the volume), it is expected that rockfall from roofs and walls of the rooms and tunnels will occur periodically, due to eventual degradation of engineered rock support and, in the longer term, due to seismic and/or glacial events. This process continues intermittently, over a period of a few hundred thousands of years, until the volume of collapsed rock has increased sufficiently to support the roof of the void. The extent of roof collapse is expected to be about 10 m above the original roof and does not affect the overlying strata of key barrier rock formations, i.e., the Georgian Bay and Queenston shales.

The concrete wall at the entrance to each emplacement room is not constructed to be water/air tight and is not expected to provide a barrier to water or gas mixing between rooms. The concrete closure walls and monolith in the access tunnels provide a barrier to gas and water movement, although their effectiveness is reduced by the surrounding HDZ and EDZ.

The degradation of the waste packages results in the generation of gases, primarily hydrogen, carbon dioxide and methane, over a period of thousands of years. Initially, the rate of gas generation is likely to be greater than the rate of gas loss due to the low permeability of the host rock resulting in an increase in gas pressure in the repository. As the wastes are degraded, the rate of gas generation eventually slows, and eventually a long-term pressure equilibrium will be approached with the geosphere.

Repository gases will contain H-3, C-14 and radon. In addition, some I-129, Cl-36 and Se-79 may be volatilized⁶. These radionuclides can be released as bulk gas phase into the shafts and the host rock. Gases can also dissolve into repository water and migrate from the repository in the water. The rate of bulk and dissolved gas migration via the shafts and EDZs is very slow due to their low permeability and small area.

Contaminants are also released from the wastes directly into repository water. Most wasteforms release contaminants relatively easily into the repository water on contact. However some contaminants within the concrete packages (e.g., resins, retube waste) can be associated

⁶ Microbially mediated reactions in surface soils can lead to the methylation of I, Cl and Se, forming volatile compounds, i.e., CH₃Cl, etc. Similar reactions could potentially occur in a repository.

initially with low solubility due to high pH. Corrosion-resistant wasteforms such as Zircaloy only release contaminants very slowly. Diffusion of contaminants can take place through any surface contacted by repository water. The release of contaminants in water, therefore, increases as the repository resaturates. Transport of contaminated water takes place in the shafts and their associated EDZs. The shafts contain a sequence of seals of concrete, bentonite-sand and asphalt that limit migration of contaminants in gas and water through the shafts. The performance of the bentonite-sand and asphalt seals in terms of resistance to gas and water flow is not expected to degrade significantly in the Deep and Intermediate Bedrock Groundwater Zone due to the stable geological environment. Sulphate attack and mechanical stresses may result in some cracking of the concrete in the shafts.

Transport of contaminants in water through the shaft might have an advective, as well as diffusive, component due to the driving head provided by the pressurized Cambrian formation that underlies the DGR and the gas pressure in the DGR itself. However, this is also counteracted by the underpressures in the Ordovician formations, which tend to pull water from the shaft. Furthermore, the relatively small cross-sectional area of the shafts limits the contaminant mass that can migrate via this route. Contaminants may also be released to the host rock, although their subsequent transport is diffusional due to the very low rock permeability and porosity.

7.3 Geosphere Evolution

The deep sedimentary rocks were laid down over 400 million years ago. These rock formations are thick, laterally extensive, and stable.

The repository is a local perturbation to the deep rock. A 'halo' region around the repository is formed where there are some effects from the repository on the host rock, such as some alteration of the porewater chemistry, redistribution of stresses, and increased gas content in the pores.

On a larger scale, the key External FEP affecting geosphere evolution is climate change, specifically glacial/interglacial cycling. Within the past million years, the rocks at the Bruce nuclear site have been subjected to multiple glaciations and this glacial cycling is expected to continue. Although global warming results in changes in groundwater recharge and flow in the Shallow Bedrock Groundwater Zone in the short term (i.e., over the next thousand years), it is expected that the impacts will not be significant from the perspective of the postclosure safety assessment.

The main impacts of glacial cycles in the Deep Bedrock Groundwater Zone are changes in the temperature, hydraulic pressure and stress regime resulting from ice-sheet loading and unloading. Changes in hydraulic pressures will lag the ice-sheet loading and unloading due to the low permeability of the rock, which will create some vertical pressure gradients. However, actual flow due to these gradients will remain limited due to the low permeability of the rock and shaft seals. Changes in the stress regime might result in repository rockfall, as described in Section 7.2, until the fallen rock becomes self-supporting to the roof.

Significant changes are likely to occur in the Shallow Bedrock Groundwater Zone during the glacial cycles. As the climate cools, the recharge to the shallow groundwater decreases due to reduced precipitation and an increased proportion of precipitation becoming surface runoff due to spring snowmelt. Discontinuous permafrost develops in the Shallow Bedrock Groundwater Zone and with time extends down to several tens of metres depth. The permafrost does not,

therefore, substantially impact on the overall conductivity of the Shallow Bedrock Groundwater Zone. The amelioration of the climate as the glacial cycle continues results in the retreat of the ice-sheet, and the melting of the permafrost. It is likely that proglacial meltwater lakes will be present.

The arrival of an ice-sheet causes changes in water flow rate and direction in the Shallow Bedrock Groundwater Zone and possibly certain formations in the Intermediate Bedrock Groundwater Zone due to the weight of the ice. It might affect hydrogeology and groundwater chemistry by moving large volumes of low-salinity and possibly oxidizing meltwater through these formations. At the Bruce nuclear site, there is evidence that the influence of the last Laurentide glaciation extended throughout the Shallow Bedrock Groundwater Zone and locally to the Salina A1 upper carbonate formation at around 300 m depth in the intermediate groundwater zone.

Taking a rate of future erosion by ice and meltwater (associated with ice-sheet advance and retreat) comparable with that estimated over the last 100,000 years, implies that of the order of 100 m of bedrock may be eroded over 1,000,000 years. This does not significantly reduce the geosphere barrier at the Bruce nuclear site given the depth of the DGR.

The Bruce nuclear site is in a tectonically stable region and is expected not to be subjected to severe seismic ground motion. Nevertheless, seismic events will occur during the timescales of interest and are expected to be one of the causes of repository rockfall within the emplacement rooms and tunnels. Other potential consequences of seismic activity, such as reactivation of existing faults, are very unlikely. No evidence of faults has been found in the vicinity of the repository, and they are not evaluated in the Normal Evolution Scenario.

Contaminants in the gas phase in the geosphere are expected to be isolated and contained within the deep geosphere due to its very low permeability. Contaminants dissolved in water migrate by diffusion through the Deep Bedrock Groundwater Zone, and then eventually into the Intermediate and Shallow Bedrock Groundwater Zones. Water in the Deep and Intermediate Bedrock Groundwater Zones is either stagnant or very slow moving, in large part due to the low permeability of the rock.

The transport of any contaminants that might eventually reach the Shallow Bedrock Groundwater Zone via the shafts, their EDZs and/or the geosphere is expected to be advection dominated in the Shallow Bedrock Groundwater Zone, and contaminated groundwater is expected to discharge into the near-shore zone of Lake Huron or its successor. The nature of transport in this region may be affected during glacial cycles through erosion/deposition, the introduction of large volumes of low-salinity and possibly oxidizing meltwater, and changes in the groundwater flow direction and discharge location.

7.4 Biosphere Evolution

Due to the depth of the DGR and the physical and chemical barrier provided by the geosphere and shaft seals, the contaminants are expected to be isolated and contained in the repository and deep geosphere. Most radionuclides will decay to negligible levels within the repository and/or geosphere. Any release to the biosphere would be at very low concentrations and at very long times (potentially in excess of a million years).

One consequence of this robust system is the need to consider the biosphere over timescales on which glacial cycling is likely to occur. Given the considerable uncertainties associated with

the resulting evolution of the biosphere, a 'reference' biosphere approach has been used, in which stylized representations of the biosphere are used to allow illustrative estimates of potential repository impact to be made.

Four future biosphere states are identified.

- **Temperate** - the characteristics of the biosphere and habits of the humans are similar to those found in the vicinity of the site today. The land is used for agricultural and recreational purposes and water is pumped from a well in the Shallow Bedrock Groundwater Zone to be used for agricultural and domestic purposes. The wetlands and other natural environments are sources of wild food. The lake is used for fishing.
- **Tundra** - the characteristics of the biosphere and habits of the humans are similar to those found in present-day tundra ecosystems. Any permafrost present is discontinuous and limited in depth to less than a few tens of metres. Groundwater continues to discharge from the Shallow Bedrock Groundwater Zone into the lake and is pumped from a well. In addition, retreat of the lake due to reduced precipitation results in exposure of lake bed sediment and may lead to some limited discharge of groundwater to a stream. Human habitation is feasible, but reduced temperatures and precipitation mean that farming is limited and there is greater reliance on wild foods. Exposure pathways associated with well water remain possible for domestic and limited agricultural use.
- **Glacial** – self-sufficient permanent human habitation in the region is very unlikely as the environment is harsh and inhospitable. Prior to the site being overrun by the ice-sheet, there may be some use of resources in the region (e.g., the lake) by temporary visitors (e.g., fishermen, nomadic people) and releases of groundwater are expected to continue to the lake basin and also potentially to other water bodies that may form in advance of the ice-sheet (if warm based). As the ice-sheet advances, sediments and bedrock are eroded due to the action of the ice and meltwater, and moraines develop at the front of the ice-sheet.
- **Post-glacial** - a large proglacial lake is likely to form and to eventually overlie the site completely for a period, before gradually receding as a result of ameliorating climatic conditions and isostatic rebound. The retreating ice-sheet results in a network of meltwater streams, which redistribute sediments resulting from ice-sheet deposition. Human habitation is unlikely initially as the exposed rocks and sands do not support life, but in due course soils develop and plants return as do migrating animals and birds, and fishing supports nomadic humans.

8. OTHER POSSIBLE EVOLUTIONS OF THE DGR SYSTEM: DISRUPTIVE SCENARIOS

In addition to consideration of the Normal Evolution Scenario, the guidelines for the preparation of the PSR and EIS required for the DGR (CEAA and CNSC 2009) and the G-320 guidance on assessing the long-term safety of radioactive waste management (CNSC 2006) both identify the need for the postclosure safety assessment to consider additional scenarios (disruptive scenarios) that examine the impacts of unlikely disruptive events that lead to possible penetration of barriers and abnormal degradation and loss of containment. Given the high quality of the geosphere at the DGR site, the Disruptive Scenarios identified here consider various very unlikely “what if” cases in which the geosphere may be bypassed. These test the robustness of the DGR system.

8.1 Identification of Disruptive Scenarios

A set of Disruptive Scenarios has been identified through evaluating the potential for the External FEPs identified in Table 3.1 to compromise the isolation and containment safety functions of the DGR system. These high-level safety functions are in turn defined in terms of several safety arguments.

The various External FEPs that might compromise these safety arguments are listed and screened in Table 8.1 to identify those that need to be considered further. As a further check, the potential for the Internal FEPs (summarized in Table 8.2) to compromise the long-term safety arguments is also considered (Table 8.3). Note that the FEPs considered under the “Contaminant Factors” category in Table 8.2 are not capable, on their own, of modifying the DGR system to an extent that results in a fundamentally different evolution of the system to that considered in the Normal Evolution Scenario. Therefore, they are not scenario generating. Rather, they modify the rate at which contaminants are released and migrate from the DGR and the magnitude and timing of any impacts. So their effects can be evaluated through considering different calculation cases for the Normal Evolution Scenario rather than through the development of Disruptive Scenarios.

The failure mechanisms identified in Table 8.1 and Table 8.3 can be grouped into four Disruptive Scenarios as discussed below and summarized in Table 8.4.

Table 8.1: External FEPs Potentially Compromising Arguments relating to the Long-term Safety of the DGR

Long-term Safety Argument	Potentially compromised by	Need to consider as failure mechanism
<p>1. The DGR is isolated from the biosphere by its depth</p>	<p>Near-surface design adopted (FEP 1.1.02).</p>	<p>No, only deep design being considered for the DGR (Section 2.2.1).</p>
	<p>Meteorite impact (FEP 1.5.01).</p>	<p>No, due to low probability of meteor impact capable of compromising safety due to relatively small panel footprint (~0.25 km²) and depth of repository (about 680 m).</p>
	<p>Exploration borehole penetrates into repository providing enhanced permeability pathway to surface environment and potential for direct exposure to waste (FEP 1.4.03 and 1.4.04).</p>	<p>Yes, although the depth (about 680 m) and relatively small panel footprint (~0.25 km²) of the DGR will mean that the annual probability of such a borehole intruding into the DGR will be very low.</p>
	<p>Mining and other underground activities resulting in excavation in the vicinity of the repository (FEP 1.4.05).</p>	<p>No, due to absence of proven commercially viable mineral resources at or below repository level (Section 2.3.5). Other underground activities are unlikely at site because the geology is uniform across a large area and so there is nothing unique at the site other than the repository (i.e., deliberate intrusion) (Section 2.3). Also, such activities would likely be preceded by exploration boreholes, as addressed above.</p>
	<p>Deliberate human intrusion into repository (FEP 1.4.15).</p>	<p>No, exclude deliberate human intrusion since it is expected that the intruders would take appropriate precaution.</p>
<p>Could discover resources that were not identified during site investigations (FEP 1.1.01) or exploit existing rocks that have become a commercially viable resource. These new resources are exploited by drilling or mining at or below repository level (FEP 1.4.04 and 1.4.05).</p>		<p>No. The host rocks are laterally extensive and uniform in properties. The lack of resources seen at the site is consistent with regional information. Even if the existing rocks became commercially viable, the DGR site is unlikely to be the mine site because of the large lateral extent of the host rocks, which extend to shallower depths elsewhere. Impact of drilling is already considered under exploration borehole (FEP 1.4.04).</p>

Long-term Safety Argument	Potentially compromised by	Need to consider as failure mechanism
2. Multiple barriers provide containment	Ice-sheet erosion resulting from climate change removes a significant thickness of rock above repository (FEP 1.2.07, 1.3.01, 1.3.02, 1.3.05). An enhanced permeability pathway is introduced through the sequence of rocks by human-induced processes (e.g., drilling activities – FEP 1.4.04). Site investigations do not identify a relatively high permeability fracture zone or fault that provides a connection between the DGR horizon and higher horizons (FEP 1.1.01). Ice-sheet erosion resulting from climate change removes a significant thickness of rock above the repository (FEP 1.2.07, 1.3.01, 1.3.02, 1.3.05). Poor construction techniques impact on the performance of the repository and shaft EDZ providing an enhanced permeability pathway to the surface environment (FEP 1.1.04). Repository and shaft not properly sealed at time of closure providing an enhanced permeability pathway to the surface environment (FEP 1.1.07). Site investigation/monitoring borehole not properly sealed at time of closure providing an enhanced permeability pathway to the surface environment (FEP 1.1.01 and 1.1.13).	No. Extrapolating the past rate of erosion implies that of the order of 100 m of bedrock may be eroded over 1,000,000 years (Section 2.2.7.2 of NWMO 2011). This would not significantly reduce the geosphere barrier at the Bruce nuclear site given the depth of the DGR (about 680 m). Yes , see discussion of seismic events and drilling activities under Argument 1. Yes. Although very unlikely (given the strong geological, hydrogeological, and geochemical evidence to the contrary, Section 2.3), such a feature cannot be categorically ruled out and so is considered in a “what if” scenario. No , see discussion of ice-sheet erosion under Argument 1. Yes , although application of OPG’s quality control will ensure that poor construction is very unlikely. Yes , although application of OPG’s quality control will ensure that poor sealing is very unlikely. Yes , although application of OPG’s quality control will ensure that poor sealing is very unlikely.

Long-term Safety Argument	Potentially compromised by	Need to consider as failure mechanism
	<p>High magnitude seismic event results in reactivation of undetected fracture zone or fault and/or failure of shaft seals which provides an enhanced permeability pathway to higher horizons (FEP 1.2.03).</p>	<p>Yes, the assessment timescales are such that a significant event with a magnitude of $M \geq 6$ may occur, even though its annual probability of occurrence within a 20 km radius of the Bruce nuclear site is around 10^{-6} (Section 2.3.8). Even then, the probability that the earthquake could actually reactivate a nearby fracture is very small since it would take a lot of energy and since there is no evidence for faults near the DGR site.</p>
	<p>Other external geological processes disrupt the DGR system, i.e., tectonic movement (FEP 1.2.01), orogeny (FEP 1.2.02), volcanic and magmatic activity (FEP 1.2.04), metamorphism (FEP 1.2.05), hydrothermal activity (FEP 1.2.06), diagenesis (FEP 1.2.08) and salt diapirism and dissolution (FEP 1.2.10).</p>	<p>No, since precluded by site's location and assessment timescales (see Table 3.2, and also related discussion in Geosynthesis, NWMO 2011).</p>
<p>3. Mass transport is diffusion-dominated at the repository depth</p>	<p>Ice-sheet meltwater penetrates into the Deep Bedrock Groundwater Zone and affects flow in this zone (FEP 1.3.07).</p>	<p>No. No evidence from site investigation of meltwater from previous glaciations penetrating the Deep Bedrock Groundwater Zone due to its low permeability and the relatively high permeability of the Shallow Bedrock Groundwater Zone (Section 4.4 of the Geosynthesis report, NWMO 2011).</p>
	<p>Ice-sheet erosion resulting from climate change removes a significant thickness of rock above the repository resulting in the establishment of an advection dominated system surrounding the DGR (FEP 1.2.07, 1.3.01, 1.3.02, 1.3.05).</p>	<p>No, see discussion of ice-sheet erosion under Argument 1.</p>
<p>4. Hydrological and chemical conditions limit contaminant mobility at the repository depth</p>	<p>Ice-sheet meltwater penetrates into the Deep Bedrock Groundwater Zone and modifies hydrogeochemical conditions in this zone (FEP 1.3.07).</p>	<p>No, see discussion of ice-sheet meltwater under Argument 3.</p>

Long-term Safety Argument	Potentially compromised by	Need to consider as failure mechanism
	Ice-sheet erosion resulting from climate change removes a significant thickness of rock above the repository and modifies hydrogeochemical conditions around the DGR (FEP 1.2.07, 1.3.01, 1.3.02, 1.3.05).	No , see discussion of ice-sheet erosion under Argument 1.
5. The groundwater at the repository depth is resilient to natural external perturbations	Ice-sheet meltwater penetrates into the Deep Bedrock Groundwater Zone and affects transport in this zone through the introduction of fresh aerobic water (FEP 1.3.07).	No , see discussion of ice-sheet meltwater under Argument 3.
	Ice-sheet loading/unloading results in reactivation of a fault and/or failure of shaft seals which provides an enhanced permeability pathway from the repository to higher horizons (FEP 1.2.11 and 1.2.13).	No , geomechanical modelling has shown that the consequences of ice-sheet loading/unloading are limited (Chapter 6 of NWMO 2011).
	Ice-sheet erosion resulting from climate change removes a significant thickness of rock above the repository (FEP 1.2.07, 1.3.01, 1.3.02, 1.3.05).	No , see discussion of ice-sheet erosion under Argument 1.
6. Resaturation of the repository with groundwater will be very slow	Rapid resaturation of repository occurs due to an enhanced permeability pathway from the repository to the surface environment, i.e., poorly constructed shaft (FEP 1.1.04), poorly sealed shaft (FEP 1.1.07), or future exploration borehole (FEP 1.4.04).	Yes , although application of OPG's quality control will ensure that poor construction and sealing is very unlikely and the depth and relatively small panel footprint mean that the annual probability of a future exploration borehole intruding into the DGR will be very low.
	Rapid resaturation of repository occurs due to an enhanced permeability pathway from the repository to the surface environment via a DGR site investigation borehole (FEP 1.1.01) or monitoring borehole (FEP 1.1.13)	No , since it is a requirement that there is a separation between any part of the repository and an existing or planned deep borehole (NWMO 2010b). Currently the closest borehole (DGR-2) is around 100 m from the DGR (Figure 2.1).

Long-term Safety Argument	Potentially compromised by	Need to consider as failure mechanism
<p>7. Institutional Controls will limit the potential for human encounter with the DGR system in the near-term after closure</p>	<p>Institutional controls on the development of the site are ineffective (FEP 1.4.02) and knowledge of the site is lost (FEP 1.4.03) in the near-term. This allows development of the site (1.4.08) and human intrusion into the repository to occur by drilling (FEP 1.4.04) and/or mining (FEP 1.4.05)</p>	<p>No. Measures will be taken in the near-term to ensure that information regarding the purpose, location, design and contents of the repository is preserved so that future generations are made aware of the consequences of any actions they may choose to take. With these institutional measures as well as general societal memory, and with the absence of commercially viable natural resources at depth, inadvertent intrusion in the near-term after closure is not considered. However, Human Intrusion is considered in the long-term.</p>

Table 8.2: Summary of Internal FEPs from the DGR FEP List

Category	FEP	FEP
2. INTERNAL FACTORS		
2.1	Waste, Waste Form & Engineered System	
	2.1.01*	Waste inventory
	2.1.02*	Waste-form characteristics
	2.1.03*	Waste-packaging characteristics
	2.1.04*	Emplacement room and access and ring tunnel characteristics
	2.1.05*	Shaft characteristics
	2.1.06*	Mechanical processes and conditions (in wastes, emplacement rooms, tunnels and shafts)
	2.1.07*	Hydraulic/hydrogeological processes and conditions (in wastes, emplacement rooms, tunnels and shafts)
	2.1.08*	Chemical/geochemical processes and conditions (in wastes, emplacement rooms, tunnels and shafts)
	2.1.09*	Biological/biochemical processes and conditions (in wastes, emplacement rooms, tunnels and shafts)
	2.1.10*	Thermal processes and conditions (in wastes, emplacement rooms, tunnels and shafts)
	2.1.11*	Gas sources (in wastes, emplacement rooms, tunnels and shafts)
	2.1.12	Radiation effects (in wastes, emplacement rooms, tunnels and shafts)
	2.1.13	Effects of extraneous materials
2.1.14	Nuclear criticality	
2.2	Geological Environment	
	2.2.01	Stratigraphy
	2.2.02	Host lithology
	2.2.03*	Disturbed zone (in geosphere)
	2.2.04*	Large-scale discontinuities (in geosphere)
	2.2.05*	Mechanical processes and conditions (in geosphere)
	2.2.06*	Hydraulic/hydrogeological processes and conditions (in geosphere)
	2.2.07*	Chemical/geochemical processes and conditions (in geosphere)
	2.2.08	Biological/biochemical processes and conditions (in geosphere)
	2.2.09*	Thermal processes and conditions (in geosphere)
	2.2.10*	Gas processes and effects (in geosphere)
	2.2.11	Geological resources (in geosphere)
2.2.12	Undetected features (in geosphere)	

Category	FEP	FEP
2.3	Surface Environment	
	2.3.01	Topography and morphology
	2.3.02	Biomes
	2.3.03*	Soil and sediment
	2.3.04	Near-surface aquifers and water-bearing features
	2.3.05*	Terrestrial surface-water bodies
	2.3.06	Coastal features
	2.3.07	Marine features
	2.3.08	Atmosphere
	2.3.09	Vegetation
	2.3.10	Animal populations
	2.3.11	Climate and weather
	2.3.12	Hydrological regime and water balance (near-surface)
	2.3.13	Erosion and deposition
	2.3.14	Ecological/biological/microbial systems
2.3.15	Biotic intrusion	
2.4	Human Behaviour	
	2.4.01	Human characteristics (physiology, metabolism)
	2.4.02	Age, gender and ethnicity
	2.4.03*	Diet and liquid intake
	2.4.04	Habits (non-diet-related behaviour)
	2.4.05*	Community characteristics
	2.4.06	Food preparation and water processing
	2.4.07	Dwellings
	2.4.08	Natural/semi-natural land and water use
	2.4.09	Rural and agricultural land and water use
	2.4.10	Urban and industrial land and water use
2.4.11	Leisure and other uses of environment	
3. CONTAMINANT FACTORS		
3.1	Contaminant Characteristics	
	3.1.01	Radioactive decay and in-growth
	3.1.02	Organics and potential for organic forms
	3.1.03	Chemical/organic toxin stability
	3.1.04	Inorganic solids/solutes

Category	FEP	FEP
	3.1.05	Volatiles and potential for volatility
	3.1.06	Noble gases
3.2	Contaminant Release and Migration Factors	
	3.2.01	Contaminant release pathways
	3.2.02*	Water-mediated migration of contaminants
	3.2.03	Solid-mediated migration of contaminants
	3.2.04	Gas-mediated migration of contaminants
	3.2.05	Atmospheric migration of contaminants
	3.2.06	Microbially/biologically-mediated processes, effects on contaminant release and migration
	3.2.07	Animal-, plant- and microbe-mediated migration of contaminants
	3.2.08	Human-action-mediated migration of contaminants
	3.2.09	Colloid-mediated migration of contaminants
	3.2.10*	Dissolution, precipitation and mineralization
	3.2.11*	Speciation and solubility (contaminant)
	3.2.12*	Sorption and desorption (contaminant)
	3.2.13*	Complexing agent effects (contaminant)
	3.2.14	Food chains and uptake of contaminants
3.3	Exposure Factors	
	3.3.01	Contaminant concentrations in drinking water, foodstuffs and drugs
	3.3.02	Contaminant concentrations in non-food products
	3.3.03	Contaminant concentrations in other environmental media
	3.3.04*	Exposure modes
	3.3.05*	Dosimetry and biokinetics
	3.3.06*	Radiological toxicity/effects
	3.3.07*	Chemical toxicity/effects
	3.3.08	Radon and radon daughter exposure

Notes: * These FEPs are sub-divided further in the FEPs Report (QUINTESSA et al. 2011b).

Table 8.3: Internal FEPs Potentially Compromising Arguments relating to the Long-term Safety of the DGR

Long-term Safety Argument	Potentially compromised by	Need to consider as failure mechanism
<p>1. The DGR is isolated from the biosphere by its depth</p>	<p>No internal FEP could result in a significant change in the depth of the repository. Note that FEP 2.3.13 relates to the erosion of surficial deposits and not bedrock.</p>	<p>-</p>
<p>2. Multiple barriers provide containment</p>	<p>An undetected feature (e.g., a fracture zone or fault) in the geosphere provides a relatively high permeability connection between the DGR horizon and higher horizons (FEPs 2.2.04 and 2.3.13)</p>	<p>Yes. Although very unlikely (given the strong geological, hydrogeological, and geochemical evidence to the contrary, Section 2.3), such a feature cannot be categorically ruled out and so is considered in a “what if” scenario.</p>
	<p>Karst features provide a relatively high permeability connection between the DGR horizon and higher horizons (FEP 2.2.04)</p>	<p>No. Section 2.3.8 of the Geosynthesis report (NWMO 2011) notes that conditions are unsuitable for karst development in the Intermediate and Deep Bedrock Groundwater Zones. Paleokarst horizons do exist but hydraulic conductivity does not appear to be significantly elevated and the horizons are not interconnected.</p>
	<p>Gas pressure in the repository could exceed lithostatic pressure and cause fracturing of geosphere (FEPs 2.1.11 and 2.2.10).</p>	<p>No. Repository pressures expected to be significantly less than the lithostatic pressure of about 17 MPa, and regional horizontal stresses of 20 - 30 MPa (see Section 8.1 of the Gas Modelling report, GEOFIRMA and QUINTESSA 2011). Any fractures would be horizontal from repository rather than vertical due to the local rock stress conditions.</p>
	<p>Various repository FEPs (e.g., FEPs 2.1.06 to 2.1.11) and geosphere FEPs (e.g., FEPs 2.2.05 to 2.2.10) can affect the rate at which contaminants are released from the DGR and migrate through the shafts and geosphere.</p>	<p>Yes. Although geological, hydrogeological, and geochemical evidence (Section 2.3) indicates that the geosphere will be robust to uncertainties in internal repository and geosphere FEPs, the possibility of such FEPs resulting in repository and shaft seal/EDZ degradation deviating from that expected cannot be categorically ruled out and so are considered in a “what if” scenario.</p>

Long-term Safety Argument	Potentially compromised by	Need to consider as failure mechanism
<p>3. Mass transport is diffusion-dominated at the repository depth</p>	<p>An undetected feature (e.g., a fracture zone or fault) in the geosphere provides a relatively high permeability connection between the DGR horizon and higher horizons (FEPs 2.2.04 and 2.3.13)</p>	<p>Yes, see discussion of undetected feature under Argument 2.</p>
<p>4. Hydrological and chemical conditions limit contaminant mobility at the repository depth</p>	<p>Gas pressure in the repository could exceed lithostatic pressure and cause fracturing of geosphere (FEPs 2.1.11 and 2.2.10).</p>	<p>No, see discussion of gas fracturing under Argument 2.</p>
<p>5. The groundwater at the repository depth is resilient to natural external perturbations</p>	<p>Various repository FEPs (e.g., FEPs 2.1.06 to 2.1.11) have the potential to modify the hydrological and chemical conditions at the repository depth.</p>	<p>No. The effects are likely to be localized to the immediate vicinity of the DGR and these FEPs can be evaluated through considering different calculation cases for the Normal Evolution Scenario rather than through the development of alternative Disruptive Scenarios.</p>
<p>6. Resaturation of the repository with groundwater will be very slow</p>	<p>Relates to External FEPs only (see Table 8.1). The impact of Internal FEPs is considered under Argument 4 above.</p>	<p>-</p>
<p>7. Institutional Controls will limit the potential for human encounter with the DGR system in the near-term after closure</p>	<p>The rate of resaturation will be affected by repository FEPs 2.1.07 to 2.1.11, and geosphere FEPs 2,2,06 and 2.2.10.</p>	<p>No. The effect of earlier resaturation can be addressed through calculation cases for the Normal Evolution Scenario that consider a range of resaturation times, rather than through the development of alternative Disruptive Scenarios.</p>
<p>Affected by External FEPs relating to Future Human Actions (see Table 8.1) rather than the Internal FEPs relating to human behaviour that responds to the Future Human Actions.</p>	<p>-</p>	<p>-</p>

Table 8.4: Potential Failure Mechanisms and Associated Scenarios

Failure Mechanism	Associated Scenario
Exploration borehole penetrates into repository providing an enhanced permeability pathway to the surface environment and potential for direct exposure to waste	Human Intrusion
Poor construction techniques impact on the performance of the repository and shaft EDZs providing an enhanced permeability pathway to the surface environment	Severe Shaft Seal Failure
Repository and shafts are not properly sealed at the time of closure, providing an enhanced permeability pathway to the surface environment	Severe Shaft Seal Failure
Long-term performance of shaft seals and EDZs deviates from that expected, due to some unexpected internal processes, resulting in an enhanced permeability pathway to the surface environment	Severe Shaft Seal Failure
Site investigation/monitoring borehole is poorly sealed at time of closure providing an enhanced permeability pathway to the surface environment	Poorly Sealed Borehole
Long-term performance of site investigation/monitoring borehole seal deviates from that expected, due to some unexpected internal processes, resulting in an enhanced permeability pathway to the surface environment	Poorly Sealed Borehole
Site investigations do not identify a relatively high permeability fracture zone or fault that provides a connection between the DGR horizon and higher horizons	Vertical Fault
Seismic event results in reactivation of an existing structural discontinuity and/or failure of shaft seals that provides an enhanced permeability pathway to higher horizons	Bounded by Vertical Fault and Severe Shaft Seal Failure
Rapid resaturation of the repository occurs due to an enhanced permeability pathway from the repository to higher horizons	Included in Human Intrusion and Severe Shaft Seal Failure

The first scenario by which the geosphere may be bypassed is human intrusion. There are no known commercially viable natural resources at or below repository level, and the DGR has a small panel footprint (~0.25 km²) and is at a depth of around 680 m. These factors limit the range of human activities that could directly impact the closed repository to a borehole unintentionally drilled into the repository as part of a future geological exploration program⁷. This situation has a low probability of occurrence. Nevertheless, it is recognized that, once controls on the use of the site are no longer effective, the possibility of inadvertent human intrusion by this method cannot be ruled out over long timescales⁸. Such a borehole could provide an enhanced permeability pathway to the surface environment and potential for direct exposure to waste. This scenario is referred to as the **Human Intrusion Scenario**.

A second scenario by which the geosphere barrier can be bypassed is via the main and ventilation shafts. These are 9.2 m and 7.5 m diameter holes that penetrate through the geosphere, but are placed away from the waste panels and carefully sealed in the preliminary design. The Normal Evolution Scenario takes account of the role of engineered barriers and assumes their performance meets design specifications; it includes an expected degree of degradation of the seals with time. The **Severe Shaft Seal Failure Scenario** considers the possibility that the seals are not fabricated or installed appropriately, or that the long-term performance of the seals and shaft/repository EDZs is poor due to unexpected physical, chemical and/or biological processes. Either situation could result in an enhanced permeability pathway to the surface. It is difficult to assign a probability to the scenario; however, it would be expected to be very unlikely due to the quality control measures that will be applied to the DGR shaft seal closure, and the multiple durable material layers in the shaft.

Another way in which the geosphere barrier can be bypassed is through the existing site characterization/monitoring boreholes. These boreholes occur in the vicinity of the DGR down to and beyond the depth of the DGR. In all cases, the boreholes are located at least 100 m from the repository. Furthermore, they will be appropriately sealed on cessation of site investigation/monitoring activities and consequently they will have no effect on the repository performance. However, if a deep borehole were not properly sealed or were to extensively degrade, then it could provide a small but relatively permeable pathway for the migration of contaminants from the repository horizon. The scenario is termed the **Poorly Sealed Borehole Scenario**. Like the Severe Shaft Seal Failure Scenario, such a situation is very unlikely due to the adoption of good engineering practice and quality control.

There is strong geological, hydrogeological, and geochemical evidence that transmissive vertical faults/fracture zones which could provide enhanced permeability pathways from the repository horizon to an overlying aquifer do not exist within the footprint or vicinity of the DGR (Section 2.3). This evidence has been gathered through a deep drilling/coring program, a 2-D seismic reflection survey, petrophysics, in-situ borehole testing and micro-seismic monitoring. Despite this evidence, a “what if” scenario is considered to investigate the safety implications of

⁷ The assessment excludes deliberate human intrusion since it is expected that the intruders would take appropriate precaution.

⁸ The repository might appear as an anomaly in any surface/airborne survey of the area, and this could encourage drilling at the site. However, the uniformity of the sediments and general lack of interesting minerals or geologic features in the area would argue against deliberate surveys of the area. Furthermore, a cautious approach to drilling might be used if such unexpected anomalies were identified that would minimise the consequences of any intrusion into the DGR.

a hypothetical transmissive vertical fault, either undetected or representing the displacement of an existing structural discontinuity. Regionally, any such discontinuities are often associated with hydrothermal dolomitized carbonate and are found to originate in the Precambrian or Cambrian and extend up to the Ordovician shales where they terminate (Armstrong and Carter 2010). The hypothetical fault is assumed to be in close proximity to the DGR and is assumed to extend beyond the Ordovician shales and into the permeable Guelph formation. The scenario is termed the **Vertical Fault Scenario**.

Other potential Disruptive Scenarios were considered, but ruled out on various grounds as described in QUINTESSA (2011) and QUINTESSA et al. (2011b). For example, no volcanic activity is anticipated in the area over the next one million years, and the probability of being hit by a large meteor capable of damaging the repository is remote. Seismic activity is possible, and likely earthquakes are included in the Normal Evolution Scenario, where their main effect is rockfall within the repository. Large earthquakes are unlikely, and their main effects on the repository are bounded by the Severe Shaft Seal Failure and Vertical Fault Scenarios, so there is no need to consider an additional earthquake scenario. Similarly, repository gas pressures are expected to be significantly less than the lithostatic pressure of about 17 MPa and the regional horizontal stresses of 20-30 MPa (see Section 8.1 of the Gas Modelling report, GEOFIRMA and QUINTESSA 2011). Therefore, they do not cause fracturing of the rock and this scenario is not evaluated. Glaciation could affect the site; it is considered within the Normal Evolution Scenario.

In order to build confidence that an appropriate set of Disruptive Scenarios has been identified using the safety function and argument approach described above, a complementary approach was also used. The approach involved reviewing each of the External FEPs identified in Table 3.1 to see whether, given the assessment context (specified in Chapter 3 of the Postclosure Safety Assessment report, QUINTESSA et al. 2011a) and the system description (given in Chapter 2 of this report), it was possible for the External FEP to have one or more alternative states to the state considered in the Normal Evolution Scenario. The results of this review are presented in Table 8.5. Those external FEPs with potential alternative states were then reviewed to see whether the alternative states would generate additional scenarios or whether they could be covered by alternative conceptualization of the Normal Evolution Scenario. The same set of four additional scenarios, identified using the safety argument approach, was identified (see Table 8.5).

Further confidence that an appropriate set of Disruptive Scenarios has been identified can be built by comparing the scenarios (additional to the “reference/base/normal evolution” scenario) considered in the postclosure safety assessments of other deep repositories. A review of the scenarios considered in deep repositories in other countries was undertaken. The results are summarized in Table 8.6⁹.

⁹ Assessments often sub-divide a given scenario down into a number of “sub-scenarios” or variant/alternative cases. For example, the exploration drilling scenario considered in SAFIR 2 has three variants: examination of the drill core; contamination of soil by drill cuttings; and preferential pathway for groundwater flow (ONDRAF/NIRAS 2001). In Nagra (2002), alternative conceptualisations of the Reference Scenario address phenomena in the near field and the geosphere where uncertainty exists about their importance for the reference radionuclide release pathway. Given that the purpose of the review was to compare the top-level scenarios, any division of a scenario into sub-scenarios or variant/alternative cases is not included in Table 8.6.

Table 8.5: Grouping of Alternative States for External FEPs into Additional Scenarios

External FEP		Potential for Alternative State(s)	Additional Scenario
1.1	Repository Factors		
	1.1.01	Site investigations Yes , consider a site investigation borehole not being properly sealed or an undetected fault/fracture zone	Poorly Sealed Borehole Vertical Fault
	1.1.02	Design of repository Yes , consider design alternatives such as grouting and backfilling	Can be covered by alternative parameterization of the Normal Evolution Scenario – no need for additional scenario
	1.1.03	Schedule and planning No , only consider operational period to 2062 (see Section 3.8 of the Postclosure Safety Assessment report, QUINTESSA et al. 2011a)	-
	1.1.04	Construction Yes , consider poor construction techniques impacting on the performance of the repository and shaft seals	Severe Shaft Seal Failure
	1.1.05	Operation Yes , consider damage of waste container during emplacement	Can be covered by alternative parameterization of the Normal Evolution Scenario – no need for additional scenario
	1.1.06	Waste allocation Yes , consider alternative options of locating certain waste packages within the repository	Can be covered by alternative parameterization of the Normal Evolution Scenario – no need for additional scenario
	1.1.07	Repository closure Yes , consider degraded performance of repository and shaft seals	Severe Shaft Seal Failure
1.1.08	Quality assurance No , a quality assurance program will be followed. However, some 'what if' states that could result from process errors that are undetected by quality assurance/quality control procedures are noted in FEPs 1.1.01, 1.1.04, 1.1.05 and 1.1.07.	-	

External FEP		Potential for Alternative State(s)	Additional Scenario
1.1.09	Repository administrative control	No , institutional controls will be in place following repository closure. Calculations for all postclosure scenarios will be undertaken from closure of the facility (2062) and so results can be produced for a range of different periods of effective institutional control without the need to generate alternative scenarios	-
1.1.10	Accidents and unplanned events	No , even if accidents and unplanned events occur, corrective actions will be taken to prevent any detrimental impacts on postclosure safety	-
1.1.11	Retrieval	No , if retrieval were to be undertaken, it would be undertaken in a manner that would not impact the long-term safety of the repository	-
1.1.12	Repository records and markers	No , records will be in place following repository closure. Calculations for all postclosure scenarios will be undertaken from closure of the facility (2062) and so results can be produced for a range of different periods of record maintenance without the need to generate alternative scenarios	-
1.1.13	Monitoring	Yes , consider monitoring borehole not being properly sealed	Poorly Sealed Borehole
1.2	Geological Processes and Effects		
1.2.01	Tectonic movement	No , given the site's tectonically stable location (Section 2.3.1) and timescales of interest (1,000,000 years)	-

External FEP		Potential for Alternative State(s)	Additional Scenario
1.2.02	Orogeny	No , given site's distance from active orogenic zones (Section 2.3.1) and timescales of interest (1,000,000 years)	-
1.2.03	Seismicity	Yes , severe seismic event could damage repository and shaft seals and/or reactive an undetected fault/fracture zone	Severe Shaft Seal Failure Vertical Fault
1.2.04	Volcanic and magmatic activity	No , given site's distance from volcanic and magmatic activity(Section 2.3.1) and timescales of interest (1,000,000 years)	-
1.2.05	Metamorphism	No , since no processes occur over the timescale of interest (1,000,000 years) that will cause metamorphism (Section 2.3.1)	-
1.2.06	Hydrothermal activity	No , given absence of drivers of hydrothermal activity over the timescales of interest, 1,000,000 years (Section 2.3.1)	-
1.2.07	Denudation and Deposition (large-scale)	No , already considered in Normal Evolution Scenario	-
1.2.08	Diagenesis	No , significant diagenesis that would affect repository safety is unlikely over the timescales of interest (1,000,000 years)	-
1.2.09	Pedogenesis	No , already considered in Normal Evolution Scenario	-
1.2.10	Salt diapirism and dissolution	No , salt deposits are not located in the vicinity of the site (Section 2.3.2)	-
1.2.11	Hydrological response to geological changes	Yes , seismic activity reactivates an undetected fault/fracture zone	Vertical Fault
1.2.12	Geomorphologic response to geological changes	No , given site's geologically stable location and timescales of interest (Section 2.3).	-
1.2.13	Deformation (elastic, plastic or brittle)	No , already considered in Normal Evolution Scenario	-

External FEP		Potential for Alternative State(s)	Additional Scenario	
1.3	Climate Processes and Effects			
	1.3.01	Global climate change	No, already considered in Normal Evolution Scenario	-
	1.3.02	Regional and local climate change	No, already considered in Normal Evolution Scenario	-
	1.3.03	Sea-level change	No, changes in sea level do not affect the site due to its elevated continental location	-
	1.3.04	Periglacial effects	No, already considered in Normal Evolution Scenario	-
	1.3.05	Local glacial and ice-sheet effects	No, already considered in Normal Evolution Scenario	-
	1.3.06	Warm climate effects (tropical and desert)	No, northerly location of site precludes tropical or hot desert conditions	-
	1.3.07	Hydrological response to climate changes	No, already considered in Normal Evolution Scenario	-
	1.3.08	Ecological response to climate changes	No, already considered in Normal Evolution Scenario	-
	1.3.09	Human behavioural response to climate changes	No, already considered in Normal Evolution Scenario	-
1.3.10	Geomorphologic response to climate changes	No, already considered in Normal Evolution Scenario	-	
1.4	Future Human Actions			
	1.4.01	Human influences on climate	No, already considered in Normal Evolution Scenario	-

External FEP		Potential for Alternative State(s)	Additional Scenario
1.4.02	Social and institutional developments	No , expect that land use change will not occur until controls on the development of the site are no longer effective. Although it is possible that certain changes in land use might be allowed during the institutional control period, it is expected that this will only occur if the change can be demonstrated to have no safety consequences.	-
1.4.03	Knowledge and motivational issues (repository)	Yes , there is human intrusion into the DGR.	Human Intrusion
1.4.04	Drilling activities	Yes , exploration borehole penetrates into the repository	Human Intrusion
1.4.05	Mining and other underground activities	No , no commercially viable mineral resources identified at the site and other underground activities are unlikely at the site because the geology is uniform across a large area and so there is nothing unique at the site.	-
1.4.06	Un-intrusive site investigation	No , no direct impact on repository safety	-
1.4.07	Surface excavations	No , no direct impact on repository safety due to depth of repository	-
1.4.08	Site Development	No , already considered in Normal Evolution Scenario	-
1.4.09	Archaeology	No , no direct impact on repository safety due to depth of repository	-
1.4.10	Water management (groundwater and surface water)	Yes , water is drawn from sources other than a well in the Shallow Bedrock Groundwater Zone (e.g., lake or river)	Can be covered by alternative parameterization of the Normal Evolution Scenario – no need for additional scenario

External FEP		Potential for Alternative State(s)	Additional Scenario
1.4.11	Explosions and crashes	No , surface explosions and crashes would have no direct impact on repository safety due to depth of repository. Rockfall might provide an ignition source for gases in repository but impact on long-term safety expected to be minimal.	-
1.4.12	Pollution	No , impact of non-repository derived contaminants is expected not to be significant	-
1.4.13	Remedial actions	No , even if remedial actions are undertaken, it is expected that they do not have a detrimental impact on long-term safety	-
1.4.14	Technological developments	No , only consider current lifestyles, consistent with CNSC (2006) and ICRP (2000)	-
1.4.15	Deliberate human intrusion	No , exclude deliberate human intrusion since it is expected that the intruders would take appropriate precaution.	-
1.5	Other External Factors		
1.5.01	Impact of meteorites and human space debris	No , due to low probability and low consequence in terms of repository safety. Even if the impact was so large that it did affect the repository, then the global consequences arising directly from the impact itself would in any case be far larger than the increased impact from the repository.	-
1.5.02	Evolution of biota	No , consistent with recommendations of ICRP (2000)	-

Table 8.6: Additional Scenarios Considered in Other Safety Assessments

Assessment	Reference	Additional Scenarios Considered
SAFIR 2 (Belgium)	ONDRAF/ NIRAS (2001)	<ul style="list-style-type: none"> • Exploitation drilling (water well) • Exploratory drilling • Greenhouse effect • Poor sealing of repository • Fault activation • Severe glacial period • Failure of engineered barriers • Gas-driven transport
Olkiluoto (Finland)	POSIVA (2010)	<ul style="list-style-type: none"> • Defective canister (early and delayed penetration) • Earthquake/rock shear • Disrupted buffer • Release affected by gas • Exploitation drilling (water well) • Exploratory drilling
Dossier Argile (France)	ANDRA (2005)	<ul style="list-style-type: none"> • Seal failure and defective plug • Defective waste and spent fuel containers • Borehole penetrating repository • Functioning of repository greatly degraded
H12 (Japan) ⁽¹⁾	JNC (2000)	<ul style="list-style-type: none"> • Climate and sea-level change • Exploitation drilling (water well) • Engineering defects
SRCan (Sweden)	SKB (2006b)	<ul style="list-style-type: none"> • Extended greenhouse effects • Disrupted buffer (e.g., due to advection, freezing) • Canister failure (e.g., due to load, shear or corrosion) • Exploitation drilling (water well) • Exploratory drilling • Rock excavation • Poorly sealed repository
Opalinus (Switzerland)	NAGRA (2002)	<ul style="list-style-type: none"> • Gas pathways • Exploitation drilling (water well) • Exploratory drilling • Poorly sealed repository
GPA (UK)	NIREX (2003)	<ul style="list-style-type: none"> • Exploratory drilling
WIPP (USA)	USDOE (2004)	<ul style="list-style-type: none"> • Mining • Exploratory drilling
Yucca Mountain (USA) ⁽²⁾	USDOE (2002)	<ul style="list-style-type: none"> • Exploratory drilling • Seismicity • Volcanic event

Notes:

1. Isolation Failure Scenarios that involve penetration of the repository (including magma intrusion, human intrusion and meteorite impact) were also considered but screened out on the grounds that they are extremely unlikely to occur. Some 'what-if' calculations were carried out instead.
2. The term 'scenario' is used in a way that differs from the other assessments reviewed. Three Thermal Load Scenarios are discussed that are design variants, while two No-action Scenarios refer to futures in which the Yucca Mountain facility does not go ahead.

It can be seen that, consistent with the DGR assessment, most assessments have identified a limited number of additional scenarios that consider the degradation/failure of engineered and natural barriers by natural processes (e.g., earthquakes, climate change) and human actions (e.g., drilling, poor quality control). Although there are some scenarios identified in Table 8.6 that are not considered in the DGR Disruptive Scenarios, these are either not relevant to the Bruce nuclear site (e.g., volcanic activity, sea-level rise, mining of resources) or have been included in the DGR's Normal Evolution Scenario (e.g., climate change, canister failure, gas generation).

The selected Disruptive Scenarios are described in Section 8.2 below. Figure 8.1 shows their locations assumed for the SA. The Disruptive Scenarios are evaluated separately rather than in combination since the individual scenarios have low probability and independent causes, and so their probabilities of occurring together are even lower

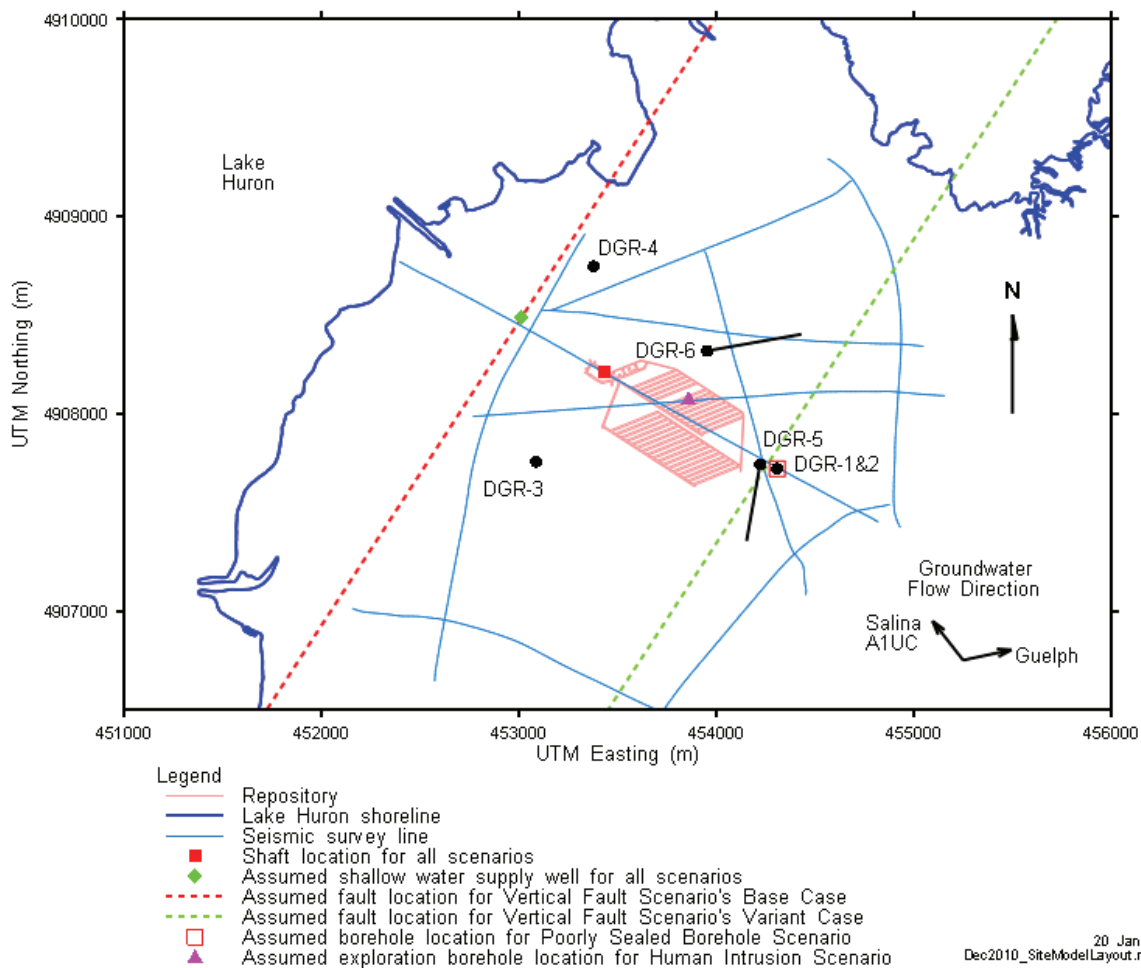


Figure 8.1: Location of Disruptive Scenarios Evaluated in the Safety Assessment

8.2 Description of Disruptive Scenarios

8.2.1 Human Intrusion Scenario

The Human Intrusion Scenario considers the same evolution of the DGR system as for the Normal Evolution Scenario with the only difference being the occurrence of human intrusion into the repository at some time after control of the site is no longer effective.

In this scenario, an exploration borehole is drilled down through the geosphere. Upon encountering the repository, the drilling crew would register a loss of drill fluid to the repository void if the repository pressure is less than the drill fluid pressure, or a surge of gas from the repository up the borehole if the repository pressure is greater than the drill fluid pressure. No significant amount of water is expected to be expelled, as the saturation of the repository is projected to be very low (less than 1% for the Normal Evolution Scenario's Reference Case, Section 5.1.1.2 of the Gas Modelling report, GEOFIRMA and QUINTESSA 2011). Current technology necessary to drill to 680 m depth would enable the drillers to ascertain the nature of the void that had been encountered, and to limit upflow from the repository (e.g., this is standard practice in sedimentary rocks where one may encounter natural gas).

In an exploration borehole, the investigators would most likely collect samples or conduct measurements at the repository level, because of its unusual properties relative to the surrounding rock. This would readily lead to the identification of high levels of radioactivity (e.g., gamma logging is a standard borehole measurement). Once the investigation was complete, the drillers would close and seal the borehole, and ensure any surface-released materials were appropriately disposed, since this is normal drilling practice. Sealing the borehole would avoid any further release of residual radioactivity directly to the surface. Therefore under normal drilling, there would be little impact even should inadvertent intrusion occur.

However, the Human Intrusion Scenario considers "what if" the intrusion is inadvertent and:

- It is not recognized that the drill has intercepted a waste repository so no safety restrictions are imposed; and
- The borehole and drill site are not managed and closed to current standards, and material from the borehole is released on surface around the drill site.

Further, the scenario also considers the long-term consequences of:

- The borehole being poorly sealed, resulting in the creation of a pathway for contaminants into permeable geosphere horizons above the repository; and
- As a very unlikely variant case, "what if" the borehole were continued down into the pressurised Cambrian Formation, and again not properly sealed.

For this scenario, therefore, contaminants could be released and humans and non-human biota exposed via four pathways:

- Direct release to the surface of pressurized contaminated gas prior to sealing of the borehole;
- Retrieval and uncontrolled dispersal of contaminated drill core debris on the site;
- Retrieval and examination of drill core contaminated with waste; and

- The long-term release of contaminated water from the repository into permeable geosphere horizons via the exploration borehole, if the borehole were continued down into the pressurized Cambrian and subsequently poorly sealed.

These releases could result in the exposure of the drill crew, laboratory technicians (who examine the drill core), residents living near the site at the time of intrusion, and site residents who might occupy the site subsequent to the intrusion event.

8.2.2 Severe Shaft Seal Failure Scenario

The shafts represent a potentially important pathway for contaminant release, and therefore the repository design includes specific measures to provide good shaft seals, taking into account the characteristics of the geosphere. The Normal Evolution Scenario considers the likely behaviour of the shaft seals and the repository/shaft EDZs; it includes some expected degree of degradation of the seals with time. The Shaft Seal Failure Scenario considers the same evolution of the DGR system and the same exposure pathways as the Normal Evolution Scenario, the difference being that there is rapid and extensive shaft seal degradation and the repository/shaft EDZs have significantly degraded properties. Like the other Disruptive Scenarios, the scenario is a bounding, “what if” scenario that is designed to investigate the robustness of the DGR system.

8.2.3 Poorly Sealed Borehole Scenario

Several site investigation/monitoring boreholes have been drilled in the vicinity of the DGR down to and beyond the depth of the DGR during the site investigation phase. The Poorly Sealed Borehole Scenario considers the consequences of one of the boreholes not being properly sealed or having a seal that extensively degrades. The evolution of the system is similar to the Normal Evolution Scenario with the key difference being that the poorly sealed borehole provides an enhanced permeability connection between the level of the repository, the overlying groundwater zones and the biosphere, thereby bypassing some of the natural geological barriers to contaminant migration from the DGR. The subsequent exposure pathways are the same as those considered in the Normal Evolution Scenario.

8.2.4 Vertical Fault Scenario

The Vertical Fault Scenario considers the hypothetical case of “what if” a transmissive vertical fault, either undetected or representing the displacement of an existing structural discontinuity that propagates from the Precambrian into the Guelph Formation in the Intermediate Bedrock Groundwater Zone, in close proximity to the repository. Such a fault could provide an enhanced permeability pathway that bypasses the Deep Bedrock Groundwater Zone, one of the natural barriers to contaminant migration from the DGR. Groundwater flow in the Guelph is assumed to be horizontal and to discharge to the lake. Consideration is given to exposure of two critical groups: one that obtains its water and fish from the lake’s near shore; and one that farms above the repository and has the same characteristics as that considered in the Normal Evolution Scenario.

9. REFERENCES

- Adams, J. 1989. Postglacial Faulting in Eastern Canada: Nature, Origin and Seismic Hazard Implications. *Tectonophysics* 163, 323-331.
- Adriaens, P., Q. Fu and D. Grbic-Galic. 1996. Bioavailability and Transformation of Highly Chlorinated Dibenzo-p-dioxins and Dibenzofurans in Anaerobic Soils and Sediments. *Environmental Science and Technology* 29, 2252-2260.
- Aitken, C.M., D.M. Jones and S.R. Larter. 2004. Anaerobic Hydrocarbon Biodegradation in Deep Subsurface Oil Reservoirs. *Nature* 431, 291-294.
- AMEC GEOMATRIX. 2011. Seismic Hazard Assessment. AMEC Geomatrix Consultants Inc. report for the Nuclear Waste Management Organization NWMO DGR-TR-2011-20 R000. Toronto, Canada.
- AMEC NSS. 2011. Radiation and Radioactivity Technical Support Document. AMEC NSS Ltd. report for Nuclear Waste Management Organization NWMO DGR-TR-2011-06 R000. Toronto, Canada.
- ANDRA 2005. Evaluation de Sûreté du Stockage Géologique. Paris, France.
- ARC. 2010. Gas Transport and Geochemical Modelling. Alberta Research Council. Technical Report CEM-19 prepared for Nuclear Waste Management Organization. Edmonton, Canada.
- Armstrong, D.K. and T.R. Carter. 2010. The Subsurface Paleozoic Stratigraphy of Southern Ontario. Ontario Geological Survey, Special Volume 7. Sudbury, Canada.
- Backblom, G. and R. Munier. 2002. Effect of Earthquakes on the Deep Repository for Spent Fuel in Sweden based on Case Studies and Preliminary Model Results. Swedish Nuclear Fuel and Waste Management Company (SKB) Technical Report TR-02-024. Stockholm, Sweden.
- Baumgartner, P. 2006. Generic Thermal-mechanical-hydraulic (THM) Data for Sealing Materials – Volume 1: Soil-water Relationships. Ontario Power Generation Report 06819-REP-01300-10122. Toronto, Canada.
- Bethke, C.M. 2008. Geochemical and Biogeochemical Reaction Modeling. Cambridge University Press. Cambridge, United Kingdom.
- BIOCLIM. 2004. Development and Application of a Methodology for taking Climate-driven Environmental Change into account in Performance Assessments. BIOCLIM Deliverable D10-12. Available from ANDRA, <http://www.andra.fr/bioclim/>.
- BIOMOVS II. 1996. Development of a Reference Biospheres Methodology for Radioactive Waste Disposal. BIOMOVS II Technical Report No. 6, published on behalf of the BIOMOVS II Steering Committee by the Swedish Radiation Protection Institute. Stockholm, Sweden.
- Bowerman, B.S., J.H. Clinton and S.R. Cowdery. 1988. Biodegradation of Ion Exchange Media. NUREG/CR-5221, BNL-NUREG-52163, Brookhaven National Laboratory, New York, USA.

- Bracke, G., W. Muller and K. Kugel. 2004. Derivation of Gas Generation Rates for the Morsleben Radioactive Waste Repository (ERAM). Proceeding of the DisTec Conference, April 26-28, Berlin, Germany.
- Brown, R.J.E. and T.L. Pewe. 1973. Distribution of Permafrost in North America and its Relationship to the Environment: A Review, 1963-1973. In: Permafrost: North American Contribution to the 2nd International Conference, 13th-28th July 1973, Yakutsk. National Academy of Sciences, Washington D.C., USA.
- CEAA and CNSC. 2009. Guidelines for the Preparation of the Environmental Impact Statement for the Deep Geologic Repository of Low- and Intermediate-Level Radioactive Wastes. Canadian Environmental Assessment Agency and Canadian Nuclear Safety Commission. Ottawa, Canada.
- CNSC. 2006. Assessing the Long-term Safety of Radioactive Waste Management. Canadian Nuclear Safety Commission Regulatory Guide G-320. Ottawa, Canada.
- CSA. 2008. Management of Low- and Intermediate-level Radioactive Waste. Canadian Standards Association Standard N292.3-08. Toronto, Canada.
- Fetter, C.W. 1994. Applied Hydrogeology (Third Edition). Prentice Hall Inc., New Jersey, USA.
- Freeman, H.D. and R.A. Romine. 1994. Hanford Permanent Isolation Barrier Program: Asphalt Technology Development. Proceedings of the 33rd Hanford Symposium on Health and Environment, Richland, USA.
- Garisto, F., P. Gierszewski and K. Wei. 2004. Third Case Study – Features, Events and Processes. Ontario Power Generation Report OPG 06819-REP-01200-10125-R00. Toronto, Canada.
- Gee, G.W., A.L. Ward, H.D. Freeman, S.O. Link, W.H. Walters, S.K. Smith, M.W. Ligojke, B.G. Gilmore, M.D. Campbell and R.A. Romine. 1994. Hanford Prototype Surface Barrier Status Report: FY 1994. Pacific Northwest Laboratory Report to USDoE, PNL-10275-UC-2010. Richland, USA
- GEOFIRMA. 2011. Postclosure Safety Assessment: Groundwater Modelling. Geofirma Engineering Ltd. report for the Nuclear Waste Management Organization NWMO DGR-TR-2011-30 R000. Toronto, Canada.
- GEOFIRMA and QUINTESSA. 2011. Postclosure Safety Assessment: Gas Modelling. Geofirma Engineering Ltd. and Quintessa Ltd. report for the Nuclear Waste Management Organization NWMO DGR-TR-2011-31 R000. Toronto, Canada.
- Glasser, F.P., M. Tyrer, K. Quillin, D. Ross, J. Pedersen, K. Goldthorpe, D. Bennett and M. Atkins. 1999. The Chemistry of Blended Cements and Backfills Intended for Use in Radioactive Waste Disposal. Environment Agency of England and Wales R&D Technical Report P98. Bristol, United Kingdom.
- GOLDER. 2003. LLW Geotechnical Feasibility Study, Western Waste Management Facility, Bruce Site, Tiverton, Ontario. Golder Associates Ltd. report for Ontario Power Generation 021-1570. Mississauga, Canada.

- GOLDER. 2011a. Aboriginal Interests Technical Support Document. Golder Associates Ltd. report for the Nuclear Waste Management Organization NWMO DGR-TR-2011-09 R000. Toronto, Canada.
- GOLDER. 2011b. Aquatic Environment Technical Support Document. Golder Associates Ltd. report for the Nuclear Waste Management Organization NWMO DGR-TR-2011-01 R000. Toronto, Canada.
- GOLDER. 2011c. Atmospheric Environment Technical Support Document. Golder Associates Ltd. report for the Nuclear Waste Management Organization Report NWMO DGR-TR-2011-02 R000. Toronto, Canada.
- GOLDER. 2011d. Geology Technical Support Document. Golder Associates Ltd. report for the Nuclear Waste Management Organization NWMO DGR-TR-2011-03 R000. Toronto, Canada.
- GOLDER. 2011e. Hydrology and Surface Water Quality Technical Support Document. Golder Associates Ltd. report for the Nuclear Waste Management Organization NWMO DGR-TR-2011-04 R000. Toronto, Canada.
- GOLDER. 2011f. Socio-economic Environment Technical Support Document. Golder Associates Ltd. report for the Nuclear Waste Management Organization NWMO DGR-TR-2011-08 R000. Toronto, Canada.
- GOLDER. 2011g. Terrestrial Environment Technical Support Document. Golder Associates Ltd. report for the Nuclear Waste Management Organization NWMO DGR-TR-2011-05 R000. Toronto, Canada.
- Guimerá, J., L. Duro, S. Jordana and J. Bruno. 1999. Effects of Ice Melting and Redox Front Migration in Fractured Rocks of Low Permeability. Swedish Nuclear Fuel and Waste Management Company (SKB) Technical Report TR-99-19. Stockholm, Sweden.
- Hallet, B. 2011. Assessment of Maximum Future Glacial Erosion – Bruce County, Georgian Bay Region, Southern Ontario. Nuclear Waste Management Organization Report NWMO DGR-TR-2011-18 R000. Toronto, Canada.
- Hanks, T. and H. Kanamori. 1979. A Moment Magnitude Scale. *Journal of Geophysical Research* 84, 2348-2350.
- Hansen, F.D. and M.K. Knowles. 2000. Design and analysis of a shaft seal system for the Waste Isolation Pilot Plant. *Reliability Engineering and System Safety* 69, 87-98.
- Herbert H.J., J. Kasbohm, H.C. Moog and K.H. Henning. 2004. Long-term behaviour of the Wyoming bentonite MX-80 in high saline solutions. *Applied Clay Science* 26, 275-291.
- Höglund, L.O. 2001. Project SAFE Modelling of Long-term Concrete Degradation Processes in the Swedish SFR Repository. Swedish Nuclear Fuel and Waste Management Company (SKB) Report R-01-08. Stockholm, Sweden.

- Holba, A.G., L. Wright, R. Levinson, B. Huizinga and M. Scheihing. 2004. Effects and impact of early-stage anaerobic biodegradation on Kuparuk River Field, Alaska. In: Cubitt, J. M., W.A. England and S. Larter (eds). *Understanding Petroleum Reservoirs: towards an Integrated Reservoir Engineering and Geochemical Approach*. Geological Society, London, Special Publications 237, 53-88.
- Holtz, R.D. and W.D. Kovacs. 1981. *An Introduction to Geotechnical Engineering*. Prentice Hall, Englewood Cliffs, USA.
- Huang, W.L., J.M. Longo and D.R. Pevear. 1993. An Experimentally Derived Kinetic Model for Smectite-to-illite Conversion and its Use as a Geothermometer. *Clays and Clay Minerals* 41, 162–177.
- IAEA. 2003. “Reference Biospheres” for Solid Radioactive Waste Disposal: Report of BIOMASS Theme 1 of the BIOSphere Modelling and ASSEssment (BIOMASS Programme). International Atomic Energy Agency-BIOMASS-6. Vienna, Austria.
- IAEA. 2004. Improvement of Safety Assessment Methodologies for Near Surface Disposal Facilities. Volume I: Review and Enhancement of Safety Assessment Approaches and Tools. International Atomic Energy Agency -ISAM-1. Vienna, Austria.
- IAEA. 2009. Determination and Use of Scaling Factors for Waste Characterization in Nuclear Power Plants. International Atomic Energy Agency Nuclear Energy Series NW-T-1.18. Vienna, Austria.
- IAEA. 2010. The Safety Case and Safety Assessment for Radioactive Waste Disposal. International Atomic Energy Agency Draft Safety Guide DS-355. Vienna, Austria.
- ICRP. 2000. Radiation Protection Recommendations as Applied to the Disposal of Long-lived Solid Radioactive Waste. International Commission on Radiological Protection Publication 81, *Annals of the ICRP* 28(4).
- INTERA. 2011. Descriptive Geosphere Site Model. Intera Engineering Ltd. report for the Nuclear Waste Management Organization NWMO DGR-TR-2011-24 R000. Toronto, Canada.
- IPCC. 2007. *Climate Change 2007: A Report of the Intergovernmental Panel on Climate Change. Volume 4: Synthesis Report*. World Meteorological Organisation and United Nations Environment Program. Geneva, Switzerland.
- JNC. 2000. H12: Project to Establish the Scientific and Technical Basis for HLW in Japan. Japan Nuclear Cycle Development Institute TN1410 2000-004. Tokai, Japan.
- Kaufhold, S. and R. Dohrmann. 2009. Stability of bentonites in salt solutions – sodium chloride. *Applied Clay Science* 45, 171-177.
- Laine, H. and P. Karttunen. 2010. Long-term Stability of Bentonite: A Literature Review. Posiva Working Report 2010-53, Eurajoki, Finland.
- Lei., S. 1999. An Analytical Solution for Steady Flow into a Tunnel. *Ground Water* 37 (1), 23-26.

- Leygraf, C. and T.E. Graedel. 2000. Atmospheric Corrosion. Wiley Interscience, New York, USA.
- Marty, N.C.M., C. Tournassat, A. Burnol, E. Giffaut and E. Gaucher. 2009. Influence of Reaction Kinetics and Mesh Refinement on the Numerical Modelling of Concrete/clay Interactions. *Journal of Hydrology* 364, 58-72.
- McMurry J., D.A. Dixon, J.D. Garroni, B.M. Ikeda, S. Stroes-Gascoyne, P. Baumgartner and T.W. Melnyk. 2003. Evolution of a Canadian Deep Repository: Base Scenario. Ontario Power Generation Report 06819-REP-01200-10092-R00. Toronto, Canada.
- Miller, W., R. Alexander, N. Chapman, I. McKinley and J. Smellie. 2000. Geological Disposal of Radioactive Wastes and Natural Analogues. Lessons from Nature and Archaeology. Waste Management Series, Volume 2. Pergamon, Amsterdam, Netherlands.
- NAGRA. 2002. Project Opalinus Clay: Safety Report, Demonstration of the Disposal Feasibility for Spent Fuel, Vitrified HLW and Long-lived ILW. Nagra Technical Report 02-05. Wettingen, Switzerland.
- NEA. 1999. Safety Assessment of Radioactive Waste Repositories – Systematic Approaches to Scenario Development – An International Database of Features, Events and Processes. A report of the Nuclear Energy Agency working group on development of a Database of Features, Events and Processes relevant to the Assessment of the Post-closure Safety of Radioactive Waste Repositories. OECD/NEA, Paris, France.
- NIREX. 2003. Generic Repository Studies: Generic Post-closure Performance Assessment. Nirex Report N/080. Harwell, United Kingdom.
- NOAA. 2010. Bathymetry of Lake Huron. <http://www.ngdc.noaa.gov/mgg/greatlakes/huron.html>. Accessed 29 June 2010. National Oceanic and Atmospheric Administration, National Geophysical Data Center, Michigan, USA.
- NWMO. 2010a. L&ILW DGR Project Data Clearance Form: Design Information for Postclosure Safety Assessment. Nuclear Waste Management Organization Filing Number DGR-REF-01929-23483. Toronto, Canada.
- NWMO. 2010b. Ontario Power Generation's Deep Geologic Repository for Low and Intermediate-Level Waste - Project Requirements. Nuclear Waste Management Organization Document DGR-PDR-00120-0001 R002. Toronto, Canada.
- NWMO. 2011. Geosynthesis. Nuclear Waste Management Organization Report NWMO DGR-TR-2011-11 R000. Toronto, Canada.
- ONDRAF/NIRAS. 2001. SAFIR 2: Safety Assessment and Feasibility Interim Report 2. ONDRAF/NIRAS Report NIROND 2001-06E. Belgium.
- OPG. 2005. Western Waste Management Facility Refurbishment Waste Storage Project: Environmental Assessment Study Report. Ontario Power Generation Report 01098-REP-07701-00002 R01. Toronto, Canada.

- OPG. 2010. Reference Low and Intermediate Level Waste Inventory for the Deep Geologic Repository. Ontario Power Generation Report 00216-REP-03902-00003-R003. Toronto, Canada.
- OPG. 2011a. OPG's Deep Geologic Repository for Low and Intermediate Level Waste: Environmental Impact Statement Ontario Power Generation Report 00216-REP-07701-00001 R000. Toronto, Canada.
- OPG. 2011b. OPG's Deep Geologic Repository for Low and Intermediate Level Waste: Preliminary Safety Report. Ontario Power Generation Report DGR-00216-SR-01320-00001 R000. Toronto, Canada.
- Pedersen, K. 2001. Project SAFE: Microbial Features, Events and Processes in the Swedish Final Repository for Low- and Intermediate-level Radioactive Waste. Swedish Nuclear Fuel and Waste Management Company (SKB) Report R-01-05. Stockholm, Sweden.
- Peltier, W.R. 2002. A Design Basis Glacier Scenario. Ontario Power Generation Report 06819-REP-01200-10069-R00. Toronto, Canada.
- Peltier, W.R. 2004. Permafrost Influences upon the Sub-surface. Ontario Power Generation Report 06819-REP-01200-10134-R00. Toronto, Canada.
- Peltier, W.R. 2011. OPG's Deep Geologic Repository for Low and Intermediate Level Waste: Long-Term Climate Change Study. Nuclear Waste Management Organization Report NWMO DGR-TR-2011-14 R000. Toronto, Canada.
- Pettersson, M. and M. Elert. 2001. Characterisation of Bitumenised Waste in SFR1. Swedish Nuclear Fuel and Waste Management Company (SKB) Report R-01-26. Stockholm, Sweden.
- POSIVA. 2010. Interim Summary Report of the Safety Case 2009. Posiva Report 2010-02. Olkiluoto, Finland
- Pratt, H.R., D.E. Stephenson, G. Zandt, M. Bouchon and A. Hustrulid. 1979. Earthquake Damage to Underground Facilities. Proceedings of Rapid Excavation and Tunneling Conference. Atlanta, USA.
- QUINTESSA. 2011. Postclosure Safety Assessment: Analysis of the Normal Evolution Scenario. Quintessa Ltd. report for the Nuclear Waste Management Organization NWMO DGR-TR-2011-26 R000. Toronto, Canada.
- QUINTESSA and GEOFIRMA. 2011. Postclosure Safety Assessment: Data. Quintessa Ltd. and Geofirma Engineering Ltd. report for the Nuclear Waste Management Organization NWMO DGR-TR-2011-32 R000. Toronto, Canada.
- QUINTESSA and SENES. 2011. Postclosure Safety Assessment: Analysis of Human Intrusion and Other Disruptive Scenarios. Quintessa Ltd. and SENES Consultants Ltd. report for the Nuclear Waste Management Organization NWMO DGR-TR-2011-27 R000. Toronto, Canada.

- QUINTESSA, GEOFIRMA and SENES. 2011a. Postclosure Safety Assessment Report. Quintessa Ltd., Geofirma Engineering Ltd. and SENES Consultants Ltd. report for the Nuclear Waste Management Organization NWMO DGR-TR-2011-25 R000. Toronto, Canada.
- QUINTESSA, SENES and GEOFIRMA. 2011b. Postclosure Safety Assessment: Features, Events and Processes. Quintessa Ltd., SENES Consultants Ltd. and Geofirma Engineering Ltd. report for the Nuclear Waste Management Organization NWMO DGR-TR-2011-29 R000. Toronto, Canada.
- Roffey, R. and A. Nordqvist. 1991. Biodegradation of Bitumen Used for Nuclear Waste Disposal. *Cellular and Molecular Lifesciences* 47, 539-542.
- Sanford, B.V., F.J. Thompson and G.H. McFall. 1985. Plate tectonics- a possible controlling mechanism in the development of hydrocarbon traps in Southwestern Ontario. *Bull. Canadian Petrol. Geol.* 33, 52-71.
- Savage, D. 2005. The Effects of High Salinity Groundwater on the Performance of Clay Barriers. Swedish Nuclear Power Inspectorate (SKI) Report 2005-54. Stockholm, Sweden.
- Savage, D., D. Noy and M. Mihara. 2002. Modelling the interaction of bentonite with hyperalkaline fluids. *Applied Geochemistry* 17, 207-223.
- Shreir, L.L., R.A. Jarman and G.T. Burstein. 1993. Corrosion. Volume 1 Metal/Environment Reactions, 3rd Edition. Butterworth-Heinemann, Oxford, United Kingdom.
- SKB. 2006a. Buffer and Backfill Process Report for the Safety Assessment SR-Can. Swedish Nuclear Fuel and Waste Management Company Technical Report TR-06-18. Stockholm, Sweden.
- SKB. 2006b. Long-term Safety for KBS-3 Repositories at Forsmark and Laxemar – A First Evaluation. Main Report of the SR-Can Project. Swedish Nuclear Fuel and Waste Management Company Report R-06-09. Stockholm, Sweden.
- Sonley, E. and G.M. Atkinson. 2005. Empirical Relationship between Moment Magnitude and Nuttli Magnitude for Small-magnitude Earthquakes in Southeastern Canada. *Seismological Research Letters* 76(6), 752-755.
- Thorne, G.A. and M. Gascoyne. 1993. Groundwater Recharge and Discharge Characteristics in Granitic Terranes of the Canadian Shield. In: Banks, S. and B. Banks (Eds.), *Memoires of the XXIVth Congress, International Association of Hydrogeologists, Hydrogeology of Hard Rock*. Oslo, Norway.
- Torstenfelt, B. 1989. Chemical Degradation of Ion Exchange Resins in a Cement Matrix – A Review. ABB Atom Report RVC 89-160. Zurich, Switzerland.
- USDOE. 2002. Final Environmental Impact Statement for a Geologic Repository for the Disposal of Spent Nuclear Fuel and High-level Radioactive Waste at Yucca Mountain, Nye County, Nevada. United States Department of Energy, Office of Civilian Radioactive Waste Management, DOE/EIS-0250. Washington D.C., USA.

- USDOE. 2004. 2004 WIPP Compliance Recertification Application (CRA) - Main Volume DOE/WIPP 04-3231, United States Department of Energy. (Available at: http://www.wipp.energy.gov/library/CRA/CRA_Index.htm).
- Whittaker, B.N. and D.J. Reddish. 1993. Subsidence Behaviour of Rock Structures. In: Brown, E.T, Fairhurst, C and Hoek, E. (Eds.), *Comprehensive Rock Engineering: Principles, Practice and Projects*, Volume 4, Excavation, Support and Monitoring. Pergamon Press, Oxford, United Kingdom.
- Wing, N.R. and G.W. Gee. 1994. Quest for the Perfect Cap. *Civil Engineering* 64, 38-41.
- WIPP. 2004. Title 40 CFR Part 191 Subparts B and C Compliance Recertification Application for the Waste Isolation Pilot Plant Appendix BARRIERS. United States Department of Energy Waste Isolation Pilot Plant. Carlsbad, USA.
- WIPP. 2009. Waste Isolation Pilot Plant Hazardous Waste Facility Permit Renewal Application September 2009: Appendix I2, Appendix A, Material Specification Shaft Sealing System Compliance Submittal Design Report. United States Department of Energy Waste Isolation Pilot Plant. Carlsbad, USA.
- Wolf, M. and R. Bachofen. 1991. Microbial Degradation of Bitumen, *Cellular and Molecular Life Sciences* 47, 542-548.
- Wu, P. 1998. Intraplate Earthquakes and Postglacial Rebound in Eastern Canada and Northern Europe. In: Wu, P. (Ed.), *Dynamics of the Ice Age Earth: A Modern Perspective*. Trans Tech Publications, Switzerland.

10. ABBREVIATIONS AND ACRONYMS

ALW	Active Liquid Waste
CNSC	Canadian Nuclear Safety Commission
CSA	Canadian Standards Association
CSH	Calcium Silicate Hydrate
DGR	Deep Geologic Repository
EA	Environmental Assessment
EDZ	Excavation Damaged Zone
EIS	Environmental Impact Statement
FEP	Features, Events and Processes
HDZ	Highly Damaged Zone
IAEA	International Atomic Energy Agency
ICRP	International Commission on Radiological Protection
ILW	Intermediate Level Waste
ISAM	Improvement of Safety Assessment Methodologies
IX	Ion Exchange
L&ILW	Low and Intermediate Level Waste
LHHPC	Low-Heat, High-Performance Cement
LLW	Low Level Waste
NWMO	Nuclear Waste Management Organization
OGW	Opportunistic Groundwater Samples
OPC	Ordinary Portland Cement
OPG	Ontario Power Generation
PCB	Polychlorinated Biphenyl
PHT	Primary Heat Transport
PSHA	Probabilistic Seismic Hazard Assessment
PSR	Preliminary Safety Report
SA	Safety Assessment

TDS	Total Dissolved Solids
T-H-E	Tile Hole Equivalent
TSD	Technical Support Document
UoT GSM	University of Toronto Glacial Systems Model
VEC	Valued Ecosystem Components
WIPP	Waste Isolation Pilot Plant
WWMF	Western Waste Management Facility

APPENDICES

THIS PAGE HAS BEEN LEFT BLANK INTENTIONALLY

APPENDIX A: MIGRATION OF GAS FROM THE DGR

A.1 MIGRATION OF FREE GAS

Although it has been identified that there is likely some free gas present in the geosphere, for simplicity it is assumed here that initially there is no free gas in the geosphere. If the gas pressure in the DGR exceeds hydrostatic pressure, then gas can begin to flow out of the DGR. The bulk gas in the rock must be at a higher pressure than hydrostatic consistent with surface tension and bubble size, also referred to as capillary pressure or suction (depending on the model). This capillary suction (pressure) will increase as the degree of water saturation decreases. The gas saturation in the rock will be determined by the saturation at which the gas pressure is equal to the sum of the hydrostatic pressure and the capillary suction (pressure). As gas migrates into the geosphere, the total volume occupied by free gas increases (repository plus geosphere) and the gas pressure decreases. Therefore, gas may not be able to migrate through the geosphere to a permeable horizon (or the ground surface) before its pressure drops to hydrostatic.

If there is sufficient gas pressure to drive migration to a permeable horizon (or the ground surface), a gas pathway will be established. Gas will migrate via this pathway while there is a pressure gradient, and via buoyancy. The pathway will close as the gas pressure decreases and the gas pathway resaturates. Dissolution of gas into water can significantly influence the opening and closure of gas pathways.

The two-phase flow properties of the geosphere are described using the van Genuchten model (Section 4.7 of the Data report, QUINTESSA and GEOFIRMA 2011). Figure A.1 shows the relative permeability of gas for the Cobourg using the data given in Table 5.15 of QUINTESSA and GEOFIRMA (2011). The permeability controlling gas flow is equal to the intrinsic permeability of the rock multiplied by the relative permeability of gas. This varies from zero at zero gas saturation to unity at full gas saturation. When fully gas saturated, the geosphere gas flow rates will be low because the intrinsic permeability of the geosphere is very low. However, the gas flow rates will be even lower when only partially gas saturated. The relative permeability for gas is ~0.001 when the gas saturation is 7.5%. There is unlikely to be any significant gas flow below this gas saturation.

Figure A.2 shows the capillary suction (pressure) in the Cobourg, using the van Genuchten model and data given in Table 5.15 of QUINTESSA and GEOFIRMA (2011). At a gas saturation of 7.5% the capillary suction equals 24 MPa. Therefore, in order for a gas saturation of 7.5% to develop in the geosphere a gas pressure of 6.25 MPa (environmental pressure) plus 24 MPa = 30 MPa is required. This is much greater than the potential DGR gas pressures described in Appendix B and indicates that significant gas migration into the geosphere is not likely to occur, and a gas pathway through the geosphere is not likely to be established.

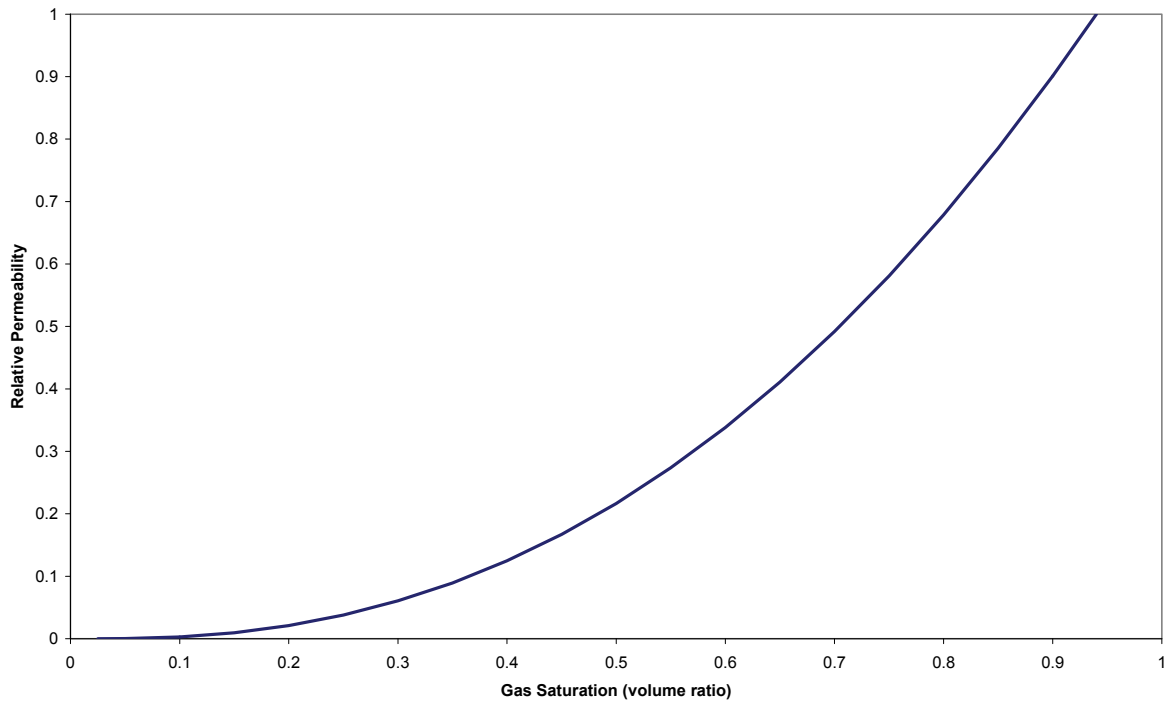


Figure A.1: Relative Permeability Curve for the Cobourg

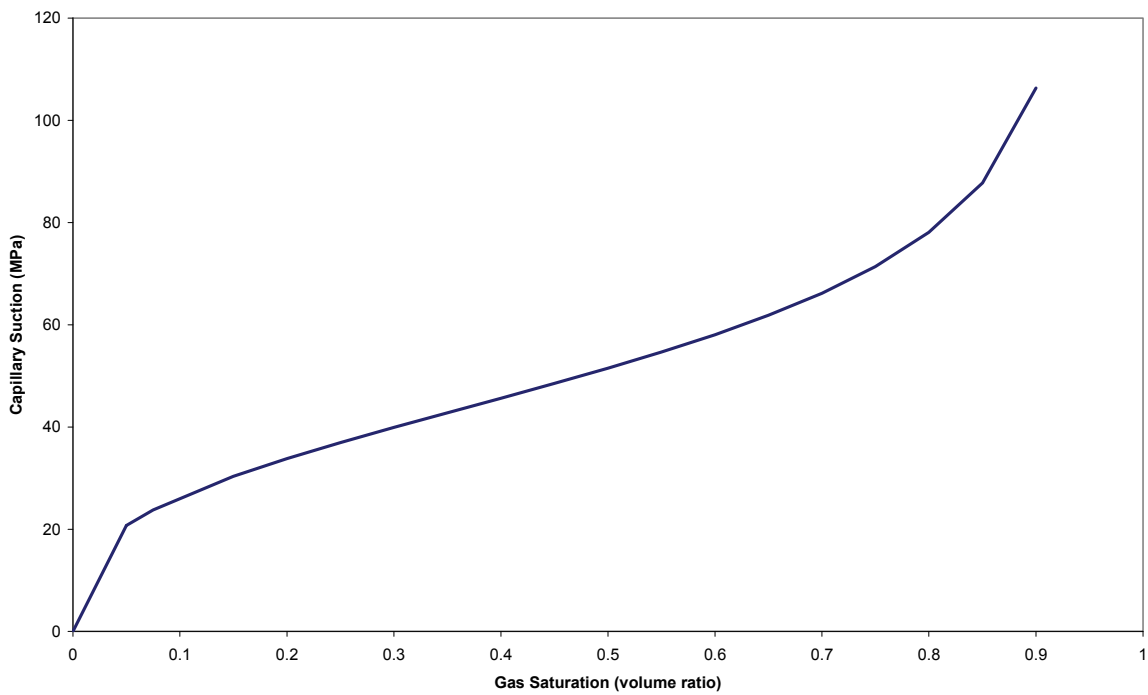


Figure A.2: Capillary Suction Curve for the Cobourg

Table A.1 shows the gas saturation at which the relative permeability is ~ 0.001 , the associated capillary suction (pressure), and the gas pressure required for gas flow. Table A.1 shows that gas will preferentially migrate through the monolith HDZ, shaft seals and shaft EDZ compared with the geosphere: the permeabilities are higher and the gas pressure required to drive gas flow is lower. Gas will flow through the monolith HDZ and then enter the shaft EDZ and bentonite-sand. However, there will be no gas flow through the monolith HDZ until the gas pressure in the DGR reaches 6.25 MPa, and no gas flow through the shaft seal or EDZ unless the gas pressure reaches 10 MPa.

Table A.1: Conditions Required for Gas Flow from the Repository

Material	Permeability (m ²) ¹	Gas saturation for Kr > 0.001 ²	Capillary Suction (MPa) ²	Environmental Pressure (MPa) ³	Gas Pressure (MPa)
Cobourg limestone	2.33E-22	0.075	24	6.25	30
Shaft Inner EDZ (Cobourg)	1.94E-20	0.075	4.8	6.25	11
Monolith	1.16E-17	0.14	0.69	6.25	6.9
Monolith HDZ	1.16E-15	7.5E-4	0 ¹	6.25	6.25
Bentonite-sand above monolith	1.16E-18	0.06	3.7	6.25	10

Notes:

1. Section 4.2 of GEOFIRMA and QUINTESSA (2011). Note there is no capillary suction in the HDZ and Kr in the HDZ fracture porosity varies linearly with saturation.
2. Calculated using data given in QUINTESSA and GEOFIRMA (2011).
3. From Figure 2.24.

If a free gas phase is present in the geosphere, then the pressure of this gas will be greater than the measured (i.e., environmental) hydraulic pressure. This means that gas in the geosphere will tend to flow or diffuse into the shaft and DGR until the pressures equilibrate with the gas pressure in the geosphere.

A.2 DIFFUSION OF DISSOLVED GAS

Gas will dissolve in water in the DGR and diffuse from the repository.

The gas composition in the DGR will likely be dominated by CH₄ at long times. Since site characterization information shows that there is methane present as a free gas phase in the Cobourg host rock, the porewaters should already be saturated with methane and, therefore, there would be little concentration gradient to drive methane from the DGR into the rock.

The following conservative calculation assumes that there is no methane present in the geosphere. The moles of methane present in the DGR can be estimated from the partial pressure of 6.6 MPa given in Table B.8 using the ideal gas law. This equates to 1.1×10^9 moles

(Table D.8), based on an unsaturated repository with a void volume of $4.18 \times 10^5 \text{ m}^3$ (Table 4.5 of the Data report, QUINTESSA and GEOFIRMA 2011), and a temperature of 295.5 K.

The Henry's constant for dissolution of methane in water in the repository is 0.004 mol/(L MPa) (Table B.2 of QUINTESSA and GEOFIRMA 2011). The dissolved concentration of methane is, therefore, $0.004 \text{ mol/(L MPa)} \times 6.6 \text{ MPa} = 0.026 \text{ mol/L}$.

For 1-D diffusion, the distance (L) a solute can diffuse in time t is approximately equal to,

$$L = (D_e t)^{0.5} \quad (\text{Drever 1997})$$

Where D_e is the effective diffusivity: taken to be $1 \times 10^{-12} \text{ m}^2/\text{s}$ based on diffusion of a non-excluded species normal to bedding (Table 5.14 of QUINTESSA and GEOFIRMA 2011). For $t = 1 \text{ Ma}$, $L = 5.6 \text{ m}$. The liquid porosity of the Cobourg is 0.015, and is similar to that of the under- and over-lying Sherman Fall and Collingwood formations. The panel footprint of the DGR is $2.39 \times 10^5 \text{ m}^2$ (Table 4.3 of QUINTESSA and GEOFIRMA 2011). The amount of methane that has diffused from the DGR in 1 million years is therefore:

$2.39 \times 10^5 \text{ m}^2 \times 5.6 \text{ m} \times 2$ (vertically upwards and downwards diffusion) $\times 0.015 \times 0.026 \text{ mol/L} \times 1000 \text{ L/m}^3 = 1 \times 10^6$ moles.

This is only 0.1% of the initial methane inventory. It shows that dissolution and diffusion of DGR methane is only a minor process, even in the absence of naturally occurring dissolved methane in the geosphere porewaters.

REFERENCES FOR APPENDIX A

- Drever, J.L. 1997. The Geochemistry of Natural Waters: Surface and Groundwater Environments. Prentice Hall, New Jersey, USA.
- GEOFIRMA and QUINTESSA. 2011. Postclosure Safety Assessment: Gas Modelling. Geofirma Engineering Ltd. and Quintessa Ltd. report for the Nuclear Waste Management Organization NWMO DGR-TR-2011-31 R000. Toronto, Canada.
- QUINTESSA and GEOFIRMA. 2011. Postclosure Safety Assessment: Data. Quintessa Ltd. and Geofirma Engineering Ltd. report for the Nuclear Waste Management Organization NWMO DGR-TR-2011-32 R000. Toronto, Canada.

APPENDIX B: POTENTIAL GAS PRESSURES IN THE DGR

B.1 INTRODUCTION

This appendix documents simple calculations to estimate potential gas pressures that could be observed within the repository, as waste is converted to gaseous forms during its evolution. They are based on the data given in the Data report (QUINTESSA and GEOFIRMA 2011) for the original preliminary design.

Based on the initial inventories (about 6.6×10^7 kg of metals and 2.2×10^7 kg of organics, Tables 4.12 and 4.10 of the Data report, QUINTESSA and GEOFIRMA 2011), this calculation estimates the total number of moles of iron (Fe), zirconium (Zr), and carbon (C) in the repository. These materials were assumed to degrade completely to generate mostly hydrogen (H_2), carbon dioxide (CO_2), and methane (CH_4) gases within the void volume of the repository. The following simplifying assumptions were made:

- No leakage of these gases;
- No influx of gas to the DGR;
- No oxygen, no nitrate, no sulphate;
- No biomass production;
- Unlimited supply of water;
- Void space of 4.2×10^5 m³ in the repository, taken from Table 4.5 of the data report (QUINTESSA and GEOFIRMA 2011); and
- Repository temperature of 22°C.

Three cases were considered and are documented in Appendix B.2 to B.4.

B.2 GAS GENERATION UNDER ANAEROBIC CORROSION & DEGRADATION WITH NO SIDERITE FORMATION AND NO METHANOGENIC REACTION (CASE1)

B.2.1 Metal Corrosion

The metals within the repository are categorized into unpassivated and passivated C-steels, passive alloys, and Zircaloy. The first three are assumed to be composed of Fe. The Zircalloys are assumed to be composed of Zr. See Table B.1 for their inventory. These metals are corroded under anaerobic conditions according to the following equations:



Therefore, 1 mole of Fe generates $4/3$ mole of H_2 ; 1 mole of Zr generates 2 moles of H_2 . Based on the Fe and Zr total moles, the amount of H_2 generated from metal corrosion was calculated to be 1.6×10^9 moles (Table B.1).

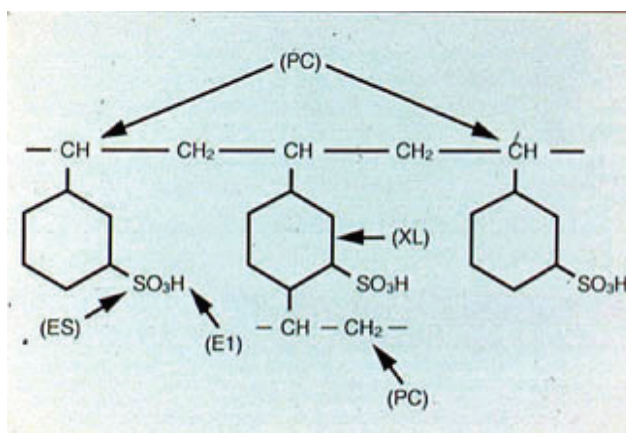
Table B.1: Iron and Zirconium Initial Inventory and Theoretical Amount of H₂ (Case 1)

Waste source	Initial Metal Mass ¹ (kg)	Initial Fe Amount (mol)	Initial Zr Amount (mol)	Theoretical H ₂ Amount (mol)	Theoretical Fe ₃ O ₄ Amount (mol)
Unpassivated C-steel	2.9E+07	5.2E+08		6.9E+08	1.7E+08
Passivated C-steel	1.6E+07	2.9E+08		3.8E+08	9.5E+07
Passive alloys	2.0E+07	3.6E+08		4.7E+08	1.2E+08
Zircaloy	6.0E+05		6.6E+06	1.3E+07	
Total	6.6E+07	1.2E+09	6.6E+06	1.6E+09	3.9E+08

Note: 1. Table 4.12 from the Data report (QUINTESSA and GEOFIRMA 2011).

B.2.2 Degradation of Organics

The organic materials are categorized into cellulosics, plastics and rubbers, and ion-exchange resins. Cellulosic materials are modelled as C₆H₁₀O₅, and plastics and rubbers are modelled as C₈H₈ (styrene). The dry ion-exchange resins consist of cation and anion resins (assumed 50 mol% each). See Figure B-1 for cation resin structure. The molecular mass for dry cation and anion resin is 0.184 and 0.193 kg/mol respectively, averaged 0.1885 kg/mol. There are 10 moles of carbon in 1 mole of dry resins, compared to 8 moles of carbon in 1 mole of polystyrene. Therefore, in order to ensure that the number of moles of carbon modelled is equal to the total amount available in the resins, the molar mass is multiplied by a factor 8/10, resulting in an equivalent mass of resin per mole of styrene monomer of 0.1508 kg/mol. The resins have an average of 10 carbon (C) atoms per mole of resins.



Note: XL: cross link; PC, polymer chain; ES, exchange site; EI, exchangeable ion

Figure B.1: Molecular Structure of Cation Resins

Table B.2 shows the initial C amount (1.3×10^9 moles). In the molecular mass column the molecular mass of cellulosic waste per mole cellulose, the mass of plastics and rubbers per mole of styrene monomer, and the mass of dry resin per mole of styrene monomer are given. Since 1 mole of C generates 1 mole of CO_2 or 1 mole of CH_4 , the theoretical total amount of CO_2/CH_4 from organic materials is 1.3×10^9 moles.

Table B.2: Carbon, Hydrogen and Oxygen Contributions from Organic Waste Sources (Case 1)

Waste source	Molecular Mass (kg/mol)	Initial Organic Mass (kg) ¹	Initial Carbon Amount (mol)	Theoretical CO_2+CH_4 Amount (mol)
Cellulosic materials	0.1620	8.2E+06	3.0E+08	3.0E+08
Plastics and rubbers	0.104	8.4E+06	6.5E+08	6.5E+08
Ion-exchange resins (dry)	0.1885	5.7E+06	3.0E+08	3.0E+08
Total		2.2E+07	1.3E+09	1.3E+09

Note: 1. Table 4.10 from the Data report (QUINTESSA and GEOFIRMA 2011).

CO_2 and CH_4 can also be estimated from the following anaerobic degradation reactions. The results are shown in Table B.3. Rubber, plastics, and resins are treated as styrene (C_8H_8).



Table B.3: CO_2 and CH_4 Generation from Organic Waste Sources (Case 1)

Waste source	Theoretical CO_2 Amount (mol)	Theoretical CH_4 Amount (mol)	Theoretical CO_2+CH_4 Amount (mol)
Cellulosic materials	1.5E+08	1.5E+08	3.0E+08
Plastics and rubbers	2.4E+08	4.0E+08	6.5E+08
Ion-exchange resins	1.1E+08	1.9E+08	3.0E+08
Total	5.1E+08	7.4E+08	1.3E+09

B.2.3 Gas Pressures

Metal corrosion and organic degradation mostly generate H_2 , CO_2 and CH_4 . In addition, initial air in the repository contains about 1.4×10^7 moles of N_2 . All O_2 in the initial air is quickly consumed by material degradation and is not considered in the scoping calculation. Based on

the initial void space in the repository and repository temperature, the maximum gas pressure in the repository was calculated to be about 17 MPa using the ideal gas law (Table B.4).

Table B.4: Maximum Repository Gas Pressure with No Siderite and No Methanogenic Reactions (Case 1)

	Theoretical Amount (mol)	Partial Pressure (MPa)
H ₂ from metal corrosion	1.6E+09	9.1
CO ₂ from organic degradation	5.1E+08	3.0
CH ₄ from organic degradation	7.4E+08	4.4
N ₂ from initial air	1.4E+07	0.1
Total	2.6E+09	16.6

B.3 GAS GENERATION UNDER ANAEROBIC CORROSION & DEGRADATION WITH SIDERITE FORMATION AND NO METHANOGENIC REACTION (CASE 2)

Because of the high HCO₃⁻ concentration, the stable corrosion product is FeCO₃ (siderite) rather than Fe₃O₄. The corrosion of carbon steel in CO₂-containing environments is given by



Therefore, 1 mole each of Fe and CO₂ will be converted to 1 mole each of FeCO₃ and H₂. Since there are 5.1 x 10⁸ moles of CO₂ (Table B.3), 5.1 x 10⁸ moles each of FeCO₃ and H₂ will be formed, and 5.1 x 10⁸ moles of Fe will be consumed. The remaining Fe (6.5 x 10⁸ moles) will be converted to Fe₃O₄ according to Equation (B.1). The theoretical amounts of iron corrosion products and H₂ are given in Table B.5.

Table B.5: Theoretical Amount of H₂ and Iron Corrosion Products (Case 2)

Waste source	Theoretical FeCO ₃ Amount (mol)	Theoretical Fe ₃ O ₄ Amount (mol)	Theoretical H ₂ Amount (mol)
Fe	5.1E+08	2.2E+08	1.4E+09
Zr			1.3E+07
Total	5.1E+08	2.2E+08	1.4E+09

Since 5.1 x 10⁸ moles of CO₂ are converted to FeCO₃, there will be no CO₂. Therefore, Table B.3 can be simplified to Table B.6.

Table B.6: CO₂ and CH₄ Generation from Organic Waste Sources (Case 2)

Waste source	Theoretical CO ₂ Amount (mol)	Theoretical CH ₄ Amount (mol)
Cellulosic materials	0	1.5E+08
Plastics and rubbers	0	4.0E+08
Ion-exchange resins	0	1.9E+08
Total	0	7.4E+08

The total amount of H₂ and CH₄ are given in Table B-5 and B-6, respectively. Based on the ideal gas law, they can be converted to partial pressures. The total gas pressure was estimated to be 12.6 MPa (Table B.7).

Table B.7: Maximum Repository Gas Pressures under Anaerobic Corrosion & Degradation with Siderite and No Methanogenic Reaction (Case 2)

	Theoretical Amount (mol)	Partial Pressure (MPa)
H ₂ from metal corrosion	1.4E+09	8.1
CO ₂ from organic degradation	0.0E+00	0.0
CH ₄ from organic degradation	7.4E+08	4.4
N ₂ from initial air	1.4E+07	0.1
Total	2.2E+09	12.6

B.4 GAS GENERATION UNDER ANAEROBIC CORROSION & DEGRADATION WITH METHANOGENIC REACTION AND NO SIDERITE FORMATION (CASE 3)

H₂ generated from anaerobic corrosion of metals can be combined with CO₂ to form CH₄ (Equation B.6).



There are a total of 1.6×10^9 moles of H₂ generated (Table B.1). It requires 3.9×10^8 moles of CO₂ to convert all H₂ to form 3.9×10^8 moles of CH₄. Therefore, 1.2×10^8 moles of CO₂ will remain. See Table B.3 for total moles of CO₂ generated (5.1×10^8 moles). The total amount of CH₄ will be increased from 7.4×10^8 moles (Table B.3) to 1.1×10^9 moles. The total gas pressure was estimated to be 7.4 MPa (Table B.8).

Table B.8: Maximum Repository Gas Pressures under Anaerobic Corrosion and Degradation with Methanogenic Reaction and No Siderite Formation (Case 3)

	Theoretical amount (mol)	Partial Pressure (MPa)
H ₂ from metal corrosion	0	0.0
CO ₂ from organic degradation	1.2E+08	0.7
CH ₄ from organic degradation	1.1E+09	6.6
N ₂ from initial air	1.4E+07	0.1
Total	1.3E+09	7.4

REFERENCE FOR APPENDIX B

QUINTESSA and GEOFIRMA. 2011. Postclosure Safety Assessment: Data. Quintessa Ltd. and Geofirma Engineering Ltd. report for the Nuclear Waste Management Organization DGR-TR-2011-32. Toronto, Canada.

APPENDIX C: CHEMICAL EVOLUTION OF THE DGR

C.1 CHEMICAL EVOLUTION

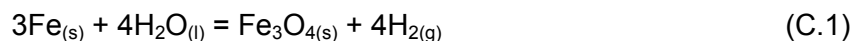
The chemistry of the host rock (Cobourg) porewater is described in Appendix C of the Data report (QUINTESSA and GEOFIRMA 2011). The impacts of chemical conditioning by cement in the DGR are also described. There are only relatively small quantities of cement in the DGR; therefore chemical conditioning by cement is only likely to affect local conditions rather than the general conditions in the DGR, for example altering pore water chemistry within wastes with concrete overpacks and the monolith.

There are significant quantities of metallic and organic wastes in the DGR that have the potential to influence not only local chemical conditions, but also the general chemical conditions in the DGR. Metals are not only present in the wastes, but also the waste packaging and DGR engineering. The potential impacts of metals and organic acids on the chemical evolution of the DGR are considered below.

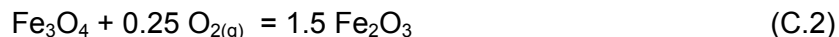
C.2 EFFECT OF CONTAINER CORROSION

As outlined in Appendix C of the Data report (QUINTESSA and GEOFIRMA 2011), models of Cobourg porewater suggest a host rock $pO_{2(g)}$ around $10^{-65.2}$ bars, which corresponds to pyrite-hematite equilibrium, a value shown to be not dissimilar to that for pyrite-siderite equilibrium. However, near-field redox conditions will be influenced by iron metal corrosion due to the large amounts of metals present in the wastes, containers and engineered components.

Iron/steel may corrode under relatively anaerobic conditions to produce magnetite (Fe_3O_4) possibly via metastable 'green rust' compounds (Wilson et al. 2006). As calculated by Wilson et al. (2006), the oxygen partial-pressure [$pO_{2(g)}$], is taken to be equal to oxygen fugacity [$fO_{2(g)}$] at 0.1 MPa and for Fe- Fe_3O_4 equilibrium, it is at a value below the stability limit of water (i.e., $H_2O_{(l)}$ - $H_{2(g)}$ equilibrium, Figure C.1). Therefore, $H_{2(g)}$ is generated when Fe(0) oxidizes to magnetite (Equation C.1):



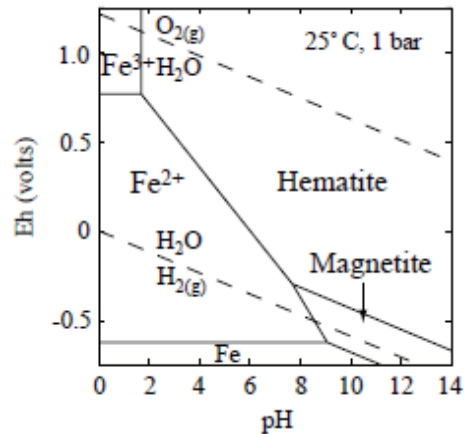
Magnetite-hematite equilibrium (Equation C.2) has also been considered as a redox buffer, in cases where iron is undergoing oxidation from Fe(II) to Fe(III) at a stage after liberation of $H_{2(g)}$ (e.g., Wilson et al. 2006):



Therefore, equilibrium expressions given in Equations C.1 and C.2 can be taken to approximately 'bracket' the range of $pO_{2(g)}$ values that may be associated with canisters that are corroding to produce iron (hydr)oxides. These values were used as input to PHREEQC models of Cobourg porewater (Table C.1). Calculations were undertaken using the Pitzer database developed for Yucca Mountain (USDOE 2007).

For cement-equilibrated Cobourg porewater, the effect of container corrosion was simply determined by repeating aqueous speciation calculations with $pO_{2(g)}$ corresponding to the aforementioned buffers assuming that magnetite buffers dissolved Fe activities and that dissolved S activities are buffered by pyrite (FeS) (thermodynamic data for the hydrolysis of this phase was taken from the 'Ilnl.dat' database, because it is not available from the Pitzer database).

The results of the models presented in Table C.1 show that the corrosion of Fe results in lower $pO_{2(g)}$ values, with no appreciable impact on pH. The lack of change to pH values reflects the assumption that $pCO_{2(g)}$ would initially be similar to that of Cobourg porewater and the fact that changes in aqueous speciation were not sufficient to lead to the development of substantial charge imbalances.



Note: Diagram taken from Wilson et al. (2006). Lower dashed line for H₂-H₂O Equilibrium and upper dashed line for H₂O-O₂ Equilibrium.

Figure C.1: Mineral Stabilities in Eh-pH Space for the System FeO-Fe₂O₃-H₂O showing the Stability Limits of Water

Table C.1: Summary of Water Chemistry Conditions in Near Field - Cobourg Porewater in the Presence of Corroding Steel

Porewater	Equilibrium Phases/Activity Buffers (SI=0)	Notes	Log p O ₂	pH	Eh(V)	log CO ₂
Non-cementitious						
Model 2 Cobourg Porewater	Anhydrite, calcite, dolomite, celestine, illite, SiO _{2(am)} Halite (-0.88).	pH based on range of calculated pCO _{2(g)} pO _{2(g)} set to pyrite-hematite equilibrium	-65.23	6.5	-0.12	-2.43
Simplified Cobourg composition at H ₂ -H ₂ O equilibrium	Calcite, dolomite, SiO _{2(am)} , magnetite, pyrite Halite (0.88) sylvite (-1.11)	Pure water equilibrated with solid phases Sulphate reduction kinetically uninhibited Input log pCO _{2(g)} =-2.4 Log pO _{2(g)} set at -83.1 Initial pH set at 6.5	-83.1	6.5	-0.38	-2.43
Simplified Cobourg composition at magnetite-hematite equilibrium	Calcite, dolomite, SiO _{2(am)} , magnetite, pyrite Halite (0.88) sylvite (-1.11)	Pure water equilibrated with solid phases Sulphate reduction kinetically uninhibited Input log pCO _{2(g)} =-2.43 Log pO _{2(g)} set at -73.2	-72.3	6.5	-0.23	-2.43
Cementitious						
Model 2 Cobourg Porewater equilibrated with cement	Calcite, celestine, portlandite, hydroxalcalite, Al-ettringite, CSH-gel, hydrogarnet	pO _{2(g)} set to pyrite-hematite equilibrium	-65.23	11.9	-0.39	-13.17
Model 2 Cobourg Porewater equilibrated with cement at H ₂ -H ₂ O equilibrium	Calcite, celestine, portlandite, hydroxalcalite, pyrite, CSH-gel, hydrogarnet	Pure water equilibrated with solid phases Log pO _{2(g)} set at -83.1 (H ₂ -H ₂ O equilibrium)	-83.1	11.9	-0.70	-13.17
Model 2 Cobourg Porewater equilibrated with cement at magnetite-hematite equilibrium	Calcite, celestine, portlandite, hydroxalcalite, pyrite, CSH-gel, hydrogarnet	Pure water equilibrated with solid phases Log pO _{2(g)} set at -73.2	-72.3	11.9	-0.54	-13.17

C.3 EFFECT OF ORGANIC ACID FORMATION

The effect of organic acid formation on the near-field water pH is considered here. Acetic acid is taken as a representative organic acid produced by waste decomposition.

The amount of acetate that may be present in a repository was calculated assuming equilibrium with cellulose (the mass of acetate is given by the ratio of degradation rates for cellulose and acetate, multiplied by cellulose mass present per given volume/total mass).

Taking a cellulose degradation rate of 5×10^{-4} /a from Table 3.21 of the Data report (QUINTESSA and GEOFIRMA 2011), assuming an acetate degradation rate¹⁰ of 1 /a, a void volume of 3.53×10^5 m² in the emplacement rooms (Table 4.5, QUINTESSA and GEOFIRMA 2011) and a total repository mass of cellulose of 8.2×10^6 kg (Table 4.10, QUINTESSA and GEOFIRMA 2011), gives an acetate concentration of 0.01 kg/m³ (6.2×10^{-5} mol/L).

Assuming that the water was the highly saline Cobourg porewater (Model 2 in Appendix C of QUINTESSA and GEOFIRMA 2011), the effect on pH was estimated using PHREEQC input for a speciation calculation where charge was balanced on pH, using the 'lnl.dat' database (which includes more organic species than the Pitzer database).

The calculated pH for model 2 Cobourg pore water is 6.2. After the addition of acetate, the pH stayed the same, as did $p\text{CO}_{2(g)}$ ($10^{-2.29}$ bars). Although the solute composition is too saline for accurate speciation given the available databases, this approach provides an indication that the magnitude of pH change due to organic acid formation from waste degradation will likely be small over the DGR.

REFERENCES FOR APPENDIX C

- GEOFIRMA and QUINTESSA. 2011. Postclosure Safety Assessment: Gas Modelling. Geofirma Engineering Ltd. and Quintessa Ltd. report for the Nuclear Waste Management Organization NWMO DGR-TR-2011-31 R000. Toronto, Canada.
- QUINTESSA and GEOFIRMA. 2011. Postclosure Safety Assessment: Data. Quintessa Ltd. and Geofirma Engineering Ltd. report for the Nuclear Waste Management Organization NWMO DGR-TR-2011-32 R000. Toronto, Canada.
- USDOE. 2007. In-Drift Precipitates/Salts Model. United States Department of Energy, ANL-EBS-MD-000045 Rev 03.
- Wilson, J., D. Savage, J. Cuadros, K.V. Ragnarsdottir and M. Shibata. 2006. The Effect of Iron on Montmorillonite Stability. (I) Background and Thermodynamic Modelling. *Geochimica et Cosmochimica Acta* 70(2), 306-322.

¹⁰ Based on Section 2.1.3.1 of the Gas Modelling report (GEOFIRMA and QUINTESSA 2011), which describes hydrolysis as being the rate limiting step in microbial degradation.

APPENDIX D: FORMATION OF METHANE AND CARBON DIOXIDE HYDRATES

Hydrates, also called clathrates, are a crystalline solid composed of water and a gas. Water forms a crystal, cage-like structure, and the gas molecules (in this case methane or carbon dioxide) can be trapped within this structure. These structures can form in any location where a free gas, water, the appropriate temperature and pressure exist.

Interest in hydrates arises from their capacity to store large volumes of gas. If a hydrate were to form, then the gas pressure in the DGR would decrease, as hydrates are able to trap relatively large amounts of methane within their structure (compared to the volume of the crystallite itself). As such, it could be considered conservative to neglect the formation of hydrates.

Figures D.1 and D.2 show the methane and carbon-dioxide hydrate stability fields respectively. The ambient temperature at the DGR horizon is 22 to 23 °C (Section 5.1 of QUINTESSA and GEOFIRMA 2011). The maximum pressure in the DGR will be 8.2 MPa at 1 million years, based on the Normal Evolution Reference Case (Section 5.1.1 and Figure 5.7 of the Gas Modelling Report, GEOFIRMA and QUINTESSA 2011). Under these conditions hydrates will not form. Under glacial conditions the temperature at the DGR horizon will fall to 17 °C (Section 5.1) and the pressure will increase by about 8% due to lithostatic loading. The pressure reached during glacial loading is below the formation pressure of methane hydrates at 17 °C. Carbon dioxide hydrates will not form under these conditions. In view of these considerations, the formation of hydrates in the DGR is conservatively neglected.

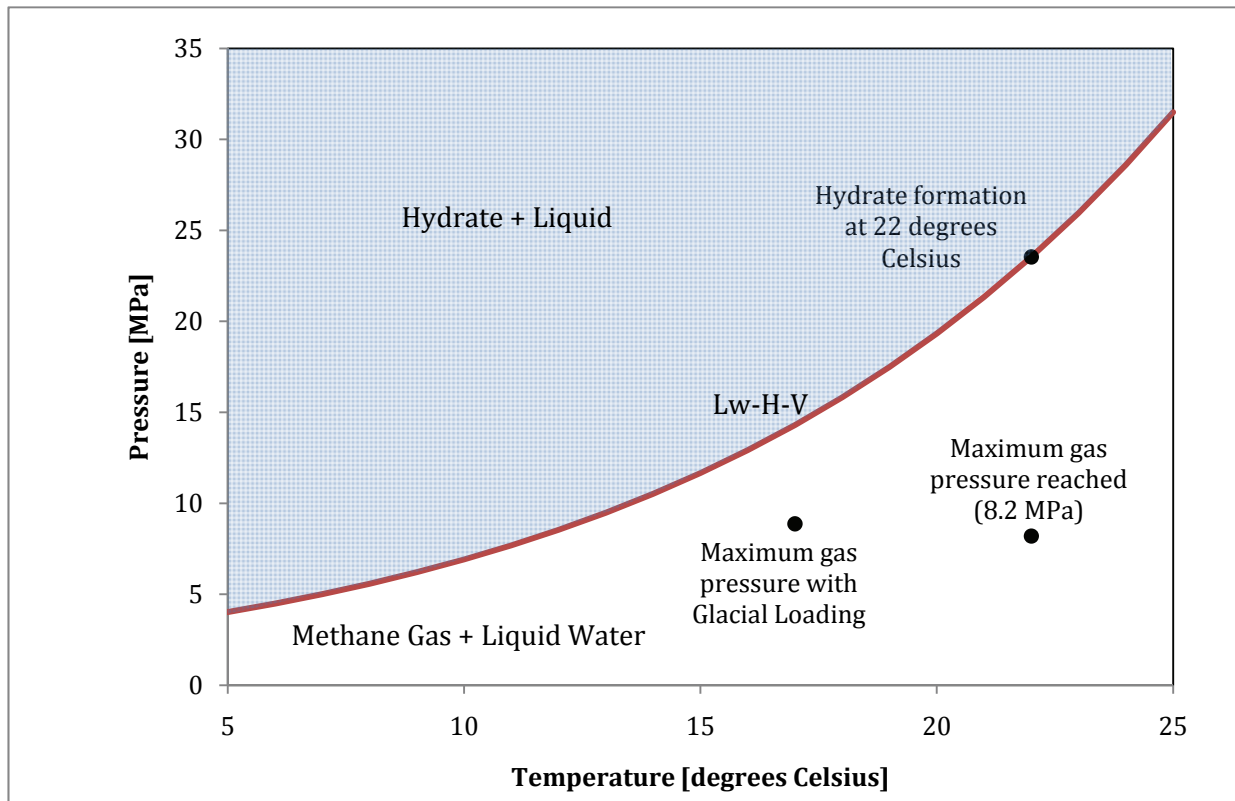


Figure D.1: Methane-Hydrate Stability Field and DGR Conditions

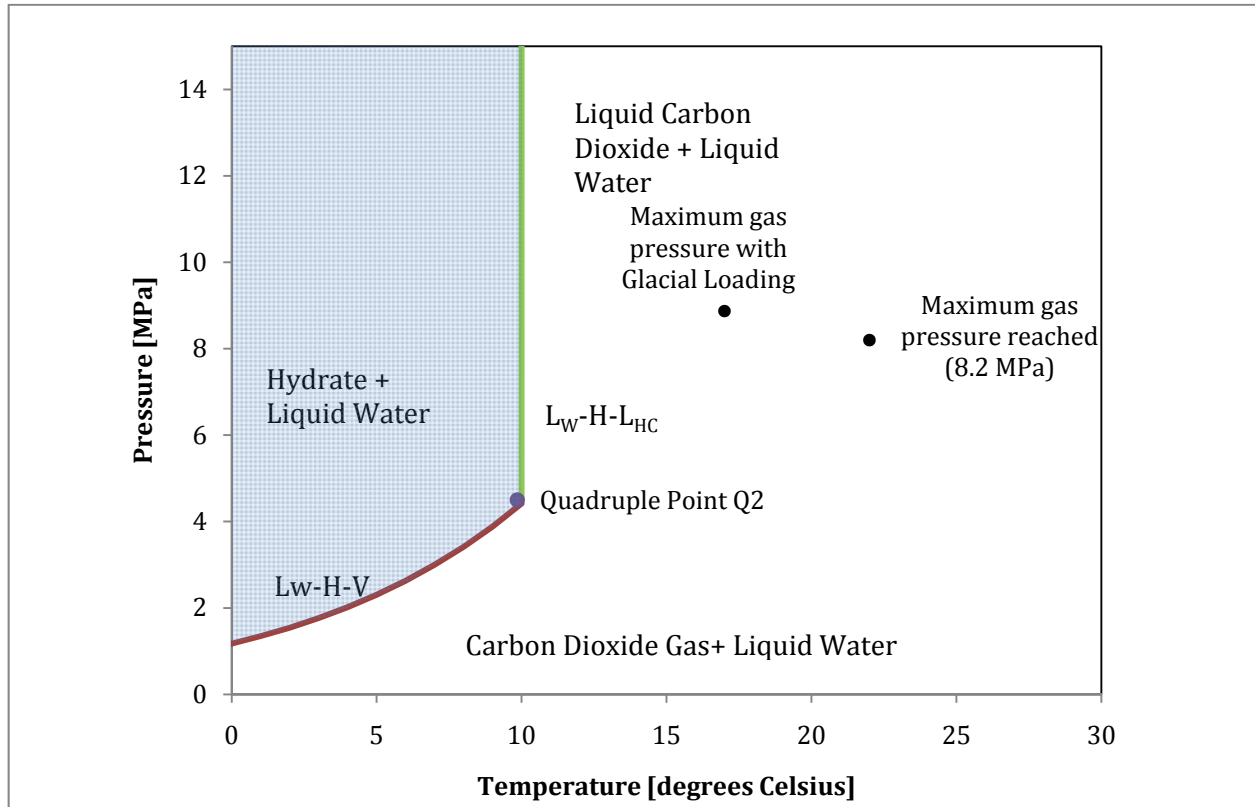


Figure D.2: Carbon Dioxide-Hydrate Stability Field and DGR Conditions

Generally, mixed gases would be even less likely to form hydrates than the pure gases. As neither carbon dioxide hydrates nor methane hydrates are expected under DGR normal or glacial loading conditions, it is not expected that mixed gas hydrates will form.

REFERENCES FOR APPENDIX D

GEOFIRMA and QUINTESSA 2011. Postclosure Safety Assessment: Gas Modelling. Geofirma Engineering Ltd. and Quintessa Ltd. report for the Nuclear Waste Management Organization NWMO DGR-TR-2011-31 R000. Toronto, Canada.

QUINTESSA and GEOFIRMA. 2011. Postclosure Safety Assessment: Data. Quintessa Ltd. and Geofirma Engineering Ltd. report for the Nuclear Waste Management Organization NWMO DGR-TR-2011-32 R000. Toronto, Canada.

APPENDIX E: ASSESSMENT OF SHAFT SEAL DEGRADATION

E.1 INTRODUCTION

The following potential degradation pathways are considered in this appendix:

- Interaction of bentonite-sand with intruding saline water and changes in smectite interlayer chemistry and swelling pressure (Appendix E.2);
- Interaction of bentonite-sand with intruding pore fluids and the potential for smectite (montmorillonite) alteration (Appendix E.3);
- Interaction of bentonite-sand with cement resulting in alteration of smectite (montmorillonite) and embrittlement (Appendix E.4);
- Cement degradation (including cement carbonation, sulphate attack, interaction of degrading cement with host rock) (Appendix E.5); and
- Asphalt degradation (Appendix E.6).

E.2 INTERACTION OF BENTONITE-SAND WITH INTRUDING SALINE WATER AND CHANGES IN SMECTITE INTERLAYER CHEMISTRY AND SWELLING PRESSURE

The interaction of bentonite with saline intruding groundwater could result in smectite (montmorillonite) interlayer ion exchange and possible changes in the physical properties of the bentonite. The interlayer occupancy of MX-80 bentonite after equilibration with Cobourg 'Model 2' porewater (taken to be a typical high salinity porewater composition to represent all shaft zones) was determined using PHREEQC with ion exchange constants and initial interlayer composition from Bradbury and Baeyens (2002) (Tables E.1 and E.2 respectively). The computed interlayer composition is given in Table E.3. The porosity of the bentonite was assumed to be the total void space porosity of 0.29 (note that a number of models have been suggested for considering porosity in bentonite; see Savage et al. 2010).

Table E.1: Ion Exchange Constants for MX-80 Bentonite

Ion exchange reaction	Log K
$XNa + K^+ = XK + Na^+$	0.6021
$2XNa + Ca^{2+} = X_2Ca + 2Na^+$	0.415
$2XNa + Mg^{2+} = X_2Mg + 2Na^+$	0.3424

Note: From Bradbury and Baeyens (2002).

Table E.2: Initial MX-80 Interlayer Occupancies

Interlayer Cation	Mol Fraction
Na	0.91
K	0.02
Mg	0.03
Ca	0.04

Note: From Bradbury and Baeyens (2002).

Table E.3: Interlayer Occupancies for MX-80 Bentonite-Sand after Equilibrium with Cobourg 'Model 2' Porewater Water

Interlayer Cation	Mol Fraction
Na	0.58
K	0.40
Ca	0.02
Mg	0.00

Note: Calculated using data from Table E.1 and E.2.

The calculations suggest that if all smectite ion-exchange sites in the bentonite/sand equilibrate with Cobourg porewater, they will become richer in exchangeable K^+ (58% of the exchange sites contain Na^+ after equilibration with Cobourg porewater (with a relatively high K content for the host geosphere) as opposed to 91% in the initial MX-80).

The volume of a cylindrical section of bentonite/sand (ventilation shaft) with vertical thickness of 1 m and excavated diameter of 7.45 m (Table 4.14 of QUINTESSA and GEOFIRMA 2011a) is $3.142 \times (3.725 \text{ m})^2 \times 1 \text{ m} \approx 43.6 \text{ m}^3$. This seal will consist of 70 wt% bentonite and 30 wt% sand, while the bentonite itself will contain 82 wt% montmorillonite, the remainder being non-swelling solid phases. The MX-80 has a dry density of 1600 kg/m^3 . This corresponds to a montmorillonite density of $1600 \text{ kg} \times 0.7 \times 0.82 \approx 918 \text{ kg/m}^3$, which when divided by the approximate molecular mass of Na-montmorillonite (367 g/mol) gives about 2500 moles of Na-montmorillonite per m^3 . If the total interlayer occupancy is taken to be ~ 0.33 moles interlayer cation per mole Na-montmorillonite, then there are $0.33 \times 0.4 = 0.132$ moles of K per mole of Na-montmorillonite once it has equilibrated with Cobourg porewater. Therefore, $0.132 \times 2500 = 330 \text{ mol/m}^3$ of K are required to produce the interlayer occupancy given in Table E.3. Multiplying this value by the volume of 1 m thick section of shaft gives $330 \times 43.6 \approx 14400$ moles of K required for whole shaft cross section.

The concentration of K in the Cobourg porewater is 0.443 molal. Therefore (assuming 1 kg water has a volume of $\sim 1 \text{ L}$), the amount of water required to provide 14400 moles, is $14400 \text{ (moles L)}/0.443 \text{ moles} \approx 32500 \text{ L}$ or 32.5 m^3 . Given a saturated porosity of 5%, this volume of water equates to a rock volume of 650 m^3 , or for a 1m thick section, a radius of 14.4 m. Therefore, assuming little K is supplied by mineral dissolution, and a geosphere effective diffusion coefficient of $3 \times 10^{-12} \text{ m}^2/\text{s}$, a geosphere K flux is approximately equal to a gradient of $440/(14.4 \text{ m} - 3.725 \text{ m}) \approx 41 \text{ mol/m}^4$, multiplied by the surface area of cylindrical section of $(2 \times 10.7 \text{ m} \times 3.142 \times 1 \text{ m}) \approx 67.2 \text{ m}^2$, multiplied by the effective diffusion coefficient ($3 \times 10^{-12} \text{ m}^2/\text{s}$) $\approx 8.3 \times 10^{-9} \text{ mol/s}$ or 0.26 mol/a . It would therefore take about 55,000 years to provide the K required for ion exchange to the outer boundary of the shaft.

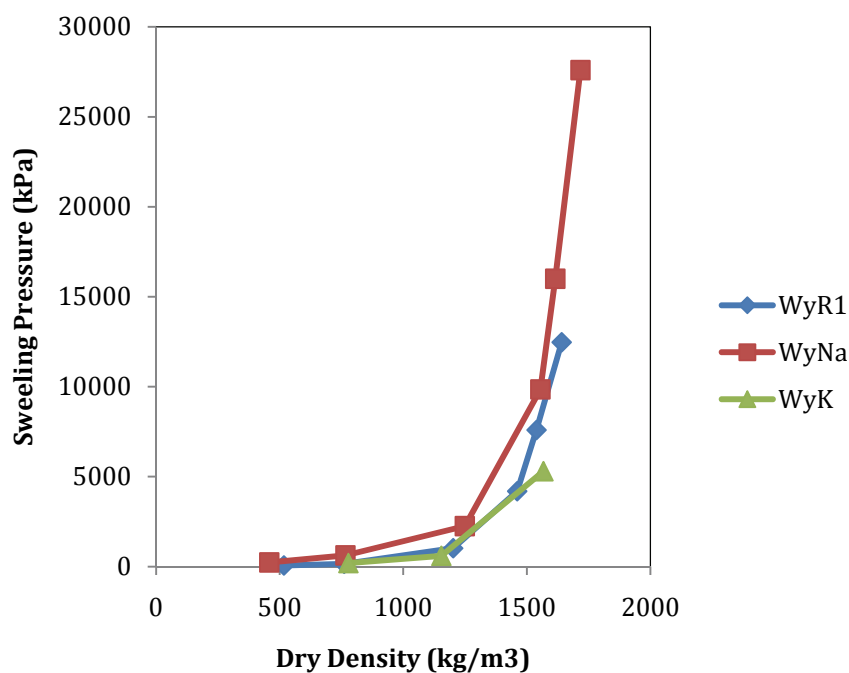
Although there is a lack of published data on the swelling pressure for bentonite with K-exchanged montmorillonite (as opposed to "K-bentonites", which may have illite layers), those available in Karnland et al. (2006) suggest that K exchange could result in a partial reduction in swelling pressure, at least under low ionic strength conditions (Figure E.1; Table E.4). The exact extent to which swelling pressure could be reduced is not clear, given the number of data points available and the shape of the curves. However, it appears that K-exchanged material probably does not have much less than half of the swelling pressure of Na-montmorillonite at a

density of $\sim 1550 \text{ kg/m}^3$. Therefore, it should be conservatively assumed that for the interlayer occupancy given in Table E.3 (0.4) results in 40% of the smectite having a swelling pressure that is reduced by $\sim 50\%$ (or a total loss in swelling pressure of $\sim 20\%$). However, several thousand years may be required for a sufficient flux of K for this to occur.

Table E.4: Swelling Pressures in the Wyoming MX-80 R1 Reference Material and the Corresponding Purified Sodium and Calcium Exchanged Clay Fraction

Material	D _d , kg/m ³	H ₂ O	0.1M	0.3M	1.0M	3.0M	0.3M	1.0M	0.1M
WyR1	517	61	35	23	16	12	23		
	761	156	123	68	37	26	79		
	1,202	1,020	1,000	800	550	100	770		
	1,461	4,190	4,240	4,000	3,150	1,240	3,690		
	1,539	7,590	7,590	7,380	6,340	4,550	6,910		
	1,641	12,470	12,350	12,170	11,520	10,220	12,020		
WyNa	458	232	115	70	44	38	115	43	112
	766	621	428	210	85	53	450	84	438
	1,249	2,248	2,125	1,634	1,074	213	2,025	1,079	1,985
	1,555	9,850	9,340	9,145	8,270	6,520	9,240	8,230	9,210
	1,615	16,000	15,400	14,900	14,240	12,600	14,900	14,100	14,960
	1,717	27,600	26,500	25,980	25,430	23,910	26,000	25,290	26,000
WyCa	502	12	9	8	8	4	8		
	789	87	69	63	51	12	66		
	1,275	1,650	1,540	1,430	970	246	1,530		
	1,580	11,285	11,040	10,800	9,870	7,980	10,880		
	1,658	21,770	21,530	21,270	20,720	17,900	21,390		
WyMg	744	90							
	1,209	1,800							
	1,564	13,400							
WyK	778	195							
	1,154	600							
	1,567	5,300							

Note: The first column of numbers shows dry clay density (D_d), the following columns show the NaCl concentrations (mol/L) in the test solutions successively in contact with the WyR1 and WyNa samples, and the CaCl₂ concentrations in the test solutions in successive contact with the WyCa samples. Pressure values in kPa (reproduced from Karnland et al. 2006).



Note: Data from Table E.4 and taken from Karnland et al. (2006). Reference, Na and K exchanged.

Figure E.1: Plots of Bentonite Swelling Pressure as a Function of Dry Density for Wyoming MX-80 Bentonite

E.3 INTERACTION OF BENTONITE-SAND WITH INTRUDING PORE FLUIDS AND THE POTENTIAL FOR SMECTITE (MONTMORILLONITE) ALTERATION

In addition to the replacement of interlayer Na for K, the potential for smectite illitization may be considered. Illite is a common K-bearing, aluminous, non-swelling 2:1 layer silicate. The K ion is essentially fixed in position between 2:1 sheets which have a higher layer charge deficit than smectites (due to substitution of Si by Al in tetrahedral sheets). Illite may exist in discrete (non-swelling) particles, or may be intercalated with other clay layer types, especially smectite, to form 'mixed layer' minerals (with restricted ability to swell). Of particular relevance is mixed layer illite/smectite which forms as smectite is gradually altered to illite.

The process of illitization (commonly associated with burial diagenesis of sediments and low grade metamorphism) involves 2:1 layer charge increase (as Al is substituted for Si in tetrahedral sheets), uptake of K into interlayer regions and the release of silica. The reaction is strongly dependent upon time, temperature and availability of K^+ .

Karnland and Birgersson (2006) evaluated a number of models for illitization and chose that described by Huang et al. (1993) to apply to the KBS crystalline rock groundwater conditions.

Huang et al. (1993) suggest the following second-order rate law for smectite illitization:

$$-\frac{dS}{dt} = A e^{-Ea/RT} K^+ S^2 \quad (E.1)$$

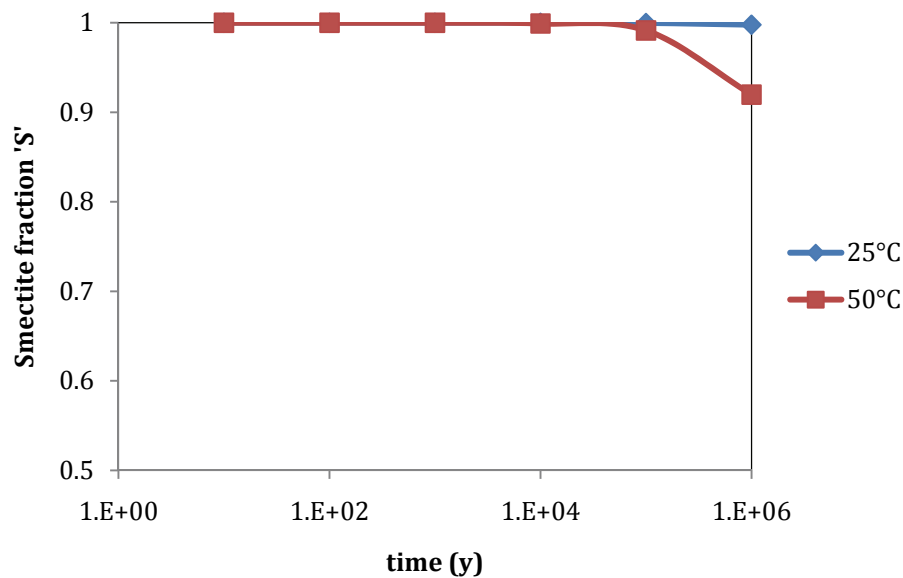
where S is smectite fraction, A is frequency factor ($8.08 \cdot 10^4 /s$), t is time (s), Ea is activation energy (28 kcal/mol or 117.15 kJ/mol), R is the gas constant, T is the temperature ($^{\circ}C$), and K^+ is expressed as a concentration (mol/L). In the case of Na dominated solutions, Huang et al. (1993) suggest that the term K^+ is replaced by C_n , where

$$C_1 = [K^+] - (([K^+]/2) \cdot ([Na^+]/2.3)) \text{ (for Na-rich fluid)} \quad (E.2)$$

$$C_2 = [K^+] - (([K^+]/2) \cdot ([Mg^{2+}]/0.05)) \text{ (for Mg-rich fluid)} \quad (E.3)$$

$$C_3 = (C_1 + C_2)/2 \text{ (for both Na and Mg-rich fluid)} \quad (E.4)$$

The maximum pore water K^+ concentration was conservatively taken to be 0.44 mol/kg (Cobourg Limestone, Table 5.4 of QUINTESSA and GEOFIRMA 2011a). A plot of S under low temperature conditions is given in Figure E.2. It is clear that smectite illitization will be of very minor importance (due mainly to the low temperature of the system) and will not adversely affect bentonite swelling. At $25^{\circ}C$, <0.01% of the smectite initially present is lost over 1 Ma. At $50^{\circ}C$ (a temperature much higher than that expected in the DGR), 92% of the smectite originally present remains.



Note: Application of the Smectite Illitization Model of Huang et al. (1993) to the Bruce nuclear site, showing smectite (montmorillonite) fraction 'S' under different temperature conditions with conservative porewater K^+ concentration of 0.443 mol/kg.

Figure E.2: Smectite (Montmorillonite) Fraction 'S' under Different Temperature Conditions

In addition to illitization, there is the theoretical potential for montmorillonite to be altered by reaction with saline solutions, including those with significant dissolved Mg^{2+} concentrations. For example, Suzuki et al. (2008) report experiments in which a crude bentonite (Kunigel V1) was reacted with simulated sea-water (Mg concentrations up to 55 millimolar), at temperatures of either 60 or 90°C over 6000 h (250 days). Mg was taken up by the bentonite during the experiments at levels over the cation exchange capacity (CEC; 0.78 meq/g for the original bentonite) at 90°C. The excess Mg was not replaced by ammonium ions, leading Suzuki et al. (2008) to suggest that an Mg solid (Mg-hydroxide) formed in the bentonite. In addition, the CEC decreased from 0.78 to 0.45 meq/g as the amount of accumulated Mg increased; the distribution coefficient (K_d) for Cs in the altered bentonite was half of that in the original bentonite; and 'potential' swelling capacity (measured as swelling power) was reduced.

Experiments in which bentonite was reacted with saline solutions have shown possible alteration to non-swelling layer silicates (e.g., Herbert et al. 2004). Herbert et al. (2008) report further experimental work where MX-80 bentonite was allowed to come into contact with solutions of varying ionic strengths and pH (0 to 15.5 M, pH of 5.3-13.2 compositions representing granite, cement, clay and salt pore waters) in both batch experiments and experiments on bentonite cells for durations of up to 3 years. With regard to smectite stability, Herbert et al. (2008) found that in all samples, montmorillonite remained the dominant solid phase (as indicated using x-ray diffraction). However, transmission electron microscopy (TEM) showed textural changes and there appeared to be some partial substitution of magnesium in octahedral sheets for aluminum and presumably a reduction in layer charge. Herbert et al. (2008) suggest that the evolution in smectite mineralogy is likely to occur in a number of steps, with montmorillonite being altered to illite/smectite mixed layers, then vermiculite/smectite mixed layers (high then low charge), followed by kaolinite/smectite/vermiculite with kaolinite as a final possible alteration product. However, large-scale, bulk changes in the mineralogy of the samples were not detected in laboratory experiments; this may have been due to kinetic constraints (low temperature, laboratory timescales).

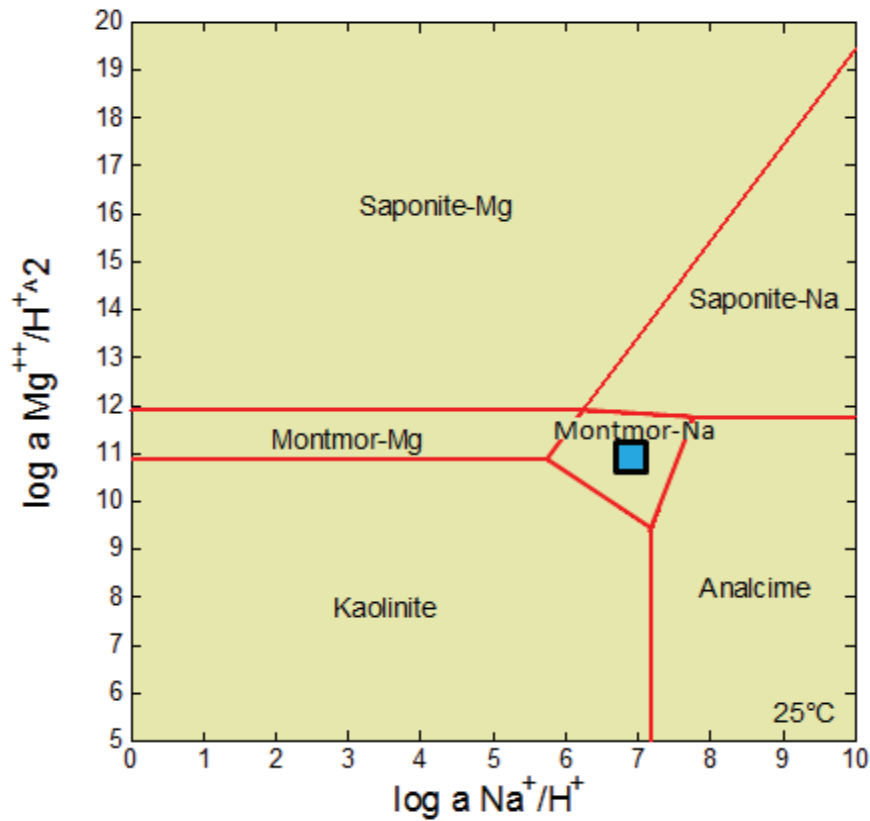
In contrast to Herbert et al. (2008), Kaufhold and Dohrmann (2009) reacted bentonite with NaCl solutions (concentration of 6M) at 60°C for five months and report that only cation exchange was observed and that x-ray diffraction suggested no major alteration of the smectite layers.

As mentioned in the review by Savage (2005), Pérez del Villar et al. (2005) and Fernández et al. (2005) investigated analogue evidence for the long-term stability of bentonite by studying the Spanish Cala de Tomate and Archidona bentonite deposits, both of which have been invaded by seawater during their geological history. Pérez del Villar et al. (2005) noted changes in exchangeable cations, BET-specific surface area and dispersibility, as a result of interaction of the Cala de Tomate deposit with saline waters, but no mineral transformation were reported. The Archidona bentonite has been invaded by seawater and meteoric water at different stages of its past history, but shows no sign of mineral alteration as a result of these processes (Fernández et al. 2005).

In order to consider the stability of montmorillonite in Mg solutions, an activity diagram was computed for the Cobourg Model 2 water composition (Figure E.3). It is clear that at dolomite equilibrium solubility, the solute activities correspond to Na-montmorillonite. If Mg activities are greater than this (and they are in some of the reported Cobourg data), it is a possibility that saponite (trioctahedral smectite) may be more stable. This would not necessarily be particularly deleterious to bentonite performance, as saponite is a smectite mineral and has the capacity to swell. However, if the mechanisms of alteration included the partial dissolution of tetrahedral sheets, or changes/disruption to the distribution of layer charges in clay crystallites, the

rheological and swelling properties of the bentonite could change. This was noted by Wilson et al. (2006) who found that montmorillonite reacted with Fe powder and NaCl solution at 250°C showed alteration of the montmorillonite to an Fe-rich smectite with reduced capacity to expand after ethylene-glycol solvation (the diagnostic test used for the identification of swelling clay by powder x-ray diffraction). This appeared to be due to the partial loss of tetrahedral Si units and an increase in H-bonding in clay crystallites (Wilson et al. 2006).

In summary, although there is some uncertainty surrounding the possibility of montmorillonite to be altered to Mg-rich clay minerals, it seems unlikely that significant degradation of hydraulic properties of the bentonite will occur due to reaction with Mg-rich waters.

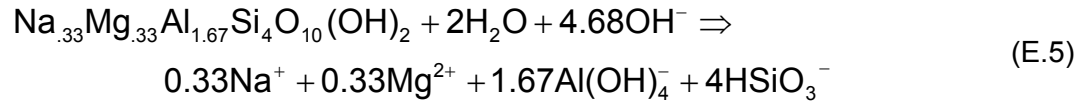


Note: Logarithmic activity diagram showing plot (solid square) of activity ratios corresponding to Cobourg porewater composition (QUINTESSA and GEOFIRMA 2011a) Coinciding with stability field of Na-Montmorillonite. Diagram constructed using Geochemist's Workbench, Bethke 2008; and the Thermodynamic Database 'thermo.com.v8.r6+'.

Figure E.3: Logarithmic Activity Diagram Showing Plot of Activity Ratios Corresponding to Cobourg Porewater Composition Coinciding with Stability Field of Na-Montmorillonite

E.4 INTERACTION OF BENTONITE-SAND WITH CEMENT RESULTING IN ALTERATION OF SMECTITE (MONTMORILLONITE) AND EMBRITTLEMENT

The dissolution of montmorillonite (typical simplified composition) in a hyperalkaline solution ($\text{pH} > 10$) can be formulated as follows (e.g., Savage et al. 2007; Gribi et al. 2008):

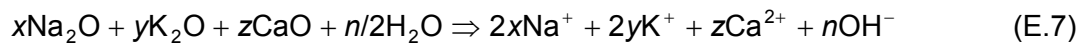


It thus takes 4.68 moles of OH^- to dissolve one mole of montmorillonite, assuming no other hydroxide-consuming or generating reactions occur (e.g., through the dissolution of accessory minerals in bentonite, or the precipitation of secondary minerals), and that no dilution of OH^- in groundwater takes place. Consequently, the mass of dissolved montmorillonite (kg) can be calculated as follows (e.g., Gribi et al. 2008):

$$\text{dissolvedmontmorillonite} = \frac{\text{mass of concrete} \times n\text{OH}^- \times M}{4.68} \quad (\text{E.6})$$

with $n\text{OH}^-$ being the amount of OH^- released per kg of concrete and M being the molar mass of montmorillonite ($M = 0.367$ kg/mol).

The degradation of a cement with x mol of Na_2O , y mol of K_2O and z mol of CaO may produce a maximum of $n = 2(x + y + z)$ mol of OH^- (e.g., Gribi et al. 2008):



The number of moles of OH^- available per kg of concrete was computed using the concrete composition given in Table E.5 and the cement compositional data from Table E.6. The values obtained were: 0.8853 mol of OH^- per kg and 2266.5 mol of OH^- per m^3 .

Table E.5: Mixing Proportions for LHHPC

Component	kg/m ³	wt%
Cement	95.6	3.94
Silica Fume	95.6	3.94
Silica Flour	190.9	7.87
Sand	881	36.34
Coarse Aggregate	1024	42.23
Superplasticizers	10.16	0.42
Water	127.27	5.25
Total Concrete Density (inc. porosity)	2560	

Note: Table 4.19 in QUINTESSA and GEOFIRMA (2011a).

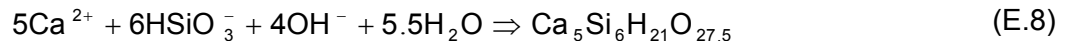
Table E.6: Cement Composition for LHHPC

Component	Concentration wt% (Cement)	Concentration Mol/kg (Concrete)
CaO	62.5	0.4391
SiO ₂	21.4	0.1403
Al ₂ O ₃	3.3	0.0128
Fe ₂ O ₃	3.8	0.0094
MgO	4.5	0.0440
Na ₂ O	0.56	0.0036
SO ₃	2.2	0.0108

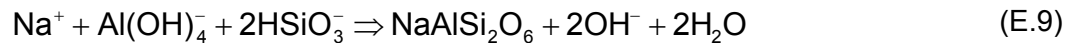
Note: Table 4.18 in QUINTESSA and GEOFIRMA (2011a).

Using the value of 0.8853 mol OH⁻ per kg and a montmorillonite molar mass of 0.367 kg/mol, this results in 0.0694 kg of montmorillonite being dissolved per kg of concrete. If the total masses of concrete and bentonite/sand mix (mass ratio of 70:30) in the shaft are taken to be 4.5 x 10⁷ kg (includes monolith and bulkheads) and 6.6 x 10⁷ kg respectively (Table 4.15 of QUINTESSA and GEOFIRMA 2011a) and the initial total mass of montmorillonite is 3.8 x 10⁷ kg (the concentration of montmorillonite in pure bentonite is 82 wt%), then the mass of montmorillonite lost is calculated to be 3.1 x 10⁶ kg (8% of the initial mass of montmorillonite).

However, as identified by Takase (2004), the mass balance issue is complicated by the nature of the potential secondary products of the cement-bentonite interaction. Growth of secondary minerals will contribute to consumption or generation of OH⁻. An example for Ordinary Portland Cement blends is precipitation of tobermorite which will enhance the pH buffering capacity of the bentonite and decrease the degree of montmorillonite dissolution by consuming hydroxyl ions:



In contrast, the precipitation of minerals such as analcime produces hydroxyl ions:



In this regard, it is likely that there will be a difference between alteration of bentonite at pH > 12 and that at lower pH. Mineralogical alteration at pH > 12 is dominated by the growth of calcium silicate hydrate solids, such as tobermorite, whereas alteration at pH < 12 is typified by zeolites (Savage et al. 2007). Secondary mineral formation at pH < 11 (i.e., at pH conditions typical of low-pH cement such as LHHPC) will therefore be zeolitic, and thus tend to extend the zone of alkaline alteration. However, the availability of silica will be limited compared with higher-pH conditions, because montmorillonite will not dissolve as readily and so the extent of the alteration zone will be restricted.

The degree of bentonite alteration is sensitive to a number of factors, such as the precise rate and mechanism of montmorillonite dissolution under conditions that are close to equilibrium, the variation of porosity and permeability with time, the composition of cement pore fluids, and the assumed crystallinity and types of secondary minerals (Savage et al. 2007).

The mass balance scoping calculations presented here do not include reaction kinetics. Montmorillonite dissolution rates measured in dilute aqueous suspensions of clay under low T, alkaline solution conditions are slow ($\sim 10^{-14}$ to 10^{-11} mol/(m² s), e.g., Bauer and Berger 1998; Sato 2004; Rozalén et al. 2008) even under far-from-equilibrium conditions. Yamaguchi et al. (2007) studied the alteration of clay in compacted bentonite-sand mixes at alkaline pH and variable temperature. Cylindrical discs consisting of 70 % bentonite and 30 % quartz sand were compacted to a density of 1600 kg/m³ and reacted with NaCl-NaOH solutions of variable pH at 50 to 170°C. Extrapolating these data to pH 10 at 25°C results in a rate of $\sim 10^{-18}$ mol/(m² s) (i.e., approximately 50 000 times less than the rate in dispersed systems), such that 10 % alteration of the clay buffer implies a duration of several million years.

In addition, the dissolution of montmorillonite reaction will be limited by slow diffusive transfer of hydroxyl ions into the bentonite. Effective diffusion coefficients for solute transport through bentonite are very low, and generally less than $\sim 10^{-10}$ m²/s. Mass transport by diffusion will therefore inhibit alkaline alteration of bentonite. A summary of reactive transport simulations undertaken over the last 10 years illustrates that alteration is generally confined to within a small zone at the cement-bentonite interface, often no more than ~ 0.1 m (Table E.7). Pore clogging at cement-bentonite interfaces due to mineral precipitation is found to limit the thickness of alteration zones (e.g., Savage et al. 2002; Marty et al. 2009).

In summary, bentonite alteration is very unlikely to be extensive through the shaft. As zones of alkaline alteration in published models have thicknesses that are confined to scales in the order of 10s of cms, a very conservative assumption may be adopted that alteration zones will not exceed 1 m in thickness.

**Table E.7: Summary of Some Cement-Clay Reaction-Transport Simulations (at 25°C)
Carried Out Over the Last Ten Years**

Solid	Initial pH	Kinetics?	Products	Alteration depth (m)	Porosity (%)	Ref
Bentonite + sand	11.3	Yes	CSH minerals, Ca-zeolite, celadonite, calcite	0.1 @ 3.2 ka	40 -> 0 @ 3.2 ka	[1]
Claystone	13.2	No	CSH minerals, sepiolite, Ca-zeolite, illite	0.6 @ 10 ka	15 -> 0 @ 2.5 ka	[2]
MX-80 (1800 kg m ⁻³)	12.5	No	Illite, zeolites, CSH minerals, saponite, chlorite	0.2 @ 100 ka	Not available	[3]
Opalinus Clay	13.5	Yes	Illite, calcite, CSH minerals, zeolites, sepiolite	0.1 @ 50 ka	11 -> 0 @ 0.1 ka	[4]
Bure clay	13.2	No	Illite, analcime, Ca-zeolites	0.15 m @ 25 ka	15 -> 2 @ 25 ka	[5]
Bentonite + sand	11	Yes	Calcite, CSH minerals, Ca-zeolites	0.01 @ 10 ka	40 -> 0 @ 10 ka	[6]
Bentonite + sand	10 - 11.5	Yes	Calcite, celadonite, Ca-zeolites, CSH minerals	0.015 @ 1 ka (pH 11)	40 -> 0 @ 1 ka (pH 11)	[7]
Claystone	12.5	Yes	Calcite, muscovite, Ca-zeolite	< 0.02 @ 0.015 ka	Porosity decrease	[8]
Bure clay	12.5	Yes	CSH minerals, calcite, Ca-zeolites, illite, saponite, hydrotalcite	0.01 @ 0.1 ka	15 -> 0 @ 0.1 ka	[9]
Generic clay	12.5	No	CSH minerals, calcite, gibbsite	0.001 @ 0.07 ka	10 -> 0 @ 0.07 ka	[10]

Notes: [1] Savage et al. (2002). [2] De Windt et al. (2004). [3] Gaucher et al. (2004). [4] Michau (2005) and Traber and Mäder (2006). [5] Trotignon et al. (2007). [6] Ueda et al. (2007). [7] Watson et al. (2007). [8] De Windt et al. (2008). [9] Marty et al. (2009). [10] Kosakowski et al. (2009),

E.5 CEMENT DEGRADATION

E.5.1 Composition and pH Buffering Associated with Low pH Cement

Degradation of the concrete can have a number of impacts on its physical properties:

- Increased porosity and permeability due to leaching of cement minerals (such as portlandite and calcium silicate hydrate (CSH) gels);
- Decreased porosity due to carbonation of cement phases and the precipitation of calcite (depending on $p\text{CO}_2$); and
- Cracking due to precipitation of secondary phases such as ettringite or gypsum.

The cement used for the concrete components of the shaft seal includes LHHPC (Tables E.5 and E.6, data from Tables 4.19 and 4.18 of the Data report, QUINTESSA and GEOFIRMA 2011a, respectively) as opposed to an OPC-based blend. This concrete comprises a cement component that is typical of OPC which is blended with highly reactive silica fume and presumably less reactive silica flour, sand and aggregate. The mass proportions of Type 50 cement and silica fume are equal. The addition of silica fume to OPC results in hydration proceeding such that the amount of portlandite ($\text{Ca}(\text{OH})_2$) produced is minimized/reduced (via reaction with silica to produce CSH). In addition, alkaline species are more strongly absorbed. The cement thereby produced reacts with water to give a relatively lower pH (generally $\text{pH} \leq 11-12$, rather than $\text{pH} \geq 12.5$ associated with free portlandite and initial dissolution of alkalis) and low heat characteristics (e.g., Cau dit Coumes, et al. 2006; Codina et al. 2008).

The principal solid phase in low-pH cement is a low Ca/Si (< 1.0) CSH gel (e.g., Savage and Benbow 2007). A maximum pH of 11 has been identified as a possible target for low-pH grouts (Bodén and Sievänen 2005), but the rationale for this is unclear (Savage and Benbow 2007). Codina et al. (2008) cite Gray and Shenton (1998) who give a pH of water equilibrated with crushed LHHPC of 10.6. Codina et al. (2008) report that after six months ageing, a cement paste with 60 wt% Portland Cement and 40 wt% silica fume (water:cement ratio of 0.5) consisted of the following phases: CSH, portlandite, C_2S , C_3S , hematite, calcite and quartz (note that clinker hydration was not complete).

Garcia Calvo et al. (2010) report a range of pore fluid pH values for low-pH cement pastes, after 90 days and 2 years equilibration, with measured pH values being lower for pastes with higher silica content. Measured pH values in these experiments ranged from 10.4-12.8 after 2 years reaction time. One of the cements was compositionally similar to the LHHPC (equal amounts of OPC and silica fume, with a water to cement mass ratio of 0.5). After 90 days, the pore fluid pH was 11.2, with a value of 11.3 after 2 years. XRD analysis showed that for this cement composition, portlandite was initially present, but had disappeared after 90 days. Low pH pastes were found to have Ca/Si ratios between 0.8 and 1.2.

In order to determine the initial CSH composition that may be present in LHHPC, a number of leaching experiments and related solid solution models may be considered. Harris et al. (2002) have published experimental data describing the leaching of CSH gels of variable Ca/Si ratio in pure water under both 'static' and 'sequential' leaching conditions. They report that to achieve a pH less than 11, the CSH gel must have a Ca/Si ratio less than 0.81. Unlike gels with a greater Ca/Si ratio, gels of $\text{Ca/Si} \leq 0.81$ do not show dramatic incongruent dissolution behaviour (Harris et al. 2002).

Not all models of CSH gel behaviour are applicable to modelling compositions where $\text{Ca/Si} < 1$. For example, some cement models using solid-solution models for CSH gel

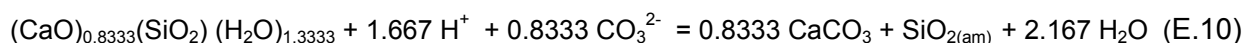
(e.g., Börjesson 1997; Walker et al. 2007) assume $\text{Ca}(\text{OH})_2$ and CaH_2SiO_4 end-members in the cement. For this choice of end-members the minimum possible Ca/Si ratio is 1 because both end members contain calcium. The Sugiyama and Fujita model (2005) also involves solid solutions, but with $\text{Ca}(\text{OH})_2$ and SiO_2 as end-members, so can potentially represent cases when $\text{Ca}/\text{Si} < 1$. Sugiyama and Fujita split the available data into two sets corresponding to data for Ca/Si ratios less than 0.833 and greater than 0.833 (0.833 is the Ca/Si ratio of tobermorite). In addition, CSH gel may be treated using ideal mixing models, such as that described by Lothenbach et al. (2008), which is based on Kulik and Kersten (2001, 2002), and in which CSH with Ca/Si values from 0.83 to 1.67, can be represented by two compositional end-members: 'jennite' $[(\text{CaO})_{1.67}(\text{SiO}_2)(\text{H}_2\text{O})_{2.1}]$ and 'tobermorite' $[(\text{CaO})_{0.83}(\text{SiO}_2)(\text{H}_2\text{O})_{1.3}]$.

Using PHREEQC (and the *lnl.dat* database, into which the Lothenbach et al. (2008) data were incorporated for ideal CSH solid solution), a CSH solid solution with $\text{Ca}/\text{Si} = 1$ gives an equilibrium pH of 11 (in pure water at 25°C, 1 bar). In contrast, a CSH solid solution composed entirely of the tobermorite end-member equilibrated with pure water produces a pH of 10.75; pure end-member jennite gives an equilibrium pH of 11.5.

Given the pH values reported by Garcia Calvo et al. (2010) and Gray and Shenton (1998), a CSH gel composition with a Ca/Si ratio of 1, may be a reasonable initial CSH composition to represent LHHPC. According to the aforementioned solid solution model, the composition is $(\text{CaO})(\text{SiO}_2)(\text{H}_2\text{O})_{1.46}$. As CSH undergoes leaching, the composition will become increasingly depleted in Ca^{2+} and some (largely hypothetical) solid solution models for low Ca/Si ratios (< 0.8) (e.g., Kulik and Kersten 2001) include compositional $\text{SiO}_{2(\text{am})}$ and tobermorite end members.

E.5.2 Cement Carbonation

For scoping calculations on LHHPC carbonation, the tobermorite compositional end-member $[(\text{CaO})_{0.83}(\text{SiO}_2)(\text{H}_2\text{O})_{1.3}]$ is used as a conservative CSH composition (low Ca/Si ratio). In addition, it has been postulated that experimental solubility data points to a minimum of dissolved Ca in the aqueous phase in equilibrium with CS-H gel of Ca/Si ~ 0.8 (Kulik and Kersten 2001). If this CSH gel composition is taken to be the primary pH buffer, it will react with dissolved carbonate to form calcite



The number of moles of Ca present in 1 m³ of LHHPC is equal to the mass of cement present (95600 g/m³, Table E.5), multiplied by the fraction of CaO (0.625, Table E.6) divided by the molecular mass of CaO (56.08 g/mol), which equals 1066 moles of CaO per m³. Given that there are 0.83 moles of Ca per mole of CSH gel, it can be assumed that there are 1279 moles of CSH $[(\text{CaO})_{0.8333}(\text{SiO}_2)(\text{H}_2\text{O})_{1.3333}]$ per m³ of concrete. However, this is for an air content of 3.2%, (i.e., per m³ of concrete, there is 0.97 m³ of solid material and 0.032 m³ of air). Therefore, there are 1279 moles of CSH per 0.97 m³ of solid material, (1321 moles per m³ when porosity = 0). Given that the reference porosity of LHHPC is 0.05, the number of moles of CSH per m³ is 1255 mol/m³. In terms of CSH/water ratio, this equates to 1255 moles of CSH per 0.05 m³ of porosity or 25.1 moles of CSH per litre of pore fluid.

The carbonate content of the water present will reflect prevailing $p\text{CO}_{2(\text{g})}$ conditions. For Cobourg 'Model 2' porewater (taken to be a typical representative background geosphere composition, Appendix C of QUINTESSA and GEOFIRMA 2011a), an ambient $\log p\text{CO}_{2(\text{g})}$ value of -2.43 was calculated. This corresponds to a total dissolved carbonate content of 6.1×10^{-4} mol/kg. Therefore, conservatively assuming that all of the dissolved carbonate present could contribute to CSH carbonation (1 mole of dissolved C resulting in 1.2 moles of CSH being

altered to calcite), each porewater replacement results in 7.32×10^{-4} moles of CSH being replaced. For all CSH to be consumed, around 21 moles of dissolved C would be required per m^3 of concrete. Given the carbonate concentration for ambient Cobourg pore water, there would need to be around 34,000 pore water replacements to completely carbonate the cement in a given volume of concrete.

The volume of a cylindrical section of concrete bulkhead with a thickness of 1 m is $3.142 \times (3.725 \text{ m})^2 \times 1 \text{ m} = 43.6 \text{ m}^3$. This would contain $1255 \text{ mol m}^{-3} \times 43.6 \text{ m}^3 \approx 5.47 \times 10^4$ moles of CSH gel. According to Equation E.10, 0.83 moles of dissolved carbonate would be required to convert 1 mole of CSH into 0.83 moles of calcite. Therefore in this case, $5.47 \times 10^4 \times 0.83 \approx 4.54 \times 10^4$ moles of carbonate would be required for complete alteration.

Among the geological formations in the Intermediate and Deep Bedrock Groundwater Zones, the Salina A1 Upper unit is reported to have the highest Darcy velocity of $1.72 \times 10^{-9} \text{ m/s}$ (0.054 m/a) (calculated using the Table 5.5 and Section 5.4.1.1 of the Data report, QUINTESSA and GEOFIRMA 2011a). Using this Darcy velocity and a flow area of $2 \times 3.725 \text{ m} \times 1 \text{ m} = 7.45 \text{ m}^2$, it would take at least $4.54 \times 10^4 \text{ mol} / (0.054 \text{ m/a} \times 7.45 \text{ m}^2 \times 0.61 \text{ mol}) \approx 185,000$ years to fully carbonate a 1 m thick section of concrete bulkhead. The other rock formations in these groundwater zones are between 1 and 5 orders of magnitude less permeable than the Salina A1, which means that cement carbonation in these zones will take significantly longer than the assessment time frame of 1 million years.

Another, perhaps more realistic approach, is to consider carbonation of CSH via diffusion of dissolved carbonate into the concrete from the geosphere. The length of time required for such a flux can be estimated. The intruding groundwater can be assumed to have a total carbonate concentration of $6.1 \times 10^{-4} \text{ mol/kg}$. For pure water equilibrated with CSH gel (tobermorite compositional end member) and calcite, a pH value of 10.7 is obtained when the $\log p\text{CO}_{2(\text{g})}$ is -8.45 and total inorganic C is $1.7 \times 10^{-5} \text{ mol/kg}$ (calculated using PHREEQC and the 'Inl.dat' database). Therefore, the concentration gradient between a typical ambient porewater and cement porewater is estimated to be $(0.61 \text{ mol/m}^3 - 0.017 \text{ mol/m}^3) / 3.725 \text{ m} \approx 0.159 \text{ mol/m}^4$. The maximum flux of total inorganic C is given by the concentration gradient (0.159 mol/m^4) multiplied by the effective diffusion coefficient ($1.25 \times 10^{-10} \text{ m}^2/\text{s}$), multiplied by surface area ($2 \times 3.725 \text{ m} \times 3.142 \times 1 \text{ m} = 23.4 \text{ m}^2$) $\approx 4.65 \times 10^{-5} \text{ mol/s}$ or $1.47 \times 10^{-2} \text{ mol/a}$.

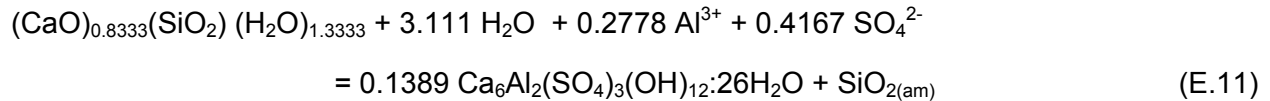
It would therefore take $4.54 \times 10^4 \text{ mol} / (1.47 \times 10^{-2} \text{ mol/a}) \approx 3.1 \times 10^6$ years for sufficient dissolved carbonate to diffuse into a 1 m thick section of concrete bulkhead to convert all of the CSH gel to calcite. This calculation assumes that the rock minerals close to the shaft are able to maintain the supply of carbonate in the rock porewater, and it does not need to diffuse inwards from porewaters further away; the actual time could be longer.

Furthermore, it seems likely that pH would fall back towards the ambient porewater pH, depending upon the nature of the evolved solid phase assemblage that develops over time. In addition, the precipitation of calcite may act to 'armour' surfaces and fill cracks thereby reducing porosities and effective diffusion coefficients. This process would reduce the ability of dissolved carbonate/bicarbonate to further react with cement surfaces (e.g., Revertigat et al. 1996).

E.5.3 Sulphate Attack

Commonly associated with cement is the issue of sulphate attack. Sulphates in solution will attack concrete by reacting with hydrated compounds in the hardened cement paste. Sulphates exist naturally in groundwater. The most common aqueous sulphate complexes are compounds of sodium, potassium, magnesium and calcium (Martino 2006).

Sulphate may react with cement to result in sulphate mineral precipitation. One reaction pathway is the production of the mineral ettringite $[\text{Ca}_6\text{Al}_2(\text{SO}_4)_3(\text{OH})_{12}\cdot 26\text{H}_2\text{O}]$, which can lead to concrete cracking. In the presumed absence of portlandite in LHHPC, the following simplified reaction may be considered, whereby low Ca/Si CSH gel (tobermorite compositional end member: $[(\text{CaO})_{0.8333}(\text{SiO}_2) (\text{H}_2\text{O})_{1.3333}]$) reacts with water, Al and SO_4^{2-} :



Therefore, to convert 1 mole of CSH gel to ettringite requires 0.417 moles of SO_4^{2-} . Part of the sulphate available for such a reaction may come from sulphate initially present in the cement blend. However, in LHHPC, only ~4 wt% of the concrete is Type 50 cement, and the sulphate content of Type 50 is only 2.2 wt%. Therefore, for the conversion of CSH gel to ettringite to occur, most of the sulphate would have to come from intruding groundwater.

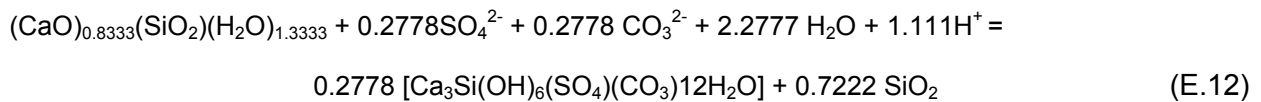
The host rock porewaters are relatively rich in SO_4^{2-} , for example, the Cobourg Model 2 porewater is saturated with respect to anhydrite (CaSO_4) (Appendix C of QUINTESSA and GEOFIRMA 2011a). It was previously shown that there are 1255 moles of CSH $[(\text{CaO})_{0.8333}(\text{SiO}_2) (\text{H}_2\text{O})_{1.3333}]$ per m^3 of LHHPC concrete. The volume of a cylindrical section of concrete bulkhead with a thickness of 1 m is $3.142 \times (3.725 \text{ m})^2 \times 1 \text{ m} \approx 43.6 \text{ m}^3$. This equates to a total of $1255 \text{ mol/m}^3 \times 43.6 \text{ m}^3 \approx 5.47 \times 10^4$ moles of CSH gel. To convert all of this to ettringite would require $5.47 \times 10^4 \times 0.4167 \approx 2.28 \times 10^4$ moles of SO_4^{2-} .

Taking the same upper Darcy velocity estimate as in Section E.5.2, $1.72 \times 10^{-9} \text{ m/s}$ (0.054 m/a), the time required for alteration of CSH to ettringite via advection is $2.28 \times 10^4 \text{ mol}/(0.054 \text{ m/a} \times 7.45 \text{ m}^2 \times 19.4 \text{ mol}) \approx 2920$ years. Alternatively the sulphate may be supplied by diffusion. The concentration gradient for SO_4 from the rock into the concrete bulkhead is difficult to estimate, given that the hydrated phase assemblage has not been ascertained for the LHHPC and it is not clear what is likely to buffer dissolved Al activities. Therefore, an illustrative range is adopted of 10 to 100 mol/m^3 per 3.725 m ≈ 2.68 to 26.85 mol/m^4 . The multiplication of these values with the effective diffusion coefficient of $1.25 \times 10^{-10} \text{ m}^2/\text{s}$ and the surface area (23.4 m^2), results in a flux range of 7.85×10^{-9} to $7.85 \times 10^{-8} \text{ mol/s}$ or 0.248 to 2.48 mol/a. Based on this range of fluxes, it would take at least 9000 to 90,000 years to completely alter CSH to ettringite. This calculation assumes that the rock minerals close to the shaft are able to maintain the supply of sulphate in the rock porewater, and it does not need to diffuse inwards from porewaters further away. In addition, a significant source of Al is required for CSH to conversion to ettringite and this will be a limiting factor.

To convert a mole of CSH gel to ettringite, 0.28 moles of Al are needed. If it is assumed that most of the more reactive Al present in the system is in the cement component of the concrete (rather than as aluminosilicate minerals in the aggregate), there are 95.6 kg $\times 0.033 \approx 3.155$ kg of Al_2O_3 present, which is equal to $3155 \text{ g}/(101.96 \text{ g/mol}) \approx 30.94$ moles. Therefore, in 1 m^3 of concrete there is only enough Al to convert around 110 moles of CSH (8.8 %). The other 1145 moles required per m^3 of concrete would have to be provided by the infiltrating water. However,

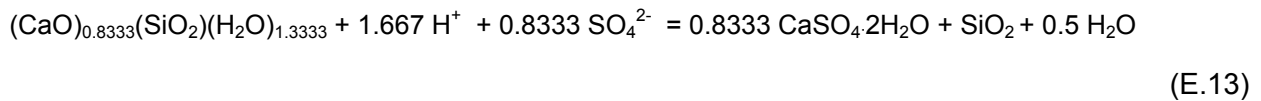
aluminosilicate minerals have a very limited solubility under circum-neutral conditions. It was calculated that for a high salinity groundwater such as Cobourg, a representative Al concentration would be given by the solubility of aluminosilicates such as illite (resulting in a calculated total dissolved Al concentration of 6.2×10^{-11} molal). The equilibrium solubility of gibbsite (Al_2O_3) in pure water at pH 7, results in a total dissolved Al concentration of 9.3×10^{-9} mol/kg. To provide 1145 moles of Al, at a concentration of 9.3×10^{-9} mol/kg, would require 1.2×10^{11} kg of solution, per m^3 of concrete. This could not happen on relevant timescales.

Another possible cement degradation pathway may be the alteration of cement to thaumasite [$\text{Ca}_3\text{Si}(\text{OH})_6(\text{SO}_4)(\text{CO}_3)12\text{H}_2\text{O}$] which tends to form at low temperatures ($< 25^\circ\text{C}$) and may result in the softening or cracking of concrete as it lacks the capacity to bind (Taylor 1990). A simplified reaction may be written, whereby CSG gel (tobermorite compositional end-member) is altered to thaumasite:



Therefore, according to Equation E.12, 0.2778 moles of sulphate (and carbonate) are required to convert one mole of CSH gel to thaumasite. Therefore, to convert all of the CSH gel present in a 1 m thick section of shaft to thaumasite, $5.47 \times 10^4 \times 0.2778 = 1.52 \times 10^4$ moles of SO_4^{2-} are required. Given the same range of illustrative sulphate diffusional fluxes discussed above, it would take in the region of 6000 to 60,000 years for complete conversion. However, Equation E.12 shows that an equimolar number of carbonate molecules are required for conversion, and the previously calculated flux for carbonation suggests that it would take approximately 1Ma to supply all of the required carbonate. Therefore, the conversion of CSH to thaumasite will be limited due to carbonate supply, which may slow the conversion to a rate similar to that of calcite formation.

In addition to the sulphate phases previously discussed, there is a possibility that gypsum may be a CSH alteration product due to sulphate attack. The formation of gypsum in OPC based cement results in potential reduction in cohesion. For the CSH taken to represent that present in LHHPC, gypsum formation may occur as follows:



As shown in Equation E.13, 0.8333 moles of sulphate are required to alter one mole of CSH gel to gypsum. The volume of a cylindrical section of concrete bulkhead with a thickness of 1 m is $3.142 \times (3.725 \text{ m})^2 \times 1 \text{ m} \approx 43.6 \text{ m}^3$. The number of moles of CSH per m^3 is 1255 moles of CSH gel per m^3 . This equates to a total of $1255 \text{ mol/m}^3 \times 43.6 \text{ m}^3 \approx 5.47 \times 10^4$ moles of CSH gel. Therefore 4.56×10^4 moles of sulphate are required for complete conversion of CSH gel to gypsum, or double the number of moles required to alter all of the CSH gel to ettringite. As with the illustrative calculations on alteration of CSH gel to ettringite, complete alteration would probably occur over the timescales of thousands to tens of thousands of years, but unlike ettringite formation, would not require a source of Al.

It should be noted that monosulphate ($3\text{CaO} \cdot \text{CaSO}_4 \cdot 12\text{H}_2\text{O}$) may gradually replace ettringite as the ratio of available alumina to sulphate increases with continued cement hydration. Most of the available sulphate within cement can dissolve immediately following addition of water, but

much of the C_3A (tricalcium aluminate) is inaccessible to the water. However, with progressive hydration, alumina is gradually released from the cement and the proportion of ettringite decreases leading to an increase in monosulphate.

E.5.4 Chloride Attack

Although there appears to be little published data on the reaction of low pH cement compositions such as LHHPC with saline solutions, one could possibly envisage the conversion of CSH to solids such as Friedel's Salt: $Ca_4Al_2(Cl)_{1.95}(OH)_{12.5} \cdot 4H_2O$ or Kuzel's Salt: $Ca_4Al_2(Cl)(SO_4)_{0.5}(OH)_{12} \cdot 6H_2O$ (e.g., Balonis et al. 2010). Friedel's salt is associated with OPC and high salinity solutions. However, the widespread conversion of CSH gel/phases to phases such as Friedel's Salt would require significant Al availability, which as previously discussed, is rather unlikely.

E.5.5 Effect of Cement Degradation on Host Rock

The cement pore water (pH ~11) will react with the host geosphere minerals. Rocks/sediments present at various horizons through which the shaft will pass include calcite, dolomites, evaporates and silicates. The elevated pH may act to destabilize calcite:



It is also possible that de-dolomitization in the vicinity of bulkheads may occur resulting the precipitation of brucite [$Mg(OH)_2$]:



This could theoretically result in shrinkage, given that the molal volumes of dolomite and calcite and brucite are: 64.365, 36.934 and 24.630 cm^3/mol .

The elevated pore water pH that results from CSH gel/mineral dissolution may also destabilize aluminosilicate minerals in the host rock and result in their dissolution. However, this would result in consumption of H^+ and a subsequent fall in porewater pH at the concrete/rock interface. Under mildly alkaline conditions (pH 8-10), aluminosilicates such as zeolites and analcime have been observed in natural systems such as alkaline lakes (Savage et al. 2007). As is the case for cement carbonation, the growth of secondary phases at the concrete/geosphere interface may result in fracture filling and the reduction of porosity, thereby limiting the capacity for further host rock alteration.

Overall, the impact of cement degradation on host rocks is expected to be limited and localized.

E.6 ASPHALT DEGRADATION

There is limited published information on degradation rates for bitumen used to encapsulate LLW/ILW. Furthermore, the composition of bitumen used in the small number of reported degradation experiments is unlikely to be the same as that employed for the seals of the DGR shaft since asphalts have widely varying compositions. However, some published experiments investigated durable bitumens and gave results that can be used to scope plausible rates of asphalt degradation in the DGR shaft.

Barletta et al. (1986) report bitumen degradation rates in soil of 5.5 $\mu m/a$, where the bitumen was intended for use with low and intermediate level waste. It is not clear if these rates were obtained under anaerobic conditions.

Roffey and Nordqvist (1991) report experimentally-determined aerobic and anaerobic degradation rates for bitumen. They found aerobic and anaerobic degradation to produce 7.2-18 millimoles $\text{CO}_2/(\text{g a})$ and 13.2-18 millimoles $\text{CO}_2/(\text{g a})$, respectively. Their samples had high surface areas of about $1 \text{ m}^2/\text{g}$, and therefore their rates are equivalent to approximately 13-18 millimoles $\text{CO}_2/(\text{m}^2 \text{ a})$. If only CO_2 is produced and the bitumen is about 80 wt% carbon, then this is roughly equivalent to a bitumen degradation rate of 0.2-0.3 $\text{g}/(\text{m}^2 \text{ a})$. Assuming a bitumen density of about $1000 \text{ kg}/\text{m}^3$, then an area of 1 m^2 of bitumen would recede at about 0.2-0.3 $\mu\text{m}/\text{a}$.

Wolf and Bachofen (1991) carried out experiments to investigate bacterial degradation of Swiss bitumen used to immobilize LLW/ILW. They reported that under aerobic conditions the bitumen degradation rate was 20 to 50 $\text{g}/(\text{m}^2 \text{ a})$. Under anaerobic conditions, the degradation rate was reported to be two orders of magnitude slower, namely 0.2-0.6 $\text{g}/(\text{m}^2 \text{ a})$. These latter values correspond to a rate of bitumen surface regression of approximately 0.2-0.6 $\mu\text{m}/\text{a}$.

Molecke (1979) reports gas generation rates from asphalt at 25°C of 0.02 millimoles $\text{CO}_2/(\text{g a})$ under saturated water or brine under aerobic conditions, and 0-0.004 millimoles $\text{CO}_2/(\text{g a})$ under anaerobic conditions. The surface area is not stated, but assuming that the 1 g samples were essentially 1 cm^3 solid cubes, the degradation rates would correspond to about 30 millimoles $\text{CO}_2/(\text{m}^2 \text{ a})$ aerobic, and less than 7 millimoles $\text{CO}_2/(\text{m}^2 \text{ a})$ or 0.1 $\mu\text{m}/\text{a}$ anaerobic.

For comparison, gas evolution from IX resins among the wastes is modelled in this assessment as a styrene degradation process (Section 4.2.1.1 of QUINTESSA and GEOFIRMA 2011b). The best estimate anaerobic degradation rate for ion-exchange resins is $5 \times 10^{-5}/\text{a}$ (Table 3.21 of QUINTESSA and GEOFIRMA 2011a). Since the molecular mass of styrene is 104.14, then 1 g styrene produces $3/104.14 \approx 0.029$ moles $\text{CO}_2 = 29$ millimoles of CO_2 . Taking the resin degradation rate then gives a CO_2 evolution rate of $29 \times 5 \times 10^{-5} = 0.00145$ millimoles of $\text{CO}_2/(\text{g a})$.

Over 1 Ma, these anaerobic degradation rates imply that a bitumen surface would recede by 0.1-0.6 m.

It is currently planned that there would be around 60 m of asphalt seal employed in the shaft (Table 4.14 of QUINTESSA and GEOFIRMA 2011a), and this seal would have a lateral surface area of about $3.14 \times 7.45 \times 60 \approx 1400 \text{ m}^2$, approximately 20% of which is bitumen. Assuming that microbial degradation would not be limited by nutrient supply or removal of microbial metabolites, the gas generation rate would be equivalent to about 15 millimoles $\text{CO}_2/(\text{m}^2 \text{ a}) \times 1400 \text{ m}^2 \times 0.2 = 4.2$ moles CO_2/a .

The rates of asphalt degradation used in these calculations are likely to be much greater than the actual rates that will occur within the shafts because:

- The bitumen degradation data were obtained from short-term (days to months) laboratory experiments; and
- In the shaft the very low permeability of the wall rocks and the seals mean that the supply of nutrients to micro-organisms involved in breaking down bitumen is likely to be limited.

The first of these points reflects the fact that lighter organic components of bitumens are known to undergo microbial degradation more rapidly than the heavier components (e.g., Aitken et al. 2004; Holba et al. 2004). Consequently, gas generation at early times in an experiment is expected to be much more rapid than at later times. For this reason alone, the

rates reported are likely to be much higher than the long-term average rate; there are also other aspects of the experiments, such as them not being nutrient-limited, which would tend to result in very high rates compared with those expected for long-term in-situ degradation within a shaft. Furthermore, asphalt tends to deform plastically and undegraded bitumen could deform to fill voids left by chemically degraded bitumen. Consequently, it is to be expected that loss of mass by chemical degradation would not necessarily be accompanied by a proportionally large increase in permeability. It has also been suggested that addition of lime to the mix could make microbial degradation of bitumen even less likely (Hansen and Knowles 2000).

It is also noteworthy that only experimental data for microbially mediated CO₂ generation from bitumen have been reported. It is likely that CH₄ would also be generated under in-situ conditions.

E.7 SUMMARY

- The montmorillonite is expected to be stable over relevant time scales. Significant alteration of smectite (montmorillonite) to illite will not occur. There is potential for porewater potassium to replace Na on the montmorillonite interlayers, which could reduce swelling pressure.
- Bentonite-sand may interact with cement resulting in alteration of smectite (montmorillonite) and embrittlement at interfaces. Conservative scoping calculations suggest that if all of the cement present in the shaft could react with bentonite, ~9% of the bentonite would be lost. However, consideration of reaction kinetics and the likelihood of pore blocking at the cement-bentonite interface, suggest that alteration will occur in spatially limited zones (conservatively taken to be up to 1 m in thickness).
- There is potential for the CSH phases present in LHHPC to undergo leaching. However, carbonation will also occur due to reaction with dissolved carbonate in host rock porewater. The rate of carbonation will be low in a diffusion-dominated system and scoping calculations suggest that it would take in the order of 10⁶ years for complete carbonation to occur, without accounting for porosity reduction due to calcite precipitation. The precipitation of calcite on surfaces (“armouring”), in pores and in cracks will result in a reduction in porosity and effective diffusion coefficient, thereby limiting the potential for further alteration.
- There is the potential for sulphate attack on the LHHPC, leading to the formation of products such as ettringite that can cause swelling and cracking. However, scoping calculations indicate that -the conversion into ettringite will be substantially limited by the low availability of Al, and that the conversion to thaumasite by the availability of carbonate. Effects are likely to be confined to the interfaces with the geosphere, given the capacity for calcite growth to result in pore blocking and the armouring of surfaces, and due to the time needed for diffusion of sufficient sulphate into the concrete from the geosphere.
- Cement dissolution and localized pH elevation may act to destabilize minerals (calcite, dolomite, aluminosilicates) in the host geosphere. However, the growth of secondary phases at the concrete/geosphere interface will result in the reduction of porosity/fracture filling, thereby limiting the capacity for further host rock alteration.
- Conservative assumptions about asphalt degradation based on short-term laboratory experiments imply that about 10% of the asphalt could degrade over a time period of a

million years. However, in reality the degradation rate is likely to be very much slower than that implied by experimental results.

REFERENCES FOR APPENDIX E

- Aitken, C.M., D.M. Jones and S.R. Larter. 2004. Anaerobic hydrocarbon biodegradation in deep subsurface oil reservoirs. *Nature* 431, 291-294.
- Balonis, M., B. Lothenbach, G. Le Saout and F.P. Glasser. 2010. Impact of chloride on the mineralogy of hydrated Portland cement systems. *Cement and Concrete Research* 40, 1009-1022.
- Barletta, R.E., B.S. Bowerman, R. Davis and C. Shea. 1986. Biodegradation testing of bitumen. *Scientific Basis for Nuclear Waste Management X, MRS Proceedings, Vol 84*. Warrendale, USA.
- Bauer, A. and G. Berger 1998. Kaolinite and smectite dissolution rate in high molar KOH solutions at 35 and 80°C. *Applied Geochemistry* 13, 905–916.
- Bethke, C.M. 2008. *Geochemical and Biogeochemical Reaction Modeling*. Cambridge University Press, Cambridge, United Kingdom.
- Bodén, A. and U. Sievänen. 2005. *Low-pH Injection Grout for Deep Repositories. Summary Report from a Co-operation Project between NUMO (Japan), Posiva (Finland) and SKB (Sweden)*. Swedish Nuclear Fuel and Waste Management Company (SKB) Report R-05-40. Stockholm, Sweden.
- Börjesson, S. 1997. *Computer Modelling of the Interaction between Water and Complex Solid Phases*. Ph.D. Thesis, Chalmers University of Technology. Göteborg, Sweden.
- Bradbury, M.H. and B. Baeyens. 2002. *Porewater Chemistry in Compacted Re-saturated MX-bentonite. Physicochemical Characterisation and Geochemical Modelling*, Paul Scherrer Institute PSI Report 02-10. Villigen, Switzerland.
- Cau Dit Coumes, C., S. Coutois, D. Nectoux, S. Leclercq and X. Bourbon. 2006. Formulating a low-alkalinity, high resistance, and low heat concrete for radioactive waste repositories. *Cement and Concrete Research* 36, 2152-2163.
- Codina, M., C. Cau Dit Coumes, P. Le Bescop, J. Verdier and J.P. Ollivier. 2008. Design and characterisation of low-heat and low-alkalinity cements. *Cement and Concrete Research* 38, 437-448.
- De Windt, L., D. Pellegrini and J. van der Lee. 2004. Coupled modeling of cement/claystone interactions and radionuclide migration. *Journal of Contaminant Hydrology* 68, 165-182.
- De Windt, L., F. Marsal, E. Tinseau and D. Pellegrini. 2008. Reactive transport modeling of geochemical interactions at a concrete/argillite interface, Tournemire site (France). *Physics and Chemistry of the Earth* 33: S295-S305.
- Fernandez, A.M., D. Arcos, M. Pelayo, M. Tsige, J.M. Fernandez-Soler, P. Rivas and L. Pérez del Villar. 2005. Natural analogues in performance assessment of a nuclear waste disposal: the Cortijo de Archidona deposit and the salinity effect. In *Clays in Natural and Engineered Barriers for Radioactive Waste Confinement*, Tours, France, p.391-392.

- Garcia Calvo, J.L., A. Hidalgo, C. Alonso and L. Fernandez Luco. 2010. Development of low-pH cementitious materials for HLRW repositories: Resistance against ground waters aggression. *Cement and Concrete Research* 40, 1290-1297.
- Gaucher, E.C., P. Blanc, J.-M. Matray and N. Michau. 2004. Modeling diffusion of an alkaline plume on a clay barrier. *Applied Geochemistry* 19, 1505-1515.
- Gray, M.N. and B.S. Shenton. 1998. For better concrete, take out some of the cement. Proceedings of the 6th ACI/CANMET Symposium on the Durability of Concrete, May 31-June 5, 1998. Bangkok, Thailand.
- Gribi, P., L. Johnson, D. Suter, P. Smith, B. Pastina and M. Snellman. 2008. Safety Assessment for a KBS-3H Spent Nuclear Fuel Repository at Olkiluoto: Process report. Swedish Nuclear Fuel and Waste Management Company (SKB) Report R-08-36. Stockholm, Sweden.
- Hansen, F.D. and M.K. Knowles. 2000. Design and analysis of a shaft seal system for the Waste Isolation Pilot Plant. *Reliability Engineering and System Safety* 69, 87-98
- Harris, A.W., M.C. Manning, W.M. Tearle and C.J. Tweed. 2002. Testing of models of the dissolution of cements - leaching of synthetic gels. *Cement and Concrete Research* 32(5), 731-746.
- Herbert H.J., J. Kasbohm, H.C. Moog and K.H. Henning. 2004. Long-term behaviour of the Wyoming bentonite MX-80 in high saline solutions. *Applied Clay Science* 26, 275-291.
- Herbert, H.J., J. Kasbohm, H. Sprenger, A.M. Fernández and C. Reichelt. 2008. Swelling pressures of MX-80 bentonite in solutions of different ionic strength. *Physics and Chemistry of the Earth* 33, S327-S342.
- Holba, A.G., L. Wright, R. Levinson, B. Huizinga and M. Scheihing. 2004. Effects and impact of early-stage anaerobic biodegradation on Kuparuk River Field, Alaska. In: Cubitt, J. M., England, W. A. and Larter, S. (Eds.) *Understanding Petroleum Reservoirs: towards an Integrated Reservoir Engineering and Geochemical Approach*. Geological Society, London, Special Publications 237, 53-88.
- Huang, W.L., J.M. Longo and D.R. Pevear. 1993. An experimentally derived kinetic model for smectite-to-illite conversion and its use as a geothermometer. *Clays and Clay Minerals* 41, 162-177.
- Karnland, O. and M. Birgersson. 2006. Montmorillonite Stability with Respect to KBS-3 Conditions. Swedish Nuclear Fuel and Waste Management Company (SKB) Technical Report TR-06-11. Stockholm, Sweden.
- Karnland, O., S. Olsson and U. Nilsson. 2006. Mineralogy and Sealing Properties of Various Bentonites and Smectite-rich Clay Materials. Swedish Nuclear Fuel and Waste Management Company (SKB) Technical Report TR-06-30. Stockholm, Sweden.
- Kaufhold, S. and R. Dohrmann. 2009. Stability of bentonites in salt solutions: sodium chloride. *Applied Clay Science* 45, 171-177.

- Kosakowski, G., P. Blum, D. Kulik, W. Pflingsten, H. Shao and A. Singh. 2009. Evolution of a generic clay/cement interface: first reactive transport calculations utilizing a Gibbs energy minimization based approach for geochemical calculations. *Journal of Environmental Science for Sustainable Society* 3, 41-49.
- Kulik, D.A. and M. Kersten. 2001. Aqueous solubility diagrams for cementitious waste stabilization systems: II, End-member stoichiometries of ideal calcium silicate hydrate solid solutions. *Journal of the American Ceramic Society* 84(12), 3017–3026.
- Kulik, D.A. and M. Kersten. 2002. Aqueous solubility diagrams for cementitious waste stabilization systems: 4. A carbonation model for Zn-doped calcium silicate hydrate by Gibbs energy minimization. *Environmental Science and Technology* 36, 2926–2931.
- Lothenbach, B., T. Matschei, G. Moschner and F.P. Glasser. 2008. Thermodynamic modelling of the effect of temperature on the hydration and porosity of Portland cement. *Cement and Concrete Research* 38(1), 1-18.
- Martino, J.B. 2006. Issues affecting the Durability of Concrete in a Deep Geologic Repository. Atomic Energy of Canada Ltd. Report 06819-REP-01200-10143-R00. Chalk River, Canada.
- Marty, N.C.M., C. Tournassat, A. Burnol, Giffaut and E. Gaucher. 2009. Influence of reaction kinetics and mesh refinement on the numerical modelling of concrete/clay interactions. *Journal of Hydrology* 364, 58-72.
- Michau, N. 2005. ECOCLAY II: Effects of Cement on Clay barrier Performance. ANDRA Report C.RP.ASCM.04.0009, ANDRA, Paris, France.
- Molecke, M. 1979. Gas Generation from Transuranic Waste Degradation: Data Summary and Interpretation. Sandia Laboratories Report SAND79-1245. Albuquerque, USA.
- Pérez del Villar, L., M. Pelayo, A.M. Fernandez, J.S. Cozar, A. Delgado, E. Reyes, J.M. Fernandez-Soler and M. Tsige. 2005. Na-smectites in the Cala de Tomate bentonite deposit (Spain): a natural analogue of the salinity effect on the bentonite barrier of a radwaste disposal. In *Clays in Natural and Engineered Barriers for Radioactive Waste Confinement*, Tours, France, 387-388.
- QUINTESSA and GEOFIRMA. 2011a. Postclosure Safety Assessment: Data. Quintessa Ltd. and Geofirma Engineering Ltd. report for the Nuclear Waste Management Organization NWMO DGR-TR-2011-32 R000. Toronto, Canada.
- QUINTESSA and GEOFIRMA. 2011b. T2GGM Version 2: Gas Generation and Transport Code. Quintessa Ltd. and Geofirma Engineering Ltd. report for the Nuclear Waste Management Organization NWMO DGR-TR-2011-33 R000. Toronto, Canada.
- Roffey, R. and A. Nordqvist. 1991. Biodegradation of bitumen used for nuclear waste disposal. *Cellular and Molecular Lifesciences* 47, 539-542.
- Rozalén, M.L., F.J. Huertas, P.V. Brady, J. Cama, S. García-Palma and J. Linares. 2008. Experimental study of the effect of pH on the kinetics of montmorillonite dissolution at 25°C. *Geochimica et Cosmochimica Acta* 72, 4224-4253.

- Sato, T., M. Kuroda, S. Yokoyama, M. Tsutsui, K. Fukushi, T. Tanaka and S. Nakayama. 2004. Dissolution mechanism and kinetics of smectite under alkaline conditions. In: R. Metcalfe and C. Walker (Eds.), International Workshop on Bentonite-Cement Interaction in Repository Environments. NUMO/Posiva, Tokyo, Japan.
- Savage, D. and S. Benbow. 2007. Low pH Cements. Swedish Nuclear Power Inspectorate (SKI) Report 2007:32. Stockholm, Sweden.
- Savage, D., D. Noy and M. Mihara. 2002. Modelling the interaction of bentonite with hyperalkaline fluids. *Applied Geochemistry* 17, 207-223.
- Savage, D. 2005. The Effects of High Salinity Groundwater on the Performance of Clay Barriers. Swedish Nuclear Power Inspectorate (SKI) Report 2005-54. Stockholm, Sweden.
- Savage, D., C. Walker, R. Arthur, C. Rochelle, C. Oda and H. Takasa. 2007. Alteration of bentonite by hyperalkaline fluids: A review of the role of secondary minerals. *Physics and Chemistry of the Earth* 32, 287-297.
- Savage, D., R. Arthur, C. Watson and J. Wilson. 2010. An Evaluation of Models of Bentonite Pore Water Evolution. Swedish Radiation Safety Authority Technical Report 2010-12. Stockholm, Sweden.
- Sugiyama, D. and T. Fujita. 2005. A thermodynamic model of dissolution and precipitation of calcium silicate hydrates. *Cement and Concrete Research* 36: 227-237.
- Suzuki, S., M. Sazarashi, T. Akimoto, M. Haginuma and K. Suzuki. 2008. A study of the mineralogical alteration of bentonite in saline water. *Applied Clay Science* 41, 190-198.
- Takase, H. 2004. Discussion on PA model development for bentonite barriers affected by chemical interaction with concrete: do we have enough evidence to support bentonite stability? In: R. Metcalfe and C. Walker (Eds.), International Workshop on Bentonite-Cement Interaction in Repository Environments. NUMO/Posiva, Tokyo, Japan, p.172-177.
- Taylor, H.F.W. 1990. *Cement Chemistry*. Academic Press, London.
- Traber, D. and U. Mäder. 2006. Reactive Transport Modelling of the Diffusive Interaction between Opalinus Clay and Concrete. Nagra Internal Report NIB 05-06. Wettingen, Switzerland.
- Trotignon, L., V. Devallois, H. Peycelon, C. Tiffreau and X. Bourbon. 2007. Predicting the long-term durability of concrete engineered barriers in a geological repository for radioactive waste. *Physics and Chemistry of the Earth* 32, 259-274.
- Ueda, H., H. Hyodo, H. Takase, D. Savage, S. Benbow, and M. Noda. 2007. Evaluation of the kinetics of cement-bentonite interaction in a HLW repository using the reactive solute transport simulator, 15th International Conference on Nuclear Engineering. JSME, Nagoya, Japan, p.ICONE15-10566.
- Walker, C.S., D. Savage, T. Tyrer and V. Ragnarsdottir. 2007. Non-ideal solid solution aqueous solution modeling of synthetic calcium silicate hydrate. *Cement and Concrete Research* 37, 502-511.

Watson, C., S. Benbow and D. Savage. 2007. Modelling the Interaction of Low pH Cements and Bentonite. Issues affecting the Geochemical Evolution of Repositories for Radioactive Waste. Swedish Nuclear Power Inspectorate Report 2007:30. Stockholm, Sweden.

Wilson, J., G. Cressey, B. Cressey, J. Cuadros, K.V. Ragnarsdottir, D. Savage and M. Shibata. 2006. The effect of iron on montmorillonite stability. (II) Experimental investigation. *Geochimica et Cosmochimica Acta* 70, 323–336.

Wolf, M. and R. Bachofen. 1991. Microbial degradation of bitumen. *Cellular and Molecular Life Sciences* 47, 542-548.

Yamaguchi, T., Y. Sakamoto, M. Akai, M. Takazawa, Y. Iida, T. Tanaka and S. Nakayama. 2007. Experimental and modeling study on long-term alteration of compacted bentonite with alkaline groundwater. *Physics and Chemistry of the Earth* 32, 298-310.

APPENDIX F: AUDIT OF COMPONENT INTERACTIONS IN THE DGR AND ITS SHAFTS

An audit has been undertaken to ensure that all key component interactions that might influence the evolution of the repository and its shafts have been identified in this report. This was undertaken in two stages. First, all the major components of the repository and its shafts were identified. Second, the Interaction Matrix (IM) approach was used to consider the potential interactions between the identified components. Consideration was given first to the repository and then to the shafts.

F.1 REPOSITORY INTERACTIONS

The following key components of the repository were identified.

- The T-H-E array, into which ILW wastes in T-H-E containers will be placed¹¹. The T-H-E array is identified explicitly because the evolution of ILW wastes placed into the array is considered to be different from that of the other ILW wastes, which are placed directly into the rooms. The T-H-E array comprises the array itself, plus the associated wastes and their containers.
- The ILW and LLW wastes, their associated containers and overpacks.
- The DGR engineering. This comprises all operational engineering that will remain post-closure and that may influence the evolution of the DGR, e.g., concrete floors, rockbolts, room end walls.
- The tunnels, including the access tunnels and the emplacement rooms.
- The concrete monolith. This forms the base of the shaft seals. It will interact with materials in the DGR, in addition to the host rock and overlying bentonite-sand seals (see Appendix F.2).
- Water and gas in the DGR. Water and gas will enable interaction between components not in physical contact. They will influence conditions in the DGR, e.g., resaturation, and are the two media that can transport contaminants.

The Interaction Matrix for the repository is presented in Figure F.1. Where component interactions are possible, they are numbered R#. The potential interaction(s) are summarized in Table F.1, and the relevant sections of this report referenced. Where interaction between components is not possible, this is indicated in Figure F.1 by “-“. For example, there is no direct interaction between the concrete monolith and ILW wastes because they are not in direct contact with each other. Interaction is only possible indirectly via water and gas, which are considered as separate components.

¹¹ Only considered in the original preliminary design.

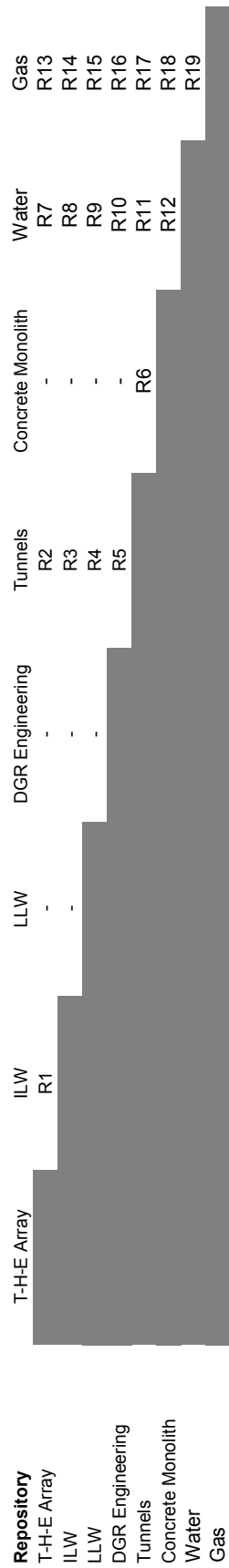


Figure F.1: Interaction Matrix for Repository Components

Table F.1: Summary of Repository Component Interactions

No.	Components	Interaction(s)	Section (this report)
R1	ILW – T-H-E array	ILW wastes in T-H-E containers are placed in the T-H-E array. This controls the elevation of the waste and hence the time at which waste-water contact can first occur.	2.1; 2.2.2
R2	Tunnels – T-H-E array	The T-H-E array supports the tunnel and prevents roof collapse.	N/A. See QUINTESSA (2011)
R3	Tunnels - ILW	Roof collapse damages the containers and overpacks. Roof collapse and container damage is assumed to occur immediately post-closure in the safety assessment models.	4.4
R4	Tunnels - LLW	Roof collapse damages the containers and overpacks. Roof collapse and container damage is assumed to occur immediately post-closure in the safety assessment models.	4.4
R5	Tunnels – DGR Engineering	DGR engineering supports the tunnels during the operational phase, but does not provide any long-term support post-closure.	4.4
R6	Concrete Monolith - Tunnels	The monolith seals the DGR tunnel system. Where the monolith supports the tunnels it prevents roof collapse.	N/A. See QUINTESSA and GEOFIRMA (2011)
R7	Water – T-H-E array	Contaminants in wastes in the T-H-E array will dissolve in water. The array is assumed not to be structurally degraded by reaction with water and therefore does not collapse.	N/A. See QUINTESSA (2011)
R8	Water - ILW	Contaminants in the wastes will dissolve in the water.	N/A. See QUINTESSA (2011)
R9	Water - LLW	Contaminants in the wastes will dissolve in the water.	N/A. See QUINTESSA (2011)
R10	Water – DGR engineering	Metal components of the DGR engineering will corrode anaerobically through reaction with water, generating gas. Concrete will condition the chemistry of the water in the DGR.	4.5.1

No.	Components	Interaction(s)	Section (this report)
R11	Water - tunnels	Water will flow from the host rock into the tunnels and eventually the DGR will resaturate.	4.3
R12	Water – concrete monolith	Water will react with the concrete and cause it to degrade.	As shaft concrete – EDZ, see Table F-2
R13	Gas – T-H-E array	CO ₂ will carbonate the cement minerals in the array.	4.5.3
R14	Gas – ILW	Gas is generated from ILW wastes. CO ₂ enhanced corrosion of metal wastes and containers will result in the precipitation of siderite.	4.5.1; 4.5.2
R15	Gas - LLW	Gas is generated from LLW wastes. CO ₂ enhanced corrosion of metal wastes and containers will result in the precipitation of siderite.	4.5.1; 4.5.2
R16	Gas – DGR engineering	CO ₂ will carbonate the cement minerals in concrete and cause CO ₂ enhanced corrosion of metals.	4.5.2; 4.5.3
R17	Gas - tunnels	The gas pressure in the tunnels will affect the potential for roof and pillar collapse, and could induce hydrofracturing of the tunnel walls if it rises to approx. >80% of lithostatic.	4.4 and see Section 6.4 of NWMO (2011)
R18	Gas – concrete monolith	CO ₂ will carbonate the cement minerals in the monolith.	4.5.3
R19	Gas- Water	The gas pressure will affect inflow of water into the DGR. CH ₄ will dissolve in water. CO ₂ will react with water – controlled by carbonate equilibria.	4.3

F.2 SHAFT INTERACTIONS

The following key components of the shaft were identified:

- The concrete monolith containing LHHPC at the base of each shaft;
- The concrete bulkheads containing LHHPC placed in each shaft in the Intermediate Bedrock Groundwater System;
- The bentonite/sand mix used for the majority of seals;
- Asphalt mastic mix used in one section of the Deep Bedrock Groundwater System;
- The concrete liner that is not removed from the sides of the shafts in the Shallow Bedrock Groundwater System;
- The compacted engineered fill (sand) used in the Shallow Bedrock Groundwater System;
- The concrete cap at the top of each shaft;

- The EDZ that is formed between the shafts and the surrounding geosphere; and
- The geosphere that surrounds the shafts.

Interaction matrices are presented in Figure F.2. As in Figure F.1, “-” in Figure F.2 indicates that interaction between components is not possible due to their physical separation. The potential interactions are described in Table F.2. The focus in Table F.2 is on processes that result in degradation of performance of shaft components rather than processes that might improve performance (e.g., precipitation of minerals in the EDZ due to interactions with other components such as the geosphere that would reduce the permeability of the EDZ).

Shallow Geosphere	Concrete Cap	Concrete (sides)	EDZ	Geosphere	Engineered Fill
Concrete Cap		S1	S2	-	S3
Concrete (sides)			S4	-	S5
EDZ				S6	-
Geosphere					-
Engineered Fill					

Intermediate Geosphere	Bentonite-Sand	Concrete Bulkheads	EDZ	Geosphere
Bentonite-Sand		I1	I2	-
Concrete			I3	-
EDZ				I4
Geosphere				

Deep Geosphere	Bentonite-Sand	Asphalt	Concrete Monolith	EDZ	Geosphere
Bentonite-Sand		D1	D2	D3	-
Asphalt			-	D4	-
Concrete Monolith				D5	D6
EDZ					D7
Geosphere					

Figure F.2: Interaction Matrices for Shaft Components

Table F.2: Summary of Shaft Component Interactions

No	Components	Interaction(s) Promoting Component Degradation	Section (this report)
S1	Concrete (cap) - Concrete (liner)	none expected	-
S2	Concrete (cap) – Damaged Zone	cement degradation	4.5.3; Appendix E.5
S3	Concrete (cap) - Eng. Fill	cement degradation	4.5.3; Appendix E.5
S4	Concrete (liner) - Damaged Zone	cement degradation	4.5.3; Appendix E.5
S5	Concrete (liner) - Eng. Fill	none expected	-
S6	Damaged Zone - Geosphere	none expected	-
I1	Bentonite - Concrete	bentonite alteration due to reaction with cement pore fluid	4.5.4; Appendix E.4
I2	Bentonite - EDZ	interlayer K exchange in smectite, possible reduction in swelling pressure or illitization	4.5.4; Appendix E.2 and E.3
I3	Concrete - EDZ	cement degradation	4.5.3, Appendix E.5
I4	EDZ - Geosphere	none expected	-
D1	Bentonite - Asphalt	none expected	-
D2	Bentonite - Concrete	bentonite alteration due to reaction with cement pore fluid	4.5.4; Appendix E.4
D3	Bentonite - EDZ	interlayer K exchange in smectite, possible reduction in swelling pressure or illitization	4.5.4; Appendix E.2 and E.3
D4	Asphalt - EDZ	asphalt degradation	4.5.5; Appendix E.6
D5	Concrete monolith - EDZ	cement degradation	4.5.3
D6	Concrete monolith - Geosphere	cement degradation minor host rock alteration	4.5.3 Appendix E.5.5
D7	EDZ - Geosphere	none expected	-

REFERENCES FOR APPENDIX F

NWMO. 2011. Geosynthesis. Nuclear Waste Management Organization Report NWMO DGR-TR-2011-11 R000. Toronto, Canada

QUINTESSA. 2011. Postclosure Safety Assessment: Analysis of the Normal Evolution Scenario. Quintessa Ltd. report for the Nuclear Waste Management Organization NWMO DGR-TR-2011-26 R000. Toronto, Canada.

QUINTESSA and GEOFIRMA. 2011. Postclosure Safety Assessment: Data. Quintessa Ltd. and Geofirma Engineering Ltd. report for the Nuclear Waste Management Organization NWMO DGR-TR-2011-32 R000. Toronto, Canada.

THIS PAGE HAS BEEN LEFT BLANK INTENTIONALLY

APPENDIX G: HOST ROCK DISSOLUTION BY CARBON DIOXIDE

The potential influence of the CO₂ on host rock dissolution by porewater was estimated by simple scoping calculations. The geochemical modelling software PHREEQC v 2.15 (Parkhurst and Appelo 1999) was used together with the “Pitzer” thermodynamic database “data0.ypf.R2” (USDOE 2007) to equilibrate a model Cobourg Formation porewater with CO₂ at a partial pressure of CO₂ of 8.9 x 10⁵ Pa (conservatively set at around a factor of two higher than the pressure for the simplified base case calculation). The composition of the porewater, henceforth termed “Model 2” porewater, was calculated using the chemical constraints given in Table G.1.

Table G.1: Chemical Constraints on “Model 2” Cobourg Formation Porewater

Parameter	Value	Constraint
Ionic Strength	4.77	
pH	6.5	Fixed to give plausible pCO ₂ in calcite-buffered system
pe	-1.993	Specified to be consistent with log pO ₂ (g), determined by pyrite – hematite equilibrium
	Concentration (molal)	
Na	2.59E+00	Reported composition, Table 2.10
Ca	2.38E-01	Reported composition, Table 2.10
Mg	9.72E-03	Dolomite equilibrium
K	4.43E-01	Reported composition, Table 2.10
Sr	1.91E-03	Celestite equilibrium
Cl	3.48E+00	Electrical neutrality
Br	2.28E-02	Reported composition, Table 2.10
SO ₄	1.94E-02	Anhydrite equilibrium
B	1.64E-02	Reported composition, Table 2.10
C	6.10E-04	Calcite equilibrium
Al	6.22E-11	Illite equilibrium
Si	9.98E-04	SiO ₂ (am) equilibrium

Again using PHREEQC and the "data0.ypf.R2" thermodynamic database, the resulting CO₂-equilibrated solution was reacted with calcite and dolomite in turn. This procedure determined how much of each mineral could be dissolved by 1 kg of the water. It was found that this quantity of water would dissolve 0.01134 moles of calcite, or 0.00551 moles of dolomite.

By making the simplifying assumption that the rock is either pure calcite or pure dolomite, upper limits were calculated for the amount of rock that would dissolve. Furthermore, it is expected that more dissolution would occur within the damaged zone than in the undamaged host rock, since the porosity of the damaged zone is around two to four times greater than that of the undamaged rock (Table 5.8 of QUINTESSA and GEOFIRMA 2011). Consequently, the porewater/solid ratio is higher in the damaged zone. Taking a damaged zone porosity of 0.06, one pore volume of the CO₂-equilibrated model Cobourg Formation porewater would dissolve 0.0027 wt% of the rock, if the rock were entirely composed of calcite, or 0.0023 wt% of the rock if the rock were entirely composed of dolomite. These values are equivalent to increases in porosity of 0.042% and 0.035% of the original porosity respectively.

In reality, the increases in porosity are likely to be much less than these values for the following reasons.

- A significant proportion of the rock is composed of minerals that are much less soluble than either calcite or dolomite. Up to 20 wt% of the Cobourg Formation consists of sheet silicates (Figure 2.27).
- The partial pressure of CO₂ is expected to be much less than the upper limit used in this calculation. The T2GGM model for the reference case had a peak pCO₂ of 7.6 x 10⁵ Pa (GEOFIRMA and QUINTESSA 2011). However, even this value is likely to over-estimate the actual value, since it takes no account of CO₂ being removed by reaction with cement in the repository.
- Dolomite and calcite in fact occur together in the rock and dissolution of dolomite is likely to be accompanied by precipitation of calcite.

These calculations should be balanced by the fact that they take no account of the time-integrated production of CO₂, but rather consider dissolution at peak pressure. The evolution of porosity over time has been investigated by ARC (2010), who studied more realistic rock compositions. Their results also indicated very little dissolution of the carbonate rock (<0.002%).

In conclusion, none of the calculated changes in rock mass would have a significant effect on the rock properties such as porosity and permeability of the surrounding carbonate rock.

REFERENCES FOR APPENDIX G

- ARC. 2010. Gas Transport and Geochemical Modelling. Alberta Research Council. Technical Report CEM-19 prepared for Nuclear Waste Management Organization. Edmonton, Canada.
- GEOFIRMA and QUINTESSA. 2011. Postclosure Safety Assessment: Gas Modelling. Geofirma Engineering Ltd. and Quintessa Ltd. report for the report for the Nuclear Waste Management Organization NWMO DGR-TR-2011-31 R000. Toronto, Canada.
- Parkhurst, D.L. and C.A.J. Appelo. 1999. User's Guide to PHREEQC (Version 2) – A Computer Program for Speciation, Batch Reaction, One-dimensional Transport, and Inverse Geochemical Calculations. US Geological Survey report Water-Resources Investigations Report 99-4259. Denver, USA.
- QUINTESSA and GEOFIRMA. 2011. Postclosure Safety Assessment: Data. Quintessa Ltd. and Geofirma Engineering Ltd. report for the Nuclear Waste Management Organization NWMO DGR-TR-2011-32 R000. Toronto, Canada.
- USDOE. 2007. In-Drift Precipitates/Salts Model. United States Department of Energy ANL-EBS-MD-000045 Rev 03. Las Vegas, USA.